Bioactive Films and Hydrogels Based on Potato Starch and Phenolic Acids Using Subcritical Water Technology

by

Junchao Zhang

A thesis submitted in partial fulfillment of the requirements for the degree of

Master of Science

in

Bioresource and Food Engineering

Department of Agricultural, Food and Nutritional Science
University of Alberta

© Junchao Zhang, 2015

Abstract

Biodegradable polymers as an eco-friendly alternative to traditional plastics have raised increasing attention by the packaging industry, especially for food and pharmaceutical applications. Phenolic acids found in many plants exert antioxidant and antimicrobial activity, which are considered beneficial to human health.

In this study, a new approach based on subcritical water (SCW) technology has been developed, which allowed the modification and production of potato starch polymers with the use of gallic acid. First, solubility behavior of gallic acid, 4-hydroxybeozic acid and 3-(4-hydroxyphenyl)-propionic acid in subcritical water was determined at different pressures and temperatures using a dynamic system. The solubility of these phenolic acids in water increased with temperature. Then, gallic acid was used to produce bioactive films and hydrogels using SCW technology. Four processing parameters, gallic acid/starch ratio, temperature, glycerol/starch ratio and pressure, were evaluated based on film structural, optical, mechanical, and functional properties. Optimum film in terms of mechanical properties was achieved using 40 mg gallic acid/g starch and 0.5 g glycerol/g starch with 5% potato starch solution at 100 °C and 30 bar. Starch bioactive hydrogels were also produced and characterized in terms of structural, physicochemical and functional properties (swelling degree, and phenolic releasing capacity). The optimum hydrogel in terms of porosity and swelling degree was found. Films produced can be potentially used as functional food packaging materials or carriers for bioactive compounds. The starch based hydrogel can also be used as an absorbent for food and non-food application.

Keywords: Phenolic acid, potato starch, bioactive film, hydrogel, subcritical water.

Acknowledgements

In the past couple of years, I have achieved more than I could even imagine. All of these would be impossible without the support, encouragement and guidance of many people in the Department of Agriculture, Food and Nutritional Science at University of Alberta.

First and foremost, I would like to express my most sincere appreciation to my supervisor, Dr. Marleny D. A. Saldaña. She has been constantly providing insightful advice and knowledge, which inspired my imagination and creativity on my thesis and life. The opportunities she provided to me were also invaluable and enriched my experience in every aspects of my academic journey.

I also want to take the opportunity to thank my lab colleagues for providing a rich and stimulating environment to study and research. Although they may come from different countries, the bonding between us and sense of family will last a lifetime. A special thank goes to Dr. Victor Alvarez for his constant help with my experiments and extra-curricular activities in Canada.

I am thankful to my lab colleagues Sergio Martinez Monteagudo, Ehsan Jenab, Deniz Ciftci, Ozan Nazim Ciftci, Oscar Benito Roman, Carla Valdivieso, Sihao Wei, Cheng Shi, Ricardo Tomas Do Couto, Nian Liu and Yujia Zhao for their constant motivation and support.

I also feel greatly indebted to my family and friends for providing a supportive environment. Particularly to my parents and my wife, who have always understood, loved and supported me through my study journey at University of Alberta in Canada.

TABLE OF CONTENTS

LIST OF TABLES

LIST OF FIGURES

xiv

NOMENCLATURE

Symbols	Name
A	Absorbance
ρ	Density
Q_{eq}	Swelling degree at equilibrium
H	Thickness
ΔP	Partial water vapor pressure difference
α	Lattice structures
L	Hunter color index L
a	Hunter color index a
b	Hunter color index b
ΔE	Total color difference
MW	Molecular weight
m	Mass
T_{600}	% Transmittance of light at 600 nm
T_m	Melting point
T_{tr}	Temperature for phase transition
T_p	Peak temperature of gelatinization
T_c	Completion temperature of gelatinization
T_o	Onset temperature of gelatinization
ΔH_m	Change of enthalpy at the melting point
ΔH_{tr}	Change of enthalpy at the phase transition
ΔH	Enthalpy change
x	Molar fraction
η	Viscosity
ε_r	Relative permitivity
ε	Dielectric constant
S	Solubility
V	Volume
YI	Yellowness index

WI	Whiteness index

ABBREVIATIONS

ABTS	2,2'-azino-bis(3-ethylbenzothiazoline-6-sulphonic acid) method
ANOVA	Analysis of variance
CMC	Carboxymethylcellulose
CFU	Colony-forming unit
CL	Chain length
DPPH	2,2-diphenyl-1-picrylhydrazyl assay
DSC	Differential scanning calorimeter
24DA	2,4-Dihydroxybenzoic acid
DHT	Dynamic holding time
EV	Equilibrium vessel
E%	Percent elongation at break
FRAP	Ferric ion reducing antioxidant power
FTIR	Fourier transform infrared spectroscopy
GA	Gallic acid
GC	Gas chromatography
HPLC	High-performance liquid chromatography
34HA	3-(4-hydroxyphenyl) -propionic acid
4HA	4-Hydroxybenzoic acid
LB	Lysogeny broth
LDPE	Low-density polyethylene
MS	Mass spectrometry
MIC	Minimum inhibitory concentration
PVC	Polyvinyl chloride
PVA	Poly(vinyl alcohol)
PCL	Polycaprolactone
RH	Relative humidity
RC	Relative crystallinity

SEM	Scanning electron microscopy
SAP	Superabsorbent polymer
SHT	Static holding time
SD	Standard deviation
SCW	Subcritical water
TEAC	Trolox equivalent antioxidant activity
TPTZ	2,4,6-tri(2-pyridyl)-s-triazine
TS	Tensile strength
UV	Ultraviolet light
WS	Water solubility
WVTR	Water vapor transmission rate
WVP	Water vapor permeability
XRD	X-Ray diffraction

Chapter 1: Introduction

1.1 Rationale

Subcritical water, as an emerging topic in recent years, has raised the attention from environmental science as well as food science. The term "subcritical water" is used to define the region of condensed phase of water between the temperature ranges from 100 °C (boiling point of water) to 374 °C (critical point of water). Other common terms such as "superheated water", "near critical water", "pressurized hot water" and "hot compressed water" have also been used. Changes in temperature and pressure alter the physical properties of water, such as viscosity, density, dielectric constant and ionic product. These distinguishing properties of subcritical water upon normal water was first discovered and reported as an extraction solvent for soil samples by Hawthorne et al. (1994). Then, numerous studies have been conducted to explore the potential of subcritical water in different food and non-food applications, especially in the hydrothermal biomass transformation and extraction (Saldaña & Valdivieso-Ramírez, 2015).

The elevated temperature of subcritical water promotes bond breakage and thus the formation of radicals. Consequently, the occurrence of radical reactions is more likely to occur in subcritical water than in the water below the boiling point at ambient pressure (Watanabe et al., 2004). The decreased relative dielectric permittivity and the increased ion product of subcritical water lead to several types of chemical reactions, like nucleophilic substitutions and eliminations (Akiya & Savage, 2002; Antal et al., 1998). One type of reaction involving water as a reactant is hydrolysis, such as hydrolysis of cellobiose in subcritical water (Sasaki et al., 2002), and lignocellulosic biomass

hydrolysis (Zhao et al., 2014). In addition, the reaction rate is considerably increased in subcritical water for acid- and base-catalyzed organic reactions (Kuhlmann et al., 1994). Notably, subcritical water can also promote a series of organic reactions that only proceed at low/high pH (Moller et al., 2011).

Phenolics are the most abundant secondary metabolites of plants, which contain one or more aromatic rings with one or more hydroxyl groups (Okarter & Liu, 2010). They have a broad distribution in the plant kingdom and are found in fruits, vegetables, grain and display diverse biological and pharmacological properties (e.g. antioxidant, antiviral, and anti-inflammatory). Phenolics in plants act as defense mechanism against pathogens, parasites as well as predators. In human diets, phenolics promote and help maintain human health by their preventive effect against various types of diseases such as cancer, cardiovascular diseases, neuropathies and diabetes (Shahidi, 2012).

Due to their protectant functions in plant, phenolics are mostly found in the outer layers of fruits and vegetables, like in the skin of orange and the bran layer of barley, which are generally not suitable for human consumption and often discarded as a waste or feed for livestock. Solvent extraction is the most commonly used method to obtain phenolics from these biomasses due to their ease of use, efficiency, and wide applicability. However, traditional solvent extraction methods, such as Soxhlet extraction, may often be time consuming (usually 2 to 4 h) with low extraction yield and also require large volume (~200 mL) of non-environmentally friendly organic solvents (e.g. methanol). To reduce the use of organic solvents, subcritical water is a feasible green solvent for extraction as it utilizes pressurized water at elevated temperatures. In recent years, subcritical water has been successfully applied to the extraction of phenolic

compounds from different plant materials, such as grape seeds, apples, spinach, eggplant, potato peel and barley hull. However, phenolic compounds are easily oxidized at high temperatures so it is very important to prove that no degradation under the proposed subcritical water conditions occurs. Therefore, it is necessary to study and understand the behavior of phenolics at elevated temperatures and pressures, which can help in the optimization of the extraction process.

Starch is a polysaccharide consisting of amylose and amylopectin, which are polymers of glucose, linear and branched, respectively. Each glucose unit potentially has three reactive hydroxyl groups that are the basis of all derivatizations. Native starch granule is insoluble in cold water and has to be exposed to a certain degree of heating and excess amount of water to undergo a proper gelatinization process. Starch gelatinization involves some irreversible changes in properties, such as granular swelling, breakage of granule structure, native crystal melting, loss of birefringence, and starch solubilisation. However, the inert properties of native starch largely limit its application in the food industry and several modification methods (physical, chemical and enzymatic) have been developed. Starch modification alters the structure and affects the hydrogen bonding in a controllable manner to enhance and extend the applications. Water acts as a plasticizer in the gelatinization process of starch and facilitates the rupture of the granule, but subcritical water can also be a catalyst or reaction medium to promote interactions between phenolics with amylose and amylopectin. Thus, the potential of subcritical water technology in starch modification is worth investigating, mainly for packaging material.

Food packaging is the major application of starch-based biodegradable polymers in the food industry. The requirements for food packaging include covering and retaining

the integrity of the food content, maintaining the food fresh, enhancing organoleptic characteristics of food such as appearance, aroma, and taste, and prevent food from environmental hazards (Zhao et al., 2008). In addition to their use in the food industry, starch-based biodegradable films are also largely applied in agriculture for three purposes: mulch film, covering of greenhouses and materials with fertilizers with controlled release (Dilara & Briassoulis, 2000). The biodegradable property of starch film eliminates the concerns about environmental pollution and promotes a sustainable growth. However, compared to the common petroleum derived plastics, biodegradable starch films still reveal some drawbacks, such as lower stiffness and greater sensitivity to water and heat. Therefore, in order to expand the use of these promising materials, new technologies, such as subcritical water can modify starch and phenolics to enhance structural, mechanical and optical properties (Aranda Saldaña et al., 2014).

1.2 Hypothesis

- Subcritical water would increase the solubility of phenolic acids where pressure might facilitate solubilisation.

- Subcritical water would promote reactivity of phenolic acid with other compounds, such as starch and glycerol.

- Starch gelatinized with phenolic acid under subcritical water condition would exert different physical and chemical properties compared to native starch.

- Films formed using subcritical water would load more phenolic acids, increasing the antioxidant and antimicrobial function of the film as food packaging material.

- Starch gel obtained during bioactive film modification can be used for hydrogel development.

1.3 Thesis objectives

The main objective of this thesis was to study reactions of starch and phenolic acids in subcritical water (SCW). Understanding the solubility behavior of phenolic acids in subcritical water is fundamental for this reaction process to be implemented as an innovative technology. Also, the use of subcritical water to replace toxic chemicals used is desirable by the food industry during the production of bioactive packaging materials. To achieve this main objective, some specific objectives were:

- Determine the solubility of phenolic acids in subcritical water to unveil the influence of pressure and temperature using a newly developed semi-continuous system.

- Study the formation and optimized mechanical and functional starch based bioactive film production with and without the addition of phenolic acids using subcritical water technology at lab scale.

- Develop and characterize starch based bioactive hydrogels for potential food and non-food applications using subcritical water technology.

1.4 References

Akiya, N., Savage, P.E. 2002. Roles of water for chemical reactions in high-temperature water. *Chemical Reviews*, **102**(8), 2725-2750.

Aranda Saldaña, M.D., Alvarez, V.H., Vasanthan, T. (2014). PCT/CA2014/000432, WO 2014 186864 A1. Modification of starches and production of new biopolymers using subcritical water technology.

Antal, M.J., Carlsson, M., Xu, X., Anderson, D.G.M. 1998. Mechanism and kinetics of the acid-catalyzed dehydration of 1- and 2-propanol in hot compressed liquid water. *Industrial & Engineering Chemistry Research*, **37**(10), 3820-3829.

Dilara, P.A., Briassoulis, D. 2000. Degradation and stabilization of low-density polyethylene films used as greenhouse covering materials. *Journal of Agricultural Engineering Research*, **76**(4), 309-321.

Hawthorne, S.B., Yang, Y., Miller, D.J. 1994. Extraction of organic pollutants from environmental solids with subcritical and supercritical water. *Analytical Chemistry*, **66**(18), 2912-2920.

Kuhlmann, B., Arnett, E.M., Siskin, M. 1994. Classical organic-reactions in pure superheated water. *Journal of Organic Chemistry*, **59**(11), 3098-3101.

Moller, M., Nilges, P., Harnisch, F., Schroder, U. 2011. Subcritical water as reaction environment: Fundamentals of hydrothermal biomass transformation. *Chemsuschem*, **4**(5), 566-579.

Okarter, N., Liu, R.H. 2010. Health benefits of whole grain phytochemicals. *Critical Reviews in Food Science and Nutrition*, **50**(3), 193-208.

Saldaña, M.D.A., Valdivieso-Ramírez, C.S. 2015. Pressurized fluid systems: Phytochemical production from biomass. *The Journal of Supercritical Fluids*, **96**, 228-244.

Sasaki, M., Furukawa, M., Minami, K., Adschiri, T., Arai, K. 2002. Kinetics and mechanism of cellobiose hydrolysis and retro-aldol condensation in subcritical and supercritical water. *Industrial & Engineering Chemistry Research*, **41**(26), 6642-6649.

Shahidi, F. 2012. Nutraceuticals, Functional foods and dietary supplements in health and disease. *Journal of Food and Drug Analysis*, **20**, 226-230.

Watanabe, M., Sato, T., Inomata, H., Smith, R.L., Arai, K., Kruse, A., Dinjus, E. 2004. Chemical reactions of C-1 compounds in near-critical and supercritical water. *Chemical Reviews*, **104**(12), 5803-5821.

Zhao, R., Torley, P., Halley, P.J. 2008. Emerging biodegradable materials: Starch- and protein-based bio-nanocomposites. *Journal of Materials Science*, **43**(9), 3058-3071.

Zhao, Y., Lu, W.J., Chen, J.J., Zhang, X.F., Wang, H.T. 2014. Research progress on hydrothermal dissolution and hydrolysis of lignocellulose and lignocellulosic waste. *Frontiers of Environmental Science & Engineering*, **8**(2), 151-161.

Chapter 2: Literature review

2.1 Phenolic acids

2.1.1 Structure and classification

Phenolic acids are classified as a subclass of a larger category of secondary plant metabolites which is commonly referred to as "phenolics" or "phenolic compounds". The term "phenolic" include over 8000 naturally occurring compounds widely spread throughout the plant kingdom (Whiting, 2001). Phenolics have at least one aromatic ring, and one or more hydroxyl substituents, including functional derivatives, such as esters, methyl ethers, glycosides, among others (Rice-Evans et al., 1996). Depending on the number of aromatic rings present, phenolic compounds are divided into two categories: simple phenol and polyphenols. Polyphenols are commonly classified as flavonoids (two phenol subunits) and tannins (three or more phenol subunits). Simple phenol possesses only one phenol subunit. A typical group of simple phenol is phenolic acid, which in general describes phenols that possess one carboxylic acid group. These naturally occurring phenolic acids in plant can be distinguished depending on their structure as benzoic acid derivatives (hydroxybenzoic acids, C6-C1) and cinnamic acid derivatives (hydroxycinnamic acids, C6-C3) (Robbins, 2003). Although the basic skeleton remains the same, the number and position of the hydroxyl groups on the aromatic ring create the variety. Phenolic acids can be found in fruits, vegetables, grains and are physically dispersed throughout the plant in seeds, leaves, roots, and stems (Kelebek et al., 2015; Martinez-Huelamo et al., 2015; Shahidi & Naczk, 1995; Siu & Wu, 2014). Gallic, caffeic, *p*-coumaric, vanillic, ferulic, and protocatechuic are phenolic acids present in various plants (Oksana et al., 2012). Other acids, such as gentisic, syringic, and 3-hydroxybenzoic

acids, are found in plants. A study of total phenolic content of 62 fruits (Fu et al., 2011) found quercetin, chlorogenic acid, kaempferol, luteolin, gallic acid and caffeic acid in these fruits. High contents of gallic acid were found in olive (50 mg/100 g), wax apple (15.31 mg/100 g) and Chinese date (13.11 mg/100 g). Giada (2013) also examined the total phenolic content in a wide variety of plants and found that the top two plants in each category were: soybean (414 mg/100g) and oat (352 mg/100g) compared to other cereals and legumes; red cabbage (186 mg/100g) and potato (150 mg/100g) compared to other vegetables；basil (4425 mg/100g) and shallot (1718 mg/100g) compared to other herbs and spices; sweet orange (1343 mg/100g) and grape fruit (893 mg/100g) compared to other fruits; and roasted cocoa bean (1305 mg/100g) compared to others like red wine (242 mg/100g) and green tea (83 mg/100g).

In the plant, only a minor fraction of phenolic acid exists in the free form, the majority of them are linked through ester, ether, or acetal bonds either to structural components of the plant (e.g. cellulose, protein, and lignin) (Andreasen et al., 2000; Barros et al., 2013; Tian et al., 2013) or to larger polyphenols (flavonoids), or smaller organic molecules (e.g., glucose, quinic, maleic, or tartaric acids) or other natural products (e.g., terpenes) (Herrmann, 1992).

2.1.2 Functionality

Phenolic acids are closely related to a variety of functions involved in plants growth and reproduction, such as nutrient uptake, protein synthesis, enzyme activity, photosynthesis, structural components, and allelopathy (Robbins, 2003). The production of phenolic acid can be stimulated by the growth condition and considered as a response to protect the plant from various environmental factors, like light (Wang & Zheng, 2001),

chilling (Kreps et al., 2002; Pennycooke et al., 2005), and irradiation (Tattini et al., 2005). Most of these functions are largely related to the antioxidant and antimicrobial activity found in nearly all phenolic acids (Table 2.1). With regard to the reactivity of the hydroxyl substituent on the aromatic ring, phenolic acids act as radical scavenging agent via hydrogen atom donation (Kolodziejczyk-Czepas et al., 2014). Other established antioxidant functionality is the radical quenching mechanisms through electron donation and singlet oxygen quenching (Hamauzu et al., 2007). Number of substituents and their position on the aromatic ring affect the stabilization and therefore affect the radical-quenching ability of these phenolic acids.

Phenolic compounds with one hydroxyl group on their aromatic ring are less effective antioxidants than phenolics with the second hydroxyl in the ortho or para position (Kylli et al., 2008). As shown in Table 2.1, although the absolute antioxidant activity varied among studies, phenolic acids such as hydrobenzoic and hydrocinnamic acids with more –OH groups on the aromatic rings showed a high antioxidant activity. However, the opposite trend was found for their antimicrobial activity, as a decreasing number of hydroxyl groups enhanced the activity of hydroxybenzoic acids, but had minor effects on hydroxycinnamic acids. Overall, hydrocinnamic acids tend to have higher antimicrobial and antioxidant activities than the hydrobenzoic acid counterparts. The electron-withdrawing property of carboxylate group in benzoic acids has a negative influence on the H-donating ability of hydroxyl group on the aromatic ring (Rice-Evans et al., 1996). However, due to the additional C=C double bond, hydrocinnamic acid was less influenced by carboxylate group and exerted a higher antioxidant activity. Also,

9

with its unsaturated chain, hydrocinnamic acids are considered more lipophilic, allowing inactivating the bacteria through the membrane (Sanchez-Maldonado et al., 2011).

Kylli et al. (2008) also examined the antioxidant activity of conjugated hydroxycinnamates to mimic the influence of esterification of phenolic acids in plants. Hydroxycinnamic acids esterified to the primary hydroxyls in glucopyranoside and arabinofuranoside are able to move more freely than in other isomers, thus enabling them to function as antioxidants more efficiently. In general, the bounded form of phenolic acid is equal or more effective than its free form. Martin and Appel (2010) also suggested that consuming phenolic compounds directly from plant foods may be more effective in combating oxidative damage in human body than in the form of dietary supplement. Phenolic acids account for approximately one-thirds of the dietary phenols and there is an increasing awareness and interest in the antioxidant behavior and potential health benefits, such as preventing coronary heart disease, stroke, and cancer (El Abbassi et al., 2014; Godos et al., 2014), associated with the consumption of these simple phenolic acids.

Table 2.1 Structure, antioxidant and antimicrobial activity of naturally occurring phenolic acids

Position of OH	Hydrobenzoic acid — Antioxidant activity*	Hydrobenzoic acid — Antimicrobial activity**	Hydrocinnamic acid — Antioxidant activity*	Hydrocinnamic acid — Antimicrobial activity**
2	0.04 (Salicylic) (Harborne, 1967)		0.99 (Harborne, 1967); 0.034 (Coumaric) (Szwajgier et al., 2005)	
3	0.84 (Herrmann, 1989)		1.21 (Harborne, 1967)	
4	0.08 (Kuhnau, 1976)	0.12 (Sanchez-Maldonado et al., 2011)	0.134 (Szwajgier et al., 2005)	0.12 (Sanchez-Maldonado et al., 2011)
2, 3	1.46 (Kuhnau, 1976)			
3, 4	1.19 (Harborne, 1967); 1.92 (Protocatechuic) (Szwajgier et al., 2005)	0.31 (Sanchez-Maldonado et al., 2011)	1.26 (Kuhnau, 1976); 1.29 (Roleira et al., 2010); 0.98 (Gaspar et al., 2009); 1.41 (Caffeic) (Szwajgier et al., 2005)	0.23 (Sanchez-Maldonado et al., 2011)
2, 5	1.04 (Gentisic) (Kuhnau, 1976)			
3, 5	2.15 (Resorcylic) (Harborne, 1967)			
4-hydroxy, 3-methoxy	1.43 (Kuhnau, 1976); 2.06 (Vanillic) (Szwajgier et al., 2005)		1.90 (Hertog et al., 1993); 0.78 (Gaspar et al., 2009); 1.36 (Ferulic) (Szwajgier et al., 2005)	0.16 (Sanchez-Maldonado et al., 2011)
3, 4, 5	3.01 (Gallic) (Block & Langseth, 1994)	0.49 (Sanchez-Maldonado et al., 2011)		
3, 5-dimethoxy, 4-hydroxy	1.36 (Kuhnau, 1976); 1.85 (Syringic) (Szwajgier et al., 2005)	0.39 (Sanchez-Maldonado et al., 2011)	0.86 (Gaspar et al., 2009); 2.02 (Sinapinic) (Szwajgier et al., 2005)	

*Total antioxidant activity (mM/L) relative to Trolox , ** MIC (g/L) against *Escherichia coli* AW 1.7

2.1.3 Extraction method

To obtain phenolic compounds from natural raw materials and perform qualitative and quantitative studies, there are a variety of extraction methods to be applied that can be classified as conventional and non-conventional methods.

Conventional methods, like Soxhlet, have been well established and used as a standard extraction method in the industry during the last century (Azmir et al., 2013). However, some drawbacks present in these conventional methods, like use of organic chemicals (e.g. methanol), long operating time, and low yield and quality of extract, have promoted the development of many non-conventional methods during the last 50 years.

Non-conventional methods, such as ultrasound-assisted extraction (Orphanides et al., 2014), microwave-assisted extraction (Baiano et al., 2014), pulse electric field (Lopez-Alfaro et al., 2013; Toepfl et al., 2006), subcritical and supercritical fluid technology (Akalin et al., 2013; Herrero et al., 2013; Kanmaz & Ova, 2013; Lukmanto et al., 2013; Singh & Saldaña, 2011; Tangkhavanich et al., 2013; Vergara-Salinas et al., 2013; Yang et al., 2013; Yoswathana & Eshiaghi, 2013), and high pressure processing (Jun, 2013) have been studied to enhance the overall yield and selectivity of phenolic compounds from plant materials. For example, subcritical water (Singh & Saldaña, 2011) was used to remove higher amounts of phenolic compounds from potato peel (82 mg/100 g) compared to methanol (46 mg/100 g) or ethanol extraction (29 mg/100 g) at 65 °C and at atmospheric pressure. Besides, after optimizing the process parameters of temperature, pressure, and static holding time, subcritical water removed high amounts of phytochemicals from potato peels in shorter time and required about 50% less solvent (160 mL) than with methanol or ethanol extraction (300 mL) (Alvarez et al., 2014).

2.1.4 Solubility measurement of phenolic acids in solvents

Solubility measurement of phenolic acids in a number of solvents is summarized in Table 2.2. The main reasons to study the solubility of phenolic acids in different solvents are:

i) Use solubility data of phenolic acids in different solvents at different temperatures to design extraction and purification process from matrices, such as cereal bran, and grape seed (Daneshfar et al., 2008; Murga et al., 2003). At the same temperature, organic solvents，such as methanol and ethanol have a higher dissolving capacity for phenolic acids compared to water. Therefore, solubility of various phenolic acids (e.g. gallic acid, syringic acid, etc.) in alcohols or their aqueous mixtures have been studied (Lim et al., 2013; Noubigh et al., 2013; Noubigh et al., 2012).

ii) Aqueous solubility data of phenolic acids under different temperatures can be used to calculate appropriate thermodynamic properties, such as Gibbs free energy, molar enthalpy of dissolution, and molar entropy of dissolution, which can be used to model and predict solubility behavior at conditions which experiments cannot be performed due to equipment limitation (Lu & Lu, 2007; Mota et al., 2008; Nouhigh et al., 2008; Queimada et al., 2009).

iii) Phenolic compounds can be found in industrial or agricultural by-products, such as waste water from olive mills (Noubigh et al., 2007b), which is characterized by its dark color, characteristic odour, acidic pH (4–5) and high organic content (4–16%) mainly composed of classes of pollutants, such as polyphenols (3–10 g/L) that may exhibit antimicrobial, ecotoxic and phytotoxic properties (Davies et al., 2003; Musculo, 2010). The evaluation of solubility of phenolic acids in waste water, mainly salt solution

can help control environmental pollution as the level of polyphenol in olive mill waste water is toxic to the ecosystem (Bhatnagar et al., 2014; Noubigh et al., 2008; Pires & Franco, 2012).

There are two methods used for solubility measurement of a phenolic acid in a solvent, one is static and the other is dynamic. In the static method, an excess amount of phenolic acid is placed with a known amount of water (e.g. 100 mL) in a three-necked round-bottom flask. Then, the flask is heated using a water bath under continuous stirring through a shaking or magnetic stirring for 1 to 6 h. To ensure that the solvent was saturated with the phenolic acid from time to time, samples are taken directly from the solution and analyzed by HPLC or using the gravimetric method (obtain the mass of solute by drying) (Lim et al., 2013). Once the concentration of phenolic acid has reached equilibrium, the amount of solute in the solvent is considered as the solubility value at the measured temperature. However, this static method is time consuming and only suitable for heat stable compounds or low temperature (< 50 ℃) measurements. For solubility measurements at high temperature, heating for some hours can induce degradation of the solute and affect the accuracy of the results. Therefore, for aqueous solubility measurements at temperatures higher than 100 °C (subcritical water), where pressure is require and a flask cannot further maintain the pressure, a dynamic method has been adopted in recent years (Chafer et al., 2007; Murga et al., 2003; Srinivas et al., 2010). In this method, solvent is pumped at a constant low flow rate (0.1-0.5 mL/min) through an equilibrium cell loaded with an excess amount of phenolic acid, then the saturated solution is diluted by a solvent before cooling and collection. In the case of supercritical CO_2, additional pressure is needed to attain the supercritical state of CO_2. After exiting

the equilibrium vessel, CO_2 becomes a gas through depressurization and precipitate the solute in the collecting vessel. Due to the similarity on polarity, solubility of phenolic acids in organic solvents, like methanol, are extremely higher than in water. For example, the solubility of p-hydrobenzoic acid in methanol at 25 ℃ is 555 g/kg, but its solubility in water is only 6 g/kg (Gracin & Rasmuson, 2002). Higher solubility of phenolic acids in organic solvent (e.g. methanol, ethanol) than water has been found (Table 2.2), which supports the use of these organic solvents in the extraction or purification process of phenolic acids. However, the toxicity of organic solvent (e.g. methanol) has been the major concern limiting its use in food applications. Any residue of organic solvent in the extracted phenolic acid (e.g. from grape seeds, potato peels, etc.) has to be completely removed before a final application. Therefore, the current focus is to isolate phenolic compounds from natural vegetable matrices using environmentally safe and efficient "green" processes such as supercritical fluid extraction (SFE) to replace conventional wet extraction. Although supercritical CO_2 has been successfully applied for the extraction of many heat labile compounds (e.g bran oil, flavors, etc.) (Choi et al., 2014; de Aguiar et al., 2014; Tarvainen et al., 2015), the solubility of phenolic acids in supercritical CO_2 are relatively low compared to water. In addition, a co-solvent like ethanol is often used to improve the extraction efficiency (Chen et al., 2009; Murga et al., 2002).

Another green environmentally friendly and cheap solvent studied recently is subcritical water, also known as pressurised hot water, and is referred to liquid water heated to temperatures above its boiling point and under pressure. The temperature has a dramatic influence on the solvent polarity, which is usually measured by the dielectric constant (ε) of water. By increasing temperate, the number of hydrogen bonds in water

decreases and resulted in a lower dielectric constant, which make subcritical water more similar to hydrocarbon solvents (Pavlovic et al., 2013). For example, at a constant pressure, an increase in water temperature results in a decrease of its dielectric constant from ~80 at 25 ℃ to ~27 at 225 ℃, which is similar to that of methanol ($\varepsilon = 33$) and ethanol ($\varepsilon= 24$) (Karasek et al., 2006; Miller et al., 1998). For this reason, the solubility of phenolic acids, hydrophobic organic compounds (e.g. benzopyrene), fatty acid and sugar in subcritical water have increased.

The solubility of gallic acid, catechin, protocatechuic acid (Srinivas et al., 2010), and salicylic acid (Kayan et al., 2010) at temperatures ranging from 25 to 200 ℃ have shown dramatic increases in solubility with increasing temperature, especially above 100℃. For example, the solubility of gallic acid at 142 ℃ was 2870 g/L, which was almost six times higher than the one at 102 ℃ (523 g/L), 227 times higher than the one at 25 ℃ (12.6 g/L), and even higher than the one in methanol (368 g/L) or ethanol (208 g/L) at 60℃ (Daneshfar et al., 2008).

Miller and Hawthorne (1998) found the solubility of benzopyrene in water increased from 0.04 (100 °C) to 6.5 μg/g (150 ℃) and even higher 1095 μg/g (250 °C). The solubility of palmitic acid in water increased from 0.12 (100 °C) to 0.18 g/100g (160 °C) and stearic acid from 0.08 (100 °C) -0.13 g/100g (180 °C), but it was also found the solubility of these fatty acid start to stabilize and further degradation occurred during measurement when temperature above 200 °C (Huang et al., 2013). The solubility of polycyclic aromatic hydrocarbons (e.g. anthracene, pyrene, chrysene, perylene, and carbazole) in subcritical water at 205 °C were signifincaly higher than the one at 100 °C by 3 orders of magnitude. For example, increasing the temperature from 100 to 205 ℃

increased the mole fraction solubility of chrysene from 13 x10^{-9} to 75 800 x 10^{-9} (Miller et al., 1998).

In addition, for water soluble compounds, such as lactose and glucose, their solubility in subcritical water also increased. Saldaña et al. (2012) found that the solubility of glucose increased from 1.44 (100 °C) to 4.24 g/g (160 °C) and lactose from 0.64 (100 °C) to 1.11 g/g (160 °C). They also found that the solubility of sugar in water was influenced by pressure. For example, the solubility of glucose at 160 °C and 120 bar was 2.61 g/g lower than the solubility (4.24 g/g) obtained at 15 bar.

Table 2.2 Solvent, temperature and method used for solubility measurement of phenolic acids in solvents.

Phenolic acid	Method	Solvent	Conditions	Solubility	Ref
Gallic acid	Shake-flask method	water	15-50 ℃	9.1-38.9 g/L	Mota et al. (2008)
		Water	20-45 °C	0.06-0.07 mole/kg	Noubigh et al. (2007a)
		(1 mole/kg) KCl +water		0.05-0.07 mole/kg	
		(1 mole/kg) NaCl+water		0.05-0.06 mole/kg	
		(1 mole/kg) LiCl+water		0.03-0.045 mole/kg	
		Water +(0-64%) methanol	20-45 ℃	$1-76 \times 10^{-3}$ mole fraction	Noubigh et al. (2013)
		Water	0-90 ℃	7.2-290 g/g	Lu and Lu (2007)
		Methanol	25-60 ℃	0.387 -0.465 g/g	Daneshfar et al. (2008)
		Ethanol		0.233-0.265 g/g	
		Water		0.015-0.08 g/g	
		Ethyl acetate		0.0129-0.0171 g/g	
		(7.2 -68.2 %) ethanol+water	20-45 ℃	$2.486-87 \times 10^{-3}$ mole fraction	Noubigh et al. (2012)
		(0-21.3%) Sodium sulfate	20-45 ℃	$1.16-1.43 \times 10^{-3}$ mole fraction	Nouhigh et al. (2008)
	Dynamic flow apparatus	Subcritical water	25-142 ℃	13-2870 g/L	Srinivas et al. (2010)
		Supercritical CO_2 + 6% ethanol	40-60 °C, 100 - 400 bar, flow rate 0.5 to 5 mL/min	$1.06-19.7 \times 10^{-7}$ mole fraction	Chafer et al. (2007)
Salicylic acid	Shake-flask method	Water	15-50 °C,	1-5.97 g/L	Mota et al. (2008)
		Water	25 ℃	0.0003 mole fraction	Matsuda et al. (2009)
		Methanol		0.1223 mole fraction	
		Ethanol		0.1450 mole fraction	
		Water	20-40 °C, 0.925 bar	0.0116-0.018 mole/kg	Pires and Franco (2012)
	Dynamic flow apparatus	Subcritical water	25-150 ℃ , 50 bar	0.47-102 mole fraction	Kayan et al. (2010)

Table 2.2 Continued. Solvent, temperature and method used for solubility measurement of phenolic acids in solvents.

Phenolic acid	Method	Solvent	Conditions	Solubility	Ref
Caffeic acid	Shake-flask method	water	15-50 °C,	0.55-2.92 g/L	Mota et al. (2008)
		Ionic liquid (bmimPF 6)	30-44 ℃	0.0012-0.0024 mole fraction	Alevizou and Voutsas (2013)
	Dynamic analytical method	Supercritical CO_2	500 bar , 40-60 °C Flow rate as low as possible	0.008-0.472x10^{-7}mole fraction	Murga et al. (2003)
trans-Cinnamic acid	Shake-flask method	water	15-50 °C,	0.21-0.85 g/L	Mota et al. (2008)
Ferulic acid	Shake-flask method	Water	15-50 ℃	0.57-2.19 g/L	Mota et al. (2008)
		Water	20-45 ℃	0.02-0.06 mole/kg	Noubigh et al. (2007a)
		(1 mole/kg) KCl +water		0.01-0.048 mole/kg	
		(1 mole/kg) NaCl+water		0.009-0.044 mole/kg	
		(1 mole/kg) LiCl+water		0.008-0.042 mole/kg	
	Dynamic analytical method	Supercritical CO_2	500 bar , 40 to 60 ℃ Flow rate as low as possible	8-433x 10^{-7}mole fraction	Murga et al. (2003)
Vanillic acid	Shake-flask method	Water	20-45 ℃	0.007-0.0164 mole/kg	Noubigh et al. (2007a)
		(1 mole/kg) KCl +water	20-45 ℃	0.005-0.014 mole/kg	Noubigh et al. (2007a)
		(1 mole/kg) NaCl+water		0.036-0.012 mole/kg	
		(1 mole/kg) LiCl+water		0.0029-0.011 mole/kg	
o-Coumaric acid	Shake-flask method	Water	15-50 ℃	0.2-1.3 g/L	Queimada et al. (2009)
p-Coumaric acid		Ionic liquid (bmimPF 6)	30-44 ℃	0.0062-0.01mole fraction	Alevizou and Voutsas (2013)
	Dynamic analytical method	Supercritical CO_2	500 bar , 40 – 60 ℃ Flow rate as low as possible	0.06-25.5x 10^{-7}mole fraction	Murga et al. (2003)

Table 2.2 Continued. Solvent, temperature and method used for solubility measurement of phenolic acids in solvents.

Phenolic acid	Method	Solvent	Conditions	Solubility	Ref
Syringic acid	Shake-flask method	(0-21.3%) Sodium Sulfate solution	25-45 ℃	$1.8\text{-}10.5\text{x}10^{-3}$ mole fraction	Nouhigh et al. (2008)
		water	15-50 ℃	1.1-5.9 g/L	Queimada et al. (2009)
		Water	20-45 ℃	0.02-0.05 mole/kg	Noubigh et al. (2007a)
		(1 mole/kg) KCl +water	20-45 ℃	0.0164-0.0539 mole/kg	
		(1 mole/kg) NaCl+water	20-45 ℃	0.0145-0.0504 mole/kg	
		(1 mole/kg) LiCl+water		0.013-0.0472 mole/kg	
Protocatechuic acid	Shake-flask method	Water	20-45 ℃	0.11-0.14 mole/kg	Noubigh et al. (2007a)
		(1 mole/kg) KCl +water		0.1-0.125 mole/kg	
		(1 mole/kg) NaCl+water		0.08-0.1 mole/kg	
		(1 mole/kg) LiCl+water		0.07-0.0942 mole/kg	
		Water	15 to 50 °C	7.6-49.3 g/L	Queimada et al. (2009)
		(0-21.3%) Sodium sulfate solution	20-45 ℃	$1.12\text{-}2.55\text{x}10^{-3}$ mole fraction	Nouhigh et al. (2008)
	Dynamic flow apparatus	Subcritical water	25-142 ℃	29-1180 g/L	Srinivas et al. (2010)
		Supercritical CO_2	40-60 °C, 100-500 bar Flow rate as low as possible	$0.48\text{-}25.9 \times 10^{-7}$ mole fraction	Murga et al. (2002)

2.2 Reaction in subcritical water media

In addition to the comparable dissolving capacity as organic solvent, at high temperature, subcritical water also produce significantly higher (up to 3 orders of magnitude) amount of ion product than at ambient temperatures, which allow it to act as an acid or base catalyst for reactions, such as hydrolysis and degradation (Krammer & Vogel, 2000; Kuhlmann et al., 1994; Wang et al., 2010b). For example, the reaction pathway of caffeic acid decomposition in SCW media as well as the antioxidant activity of the resulted products was investigated by Khuwijitjaru et al. (2014). They found that by heating caffeic acid in subcritical water (160 to 240 °C) for 30 to 1080s, 80 to 90 % caffeic acid was degraded to hydroxytyrosol, protocatechuic aldehyde or 4-vinylchatechol. However, this degradation did not significantly reduce the total antioxidant activity due to the comparable antioxidant activity of degraded products compared to caffeic acid.

Besides, subcritical water was used to hydrolyze biomass to produce sugars and recover bioactive compounds trapped in the biomass. Hydrolysis of biopolymers in SCW, such as lentil husk, barley hull, lupin hull, and flax hull have been studied in our laboratory (Saldaña & Valdivieso-Ramírez, 2015). Marine biomasses, such as seed weed, were also investigated by other researchers for hydrolysis and liquefaction (Kang et al., 2014; Meillisa et al., 2015). Brown seaweed (*Phaeophyta*) is mainly consisted of alginate, which is an unbranched hetero-polysaccharide. Glucose, mannose, and galactose found in brown seaweed contain essential compounds that can be converted into valuable intermediate products, such as gulose, which has been reported to be a building block in the synthesis of nucleoside analogues, and useful as potential anticancer compounds

(Sugiura et al., 2007). A recent study (Meillisa et al., 2015) found that using subcritical water at 180–260 °C (15-65 bar), with a ratio of alginate to water of 1:25 (w/v) can recover 2.2-2.7 g gulose/L alginate solution. Although adding a catalyst (1% formic acid) increase the recover amount of gulose to 5.5-6.5 g/L, it also produces rate. However, the addition of acid during hydrolysis produced by-product compounds, such as hydroxymethylfurfural, levulinic acid, and furan aldehyde, which need to be removed before further applications.

Furthermore, subcritical water also had improved transport properties (high diffusion coefficient and thermal conductivity, and low viscosity), which make subcritical more similar to a gas than a liquid for better mass transfer and therefore elevates reaction rates (Kruse & Gawlik, 2003). For example, the synthesis of flavanones are generally prepared by reacting chalcones with catalytic amount of I_2 in DMSO and refluxing for 20-40 min, followed by cold water filtration and washing by sodium thiosulphate for removing excess iodine (Ghodile et al., 2012). By using this conventional method, 62-65% production yield of flavanones is achieved. However, by reacting 2-hydroxyacetophenone and benzaldehyde in subcritical water at 250 °C, 69 bar for 60 min can achieve 64% yield production of flavanones and no side reaction or by-products (Sirin et al., 2013). In addition, Abdelmoez and Yoshida (2007) successfully used subcritical water to crosslink without using any other catalyst. The synthesis of their polymerized bovine serum albumin processes were carried out using subcritical water in a batch reactor at 250 °C for a very short reaction time (1 min).

2.3 Starch modification

Recently, a trend of minimizing the harmful impact of chemicals on the environment as well as seeking effective alternatives to deplete petrochemical resources has generated a high demand for bio-based polymers (Gulrez et al., 2011). Starch is one promising candidate that can be utilized in the synthesis of bio-polymers with a number of benefits. Starch is non-toxic, biodegradable, biocompatible, abundant, relatively inexpensive and friendly for the environment. Native starch is produced in the plant and stored as an energy source to support its growth during germination (Ball & Morell, 2003). Starches from different botanical origins may exhibit distinct shape, size, composition (e.g. high amylose or waxy starch) and other constituents (e.g. lipid) of the starch granules (Halley et al., 2007).

In general, starch serves as a filler, and thickening agent in the food industry. This thesis focuses on the modification of starch for two non-food applications: starch based packaging material (film) and super-absorbent (hydrogel).

2.3.1 Formation of starch based polymer network

Starch is a polysaccharide which consists of two major components (Figure 2.1): linear amylose (poly-α-1, 4-D-glucopyranoside) and branched amylopectin (poly-α-1, 4-D-glucopyranoside and α-1, 6-D-glucopyranoside) (Rodriguez et al., 2006).
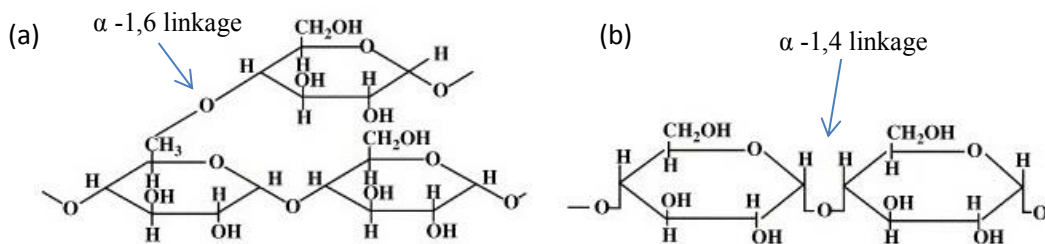
Figure 2.1 Building units of starch: (a) amylopectin and (b) amylose (Adapted from Amanullah & Yu, 2005)

23

The production of starch based films and hydrogels require the transformation of individual starch granules to a polymer network, which are achieved through two major steps, gelatinization and retrogradation. Native starch granules cannot be properly gelatinized without heating in excess of water (Jay-lin, 2003). Therefore, the first step in the production of starch films often involves heating starch in excess water. At the beginning of the gelatinization, with the assistant of heat, water is able to penetrate into the starch granule, which results in the irreversible swelling and breakage of granule structure (Wang et al., 2010a). The temperature at which starch granules lose structure and start swelling in the presence of excess water is known as the gelatinization temperature, which is commonly measured by a differential scanning calorimeter (DSC) (Jay-lin, 2003). As shown in Table 2.3, starches of different botanical sources exhibit different gelatinization temperatures, which are attributed to the different composition (amylose content), size and shape of starch granule (Buléon et al., 1998). The gelatinization temperature varies substantially during heating. For example, the onset gelatinization temperature of normal rice is 70.3 °C then increases to 76.2°C when reaches the peak of gelatinization and is completed at 80.2 °C. During gelatinization, cross-linkages between the starch chains are broken, and amylose leaches out into the aqueous solution. This gradual dissolving process of starch granules allows further hydration until the whole structure of the starch granules are completely disintegrated (Endres et al., 1994; Smits et al., 2003). The granule size of starch can also influence the degree of swelling and consequently influence the uniformity of the gel. Puncha-Arnon et al. (2008) found that larger size granules such as potato (47 μm) and canna (52 μm) starches are more prone to swelling than small granule starches like rice starch (7 μm) during

24

gelatinization, as heating at 100 °C for 20 min, most of the highly swelled potato starch granules were broken into small pieces and formed a homogeneous gel, while rice starch granules were not completely swelled and still in porous granule shape.

With the presence of high concentration of amylose after gelatinization, retrogradation of starch gel can be triggered by lowering the temperature, which promote the association between starch molecules (mainly amylose) and formed ordered double helical structure network (Liu & Han, 2005). The association between linear amylose molecules takes place quickly at the first stage of retrogradation and promote the formation of double helices hydrogen bonding. Amylose molecules also re-associate with the branch chain of amylopectin through the intermolecular hydrogen and form crystalline lamellae composed of double helices of amylopectin short chains (Masakuni & Susumu, 2002). On the other hand, compared with amylose, re-association between amylopectin in gelatinized starch granule is relatively slow due to its high molecular weight and branched structure (Goodfellow & Wilson, 1990; Zobel, 1988). In consequence of retrogradation the intermolecular distances between starch molecules reduce and eliminate water from gel. Therefore, retrogradation also promotes dehydration of the gel and often observed as occurrence of water on gel surface, which is known as synaeresis (Karim et al., 2000; Napierala, 1998). It was also found that starch with smaller size granule like cereal starches are less susceptible to retrogradation than large size starch granules like potato (Narpinder & Lovedeep, 2004; Sobolewska-Zielinska & Fortuna, 2010). In addition, the surface of the dried gel formed from potato starch at 70 or 100 °C was smoother than those formed by canna, mung bean and rice starches

(Puncha-Arnon et al., 2008), which suggest the benefit of using potato starch as raw material for bioplastic application.

Therefore, starches (e.g. tube starch) with large granule size tend to swell and gelatinize more completely compare to small size starch (e.g. cereal starch). In addition, gelatinized gels from large size starch granule can re-associate faster and form the dehydrated materials (e.g. film, hydrogel) in a short time than small size starch granules.

Table 2.3 Physical properties of some common starches from different botanical origin

Starch	Amylose %	Gelatinization temperature(°C)			ΔH (J/g)	Granule size (μm)	Ref
		T_0	T_p	T_c			
Canna	23.9	69.6	72.4	75.8	17.1	10-152	Puncha-Arnon et al. (2008)
Potato	16.8	62.0	65.8	72	17.2	8-131	Puncha-Arnon et al. (2008)
Mung bean	22.9	63.9	70.1	77.5	12.8	6-61	Puncha-Arnon et al. (2008)
Rice	11.4	71.8	75.2	79.5	15.1	2-24	Puncha-Arnon et al. (2008)
Cassava	17	68.2	75.5	11.8	11.8	3-28	Moorthy (2002)
Corn	29.4	64.1	69.4	74.9	12.3	2-16	Jane et al. (1999); Jane et al. (1992); Moorthy (2002)
Wheat	28.8	57.1	61.6	66.2	10.7	3-34	Jane et al. (1999); Moorthy (2002)
Sorghum	29.8	67.1	70.7	75.5	13.8	3-27	Ai et al. (2011); Moorthy (2002)
Barley	25.5	56.3	59.5	62.9	10	2-35	Jane et al. (1999); Sun and Henson (1990)
Tapioca	23.5	64.3	68.3	74.4	14.7	3-28	Herceg et al. (2013); Jane et al. (1999)

Onset temperature (To), peak temperature (Tp), completion temperature (Tc), and enthalpy change (ΔH) of starch gelatinization.

2.3.2 Modification for starch based films

Food packaging is the major application of starch-based biodegradable polymers in the food industry. The requirements for food packaging include covering and retaining the integrity of the food content, keeping food fresh, enhancing organoleptic characteristics of food such as appearance, aroma, and taste, and prevent food from environmental hazards (e.g. microorganism, dust) (Zhao et al., 2008). Traditional food packaging materials, such as low-density polyethylene (LDPE), and polyvinyl chloride (PVC) may impose severe pollution to the environment if not recycle or dispose properly

26

(de Abreu et al., 2012). Starch based film is a possible alternative for food packaging to overcome those environmental concerns due to its biodegradability. However, the high biodegradability of conventional starch-based packaging materials also reduces its durable and stable of packaging materials under high moisture conditions (Wittaya, 2012). Besides, the film made of starch is not completely inert and migration of substances (e.g. moisture, oxygen) into the food might occur (Noun & Nafchi, 2014). To overcome these problems and enhance its performance, new starch-based packaging materials are being developed and investigated through chemically, physically, mechanically and/or combined with polymeric additives as shown in Table 2.4. Most modifications were conducted after starch gelatinization, where the −OH of the starch molecules are exposed, allowing the incorporation of functional additives such as corn starch nanoparticles, or gallic acid.

Depending on the additives used, the functional, mechanical or barrier properties of starch films are altered. As oxidation of lipids and bacterial growth have been the major concerns for food safety and quality, various antioxidant or antimicrobial compounds (e.g. phenolic acid extracts, or essential oils) have been used in films. Pyla et al. (2010) incorporated thermally processed tannic acid (autoclaving fresh tannic acid for 20 mins) into a corn starch film with a final concentration around 0.45 mg tannic acid/ 10 cm diameter disc), allowing 100% release of tannic acid that had a strong antimicrobial activity against *E. coli* O157:H7 and *L. monocytogenes* with inhibition of 5-7 Log/ mL in 24 h. Noun and Nafchi (2014) used Betel leaf extract to modify sago starch film, increasing antimicrobial activity with an increase concentration of extract added. But, the tensile strength of the film significantly decreased from 7 to 3 MPa along with the

increase concentration of betel leaf extract, while the elongation significantly increased from 80 to 120%. Interestingly, they found that with an increase concentration of extract from 20 to 30%, the elongation significantly reduced from 120 to 70%, which indicates that an optimum concentration to balance the antimicrobial properties and mechanical properties are required. Mathew and Abraham (2008) also found the optimum concentration of ferulic acid in starch-chitosan film in terms of mechanical properties. By adding 75 mg ferulic acid/100 g of blend solution (1% w/v starch and 2% w/v chitosan), the film not only exerted an improved antioxidant activity against lipid oxidation of fresh linoleic acid, but also reduced water vapor permeability from 1.41 to 1.15 x 10^{-2}(g mm $KPa^{-1}h^{-1}m^{-2}$) and oxygen permeability from 3.7 to 0.91 (cm^3m m^{-2} day^{-1} kPa^{-1}), mainly due to crosslinking induced by ferulic acid between chitosan and starch through hydrogen bonding found by FTIR.

Without chemical modification, the bonding formed is generally hydrogen bonding or intermolecular interaction between the hydroxyl group of the starch with the functional group of the additive (e.g. amide group of the oxidized ferulic acid), which are weaker than chemical bonds like covalent bond. Polymer network formed by a weak bonding like hydrogen bond is not stable, and therefore can facilitate the release of bioactive components (e.g. tannic acid, ferulic acid, etc.) to the food matrix in contact with the film and exert antimicrobial or antioxidant activity. Unstable network formed by hydrogen bonding also results in poor mechanical properties. The mechanical properties of petroleum based plastics, like low density polyethylene (tensile strength of 10 - 31 MPa and elongation of 600 to 900%), are relatively higher compared to films made of starch (tensile strength of 2-10 MPa and elongation of 55%) (Dai et al., 2015). Therefore,

additives such as nanoparticles of TiO_2 (Khanmirzaei & Ramesh, 2014), natural polymers (e.g. chitosan) or polymers (vinyl alcohol, PVA) were incorporated into starch films to improve the mechanical properties and barrier properties. By adding taro starch nanoparticles into corn starch film, the tensile strength of the film significantly increased by 2 MPa and elongation increased by 30% compared to the control (Dai et al., 2015). However, the compatibility of these additives, especially synthetic ones (e.g. PVA) with starch is relatively low and phase separation between starch and these additives was earlier reported (Lawton, 1996; Lawton & Fanta, 1994). Therefore, more effective methods to increase the compatibility between starch and synthetic polymers and improve the film properties by chemical modification of the synthetic polymers and starch are currently being investigated. Starch chemical modifications include mainly grafting, and crosslinking (Abdel-Halim & Al-Deyab, 2014; González & Villanueva, 2011; Hu et al., 2013; Kim et al., 2002; Kim & Lee, 2002; Moad, 2011), which were discussed below.

In native starch, amylose and amylopectin are cross-linked through hydrogen bonds, which can be easily broken by hot water or acidic water. Therefore, chemical modifications mainly focus on crosslinking the starch molecules by covalent bond (Lopez et al., 2008). There are two main pathways to replace the hydrogen bond between starch molecules and induce polymerization in the starch network: a) adding a crosslinking agent which reacts with the –OH group on the amylose and amylopectin through condensation reaction (e.g. citric acid) (Figure 2.2), and b) replacing the –OH group of the amylose and amylopectin by more reactive functional group (e.g. hydroxyl radical) to form covalent bonding (e.g. grafting, oxidation) (Figures 2.3-2.4). In addition, both

pathways need a catalyst (e.g. sodium hypophosphite) to start the reaction. Otherwise, the bonding formed is still hydrogen bond.

As seen from Figure 2.2, in the presence of an acid catalyst sodium hypophosphite, cellulose and starch with a considerable number of hydroxyl groups can be cross-linked by poly-carboxylic acids like citric acid through intra and inter condensation reaction. Reddy and Yang (2010) reported that the optimum formulation was first mixing 3% (w/w) corn starch dispersion with 15% glycerol, 5% citric acid and sodium hypophosphite (50% w/w, on the weight of citric acid used). Then, the starch solution containing the cross-linking agent and catalyst was heated to 90 °C for 20 min, cooled to 65 °C and air dried at room temperature for 48 h. The cast film was then cured at 165 °C for 5 min to allow the cross-linking reaction to occur. Corn starch film cross-linked under this optimum condition had a tensile strength of 25 MPa, which was 150% higher compared to the control. Besides, they also found that the optimum concentration of citric acid in starch solution was 5%. Low concentrations of citric acid (<5 %) can induce inadequate cross-linking between the starch molecules and resulted in poor tensile strength. However, an excess cross-linking agent (5-14%) can also limit the mobility of the starch molecules, leading to low tensile strength of 8 MPa.
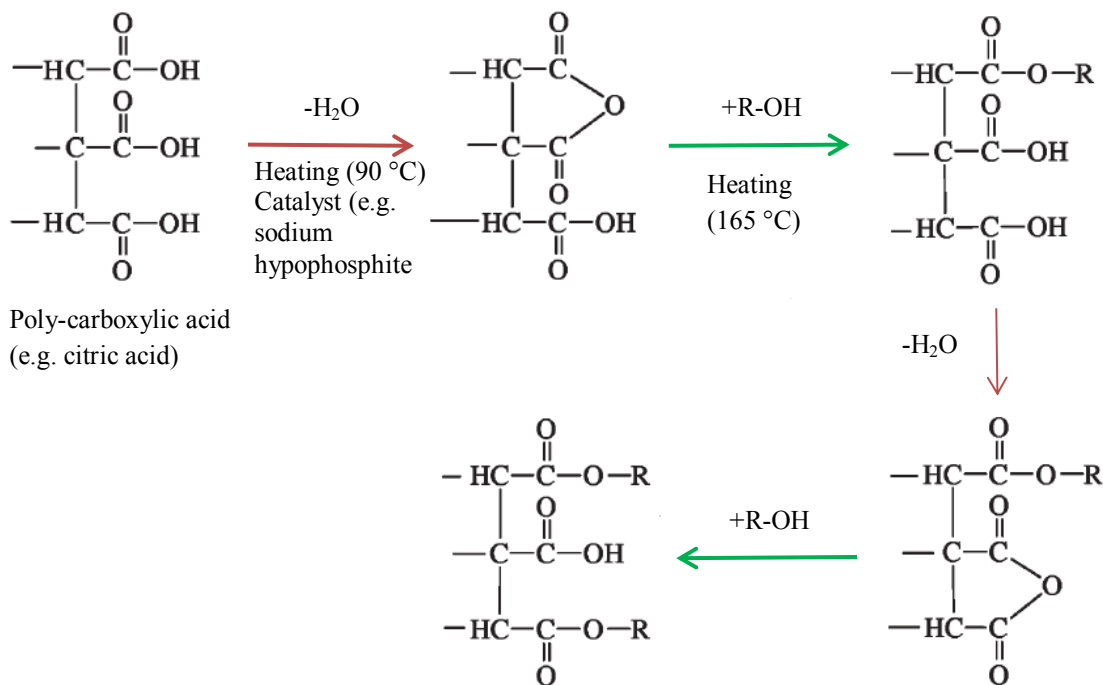
Figure 2.2 Mechanism of cross-linking cellulose or starch using poly-carboxylic acids in the presence of acid catalysts. R represents cellulose or starch (Reddy & Yang, 2010; Yang & Wang, 1996; Yang et al., 1997)

Briefly, for grafting, a polymeric material like starch is subjected to a pretreatment (e.g. oxidation) to induce ionization and subsequently the formation of free radicals. The ionized material become active at the surface and further reacts through polymerization, forming a three-dimensional cross-linked network (Figure 2.3). Grafting involves polymerization of a monomer (e.g. ε-caprolactone) on the backbone of a preformed polymer. The polymer chains are activated by the action of chemical reagents or high energy radiation treatment (e.g. electron beam). The growth of functional monomers on activated macro-radicals lead to branching and further cross-linking. Grafting and polymerization of caprolactone on starch by the use of different catalysts (Lewis acid catalyst, aluminum alkoxide; and triethyl aluminium) achieved a high conversion (>98%) (Ayoub & Rizvi, 2009). However, only using triethyl aluminium obtained a 95% grafting

efficiency compare to 30% for the other two catalysts. The reason for this difference can be due to the formation of starch–aluminium alkoxides by the reaction of triethyl aluminium with starch, which then acted as an initiator for lactone polymerization. This grafting modification allowed the production of starch/polycaprolactone (PCL) film with a tensile strength of 16 MPa and elongation percent of 275% (Narayan et.al., 1999). Another study grafting lactic acid on the starch/PVA significantly increased the tensile strength from 12 to 20 MPa and elongation from 113 to 208%, In addition, the water absorption was significantly reduced from 140 to 70% (Hu et al., 2013).
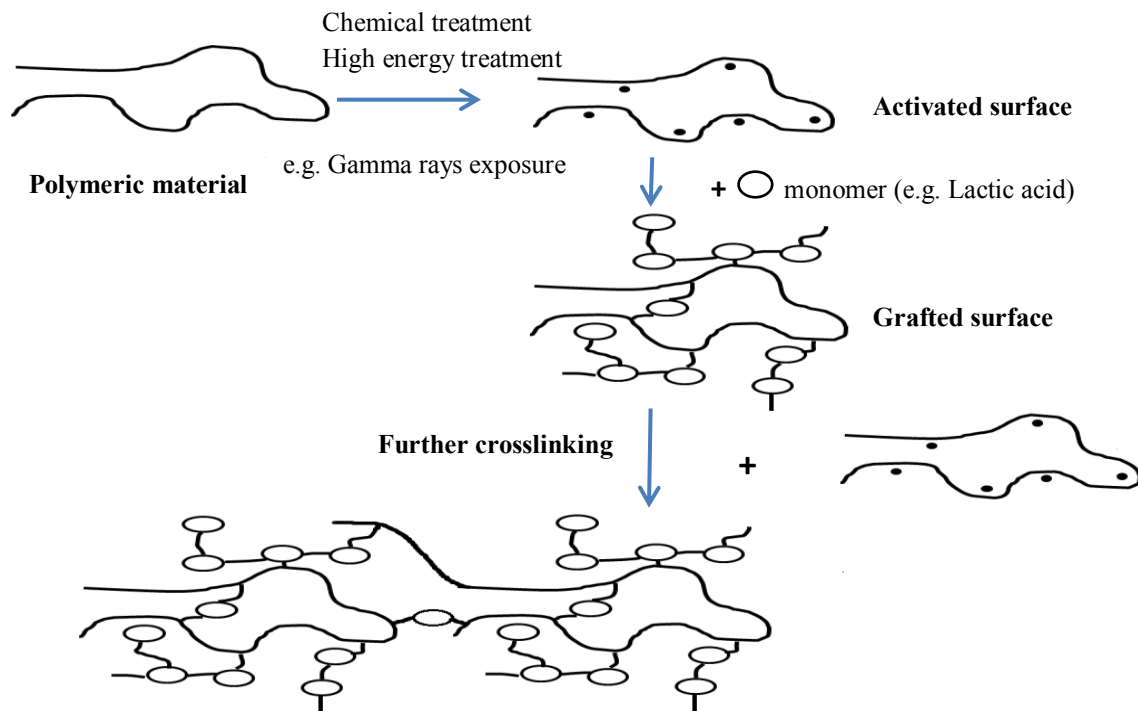
Figure 2.3 Grafting of a monomer on preformed polymeric backbone leading to infinite branching and crosslinking (Adapted from Gulrez & Al-Assaf, 2011).

Table 2.4 Modification of starch based films

Starch	Additives	Film formation	Improvement	Ref
Sago starch 4% (w/w water)	Betel leaf extract (0%, 5%, 10%, 20%, and 30%, w/w mixture)	-Gelatinizing the starch at 90 °C for 45 min -Cooled to 40–45 °C, add extract -Dry in the oven at 40 °C for 20 h -Conditioned at 23 °C, 50 % RH	-Elongation increase from 80% to 110% with 20% extract -Antimicrobial activity increase by 13-18 mm (diameter of inhibition zone) for Gram-positive bacteria and 12-14 mm for Gram-negative bacteria	Noun and Nafchi (2014)
Corn starch 7.5% (w/w water)	Taro starch nanoparticles 0%, 0.5%, 2%, 5%, 10% and 15% (w/w starch)	-Gelatinizing the starch at 100 °C for 30 min -Cooling to 60 °C, add starch nanoparticle -Dry at 45 °C over 8 h, -Conditioned at 23°C, 67% RH	-Water vapor permeability reduced from 2.74 to 1.34 (10^{-7} g Pa^{-1} h^{-1} m^{-1}) with 15 % nanoparticles -Elongation increase from 57% to 87% with 10% nanoparticles	Dai et al. (2015)
Potato starch 1% (w/v water)	Oxidized ferulic acid, chitosan (5, 50, 75 100 and 200 mg/ 100 g of blend solution (40 ml of 2% chitosan solution, 40 ml of 1% starch solution))	-Gelatinizing the starch at 90 °C for 20 min, -Add chitosan, oxidized ferulic acid -Dry at 50 °C for 50 h -Conditioned at 25°C 50% RH	With 75 mg/100g ferulic acid -Tensile strength increase from 45 to 62 MPa -Lipid peroxide value reduced from 28.5 to 11.5 (mg/kg) -Water vapor permeability decrease from 1.41 to 1.15 x10^{-2} g mm kPa^{-1} h^{-1}m^{-2} -Oxygen transmission rates decrease from 3.7 to 0.91cm^{3}mm^{-2}day^{-1} kPa^{-1})	Mathew and Abraham (2008)
Corn starch 3.5% (w/v water)	Corn starch nanoparticle (0.5 % ,w/v starch solution)	-Gelatinizing the starch at 100 ℃ for 1 h -Cooling to 70 ℃, add starch nanoparticles -Dry for over 8 h at 45 ℃ -Conditioned at 25 ℃, 53% RH	-WVP decrease from 2.59 to 1.49 10^{-7} g Pa^{-1} h^{-1} m^{-1})	Shi et al. (2013)
Potato starch 4% (w/w water)	Potassium sorbate (PS) (0.05, 0.075and 0.1 g PS/g starch)	-Gelatinizing the starch with PS at 90 °C for 10 min, -Dry for over 20 h at 50 °C -Conditioned at 25 °C, RH = 50%	With 0.1 g PS/g starch -Antimicrobial effect against *Aspergillus niger* increase from 0 to 532 mm^2(Inhibitory zone) -Elongation increase from 80% to 120%	Hassan et al. (2014)

Table 2.4 Continued. Modification of starch based films

Starch	Additives	Film formation	Improvement	Ref
Corn starch 2% (w/w water)	Sodium caseinate 2% (w/w water) mixing with starch solution in ratios of 1:0, 0.75:0.25, 0.5:0.5 and 0:1	-Gelatinizing the starch with sodium caseinate mixture at 95 °C for 5 min, -Dry for over 48 h at 20 °C with RH = 45%	Without starch -Elongation increase from 2 to 23% -Gloss (60°) increase from 71 to 81.6	Jimenez et al. (2012)
Corn starch 10% (w/w water)	Thermally processed tannic acid (0.45, 1.125, 2.25, 3.375, 4.5 mg per disc)	-Boiled starch mixture for 15 min -Add PTA and dried at room temperature to constant weight	With 4.5 mg tannic acid/ disc -Antimicrobial activity against *E.coli* increased from 0 to 19 mm (diameter of inhibition zone) and 16 mm for *L. monocytogenes*	Pyla et al. (2010)
Tapioca starch 5% (w/w water)	Pullulan 0 to 10% (w/w water)	-Gelatinizing the starch with pullulan mixture at 95 °C for 8 min -Dry at 50 °C -Condition for 2h with RH = 50%	With 10% Pullulan -Elongation increase from 4 to 6% -Improve stability with reduced moisture absorption during storage	Jong-Yea et al. (2014)
Corn starch 4% (w/w water)	ε-poly-ʟ-lysine (0, 2, 4, 6, 8 and 10 g/100 g starch)	-Gelatinizing the starch at 100 °C for 40 min, -Add glycerol and ε-poly-ʟ-lysine -Dry at 50 °C for 4 h	-Tensile strength increase from 15 to 32 MPa and elongation increase from 9 to 21% with 10g ε-poly-ʟ-lysine /100g - Antimicribical activity against *E. coli* incearse from 0 to 107 mm^2 and fro *B. subtilis* increase from 0 to 127 mm^2 with 6g ε-poly-ʟ-lysine /100g (Inhibitory zone area)	Zhang et al. (2015)
Corn starch 5% (w/w water)	Citric acid 0 to 15 % (w/w water)	The starch solution containing the cross-linking agent (citric acid) and catalyst (sodium hypophosphite) was heated to 90 °C for 20 min -Cooled to 65 °C and poured onto Teflon-coated glass plates. -Air dry for about 48 h -Use a hot air oven at 165 °C for the cross-linking reaction to occur. -Dry at 23 °C and 50% RH	With 5% citric acid -Tensile strength increase from 8 to 22 MPa -Weight loss in formic acid for 24 h at 20 °C decrease from 50 to 17 %	Reddy and Yang (2010)

Table 2.4 Continued. Modification of starch based films

Starch	Additives	Film formation	Improvement	Ref
Lactic acid grafted corn starch 6% (w/w water)	poly(vinyl alcohol) (PVA) 5% (w/w water)	-Gelatinization of 1.5g corn starch in NaOH at 75 °C for1 h -with dimethyl sulfoxide and lactic acid at 90 °C under vacuum for 9 h. Cooled down to room temperature, remove lactic acid monomer with actone, and dried at 80 °C. -PVA and Starch-g-PLA mixture heating at 95 °C for 30 min, -Add glutaraldehyde (catalyst for crosslink) for another 25 min at 85 °C. -Neutralize the remanent glutaraldehyde with ammonium chloride -Dry at 65 °C for 5 h	After grafting with lactic acid -Tensile strength increase from 11 to 20 MPa -Elongation increase 113 to 208% -Water absorption decrease from 142 to 70%	Hu et al. (2013)

2.3.2.1 Plasticizer

Films used in the food industry need to have good elasticity and flexibility, a low brittleness, and a high toughness to prevent cracking during handling and storage (Barreto et al., 2003). Therefore, plasticizers of low molecular weight (nonvolatile) are typically added to the film–forming solutions to increase %E values and decrease TS of starch based films. Plasticizers, such as water, glycerol, are usually low molecular weight compounds with high amount of hydroxyl group. Therefore, it can easily penetrate and increase the free volume in the amorphous phase and reduce interaction between the starch polymer chains (Myllarinen et al., 2002). Some commonly used plasticizers are propylene glycol (Jagannath et al., 2006), xylitol (Muscat et al., 2012), glycerol (Cerqueira et al., 2012), polyethylene glycol (Bourtoom et al., 2006), sucrose (Veiga-Santos et al., 2007), and water. Compare to glycerol and sorbitol plasticized starch films, film plasticized with monosaccharaides, like glucose, mannose, fructose, exert better physical properties with regard to tensile strength and elongation, but lower water vapor permeability (Zhang & Han, 2006).

On the other hand, the presence of sugar in the water increases the gelatinization temperature of starch. Since sugar has the ability to compete with water against starch, this results in a low water activity in the system and largely reduction in the plasticization effect of water (Maaurf et al., 2001). Thus, in addition to the type of plasticizer used in film, the concentration of plasticizers in the mixture can be critical to exert and maintain the plasticization effect (Godbillot et al., 2006). Especially for water, which is a natural diluent and could exhibit plasticization and/or anti-plasticization effect on some films depending on the amount absorbed by the film matrix (Pushpadass & Hanna, 2009). Thus, the relative humidity of the surrounding environment may induce changes in the

film moisture content, affecting film properties accordingly (Saiah et al., 2009). The amount of plasticizer added into hydrocolloid film–forming preparations vary between 10 and 60% by weight of the hydrocolloid.

High concentration may lead to phase separation in starch-plasticizer solution, while low concentration may induce anti-plasticization effect (Seow et al., 1999). Once anti-plasticization has occurred, the resulting film starts to increase its rigidity and reduce its flexibility, which make the plasticized film even stiffer than non-plasticized starch film (Chang et al., 2006). One explanation for anti-plasticization effect is that when low concentration of plasticizer is presented with starch solution, plasticizers are starting to bind starch molecule so tight that actually occupy the site initially occupied by water molecule and therefore reduce the mobility of starch fragment in the solution and form a rigid film (Mali et al., 2008). It is found that preparing starch film with 20% (dry weight) combined plasticizer (glycerol and xylitol) provided better water vapor barrier properties, and reasonable elongation, tensile strength, modulus of elasticity than using glycerol or xylitol alone (Muscat et al., 2012).

2.3.2.2 Techniques for production of starch based bioactive films

The production of starch-based films adopts similar process technologies widely used in the processing of traditional petroleum-based plastics, such as extrusion, injection molding, film blowing and solution casting (Liu et al., 2009). This thesis only describes the most common technologies used to produce starch films: solution casting, extrusion and film blowing.

2.3.2.2.1 Solution casting

As a simple technique, casting starch-based films have been widely reported at laboratory scale (Bourtoom & Chinnan, 2008; Dai et al., 2010; Fakhoury et al., 2012;

Koch et al., 2010; Li et al., 2011; Mathew & Abraham, 2008), and typically includes four basic steps: solution preparation, heating, casting and drying. The starch solution is typically prepared by mixing 2-10% of starch directly with cold water and then the film-forming solution is transferred quantitatively to a Brabender viscograph cup, in which the solution is heated from room temperature to 100℃ or higher so that gelatinization occurs (Çalgeris et al., 2012). After maintaining at the same heating temperature for 10 min while being constantly shaken or blended, the gelatinized suspensions are cooled to around 80℃ and approximately 0.8-1.2% plasticizers (e.g. glycerol) is added (Koch et al., 2010). Then, during the casting process, the heated solution is immediately poured onto a teflon or acrylic petri dish, and left to dry in an oven at about 23-35℃ for several days. The thickness of the final cast films can be controlled by the quantity of starch suspension poured onto the plate. The advantage of solution casting is simple and easy to prepare films in the lab for different variety of formulas. However, solution casting cannot produce films on a large scale with a consistent thickness.

2.3.2.2.2 Extrusion

Extrusion is the most widely used technique to process starch-based polymers. Compared to solution casting, extrusion had the ability to handle high-viscosity polymers in the absence of solvents, the broad range of processing conditions (0–500 bar and 70–500 ℃) enable it to meet different operation requirements, and control the residence times during distribution (Duin et al., 2001). A twin-screw extruder with a slit or flat film die is typically chosen to produce starch based sheets or films. Together with the extrusion is a take-off device used for orientation and stretching of the film (Fishman et al., 2006; Galdeano et al., 2009; Thuwall et al., 2006; Zhang et al., 2012). Before the

extrusion, starch, plasticizers (e.g. water, glycerol) and other additives (e.g. fiber, gelatin, etc.) are first mixed well and placed in the hopper or feeder. Then, the mixture is forced through the barrel of the extruder, starch gelatinizes and restructures into a free-flowing material until it emerges from the die. Then, it is cooled below the melting temperature (Su et al., 2009).

Besides the previous extrusion method, a two-stage sheet/film extrusion processing technique is also reported in few studies (Fishman et al., 2006; Galdeano et al., 2009; Leblanc et al., 2008). With this technique, starch blends are first extruded in a single-screw extruder to small pellets. Keeping the pellets at room temperature for few hours promotes stress-relaxation and stabilization (Leblanc et al., 2008). Then, these pellets undergo through a second extrusion in the same single-screw extruder and form flat sheets or films. Although this two-stage extrusion technique may be more time-consuming, it can be used to produce high quality starch sheets or films due to the high-pressure capacity of the single-screw extruder, which is able to overcome the high viscosity (Mościcki et al., 2012).

2.3.2.2.3 Film blowing process

Film blowing technology is quite similar to the extrusion process, except that it has the air blowing component. Typically, blown film extrusion is carried out in vertical direction, however horizontal and downward extrusion processes are now becoming more common (Andreuccetti et al., 2012; Gao et al., 2012; Ramirez-Arreola et al., 2012). Film blowing extrusion procedure consists of four main steps:

Mixing -- Inside the extruder, starch solution goes through the same procedure as regular extrusion, becoming a continuous, viscous liquid. While in blowing extrusion, an annular die is used at the end of the extrusion.

Extrusion and injection--Air is injected through a hole in the center of this die, and the pressure causes the extruded starch liquid to expand into a bubble (Ramírez-Arreola et al., 2012). Equal amount of air should be entering and leaving the bubble to ensure even and constant pressure is maintained. By controlling this, a film with uniform thickness can be obtained (Mościcki et al., 2012).

Pulling and cooling--The bubble is pulled continually upwards from the die and a cooling ring blows air onto the film. Cold air can be also injected from the internal of bubble to exert the cooling effect. This reduces the temperature inside the bubble, while maintaining the bubble diameter (Gao et al., 2012).

Extension--After solidification at the frost line, the film moves into a set of nip rollers, which collapse the bubble and flatten it into two flat film layers. The puller rolls pull the film onto windup rollers. The film passes through idler rolls during this process to ensure that there is uniform tension in the film (Gao et al., 2012).

2.3.3 Starch based hydrogel

Hydrogel is a highly swollen, hydrophilic three dimensional cross-linked network structure, and has the ability to absorb considerable amount of water or aqueous fluids (10 to 1000 times of their original weight) in a relatively short period of time (Chavda et al., 2014; Halim et al., 2014; Omidian et al., 2014; Oyen, 2014). The physical structure of hydrogels can be produced in the form of particle (nonporous or porous) or foam (porous), depending on the synthesis process used (Ahmed, 2013). Porous hydrogels are prepared using techniques, such as freeze drying (Elbert, 2011), microemulsion formation, use of a

foaming aid (glacial acetic acid and sodium bicarbonate) (Kabiri et al., 2003) and phase separation (Chirila et al., 1993). Nonporous hydrogels are simply produced by drying under vacuum and mechanically grinded into powder. However, porous hydrogels have a faster and higher water absorption capacity than non-porous hydrogels and therefore preferred by the modern industry (Nochos et al., 2008; Zhang et al., 2006). For example, the equilibrium water absorbency of porous starch-g-poly (acrylic acid-cosodium acrylate) superabsorbent hydrogels was higher than the non-porous one by 200 g water/ g hydrogel (Zhang et al., 2006).

2.3.3.1 Synthesis of starch based hydrogels

Depending on the type of crosslinking, hydrogels can be divided into two groups: physical hydrogels and chemical hydrogels. In physical hydrogel, the gel networks were cross-linked through polymer complexation or secondary forces, like ionic, hydrogen bonding or hydrophobic interaction (Figure 2.4).

Physically cross-linked hydrogels are formed after cooling hot solutions of polysaccharides (e.g. starch, carrageenan, etc.). The gel formation is due to helix-formation, association of the helices, and forming junction zones (Funami et al., 2007). For example, heating starch in excess water induces gelatinization of starch granule and promotes the crosslinking between polymer chains or polymer to water through hydrogen bonds. In addition, amylose also formed double helices rod and re-associated with each other to form aggregates (Figure 2.4b).

Ionic polymers can be cross-linked by the addition of di- or trivalent counter ions (e.g. Ca^{2+}, $2Cl^-$) into a gelling polyelectrolyte solution (e.g. Na^+ alginate$^-$) of opposite charges (Figure 2.4a). For example, Due to the presence of free amino groups, chitosan is a cationic polyelectrolyte, which can be dissolved in aqueous acidic solutions in the

41

ionized state. Chitosan-glycerolphosphate hydrogel films were formed based on the ionic interaction between negatively charged and positively charged chitosan. Hydrogel films formed from this interaction exerted a better elasticity, lower tensile strength, and higher hydrophilicity compared to the control of chitosan alone (Zhao et al., 2009).

Similar to the ionic interaction between small ion and ionic polymers, complex coacervate gels can be formed by mixing a polyanionic polymer with a polycation polymer. The polymers with opposite charges stick together and form soluble and insoluble complexes depending on the concentration and pH of the respective solutions (Figure 2.4c). One example is coacervating polyanionic xanthan with polycationic chitosan (Magnin et al., 2004). In addition, proteins below its isoelectric point are positively charged and likely to associate with anionic hydrocolloids and form polyion complex hydrogel of a complex coacervate (Magnin et al., 2004).

Hydrogen bonds can be formed between polar groups (H, C, N, O, and F) with other polar groups on the same or different polymer chains. Polysaccharides have –OH group on their backbone, which allow them to form a hydrogen bonding network. However, the dissolution of the gel in water also depends on the hydrogen bonding of the polymer with water. Therefore, the hydrogen bond formed in hydrogels between polymer chains need to be stronger than the hydrogen bonding formed with water. Therefore, before physically linked through hydrogen bonding, native polysaccharides were usually chemically modified (e.g. replacing the –OH with –COOH). Like carboxymethyl cellulose crosslinked hydrogel, which use 1,3-diaminopropane as a crosslink agent and a small amount of triethylamine as a catalyst. They found that if carboxyl groups of cellulose are fully protonated (COOH), hydrogen bonds were formed as shown in Figure

2.4d, reducing the water uptake of the gels. However, when they were ionized (COO⁻), they produced electrostatic repulsion which opened the network and increased water uptake of the hydrogel. Zhao et al. (2011) also found that the formation of hydrogen bond is pH dependent and by lowering the pH of aqueous solution of polymers carrying carboxyl groups (carboxymethyl cellulose), a hydrogel can be formed through hydrogen bonding.

Hydrogels can also be physically linked through hydrophobic interactions, which is referred to the aggregation of hydrophobic groups (e.g. methyl groups into methyl cellulose, or protein) to minimize their interactions to water molecules (Figure 2.4e). Gum Arabic is a polysaccharide with three proteins with different molecular weight, which accounts for 2-3% of its structure (Islam et al., 1997) Aggregation of the protein components can be induced by heat treatment when low molecular weight protein is associated with each other that result in high concentrations of high molecular weight fraction. This aggregation of hydrophobic components of protein subsequently produces a hydrogel with enhanced mechanical properties and water binding capability (Aoki et al., 2007).

Physically cross-linked hydrogels can also be achieved by intramolecular entanglements using freeze-thaw cycles. The mechanism involves the formation of microcrystals as physical crosslinkers in the structure during freeze-thawing process. Examples of this type of gelation were freeze-thawed gels of complex hydrogels of poly(vinyl alcohol) (PVA) and sodium carboxymethylcellulose (CMC) formed in 0.1M HCl (Xiao & Gao, 2008) as shown in Figure 2.4f. PVA microcrystals domains served as

a crosslinking agent, allowing intramolecular entanglements between CMC and PVA to form the gel network.
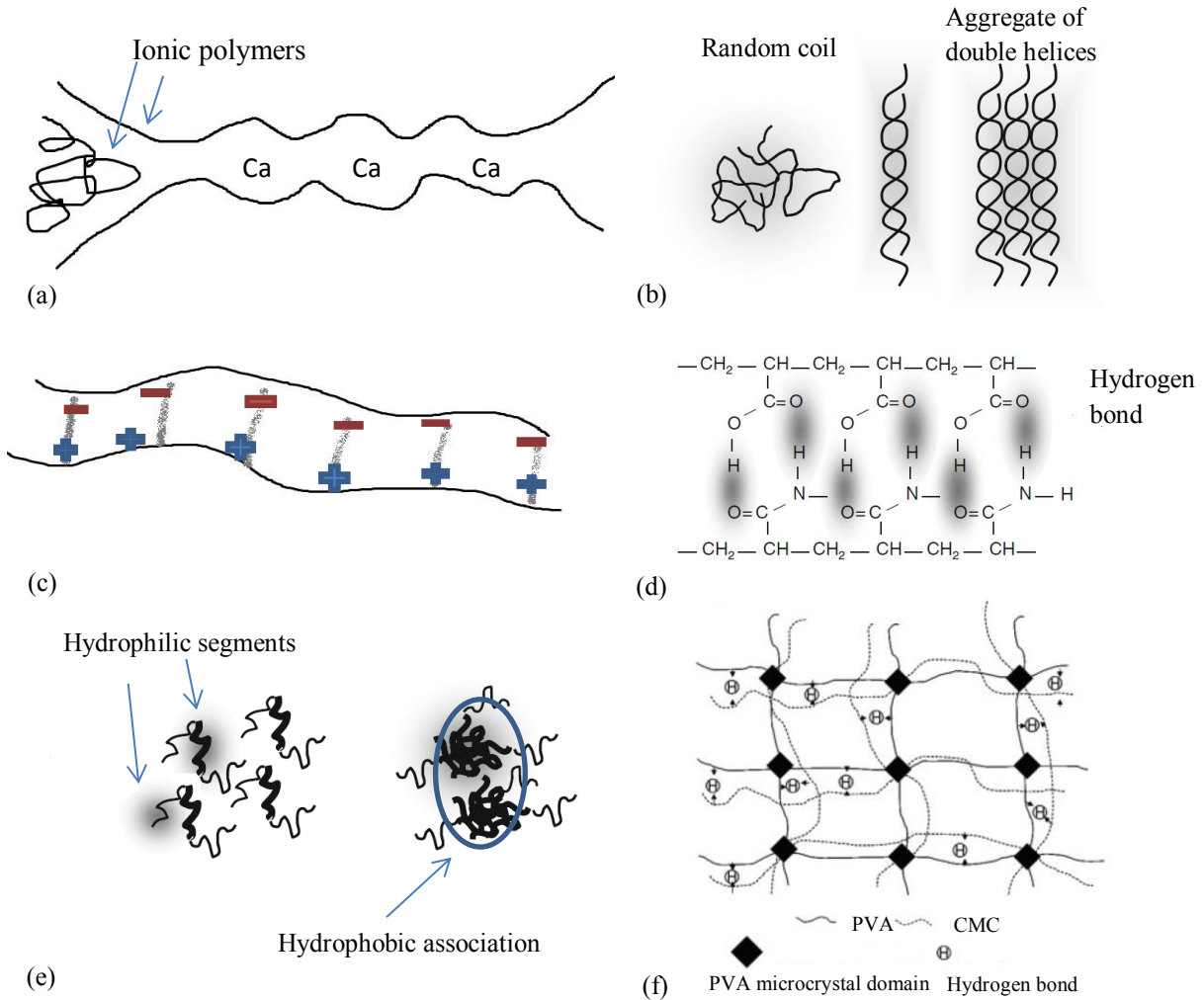
Figure 2.4 Examples of hydrogels physically cross-linked by ion–polymer complexation (a), chain aggregation (b), polymer–polymer complexation (c), hydrogen bonding (d), hydrophobic association (e), and microcrystal interaction (f). Adapted from Omidian & Park (2012), and Xiao & Gao (2008).

Physically cross-linked networks can be interrupted by changes in environmental conditions, such as application of stress (Rosiak & Yoshii, 1999). Due to the limited interaction between –OH groups on the starch, starch based hydrogels are mainly formed through chemical modification, which are covalently cross-linked networks that can be synthesized through two major pathways: A) graft copolymerization of vinyl monomers

on polysaccharide in the presence of a cross-linker; and B) direct crosslinking between polysaccharide. The mechanism for these two pathways are the same as discussed in the chemical modification of starch film in previous Section 2.2.2 (Figure 2.2.), which all involved the generation of free radicals from an initiator or crosslinker or both.

Briefly, in graft copolymerization, generally a polysaccharide reacts with an initiator by either of two separate ways. First, the –OH groups on starch were attacked by a free radical initiator, such as ceric ammonium nitrate, and then formed redox pair-based complexes(Alonso Dena-Aguilar et al., 2011; Parvathy & Jyothi, 2012). These complexes subsequently dissociated and started to homogeneously cleavage the C-C bond on the starch backbone, which resulted in the production of carbon radicals on the polysaccharide substrate. These carbon radicals initiate the graft polymerization of the vinyl monomers (e.g. acrylic acid) and cross-linker (e.g. glutaraldehyde) on the substrate. Another way of initiation required a thermal initiator to be activated by heat, such as ammonium persulfate to abstract hydrogen radicals from the -OHs of starch to produce the initiating radicals on the polysaccharide backbone (Fares et al., 2010).

Instead of crosslinking polymer chains through the use of several crosslinking agent units, starch hydrogels can also be direct cross-linking of polysaccharides through polyvinylic compounds (e.g., divinyl sulphone) or polyfunctional compounds (e.g., glycerol, epichlorohydrine and glyoxal). For example, cellulose-based superabsorbent hydrogel can be prepared via direct cross-linking of sodium carboxymethyl cellulose or hydroxyethyl cellulose by $POCl_3$ or citric acid (Demitri et al., 2008; Sannino et al., 2003).

Grafting and crosslinking can also be initiated by the use of high-energy radiation, which mainly relies on producing free radicals in the polymer following the exposure to

the high energy source, such as gamma ray, x-ray or electron beam. Radiation cross-linking is a widely used technique since it avoids the use of chemical additives and therefore retaining the biocompatibility of the biopolymer. Also, modification and sterilization can be achieved in a single step and hence it is a cost effective process to modify biopolymers having their end-use specifically in biomedical applications.

2.3.4 Applications of starch based biodegradable polymers

2.3.4.1 In food packaging

When a starch film is used as a packaging material or directly applied on the food, consumers expect the film to fulfill its duty on protecting the food inside, extending the shelf-life. The chemical composition of the food surface is dynamic and can be altered during storage by food metabolism, microbial respiration, gas solubility and permeability of the film. The composition and concentration of gas within the package can be affected by microbial activity, which could be the result of high water vapor permeability of the film (Hager et al., 2012). Therefore, in terms of chemical composition and structure of the film, the characteristics of the product, and the storage conditions, modified starch film can provide barrier properties against gas, water vapor and aroma (Fontes et al., 2011). A soy starch and gelatin based bioactive film was recently produced with addition of extracts containing mainly essential oils, such as α-pinene and limonene (Khalil et al., 2013). They tested this active film on 11 different food matrices and found that this film significantly extended the shelf-life by 9 to 200% of solid and semi-solid food, such as salami, artificial cheese, and the refrigerated pizza dough, compared to the control.

2.3.4.2 In agriculture

Besides the use in the food industry, starch-based biodegradable film can be used in agriculture, such as mulch film, covering greenhouses and fertilizers controlled release

films (Dilara & Briassoulis, 2000). Generally, the disposal methods of traditional plastic films are landfill, recycling or incineration, which are all time-consuming, not economic and may lead to environmental pollution (Khoramnejadian et al., 2011). On the other hand, the efficiency of fertilizers is fundamental for the growth of agricultural products. However, problems like surface runoff, leaching and vaporization hinder the utility of fertilizers and promote its loss to the surrounding environment, which leads to environmental problems (Dave et al., 1999; Guo et al., 2005). The generation of starch-based biodegradable polymers provides a possible solution to overcome the mentioned problems. These films control the release of fertilizers in a more efficient way, which in turn reduces the loss of fertilizers and environment pollution (Chen et al., 2008). Starch-based films can also be directly ploughed into soil and naturally degraded without leaving any toxic residue (Malinconico et al., 2002). Li et al. (2014) buried two commercially available starch based films (BioAgri Ag-Film and BioTelo Agri) in an open field tomato production system in three different locations in the USA for 24 months and they found that both films achieved 80-90% degradation in 12 months and 100% in 24 months. But, they also found the high pH and temperature of soil can influence the degradation rate of these starch films, as alkaline soil and high soil temperature tend to degrade the film.

2.3.4.3 In the medical field

Hydrogel formed from poly(acrylamide)/poly(acrylic acid) through hydrogen bonding swells when increasing temperature and de-swells after lowering the temperature (Ilmain et al., 1991). Therefore, physically cross-linked hydrogel were considered as a control released media for delivering molecules after a specific stimulation (e.g. pH). For example, a glucose sensitive hydrogel membrane was developed to allow controlled release of insulin. The porosity of hydrogel changes

depending on the concentration of glucose present, which allows control the diffusion rate of protein (e.g. insulin) through the hydrogel (Tang et al., 2004; Tang et al., 2003). Besides, hydrogel can also be used for wound healing. For example, Pal et al. (2006) developed a novel membrane of hydrogels prepared by crosslinking of polyvinyl alcohol with heat-treated corn-starch suspension, which cannot only protect injured skin but also keep it appropriately moist to speed the healing process.

Modified starch film can also act as a carrier for drug release. Çalgeris et al. (2012) found that by blending 2% (w/w) lignin with corn starch film, the mechanical as well as water absorption properties of the films were significantly improved. In addition, this film can also control the release of the load drug ciprofloxacin in response to the pH of the medium. Only 75% of ciprofloxacin was released in a medium with pH of 7.5, while almost 100% was released in a medium of pH 1.0.

2.3.4.4 Use as a superabsorbent polymer (SAP)

Based on the report of "Super Absorbent Polymers Market" by MarketsandMarkets, (2014), SAP in baby diapers shared more than 75% of the global super absorbent polymer market in 2013. SAP in baby diapers market will grow at a rate of 5.2% till 2019 and reach a value of $8.6 billion. Due to the hydrophilic nature of starch, modified starch hydrogel can exert significantly higher water absorbency up to 20000%, which is 10 to 100 times more compared to normal absorbent, such as tissue paper (400%), soft polyurethane sponge (1050%), wood pulp fluff (1200%) and cotton ball (1890%) (Zohuriaan-Mehr & Kabiri, 2008). Therefore, Starch based hydrogels are used as superabsorbent in many hygiene products, such as baby diaper, sanitary napkin, female tampon, and child training pants. Kuang et al. (2011) produced starch-based superabsorbent hydrogel by radical polymerization of starch sulfate containing vinyl

48

groups in the presence or absence of acrylic acid as a comonomer and porous structure was produced through a gas blowing process. The best superabsorbent produced in their study was able to absorb 200 times weight of water compared to its own dried weight in 50 s. In addition to this fast swelling capacity, this starch based hydrogel can also be 100% degraded by microorganisms and hydrolytic enzymes in 150 h.

Starch-based superabsorbent can also be effectively used to remove heavy metals, dyes, hazards (toxic acid, or organic solvent) from wastewater. Water contamination with heavy metals, including arsenic (As), mercury (Hg), lead (Pb), copper (Cu), nickel (Ni), Zinc (Zn), magnesium (Mg), cadmium (Cd) and selenium (Se), has become health threat worldwide (Ekebafe et al., 2012). Chemical modification of starch using vinyl or other grafts has been a successful and affordable approach in the production of starch-based hydrogels for the adsorption of heavy metals (Abdel-Halim & Al-Deyab, 2014; Guclu et al., 2010; Sadeghi et al., 2014). Ekebafe et al. (2012) formed a starch based hydrogel from grafting and polymerizing cassava starch with acrylonitrile. This hydrogel chelated metal ions by forming a chelating complex and retain heavy metals (72 mg Pb/g, 76.6 mg Cu/g and 86.5 mg Ni/g of hydrogel) within its hydrogel network structure in 30 min. In addition, 99.6% of heavy metal absorbed by this hydrogel can be released by acid stripping with 2% HCl, allowing this product to be reused.

2.4 References

Abdel-Halim, E.S., Al-Deyab, S.S. 2014. Preparation of poly(acrylic acid)/starch hydrogel and its application for cadmium ion removal from aqueous solutions. *Reactive & Functional Polymers*, **75**, 1-8.

Abdelmoez, W., Yoshida, H. 2007. Mechanical and thermal properties of a novel protein-based plastic synthesized using subcritical water technology. *Macromolecules*, **40**(26), 9371-9377.

Ahmed, E.M. 2013. Hydrogel: Preparation, characterization, and applications. *Journal of Advanced Research*, http://dx.doi.org/10.1016/j.jare.2013.07.006, In press.

Ai, Y.F., Medic, J., Jiang, H.X., Wang, D.H., Jane, J.L. 2011. Starch characterization and ethanol production of sorghum. *Journal of Agricultural and Food Chemistry*, **59**(13), 7385-7392.

Akalin, M.K., Karagoz, S., Akyuz, M. 2013. Supercritical ethanol extraction of bio-oils from German beech wood: Design of experiments. *Industrial Crops and Products*, **49**, 720-729.

Alevizou, E.I., Voutsas, E.C. 2013. Solubilities of p-coumaric and caffeic acid in ionic liquids and organic solvents. *Journal of Chemical Thermodynamics*, **62**, 69-78.

Alonso Dena-Aguilar, J., Jauregui-Rincon, J., Bonilla-Petriciolet, A., Ernestina Medina-Ramirez, I., Romero-Garcia, J. 2011. Graft copolymerization of poly(acrylonitrile) and vinyl acetate on starch via free radical in solution: Synthesis and characterization. *Afinidad*, **68**(553), 195-202.

Alvarez, V.H., Cahyadi, J., Xu, D.Y., Saldaña, M.D.A. 2014. Optimization of phytochemicals production from potato peel using subcritical water: Experimental and dynamic modeling. *Journal of Supercritical Fluids*, **90**, 8-17.

Amanullah, M., Yu, L. 2005. Environment friendly fluid loss additives to protect the marine environment from the detrimental effect of mud additives. *Journal of Petroleum Science and Engineering*, **48**(3-4), 199-208.

Andreasen, M.F., Christensen, L.P., Meyer, A.S., Hansen, A. 2000. Content of phenolic acids and ferulic acid dehydrodimers in 17 rye (*Secale cereale* L.) varieties. *Journal of Agricultural and Food Chemistry*, **48**(7), 2837-2842.

Andreuccetti, C., Carvalho, R.A., Galicia-Garcia, T., Martinez-Bustos, F., Gonzalez-Nunez, R., Grosso, C.R.F. 2012. Functional properties of gelatin-based films containing Yucca schidigera extract produced via casting, extrusion and blown extrusion processes: A preliminary study. *Journal of Food Engineering*, **113**(1), 33-40.

Aoki, H., Katayama, T., Ogasawara, T., Sasaki, Y., Al-Assaf, S., Philllps, G.O. 2007. Characterization and properties of *Acacia senegal* (L.) willd. var. Senegal with enhanced properties (Acacia (sen) SUPER GUM (TM)): Part 5. Factors affecting the emulsification of Acacia senegal and Acacia (sen) SUPER GUM (TM). *Food Hydrocolloids*, **21**(3), 353-358.

Ayoub, A.S., Rizvi, S.S.H. 2009. An overview on the technology of cross-linking of starch for nonfood applications. *Journal of Plastic Film & Sheeting*, **25**(1), 25-45.

Azmir, J., Zaidul, I.S.M., Rahman, M.M., Sharif, K.M., Mohamed, A., Sahena, F., Jahurul, M.H.A., Ghafoor, K., Norulaini, N.A.N., Omar, A.K.M. 2013. Techniques for extraction of bioactive compounds from plant materials: A review. *Journal of Food Engineering*, **117**(4), 426-436.

Baiano, A., Bevilacqua, L., Terracone, C., Conto, F., Nobile, M.A.d. 2014. Single and interactive effects of process variables on microwave-assisted and conventional extractions of antioxidants from vegetable solid wastes. *Journal of Food Engineering*, **120**, 135-145.

Ball, S.G., Morell, M.K. 2003. From bacterial glycogen to starch: Understanding the biogenesis of the plant starch granule. *Annu Rev Plant Biol*, **54**, 207-33.

Barreto, P.L.M., Roeder, J., Crespo, J.S., Maciel, G.R., Terenzi, H., Pires, A.T.N., Soldi, V. 2003. Effect of concentration, temperature and plasticizer content on rheological properties of sodium caseinate and sodium caseinate/sorbitol solutions and glass transition of their films. *Food Chemistry*, **82**(3), 425-431.

Barros, F., Dykes, L., Awika, J.M., Rooney, L.W. 2013. Accelerated solvent extraction of phenolic compounds from sorghum brans. *Journal of Cereal Science*, **58**(2), 305-312.

Bhatnagar, A., Kaczala, F., Hogland, W., Marques, M., Paraskeva, C.A., Papadakis, V.G., Sillanpaa, M. 2014. Valorization of solid waste products from olive oil industry as potential adsorbents for water pollution control-a review. *Environmental Science and Pollution Research*, **21**(1), 268-298.

Block, G., Langseth, L. 1994. Antioxidant vitamins and disease prevention. *Food Technology*, **48**(7), 80-84.

Bourtoom, Chinnan, M.S., Jantawat, P., Sanguandeekul, R. 2006. Effect of plasticizer type and concentration on the properties of edible film from water-soluble fish proteins in surimi wash-water. *Food Science and Technology International*, **12**(2), 119-126.

Bourtoom, T., Chinnan, M.S. 2008. Preparation and properties of rice starch–chitosan blend biodegradable film. *LWT - Food Science and Technology*, **41**(9), 1633-1641.

Buléon, A., Colonna, P., Planchot, V., Ball, S. 1998. Starch granules: Structure and biosynthesis. *International Journal of Biological Macromolecules*, **23**(2), 85-112.

Çalgeris, İ., Çakmakçı, E., Ogan, A., Kahraman, M.V., Kayaman-Apohan, N. 2012. Preparation and drug release properties of lignin-starch biodegradable films. *Starch - Stärke*, **64**(5), 399-407.

Cerqueira, M.A., Souza, B.W.S., Teixeira, J.A., Vicente, A.A. 2012. Effect of glycerol and corn oil on physicochemical properties of polysaccharide films - A comparative study. *Food Hydrocolloids*, **27**(1), 175-184.

Chafer, A., Fornari, T., Stateva, R.P., Berna, A., Garcia-Reverter, J. 2007. Solubility of the natural antioxidant gallic acid in supercritical CO_2+ethanol as a cosolvent. *Journal of Chemical and Engineering Data*, **52**(1), 116-121.

Chang, Y.P., Karim, A.A., Seow, C.C. 2006. Interactive plasticizing-antiplasticizing effects of water and glycerol on the tensile properties of tapioca starch films. *Food Hydrocolloids*, **20**(1), 1-8.

Chavda, H., Chavada, G., Patel, J., Rangpadiya, K., Patel, C. 2014. Topical vaginal drug delivery system based on superporous hydrogel hybrids. *Protein and Peptide Letters*, **21**(11), 1176-1184.

Chen, L., Xie, Z., Zhuang, X., Chen, X., Jing, X. 2008. Controlled release of urea encapsulated by starch-g-poly(l-lactide). *Carbohydrate Polymers*, **72**(2), 342-348.

Chen, Y.-P., Chen, Y.-M., Tang, M. 2009. Solubilities of cinnamic acid, phenoxyacetic acid and 4-methoxyphenylacetic acid in supercritical carbon dioxide. *Fluid Phase Equilibria*, **275**(1), 33-38.

Chirila, T.V., Constable, I.J., Crawford, G.J., Vijayasekaran, S., Thompson, D.E., Chen, Y.-C., Fletcher, W.A., Griffin, B.J. 1993. Poly(2-hydroxyethyl methacrylate) sponges as implant materials: in vivo and in vitro evaluation of cellular invasion. *Biomaterials*, **14**(1), 26-38.

Choi, J.-S., Cheon, E.J., Kim, T.-U., Moon, W.-S., Kim, J.-W., Kim, M.-R. 2014. Genotoxicity of rice bran oil extracted by supercritical CO_2 extraction. *Biological & Pharmaceutical Bulletin*, **37**(12), 1963-1970.

Dai, H., Chang, P.R., Geng, F., Yu, J., Ma, X. 2010. Preparation and properties of starch-based film using N,N-bis(2-hydroxyethyl)formamide as a new plasticizer. *Carbohydrate Polymers*, **79**(2), 306-311.

Dai, L., Qiu, C., Xiong, L., Sun, Q. 2015. Characterisation of corn starch-based films reinforced with taro starch nanoparticles. *Food Chemistry*, **174**, 82-88.

Daneshfar, A., Ghaziaskar, H.S., Homayoun, N. 2008. Solubility of gallic acid in methanol, ethanol, water, and ethyl acetate. *Journal of Chemical and Engineering Data*, **53**(3), 776-778.

Dave, A.M., Mehta, M.H., Aminabhavi, T.M., Kulkarni, A.R., Soppimath, K.S. 1999. A review on controlled release of nitrogen fertilizers through polymeric membrane devices. *Polymer-Plastics Technology and Engineering*, **38**(4), 675-711.

Davies, L.C., Vilhena, A., Novais, J.M., Martins-Dias, S. 2003. Modelling of olive mill wastewater characteristics. in: *Water Pollution Vii: Modelling, Measuring and Prediction*, (Eds.) C.A. Brebbia, D. Almorza, D. Sales, Vol. 9, pp. 313-322.

de Abreu, D.A.P., Cruz, J.M., Losada, P.P. 2012. Active and intelligent packaging for the food Industry. *Food Reviews International*, **28**(2), 146-187.

de Aguiar, A.C., dos Santos, P., Coutinho, J.P., Barbero, G.F., Godoy, H.T., Martinez, J. 2014. Supercritical fluid extraction and low pressure extraction of Biquinho pepper (*Capsicum chinense*). *LWT-Food Science and Technology*, **59**(2), 1239-1246.

Demitri, C., Del Sole, R., Scalera, F., Sannino, A., Vasapollo, G., Maffezzoli, A., Ambrosio, L., Nicolais, L. 2008. Novel superabsorbent cellulose-based hydrogels crosslinked with citric acid. *Journal of Applied Polymer Science*, **110**(4), 2453-2460.

Dilara, P.A., Briassoulis, D. 2000. Degradation and stabilization of low-density polyethylene films used as greenhouse covering materials. *Journal of Agricultural Engineering Research*, **76**(4), 309-321.

Duin, M.v., Machado, V., Cocas, J. 2001. A look inside extruder evolution of chemistry, morphology and rheology along the extruder axis during reactive processing and blending. *Macromolecular Symposia*, **170**(1), 29-39.

Ekebafe, L.O., Ogbeifun, D.E., Okieimen, F.E. 2012. Removal of heavy metals from aqueous media using native cassava starch hydrogel. *African Journal of Environmental Science and Technology*, **6**(7), 275-282.

El Abbassi, A., Khalid, N., Zbakh, H., Ahmad, A. 2014. Physicochemical characteristics, nutritional properties, and health benefits of argan oil: A Review. *Critical Reviews in Food Science and Nutrition*, **54**(11), 1401-1414.

Elbert, D.L. 2011. Liquid–liquid two-phase systems for the production of porous hydrogels and hydrogel microspheres for biomedical applications: A tutorial review. *Acta Biomaterialia*, **7**(1), 31-56.

Endres, H.J., Krammerstetter, H., Hobelsberger, M. 1994. Plasticization behavior of different native starches. *Starch-Starke*, **46**(12), 474-480.

Fakhoury, F.M., Maria Martelli, S., Canhadas Bertan, L., Yamashita, F., Innocentini Mei, L.H., Collares Queiroz, F.P. 2012. Edible films made from blends of manioc starch and gelatin – Influence of different types of plasticizer and different levels of macromolecules on their properties. *LWT - Food Science and Technology*, **49**(1), 149-154.

Fares, M.M., El-Faqeeh, A.S., Ghanem, H., Osman, M.E., Hassan, E.A. 2010. Hydrogels of starch-g-(tert-butylacrylate) and starch-g-(n-butylacrylate) copolymers synthesis and formation. *Journal of Thermal Analysis and Calorimetry*, **99**(2), 659-666.

Fishman, M.L., Coffin, D.R., Onwulata, C.I., Willett, J.L. 2006. Two stage extrusion of plasticized pectin/poly(vinyl alcohol) blends. *Carbohydrate Polymers*, **65**(4), 421-429.

Fontes, L.C.B., Ramos, K.K., Sivi, T.C., Queiroz, F.P.C. 2011. Biodegradable edible films from renewable sources-potential for their application in fried foods. *American Journal of Food Technology*, **6**(7), 555-567.

Fu, L., Xu, B.T., Xu, X.R., Gan, R.Y., Zhang, Y., Xia, E.Q., Li, H.B. 2011. Antioxidant capacities and total phenolic contents of 62 fruits. *Food Chemistry*, **129**(2), 345-350.

Funami, T., Hiroe, M., Noda, S., Asai, I., Ikeda, S., Nishinari, K. 2007. Influence of molecular structure imaged with atomic force microscopy on the rheological behavior of carrageenan aqueous systems in the presence or absence of cations. *Food Hydrocolloids*, **21**(4), 617-629.

Galdeano, M.C., Grossmann, M.V.E., Mali, S., Bello-Perez, L.A., Garcia, M.A., Zamudio-Flores, P.B. 2009. Effects of production process and plasticizers on stability of films and sheets of oat starch. *Materials Science and Engineering: C*, **29**(2), 492-498.

Gao, W., Dong, H., Hou, H., Zhang, H. 2012. Effects of clays with various hydrophilicities on properties of starch-clay nanocomposites by film blowing. *Carbohydrate Polymers*, **88**(1), 321-328.

Gaspar, A., Garrido, E.M., Esteves, M., Quezada, E., Milhazes, N., Garrido, J., Borges, F. 2009. New insights into the antioxidant activity of hydroxycinnamic acids: Synthesis and physicochemical characterization of novel halogenated derivatives. *European Journal of Medicinal Chemistry*, **44**(5), 2092-2099.

Ghodile, N.G., Rajput, P.R., Banewar, V.W., Raut, A.R. 2012. Synthesis and antimicrobial activity of some chalcones and flavones having 2-hydroxy acetophenone moiety. *International Journal of Pharma and Bio Sciences*, **3**(3), P-389-P-395.

Giada, M.d.L.R. 2013. Food phenolic compounds: Main classes, sources and their antioxidant power. in: *Oxidative Stress and Chronic Degenerative Diseases - A Role for Antioxidants*, (Eds.) J.A. Morales-Gonzalez, InTech Croatia, pp. 87-112.

Godbillot, L., Dole, P., Joly, C., Roge, B., Mathlouthi, M. 2006. Analysis of water binding in starch plasticized films. *Food Chemistry*, **96**(3), 380-386.

Godos, J., Pluchinotta, F.R., Marventano, S., Buscemi, S., Li Volti, G., Galvano, F., Grosso, G. 2014. Coffee components and cardiovascular risk: Beneficial and detrimental effects. *International Journal of Food Sciences and Nutrition*, **65**(8), 925-936.

González, R.M., Villanueva, M.P. 2011. 19 - Starch-based polymers for food packaging. in: *Multifunctional and Nanoreinforced Polymers for Food Packaging*, (Ed.) J.-M. Lagarón, Woodhead Publishing, pp. 527-570.

Goodfellow, B.J., Wilson, R.H. 1990. A fourier-transform IR study of the gelation of amylose and amylopectin. *Biopolymers*, **30**(13-14), 1183-1189.

Gracin, S., Rasmuson, A.C. 2002. Solubility of phenylacetic acid, p-hydroxyphenylacetic acid, p-aminophenylacetic acid, p-hydroxybenzoic acid, and ibuprofen in pure solvents. *Journal of Chemical and Engineering Data*, **47**(6), 1379-1383.

Guclu, G., Al, E., Emik, S., Iyim, T.B., Ozgumus, S., Ozyurek, M. 2010. Removal of Cu^{2+} and Pb^{2+} ions from aqueous solutions by starch-graft-acrylic acid/montmorillonite superabsorbent nanocomposite hydrogels. *Polymer Bulletin*, **65**(4), 333-346.

Gulrez, S.K.H., Al-Assaf, S., Glyn, O.P. 2011. Hydrogels: Methods of preparation, characterisation and applications. in: *Progress in Molecular and Environmental Bioengineering – From Analysis and Modeling to Technology Applications*, (Eds.) A. Carpi, InTech Croatia, pp 118-150.

Guo, M.Y., Liu, M.Z., Zhan, F.L., Wu, L. 2005. Preparation and properties of a slow-release membrane-encapsulated urea fertilizer with superabsorbent and moisture preservation. *Industrial & Engineering Chemistry Research*, **44**(12), 4206-4211.

Hager, A.S., Vallons, K.J., Arendt, E.K. 2012. Influence of gallic acid and tannic acid on the mechanical and barrier properties of wheat gluten films. *Journal of Agricultural and Food Chemistry*, **60**(24), 6157-63.

Halim, S.A.A., Yehia, S.A., El-Nabarawi, M.A. 2014. Chromium picolinate loaded superporous hydrogel and superporous hydrogel composite as a controlled release device: in vitro and in vivo evaluation. *Journal of Drug Delivery Science and Technology*, **24**(4), 326-337.

Halley, P.J., Truss, R.W., Markotsis, M.G., Chaleat, C., Russo, M., Sargent, A.L., Tan, I., Sopade, P.A. 2007. A review of biodegradable thermoplastic starch polymers. *American Chemical Society*, **978**, 287-300.

Hamauzu, Y., Inno, T., Kume, C., Irie, M., Hiramatsu, K., Yasui, H. 2007. Some health beneficial properties of phenolics from chinese quince, quince and apple. in: *Proceedings of the 1st International Symposium on Human Health Effects of Fruits and Vegetables*, (Ed.) Y. Desjardins, pp. 417-423.

Harborne, J.B. 1967. *Comparative biochemistry of the flavonoids*. Academic Press, London; New York, pp. 1-383.

Hassan, B., Hossein Azizi, M., Mohsen, B., Zohreh, H.-E. 2014. Effect of potassium sorbate on antimicrobial and physical properties of starch-clay nanocomposite films. *Carbohydrate Polymers*, **110**, 26-31.

Herceg, Z., Batur, V., Jambrak, A.R., Vukusic, T., Gmajnicki, I., Spoljaric, I. 2013. The effect of tribomechanical micronization and activation on rheological, thermophysical, and some physical properties of tapioca starch. *International Journal of Carbohydrate Chemistry*, **2013**, Article ID 657951, 7 pp.

Herrero, M., Castro-Puyana, M., Mendiola, J.A., Ibanez, E. 2013. Compressed fluids for the extraction of bioactive compounds. *Trac-Trends in Analytical Chemistry*, **43**, 67-83.

Herrmann, K. 1992. Contents of principle plant phenols in fruit. *Fluessiges Obst*, **59**(2), 66-70.

Herrmann, K. 1989. Occurrence and content of hydroxycinnamic and hydroxybenzoic acid compounds in foods. *Critical Reviews in Food Science and Nutrition*, **28**(4), 315-347.

Hertog, M.G.L., Feskens, E.J.M., Hollman, P.C.H., Katan, M.B., Kromhout, D. 1993. Dietary antioxidant flavonoids and risk of coronary heart-disease - the zutphen elderly study. *Lancet*, **342**(8878), 1007-1011.

Hu, Y., Wang, Q., Tang, M. 2013. Preparation and properties of starch-g-PLA/poly(vinyl alcohol) composite film. *Carbohydrate Polymers*, **96**(2), 384-388.

Huang, P.-p., Yang, R.-f., Qiu, T.-q., Fan, X.-d. 2013. Solubility of fatty acids in subcritical water. *Journal of Supercritical Fluids*, **81**, 221-225.

Ilmain, F., Tanaka, T., Kokufuta, E. 1991. Volume transition in a gel driven by hydrogen bonding. *Nature*, **349**(6308), 400-401.

Islam, A.M., Phillips, G.O., Sljivo, A., Snowden, M.J., Williams, P.A. 1997. A review of recent developments on the regulatory, structural and functional aspects of gum arabic. *Food Hydrocolloids*, **11**(4), 493-505.

Jagannath, J.H., Nanjappa, C., Das Gupta, D., Bawa, A.S. 2006. Studies on the stability of an edible film and its use for the preservation of carrot (*Daucus carota*). *International Journal of Food Science and Technology*, **41**(5), 498-506.

Jane, J., Chen, Y.Y., Lee, L.F., McPherson, A.E., Wong, K.S., Radosavljevic, M., Kasemsuwan, T. 1999. Effects of amylopectin branch chain length and amylose content on the gelatinization and pasting properties of starch. *Cereal Chemistry*, **76**(5), 629-637.

Jane, J., Shen, L., Wang, L., Maningat, C.C. 1992. Preparation and properties of small-particle corn starch. *Cereal Chemistry*, **69**(3), 280-283.

Jay-lin, J. 2003. Starch. in: *Chemical and Functional Properties of Food Saccharides*, (Eds.) P. Tomasik, CRC Press, USA, pp 91-96.

Jimenez, A., Jose Fabra, M., Talens, P., Chiralt, A. 2012. Effect of sodium caseinate on properties and ageing behaviour of corn starch based films. *Food Hydrocolloids*, **29**(2), 265-271.

Jong-Yea, K., Yoon-Gyoung, C., Sae Ron Byul, K., Seung-Taik, L. 2014. Humidity stability of tapioca starch-pullulan composite films. *Food Hydrocolloids*, **41**, 140-145.

Jun, X. 2013. High-pressure processing as emergent technology for the extraction of bioactive ingredients from plant materials. *Critical Reviews in Food Science and Nutrition*, **53**(8), 837-852.

Kabiri, K., Omidian, H., Hashemi, S.A., Zohuriaan-Mehr, M.J. 2003. Concise synthesis of fast-swelling superabsorbent hydrogels: Effect of initiator concentration on porosity and absorption rate. *Journal of Polymer Materials*, **20**(1), 17-22.

Kang, D.H., Hyeon, J.E., You, S.K., Kim, S.W., Han, S.O. 2014. Efficient enzymatic degradation process for hydrolysis activity of the carrageenan from red algae in marine biomass. *Journal of Biotechnology*, **192**, 108-113.

Kanmaz, E.O., Ova, G. 2013. The effective parameters for subcritical water extraction of SDG lignan from flaxseed (*Linum usitatissimum* L.) using accelerated solvent extractor. *European Food Research and Technology*, **237**(2), 159-166.

Karasek, P., Planeta, J., Roth, M. 2006. Solubility of solid polycyclic aromatic hydrocarbons in pressurized hot water: Correlation with pure component properties. *Industrial & Engineering Chemistry Research*, **45**(12), 4454-4460.

Karim, A.A., Norziah, M.H., Seow, C.C. 2000. Methods for the study of starch retrogradation. *Food Chemistry*, **71**(1), 9-36.

Kayan, B., Yang, Y., Lindquist, E.J., Gizir, A.M. 2010. Solubility of benzoic and salicylic acids in subcritical water at temperatures ranging from (298 to 473) K. *Journal of Chemical and Engineering Data*, **55**(6), 2229-2232.

Kelebek, H., Selli, S., Gubbuk, H., Gunes, E. 2015. Comparative evaluation of volatiles, phenolics, sugars, organic acids and antioxidant properties of Sel-42 and Tainung papaya varieties. *Food Chemistry*, **173**, 912-9.

Khalil, M.S., Ahmed, Z.S., Elnawawy, A.S. 2013. Evaluation of the physicochemical properties and antimicrobial activities of bioactive biodegradable films. *Jordan Journal of Biological Sciences (JJBS)*, **6**(1), 51-60.

Khanmirzaei, M.H., Ramesh, S. 2014. Nanocomposite polymer electrolyte based on rice starch/ionic liquid/TiO_2 nanoparticles for solar cell application. *Measurement*, **58**, 68-72.

Khoramnejadian, S., Zavareh, J.J., Khoramnejadian, S. 2011. Bio-based plastic a way for reduce municipal solid waste. in: *2011 International Conference on Green Buildings and Sustainable Cities*, (Eds.) P. Secondini, X. Wu, S. Tondelli, J. Wu, H. Xie, Vol. 21, Elsevier Science Bv. Amsterdam, pp. 489-495.

Khuwijitjaru, P., Suaylam, B., Adachi, S. 2014. Degradation of caffeic acid in subcritical water and online HPLC-DPPH assay of degradation products. *Journal of Agricultural and Food Chemistry*, **62**(8), 1945-1949.

Kim, D.H., Na, S.K., Park, J.S., Yoon, K.J., Ihm, D.W. 2002. Studies on the preparation of hydrolyzed starch-g-PAN (HSPAN)/PVA blend films—effect of the reaction with epichlorohydrin. *European Polymer Journal*, **38**(6), 1199-1204.

Kim, M., Lee, S.-J. 2002. Characteristics of crosslinked potato starch and starch-filled linear low-density polyethylene films. *Carbohydrate Polymers*, **50**(4), 331-337.

Koch, K., Gillgren, T., Stading, M., Andersson, R. 2010. Mechanical and structural properties of solution-cast high-amylose maize starch films. *International Journal of Biological Macromolecules*, **46**(1), 13-9.

Kolodziejczyk-Czepas, J., Nowak, P., Kowalska, I., Stochmal, A. 2014. Biological activity of clovers - free radical scavenging ability and antioxidant action of six Trifolium species. *Pharmaceutical Biology*, **52**(10), 1308-1314.

Krammer, P., Vogel, H. 2000. Hydrolysis of esters in subcritical and supercritical water. *The Journal of Supercritical Fluids*, **16**(3), 189-206.

Kreps, J.A., Wu, Y.J., Chang, H.S., Zhu, T., Wang, X., Harper, J.F. 2002. Transcriptome changes for Arabidopsis in response to salt, osmotic, and cold stress. *Plant Physiology*, **130**(4), 2129-2141.

Kruse, A., Gawlik, A. 2003. Biomass conversion in water at 330-410 degrees C and 30-50 MPa. Identification of key compounds for indicating different chemical reaction pathways. *Industrial & Engineering Chemistry Research*, **42**(2), 267-279.

Kuang, J., Yuk, K.Y., Huh, K.M. 2011. Polysaccharide-based superporous hydrogels with fast swelling and superabsorbent properties. *Carbohydrate Polymers*, **83**(1), 284-290.

Kuhlmann, B., Arnett, E.M., Siskin, M. 1994. Classical organic-reactions in pure superheated water. *Journal of Organic Chemistry*, **59**(11), 3098-3101.

Kuhnau, J. 1976. The flavonoids. A class of semi-essential food components: Their role in human nutrition. *World review of nutrition and dietetics*, **24**, 117-91.

Kylli, P., Nousiainen, P., Biely, P., Sipila, J., Tenkanen, M., Heinonen, M. 2008. Antioxidant potential of hydroxycinnamic acid glycoside esters. *Journal of Agricultural and Food Chemistry*, **56**(12), 4797-4805.

Lawton, J.W. 1996. Effect of starch type on the properties of starch containing films. *Carbohydrate Polymers*, **29**(3), 203-208.

Lawton, J.W., Fanta, G.F. 1994. Glycerol-plasticized films prepared from starch—poly(vinyl alcohol) mixtures: Effect of poly(ethylene-co-acrylic acid). *Carbohydrate Polymers*, **23**(4), 275-280.

Leblanc, N., Saiah, R., Beucher, E., Gattin, R., Castandet, M., Saiter, J.-M. 2008. Structural investigation and thermal stability of new extruded wheat flour based polymeric materials. *Carbohydrate Polymers*, **73**(4), 548-557.

Li, C., Moore-Kucera, J., Miles, C., Leonas, K., Lee, J., Corbin, A., Inglis, D. 2014. Degradation of potentially biodegradable plastic mulch films at three diverse U.S. Locations. *Agroecology and Sustainable Food Systems*, **38**(8), 861-889.

Li, M., Liu, P., Zou, W., Yu, L., Xie, F., Pu, H., Liu, H., Chen, L. 2011. Extrusion processing and characterization of edible starch films with different amylose contents. *Journal of Food Engineering*, **106**(1), 95-101.

Lim, J., Jang, S., Cho, H.K., Shin, M.S., Kim, H. 2013. Solubility of salicylic acid in pure alcohols at different temperatures. *Journal of Chemical Thermodynamics*, **57**, 295-300.

Liu, Han. 2005. Film-forming characteristics of starches. *Journal of Food Science*, **70**(1), E31-E36.

Liu, Xie, F., Yu, L., Chen, L., Li, L. 2009. Thermal processing of starch-based polymers. *Progress in Polymer Science*, **34**(12), 1348-1368.

Lopez-Alfaro, I., Gonzalez-Arenzana, L., Lopez, N., Santamaria, P., Lopez, R., Garde-Cerdan, T. 2013. Pulsed electric field treatment enhanced stilbene content in Graciano, Tempranillo and Grenache grape varieties. *Food Chemistry*, **141**(4), 3759-65.

Lopez, O.V., Garcia, M.A., Zaritzk, N.E. 2008. Film forming capacity of chemically modified corn starches. *Carbohydrate Polymers*, **73**(4), 573-581.

Lu, L.L., Lu, X.Y. 2007. Solubilities of gallic acid and its esters in water. *Journal of Chemical and Engineering Data*, **52**(1), 37-39.

Lukmanto, S., Roesdiyono, N., Ju, Y.-H., Indraswati, N., Soetaredjo, F.E., Ismadji, S. 2013. Supercritical CO_2 extraction of phenolic compounds in roselle (*hibiscus sabdariffa l.*). *Chemical Engineering Communications*, **200**(9), 1187-1196.

Maaurf, A.G., Mana, Y.B.C., Asbi, B.A., Junainah, A.H., Kennedy, J.F. 2001. Gelatinisation of sage starch in the presence of sucrose and sodium chloride as assessed by differential scanning calorimetry. *Carbohydrate Polymers*, **45**(4), 335-345.

Magnin, D., Lefebvre, J., Chornet, E., Dumitriu, S. 2004. Physicochemical and structural characterization of a polyionic matrix of interest in biotechnology, in the pharmaceutical and biomedical fields. *Carbohydrate Polymers*, **55**(4), 437-453.

MarketsandMarkets. 2014. Super Absorbent Polymers Market by Type (sodium polyacrylate, polyacrylate/polyacrylamide copolymer, & Others) & by Application (Baby Diapers, Adult Diapers, Women Sanitary Napkins, Agriculture, & Others) - Global Trends & Forecast to 2019. Retrived from https://medium.com/@evalynbaileys/super-absorbent-polymers-market-by-type-application-forecast-to-2019-4a52d350fe61

Mali, S., Grossmann, M.V.E., Garcia, M.A., Martino, M.N., Zaritzky, N.E. 2008. Antiplasticizing effect of glycerol and sorbitol on the properties of cassava starch films. *Brazilian Journal of Food Technology*, **11**(3), 194-200.

Malinconico, M., Immirzi, B., Massenti, S., La Mantia, F.P., Mormile, P., Petti, L. 2002. Blends of polyvinylalcohol and functionalised polycaprolactone. A study on the melt extrusion and post-cure of films suitable for protected cultivation. *Journal of Materials Science*, **37**(23), 4973-4978.

Martin, K.R., Appel, C.L. 2010. Polyphenols as dietary supplements: A double-edged sword. *Nutrition and Dietary Supplements*, **2**, 1-12.

Martinez-Huelamo, M., Tulipani, S., Estruch, R., Escribano, E., Illan, M., Corella, D., Lamuela-Raventos, R.M. 2015. The tomato sauce making process affects the bioaccessibility and bioavailability of tomato phenolics: A pharmacokinetic study. *Food Chemistry*, **173**, 864-72.

Masakuni, T., Susumu, H. 2002. Gelatinization mechanism of potato starch. *Carbohydrate Polymers*, **48**, 397-401.

Mathew, S., Abraham, T.E. 2008. Characterisation of ferulic acid incorporated starch–chitosan blend films. *Food Hydrocolloids*, **22**(5), 826-835.

Matsuda, H., Kaburagi, K., Matsumoto, S., Kurihara, K., Tochigi, K., Tomono, K. 2009. Solubilities of salicylic acid in pure solvents and binary mixtures containing cosolvent. *Journal of Chemical and Engineering Data*, **54**(2), 480-484.

Meillisa, A., Woo, H.-C., Chun, B.-S. 2015. Production of monosaccharides and bio-active compounds derived from marine polysaccharides using subcritical water hydrolysis. *Food Chemistry*, **171**, 70-77.

Miller, D.J., Hawthorne, S.B. 1998. Method for determining the solubilities of hydrophobic organics in subcritical water. *Analytical Chemistry*, **70**(8), 1618-1621.

Miller, D.J., Hawthorne, S.B., Gizir, A.M., Clifford, A.A. 1998. Solubility of polycyclic aromatic hydrocarbons in subcritical water from 298 K to 498 K. *Journal of Chemical and Engineering Data*, **43**(6), 1043-1047.

Moad, G. 2011. Chemical modification of starch by reactive extrusion. *Progress in Polymer Science*, **36**(2), 218-237.

Moorthy, S.N. 2002. Physicochemical and functional properties of tropical tuber starches: A review. *Starch-Starke*, **54**(12), 559-592.

Mościcki, L., Mitrus, M., Wójtowicz, A., Oniszczuk, T., Rejak, A., Janssen, L. 2012. Application of extrusion-cooking for processing of thermoplastic starch (TPS). *Food Research International*, **47**(2), 291-299.

Mota, F.L., Queimada, A.J., Pinho, S.P., Macedo, E.A. 2008. Aqueous solubility of some natural phenolic compounds. *Industrial & Engineering Chemistry Research*, **47**(15), 5182-5189.

Murga, R., Sanz, M.T., Beltran, S., Cabezas, J.L. 2002. Solubility of some phenolic compounds contained in grape seeds, in supercritical carbon dioxide. *Journal of Supercritical Fluids*, **23**(2), 113-121.

Murga, R., Sanz, M.T., Beltran, S., Cabezas, J.L. 2003. Solubility of three hydroxycinnamic acids in supercritical carbon dioxide. *Journal of Supercritical Fluids*, **27**(3), 239-245.

Muscat, D., Adhikari, B., Adhikari, R., Chaudhary, D.S. 2012. Comparative study of film forming behaviour of low and high amylose starches using glycerol and xylitol as plasticizers. *Journal of Food Engineering*, **109**(2), 189-201.

Musculo, A. 2010. Special Issue: Olive mill waste water in the Mediterranean area. *Terrestrial and Aquatic Environmental Toxicology*, **4**(Special Issue 1), 1-119.

Myllarinen, P., Partanen, R., Seppala, J., Forssell, P. 2002. Effect of glycerol on behaviour of amylose and amylopectin films. *Carbohydrate Polymers*, **50**(4), 355-361.

Narayan, R., Krishnan, M., Snook, J.B., Gupta, A. and Dubois, P. 1999. Bulk reactive extrusion polymerisation process producing aliphatic ester polymer Compositions, US Patent No. 5969089.

Napierala, D.M. 1998. Observations on the ageing of potato starch pastes modified with complexing agent. *Zywnosc Technologia Jakosc*, **5**(4), 173-180.

Narpinder, S., Lovedeep, K. 2004. Morphological, thermal, rheological and retrogradation properties of potato starch fractions varying in granule size. *Journal of the Science of Food and Agriculture*, **84**(10), 1241-1252.

Nochos, A., Douroumis, D., Bouropoulos, N. 2008. In vitro release of bovine serum albumin from alginate/HPMC hydrogel beads. *Carbohydrate Polymers*, **74**(3), 451-457.

Noubigh, A., Abderrabba, M., Provost, E. 2007a. Temperature and salt addition effects on the solubility behaviour of some phenolic compounds in water. *Journal of Chemical Thermodynamics*, **39**(2), 297-303.

Noubigh, A., Aydi, A., Mgaidi, A., Abderrabba, M. 2013. Measurement and correlation of the solubility of gallic acid in methanol plus water systems from (293.15 to 318.15) K. *Journal of Molecular Liquids*, **187**, 226-229.

Noubigh, A., Cherif, M., Provost, E., Abderrabba, M. 2008. Solubility of some phenolic compounds in aqueous alkali metal nitrate solutions from (293.15 to 318.15) K. *Journal of Chemical Thermodynamics*, **40**(11), 1612-1616.

Noubigh, A., Jeribi, C., Mgaidi, A., Abderrabba, M. 2012. Solubility of gallic acid in liquid mixtures of (ethanol plus water) from (293.15 to 318.15) K. *Journal of Chemical Thermodynamics*, **55**, 75-78.

Noubigh, A., Mgaidi, A., Abderrabba, M., Provost, E., Furst, W. 2007b. Effect of salts on the solubility of phenolic compounds: Experimental measurements and modelling. *Journal of the Science of Food and Agriculture*, **87**(5), 783-788.

Nouhigh, A., Cherif, M., Provost, E., Abderrabba, M. 2008. Solubility of gallic acid, vanillin, syringic acid, and protocatechuic acid in aqueous sulfate solutions from (293.15 to 318.15) K. *Journal of Chemical and Engineering Data*, **53**(7), 1675-1678.

Noun, L., Nafchi, A.M. 2014. Antibacterial, mechanical, and barrier properties of sago starch film incorporated with betel leaves extract. *International Journal of Biological Macromolecules*, **66**, 254-259.

Oksana, S., Marian, B., Mahendra, R., Bo, S. 2012. Plant phenolic compounds for food, pharmaceutical and cosmetics production. *Journal of Medicinal Plants Research*, **6**(13), 2526-2539.

Omidian, H., Mastropietro, D., Kandalam, U. 2014. Swelling, strength, and biocompatibility of acrylate-based superporous hydrogel hybrids. *Journal of Bioactive and Compatible Polymers*, **29**(1), 66-80.

Omidian, H., Park, K. 2012. Hydrogels. in: *Fundamentals and Applications of Controlled Release Drug Delivery*, (Eds.) J. Siepmann, R.A. Siegel, M.J. Rathbone, Springer US, pp. 75-105.

Orphanides, A., Goulas, V., Gekas, V. 2014. Introducing the concept of sono-chemical potential: A phenomenological model for ultrasound assisted extraction. *Journal of Food Engineering*, **120**, 191-196.

Oyen, M.L. 2014. Mechanical characterisation of hydrogel materials. *International Materials Reviews*, **59**(1), 44-59.

Pal, K., Banthia, A., Majumdar, D. 2006. Preparation of transparent starch based hydrogel membrane with potential application as wound dressing. *Trends Biomater Artif Organs*, **20**(1), 59-67.

Parvathy, P.C., Jyothi, A.N. 2012. Synthesis, characterization and swelling behaviour of superabsorbent polymers from cassava starch-graft-poly(acrylamide). *Starch-Starke*, **64**(3), 207-218.

Pavlovic, I., Knez, Z., Skerget, M. 2013. Subcritical water - a perspective reaction media for biomass processing to chemicals: Study on cellulose conversion as a model for biomass. *Chemical and Biochemical Engineering Quarterly*, **27**(1), 73-82.

Pennycooke, J.C., Cox, S., Stushnoff, C. 2005. Relationship of cold acclimation, total phenolic content and antioxidant capacity with chilling tolerance in petunia (Petunia × hybrida). *Environmental and Experimental Botany*, **53**(2), 225-232.

Pires, R.F., Franco, M.R., Jr. 2012. Solubility of salicylic acid in water plus salt (NaCl, KCl, NaBr, Na_2SO_4 and K_2SO_4) at 293.5-313.3 K. *Fluid Phase Equilibria*, **330**, 48-51.

Puncha-Arnon, S., Pathipanawat, W., Puttanlek, C., Rungsardthong, V., Uttapap, D. 2008. Effects of relative granule size and gelatinization temperature on paste and gel properties of starch blends. *Food Research International*, **41**(5), 552-561.

Pushpadass, H.A., Hanna, M.A. 2009. Age-Induced changes in the microstructure and selected properties of extruded starch films plasticized with glycerol and stearic acid. *Industrial & Engineering Chemistry Research*, **48**(18), 8457-8463.

Pyla, R., Kim, T.-J., Silva, J.L., Jung, Y.-S. 2010. Enhanced antimicrobial activity of starch-based film impregnated with thermally processed tannic acid, a strong antioxidant. *International Journal of Food Microbiology*, **137**(2-3), 154-160.

Queimada, A.J., Mota, F.L., Pinho, S.P., Macedo, E.A. 2009. Solubilities of biologically active phenolic compounds: Measurements and modeling. *Journal of Physical Chemistry B*, **113**(11), 3469-3476.

Ramirez-Arreola, D.E., Robledo-Ortiz, J.R., Moscoso, F., Arellano, M., Rodrigue, D., Gonzalez-Nunez, R. 2012. Film processability and properties of polycaprolactone/thermoplastic starch blends. *Journal of Applied Polymer Science*, **123**(1), 179-190.

Ramírez-Arreola, D.E., Robledo-Ortiz, J.R., Moscoso, F., Arellano, M., Rodrigue, D., González-Núñez, R. 2012. Film processability and properties of polycaprolactone/thermoplastic starch blends. *Journal of Applied Polymer Science*, **123**(1), 179-190.

Reddy, N., Yang, Y. 2010. Citric acid cross-linking of starch films. *Food Chemistry*, **118**(3), 702-711.

Rice-Evans, C.A., Miller, N.J., Paganga, G. 1996. Structure-antioxidant activity relationships of flavonoids and phenolic acids. *Free Radical Biology and Medicine*, **20**(7), 933-956.

Robbins, R.J. 2003. Phenolic acids in foods: An overview of analytical methodology. *Journal of Agricultural and Food Chemistry*, **51**(10), 2866-2887.

Rodriguez, M., Oses, J., Ziani, K., Mate, J.I. 2006. Combined effect of plasticizers and surfactants on the physical properties of starch based edible films. *Food Research International*, **39**(8), 840-846.

Roleira, F.M.F., Siquet, C., Orrù, E., Garrido, E.M., Garrido, J., Milhazes, N., Podda, G., Paiva-Martins, F., Reis, S., Carvalho, R.A., Silva, E.J.T.d., Borges, F. 2010. Lipophilic phenolic antioxidants: Correlation between antioxidant profile, partition coefficients and redox properties. *Bioorganic & Medicinal Chemistry*, **18**(16), 5816-5825.

Rosiak, J.M., Yoshii, F. 1999. Hydrogels and their medical applications. *Nuclear Instruments and Methods in Physics Research Section B: Beam Interactions with Materials and Atoms*, **151**(1–4), 56-64.

Sadeghi, M., Mohammadinasab, E., Shafiei, F., Mansouri, L., Khodabakhshi, M.J. 2014. Removal of heavy metals from aqueous solutions by starch-poly(AN) hydrogels. *Journal of Biodiversity and Environmental Sciences (JBES)*, **4**(4), 271-275.

Saiah, R., Sreekumar, P.A., Leblanc, N., Saiter, J.M. 2009. Structure and thermal stability of thermoplastic films based on wheat flour modified by monoglyceride. *Industrial Crops and Products*, **29**(1), 241-247.

Saldaña, M.D.A., Alvarez, V.H., Haldar, A. 2012. Solubility and physical properties of sugars in pressurized water. *Journal of Chemical Thermodynamics*, **55**, 115-123.

Saldaña, M.D.A., Valdivieso-Ramírez, C.S. 2015. Pressurized fluid systems: Phytochemical production from biomass. *The Journal of Supercritical Fluids*, **96**, 228-244.

Sanchez-Maldonado, A.F., Schieber, A., Ganzle, M.G. 2011. Structure-function relationships of the antibacterial activity of phenolic acids and their metabolism by lactic acid bacteria. *Journal of Applied Microbiology*, **111**(5), 1176-1184.

Sannino, A., Esposito, A., De Rosa, A., Cozzolino, A., Ambrosio, L., Nicolais, L. 2003. Biomedical application of a superabsorbent hydrogel for body water elimination in the treatment of edemas. *Journal of Biomedical Materials Research Part A*, **67A**(3), 1016-1024.

Seow, C.C., Cheah, P.B., Chang, Y.P. 1999. Antiplasticization by water in reduced-moisture food systems. *Journal of Food Science*, **64**(4), 576-581.

Shahidi, F., Naczk, M. 1995. *Phenolics in Food and Nutraceuticals*. Taylor & Francis.

Shi, A.-m., Wang, L.-j., Li, D., Adhikari, B. 2013. Characterization of starch films containing starch nanoparticles: Part 1: Physical and mechanical properties. *Carbohydrate Polymers*, **96**(2), 593-601.

Singh, P.P., Saldaña, M.D.A. 2011. Subcritical water extraction of phenolic compounds from potato peel. *Food Research International*, **44**(8), 2452-2458.

Sirin, Y.Z., Demirkol, O., Akbaslar, D., Giray, E.S. 2013. Clean and efficient synthesis of flavanone in sub-critical water. *Journal of Supercritical Fluids*, **81**, 217-220.

Siu, K.-C., Wu, J.-Y. 2014. Enhanced release of tanshinones and phenolics by nonionic surfactants from Salvia miltiorrhiza hairy roots. *Engineering in Life Sciences*, **14**(6), 685-690.

Smits, A.L.M., Kruiskamp, P.H., van Soest, J.J.G., Vliegenthart, J.F.G. 2003. The influence of various small plasticisers and malto-oligosaccharides on the retrogradation of (partly) gelatinised starch. *Carbohydrate Polymers*, **51**(4), 417-424.

Sobolewska-Zielinska, J., Fortuna, T. 2010. Retrogradation of starches and maltodextrins of various origin. *Acta Scientiarum Polonorum - Technologia Alimentaria*, **9**(1), 71-81.

Srinivas, K., King, J.W., Howard, L.R., Monrad, J.K. 2010. Solubility of gallic acid, catechin, and protocatechuic acid in subcritical water from (298.75 to 415.85) K. *Journal of Chemical and Engineering Data*, **55**(9), 3101-3108.

Su, B., Xie, F., Li, M., Corrigan, P.A., Yu, L., Li, X., Chen, L. 2009. Extrusion processing of Starch Film. *International Journal of Food Engineering*, **5**(1).

Sugiura, Y., Matsuda, K., Yamada, Y., Nishikawa, M., Shioya, K., Katsuzaki, H., Imai, K., Amano, H. 2007. Anti-allergic phlorotannins from the edible brown alga,. *Food Science and Technology Research*, **13**(1), 54-60.

Sun, Z., Henson, C.A. 1990. Degradation of native starch granules by barley alpha-glucosidases. *Plant Physiology*, **94**(1), 320-327.

Szwajgier, D., Pielecki, J., Targonski, Z. 2005. Antioxidant activities of cinnamic and benzoic acid derivatives. *Acta Scientiarum Polonorum - Technologia Alimentaria*, **4**(2), 129-142.

Tang, M., Zhang, R., Bowyer, A., Eisenthal, R., Hubble, J. 2004. NAD-sensitive hydrogel for the release of macromolecules. *Biotechnology and Bioengineering*, **87**(6), 791-796.

Tang, M., Zhang, R., Bowyer, A., Eisenthal, R., Hubble, J. 2003. A reversible hydrogel membrane for controlling the delivery of macromolecules. *Biotechnology and Bioengineering*, **82**(1), 47-53.

Tangkhavanich, B., Oishi, Y., Kobayashi, T., Adachi, S. 2013. Properties of rice stem extracts obtained by subcritical water/ethanol treatment. *Food Science and Technology Research*, **19**(4), 547-552.

Tarvainen, M., Nuora, A., Quirin, K.-W., Kallio, H., Yang, B. 2015. Effects of CO_2 plant extracts on triacylglycerol oxidation in Atlantic salmon during cooking and storage. *Food Chemistry*, **173**, 1011-21.

Tattini, M., Guidi, L., Morassi-Bonzi, L., Pinelli, P., Remorini, D., Degl'Innocenti, E., Giordano, C., Massai, R., Agati, G. 2005. On the role of flavonoids in the

integrated mechanisms of response of Ligustrum vulgare and Phillyrea latifolia to high solar radiation. *New Phytologist*, **167**(2), 457-470.

Thuwall, M., Boldizar, A., Rigdahl, M. 2006. Extrusion processing of high amylose potato starch materials. *Carbohydrate Polymers*, **65**(4), 441-446.

Tian, X., Xie, J., Zhao, Y., Lu, H., Liu, S., Qu, L., Li, J., Gai, Y., Jiang, X. 2013. Sense-, antisense- and RNAi-4CL1 regulate soluble phenolic acids, cell wall components and growth in transgenic Populus tomentosa Carr. *Plant Physiology and Biochemistry*, **65**, 111-119.

Toepfl, S., Mathys, A., Heinz, V., Knorr, D. 2006. Review: Potential of high hydrostatic pressure and pulsed electric fields for energy efficient and environmentally friendly food processing. *Food Reviews International*, **22**(4), 405-423.

Veiga-Santos, P., Oliveira, L.M., Cereda, M.P., Scamparini, A.R.P. 2007. Sucrose and inverted sugar as plasticizer. Effect on cassava starch-gelatin film mechanical properties, hydrophilicity and water activity. *Food Chemistry*, **103**(2), 255-262.

Vergara-Salinas, J.R., Bulnes, P., Carolina Zuniga, M., Perez-Jimenez, J., Lluis Torres, J., Luisa Mateos-Martin, M., Agosin, E., Perez-Correa, J.R. 2013. Effect of pressurized hot water extraction on antioxidants from grape pomace before and after enological fermentation. *Journal of Agricultural and Food Chemistry*, **61**(28), 6929-6936.

Wang, L., Xie, B., Shi, J., Xue, S., Deng, Q., Wei, Y., Tian, B. 2010a. Physicochemical properties and structure of starches from Chinese rice cultivars. *Food Hydrocolloids*, **24**(2-3), 208-216.

Wang, R.C., Neon, T.L., Kobayashi, T., Miyake, Y., Hosoda, A., Taniguchi, H., Adachi, S. 2010b. Degradation kinetics of glucuronic acid in subcritical water. *Bioscience Biotechnology and Biochemistry*, **74**(3), 601-605.

Wang, S.Y., Zheng, W. 2001. Effect of plant growth temperature on antioxidant capacity in strawberry. *Journal of Agricultural and Food Chemistry*, **49**(10), 4977-4982.

Whiting, D.A. 2001. Natural phenolic compounds 1900-2000: A bird's eye view of a century's chemistry. *Natural Product Reports*, **18**(6), 583-606.

Wittaya, T. 2012. Rice Starch-Based Biodegradable Films: Properties Enhancement. in: *Structure and Function of Food Engineering*, (Eds.) A.A. Eissa, InTech Croatia, pp. 103-134.

Xiao, C., Gao, Y. 2008. Preparation and properties of physically crosslinked sodium carboxymethylcellulose/poly(vinyl alcohol) complex hydrogels. *Journal of Applied Polymer Science*, **107**(3), 1568-1572.

Yang, C.Q., Wang, X.L. 1996. Formation of cyclic anhydride intermediates and esterification of cotton cellulose by multifunctional carboxylic acids: An infrared spectroscopy study. *Textile Research Journal*, **66**(9), 595-603.

Yang, C.Q., Wang, X.L., Kang, I.S. 1997. Ester crosslinking of cotton fabric by polymeric carboxylic acids and citric acid. *Textile Research Journal*, **67**(5), 334-342.

Yang, Y.-C., Wei, M.-C., Huang, T.-C., Lee, S.-Z. 2013. Extraction of protocatechuic acid from *Scutellaria barbata* D. Don using supercritical carbon dioxide. *Journal of Supercritical Fluids*, **81**, 55-66.

Yoswathana, N., Eshiaghi, M.N. 2013. Subcritical water extraction of phenolic compounds from mango seed kernel using response surface methodology. *Asian Journal of Chemistry*, **25**(3), 1741-1744.

Zhang, Han. 2006. Mechanical and thermal characteristics of pea starch films plasticized with monosaccharides and polyols. *Journal of Food Science*, **71**(2), 109-118.

Zhang, Yuan, X., Thompson, M.R., Liu, Q. 2012. Characterization of extruded film based on thermoplastic potato flour. *Journal of Applied Polymer Science*, **125**(4), 3250-3258.

Zhang, J., Wang, L., Wang, A. 2006. Preparation and swelling behavior of fast-swelling superabsorbent hydrogels based on starch-g-poly (acrylic acid-co-sodium acrylate). *Macromolecular Materials and Engineering*, **291**(6), 612-620.

Zhang, L., Li, R., Dong, F., Tian, A., Li, Z., Dai, Y. 2015. Physical, mechanical and antimicrobial properties of starch films incorporated with epsilon-poly-L-lysine. *Food Chemistry*, **166**, 107-114.

Zhao, G.H., Kapur, N., Carlin, B., Selinger, E., Guthrie, J.T. 2011. Characterisation of the interactive properties of microcrystalline cellulose-carboxymethyl cellulose hydrogels. *International Journal of Pharmaceutics*, **415**(1-2), 95-101.

Zhao, Q.S., Ji, Q.X., Xing, K., Li, X.Y., Liu, C.S., Chen, X.G. 2009. Preparation and characteristics of novel porous hydrogel films based on chitosan and glycerophosphate. *Carbohydrate Polymers*, **76**(3), 410-416.

Zhao, R., Torley, P., Halley, P.J. 2008. Emerging biodegradable materials: Starch- and protein-based bio-nanocomposites. *Journal of Materials Science*, **43**(9), 3058-3071.

Zobel, H.F. 1988. Molecules to granules: A comprehensive starch review. *Starch - Stärke*, **40**(2), 44-50.

Zohuriaan-Mehr, M.J., Kabiri, K. 2008. Superabsorbent polymer materials: A review. *Iranian Polymer Journal*, **17**(6), 451-477.

Chapter 3: Solubility measurement of phenolic acids in subcritical water[1]

3.1 Introduction

Phenolic acids are naturally present in fruits (Silva et al., 2014), vegetables (Hunaefi et al., 2013; Smitha & Shylaja, 2014), spices (Dada et al., 2013), aromatic herbs (Jin et al., 2014) as well as in biomass of citrus fruit peel (Ho et al., 2014), and vegetable solid waste (Baiano et al., 2014). Phenolic acids have attracted considerable interest as a number of proven biological activities has been demonstrated, such as antioxidants (Alberto et al., 2001), anti-inflammatory (Kawada et al., 2001), antifungal (Zhong et al., 2005), and anti-carcinogenic properties (Garcia-Perez et al., 2013). They have been widely used as raw materials for the synthesis of different molecules with industrial interest in cosmetics and pharmaceutical products (Mota et al., 2008).

The extraction of phenolic acids from these matrices can be achieved by subcritical water (SCW) technology. Subcritical water, also known as pressurised hot water, is referred to liquid water heated to temperatures above its boiling point under pressure, which can be considered as a "green" environmentally friendly and cheap solvent. Therefore, an understanding of phenolic acids solubility in water as a function of temperature and pressure is critical to design and optimize SCW extraction and reaction processes.

Although there is a wealth of data available in the literature for the solubility of phenolic acids in water below 100 °C (Daneshfar et al., 2008; Gracin & Rasmuson, 2002; Lu & Lu, 2007; Mota et al., 2008; Nouhigh et al., 2008; Queimada et al., 2009), scarce

---

[1]A version of this chapter was submitted to Journal of Chemical Thermodynamics

data are available at temperatures above 100 °C. Solubility of few phenolic acids in SCW was reported. The solubility of gallic acid, catechin, protocatechuic acid (Srinivas et al., 2010), benzoic and salicylic acid (Kayan et al., 2010) at temperatures ranging from 25 to 200 ℃ increased with increasing temperature. However, the influence of pressure on the solubility of phenolic acids in SCW was not assessed.

The objective of this study was to present a new experimental procedure to determine phenolic acid solubility in pressurised water. The solubility of gallic acid, 2,4-dihydroxybenzoic acid, 3-(4-hydroxyphenyl)-propionic acid, and 4-hydroxybenzoic acid in SCW were obtained at temperatures ranging from 23 to 150 °C and at pressures of 50 and 120 bar using a dynamic high pressure equilibrium method.

3.2 Materials and methods

3.2.1 Materials

Gallic acid (98% purity) was purchased from Fisher Scientific (Ottawa, ON, Canada). 2,4-Dihydroxybenzoic acid (≥97% purity), 4-hydroxybenzoic acid (99% purity, ReagentPlus® grade) and 3-(4-hydroxyphenyl)-propionic acid (98% purity) were acquired from Sigma-Aldrich (St. Louis, MO, USA). Washed and calcined silicon dioxide (Analytical reagent grade, Sigma-Aldrich, St. Louis, MO, USA) was used to distribute the phenolic acid in the equilibrium vessel (EV). Purified water from a Milli-Q system (Millipore, Bellerica, MA, USA) was used as the solvent. The water was degassed in an ultrasonic bath (Model FS30H, Fisher Scientific, Ottawa, ON, Canada) for 20 min previous to each experiment. Anhydrous ethanol (Sigma-Aldrich, St. Louis, MO, USA) was used as a dilution solvent in all the experiments.

68

3.2.2 Methods

3.2.2.1 Dynamic high pressure equilibrium unit

The solubility of phenolic acid was measured in a modified dynamic high pressure unit (Saldaña et al., 2012) as shown in Figure 3.1. The unit has three pumps, a heated high pressure equilibrium vessel, three pre-heaters, an ice-water cooling system, a digital pressure gauge, and a back pressure regulator. The equilibrium vessel (EV) and the pre-heaters are placed inside a modified convection oven (Isotemp™ 500 Series Economy Lab Oven, Fisher Scientific Co. Inc, Ottawa, ON, Canada) and heated by band heaters (Trutemp, Edmonton, AB, Canada). The temperature of the high pressure vessel and the pre-heaters were monitored by K-type thermocouples. The pre-heater and cooling systems have 150 cm of tubing length with an external diameter of 0.32 cm (Swagelok Valve & Fitting Inc, Edmonton, AB, Canada). The digital pressure gauge model is DPI #104 (Groby, Leicestershire, UK). A GILSON model 305 pump (pump 1) (Guelph, ON, Canada) was used to pump water into the equilibrium vessel, another GILSON model 307 pump (pump 2) (Guelph, ON, Canada) was used to add the dilution water at the exit of the equilibrium vessel and another GILSON model 307 pump (pump 3) (Guelph, ON, Canada) was used to add ethanol to the aqueous diluted solution.

The EV used consisted of stainless steel tubing fitted with proper end fittings (Swagelok Valve & Fitting Inc, Edmonton, AB, Canada). Measurements below 100 °C were performed in an EV with an internal diameter and a length of 0.635 and 7 cm, respectively, while measurements equal or above 100 °C were performed in an EV with an internal diameter and a length of 2.54 and 8 cm, respectively. A change in reactor size is due to increased solubility of phenolic acid in water at high temperatures.
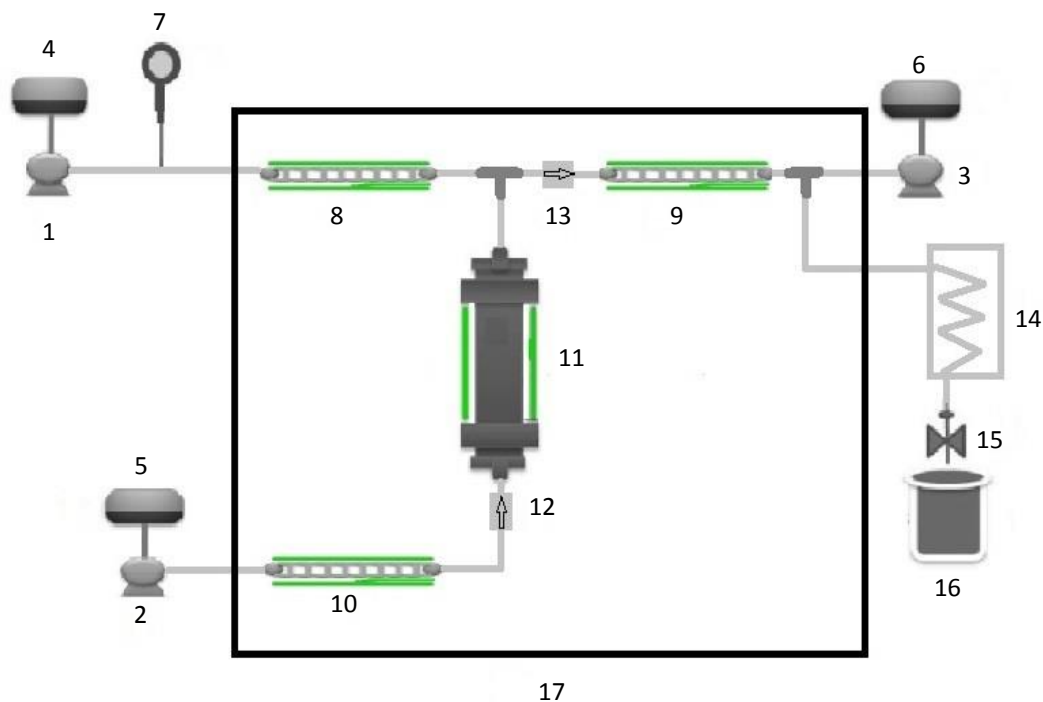
Figure 3.1 Dynamic flow high pressure unit: 1-3. HPLC pump with pressure indicator, 4-5. Water reservoir, 6. Ethanol reservoir, 7. Pressure gauge, 8-10. Pre-heating system, 11. High pressure equilibrium vessel, 12-13. Check valve, 14. Cooling system, 15. Pressure regulator, 16. Sample collection and 17. Oven.

3.2.2.2 Solubility measurement

Solubility measurements were conducted at 23, 50, 75, 100, 125 and 150 ℃ and 50 or 120 bar. First, the phenolic acid was mixed with silicon dioxide (1:2 w/w ratio) and loaded into the EV. Then, the EV was filled with water and the dilution pumps (pumps 2 and 3) supplied solvent at the required flow rate to maintain the pressure at 50 or 120 bar using the back pressure regulator. After reaching the required temperature, pressure, and static holding time (SHT), water was pumped through the EV and samples of the solution were collected in 7 mL plastic vials every minute for 30-60 min, depending on time to reach equilibrium. The refractive index of collected samples was used to detect the steady state equilibrium, which was usually achieved after 5 min of SHT and 10 to 30 min of dynamic holding time (DHT). Five samples from the steady state equilibrium were

70

analyzed for the total phenolic content. Samples collected at 125 and 150 ℃ were also analyzed by HPLC-UV to examine any potential thermal degradation. All solubility measurements were conducted in duplicate.

The aqueous solubility of the phenolic acid obtained from the total phenolic analysis can be expressed in terms of mole fraction (x_i) using

$$x_i = \frac{1}{1 + \dfrac{MW_i}{S * MW_w}} \tag{3.1}$$

where MW_i and MW_w are the molecular weights (g/mole) of the phenolic acid and water, respectively, and S is the phenolic acid content in the solution (gram of phenolic acid/gram of water).

3.2.2.3 Refractive index measurement

The refractive index of each sample collected was measured using a refractometer (Model RE50, Mettler Toledo, Tokyo, Japan) at room temperature (24 ℃). A series of dilutions were performed for a saturated phenolic acid solution. The refractive indexes of these solutions were also measured in duplicate.

3.2.2.4 Phenolic content analysis

The phenolic content of the solutions were determined by colorimetric and HPLC analysis. The colorimetric analysis was performed to determine the total phenolics content in the solution. HPLC analysis was used to monitor degradation of phenolic acid at high temperatures.

3.2.2.4.1 **Total phenolic content assay**

Total phenolic content was determined by the Folin–Ciocalteau method as previously reported (Alvarez et al., 2014; Sarkar et al., 2014). First, 0.04 mL of the solution was

mixed with 3.16 mL of distilled water and placed in the vortex for 10 s each test tube. Milli-Q water (0.04 mL) was used as a blank. Then, 0.2 mL of Folin-Ciocalteau's phenol reagent was added into the sample solution and placed in the vortex for 10 s each test tube. After 6 min of reaction, 0.6 mL of sodium carbonate solution was added to the mixture and placed in the vortex for 10 s each test tube. After incubating in a dark place at room temperature for 2 h, all samples were measured for absorbance at wavelengths from 400 to 800 nm in a spectrophotometer (Genova, Barioworld Scientific, Essex, UK) using plastic cuvettes. Scanning a range of wavelengths allowed identification and estimation of the absorbance of each phenolic acid. Standard phenolic acid solutions were prepared for the quantification of total phenolic content. Total phenolic content was expressed as milligrams of gallic acid equivalents per gram of sample solution. All measurements were performed at least in duplicate.

3.2.2.4.2   HPLC and mass spectrometry (MS) analysis

HPLC analysis for phenolics was performed in a Shimadzu Scientific HPLC system (Shimadzu Scientific Instruments Inc., Columbia, MD, USA) following the methodology reported by Singh and Saldaña (2011). The mobile phase consisted of 0.5% formic acid in water (eluent A) and 0.5% formic acid in methanol (eluent B). An amount of 0.025 mL of the phenolic compound solution was mixed with 0.975 mL of methanol and placed in the injection vial. An amount of $10 \mu L$ of the mixture was analyzed using a Phenomenex Luna 5u C18 column (4.6 mm x 150 mm, 5 µm particle size) (Phenomenex, Torrance, CA, USA) with a Supelcosil LC 18 guard column (4.6 mm x 75 mm, 20-40 µm particle size) (Supelco, Bellefonte, PA, USA). The following HPLC gradient program was used: 84% A: 16 to 19% B (15 min); 19 to 27% B (10 min); 27 to 41% B (1 min); 41 to 65% B

(10 min); 65 to 100% B (6 min); hold at 100% B (2min); 100% B to 16% B (1 min); 1 mL min^{-1} flow rate. The samples containing phenolic acids were monitored at 280 nm using an SPD-M20A Diode Array Detector. The concentration of phenolic acids in the samples analyzed using HPLC was calculated and recorded using Shimadzu Class VP software.

The identification of resorcinol was performed using a 1200 series HPLC unit and diode array detector (DAD) (Agilent Technologies, Palo Alto, CA, USA) connected to a 4000 Q TRAP LC-MS/MS System (MDS SCIEX, Applied Biosystems, Streetsville, ON, Canada). LC-MS/MS analysis was performed using atmospheric pressure electrospray ionization in negative mode.

3.2.2.5 Differential scanning calorimetry (DSC) analysis

DSC analysis allowed the measurements of melting point, enthalpy of fusion, temperature of solid–solid phase transitions and enthalpy of solid–solid phase transitions. Thermograms of the studies were obtained using a differential scanning calorimetry (Q100 V9.8 Build 296 unit, TA Instruments Company, UT, USA). Phenolic acid samples of 3 to 7 mg were sealed hermetically into a pan and heated under a stream of nitrogen in the measuring cell, while using an empty crucible as a reference. Mixtures of water and phenolic acid of 3 to 6 mg were analyzed in a sealed pan, which can keep pressures up to 25 bar. Estimates of the phase transitions were obtained from a 10°C min^{-1} temperature program from room temperature to 200 ℃ and 350 ℃ for water + phenolic acid and pure phenolic acid, respectively. Data were analyzed using the Advantage Software v5.5.3.

3.2.2.6 Statistical analysis

Minitab statistical software (version 17, Minitab Inc, PA, USA) was used to conduct analysis of variance (ANOVA) between data values. Tukey's pairwise test was used to identify significant difference at $p < 0.05$ between means of each sample.

3.3 Results and Discussion

3.3.1 Apparatus design for solubility measurement

To setup and conduct a robust experiment, preliminary studies on solubility measurements using SCW (Saldaña et al., 2012) showed the need to fulfill the following six basic requirements: i) avoid precipitation of the solute in the collection vial, ii) guarantee the right phase equilibria of the compounds in the unit, iii) avoid contamination in the EV, iv) reach equilibration time needed to achieve the maximum solubilisation, v) select the right direction of the flow inside the reactor, and vi) prove stability of phenolic acid during the measurement and before analysis.

3.3.1.1 Avoiding precipitation of the solute in the collection vial

Literature reported aqueous solubility of gallic acid of 0.015 g/g (1 bar, 25 °C) (Daneshfar et al., 2008) and 2.9 g/g (3.5 bar, 143 °C) (Srinivas et al., 2010). Then, a dilution of ~191 times with water should be used to avoid precipitation of the gallic acid at the exit of the EV. Literature reported solubility of gallic acid in methanol and ethanol at 25 °C and 1 bar are 0.3 and 0.2 g/g (Daneshfar et al., 2008), respectively. These solubility data show methanol or ethanol as better alternative co-solvents to dilute gallic acid or other phenolic acid at the exit of the EV to avoid its precipitation.

3.3.1.2 Phase equilibria

Water, methanol or ethanol used to avoid precipitation of phenolic acids should be in the liquid state to obtain the correct aqueous solubility of the solid solute. The solution in the liquid state is warranted by the use of sufficient pressure at the selected temperature. Therefore, an understanding of the vapor-liquid equilibrium of the solvent used is essential. The saturated vapor pressure, viscosity (η), density (ρ) and relative permitivity (ε_r) of water, and saturated vapor pressure for water + ethanol (1:4 w/w) and water + methanol (1:4 w/w) at various temperatures are shown in Table 3.1. The saturated vapor pressure for aqueous ethanol or methanol was calculated by the Wilson model activity coefficient.

Due to its low toxicity, ethanol was selected as a co-solvent to avoid precipitation of the phenolic acid. Aqueous ethanol solution also has a lower vapor pressure than aqueous methanol solution, as shown in Table 3.1. To prevent the precipitation of phenolic acids after cooling, the addition of ethanol was required for experiments performed from 23 to 150 ° C. The optimization of water and ethanol flow rates, SHT and DHT were carried out using "the one factor at the time" experimental design method. The validation of the optimized variables was conducted by comparing the solubility values obtained with two different amounts of loaded phenolic acid in the EV. If the solubility values were similar, then the optimal values used were considered as validated and the amount of phenolic acid loaded in the high pressure vessel was adequate.

Table 3.1 Influence of temperature on vapour pressure of aqueous solutions, viscosity (η), density (ρ) and relative permittivity (ε_r) for water at 50 bar

T	Vapor pressure (bar)			η[3]	ρ[3]	ε_r[4]
(°C)	w[1]	w:m[2] (1:4 w/w)	w:e[2] (1:4 w/w)	(μ Pa s)	(g cm^{-3})	
25	0.02	0.14	0.08	888.99	0.999	78.6
50	0.12	0.46	0.28	547.71	0.990	70.0
75	0.38	1.26	0.86	379.00	0.977	62.4
100	1.01	2.99	2.18	283.05	0.961	55.6
125	2.32	6.26	4.83	223.33	0.941	49.5
150	4.75	11.91	9.61	183.60	0.920	44.1

w: water, m: methanol, and e: ethanol. [1] DIADEM public (2000), [2] Alvarez et al. (2011), [3] NIST (2014), [4] Floriano & Nascimento (2004)

3.3.1.3 Avoid contamination in the equilibrium vessel

The configuration of the solubility unit should avoid contamination of the reactor when other solvent (e.g. ethanol) is added at the exit of the reactor. Experiments demonstrated that the distance between the exit of the reactor and the point of dilution is critical to avoid contamination of the EV with the solvent. Even though an optimal distance can be determined at some conditions of temperature and pressure for a specific phenolic acid; this configuration would not be of general use. Because for some conditions at the point of dilution, gradients of pressure and the use of other solvent can disturb the equilibrium in the EV. To overcome these problems, the solubility unit should use a first dilution at the exit of the reactor with a flow rate of water no higher than the flow rate inside the EV and a second dilution with a convenient flow rate of the other solvent after the first dilution. Moreover, the use of one-way check valves was required to prevent solvents coming back to the EV.

3.3.1.4 Equilibration time

Once the system reached the required temperature and pressure, a static holding time (SHT) followed by a dynamic holding time (DHT) is needed to attain equilibrium. These equilibration times guaranteed maximum phenolic acid solubilisation in water at a selected temperature and pressure. The SHT and DHT work similarly to a batch and a semi-batch operation, respectively.

The proposed dynamic continuous flow method requires a large amount of solute but only a short equilibration time. The identification of the optimal SHT and DHT were achieved by analysing values of solubility obtained at different conditions of pressure and temperature. The optimal SHT was selected when the highest value of solubility was obtained without degradation of the phenolic acid. The optimal DHT was established when a constant concentration was obtained throughout the time of solubilisation by comparing the refractive index values of the collected samples. Also, the degradation of the phenolic acid was verified using high performance liquid chromatography with UV detector (HPLC-UV) and colorimetric analysis.

The solubility of gallic acid in water at 75 °C and 120 bar using three different SHT of 0, 15, and 25 min had similar UV-VIS spectrum (Figure 3.2 a) and no degradation was detected. However, at 150 °C and 120 bar, the solubility values were different at 0 and 5 min of SHT as visualized by different profiles of the UV-VIS spectrum indicated thermo-catalytic cracking of gallic acid (Figure 3.2b). Moreover, after dissolution of gallic acid at 75 ℃ and 120 bar after a SHT of 0 min, a DHT of 10 min to reach maximum solubility was used. This total equilibration time of 10 min was not extended to other temperatures since the tendency for phenolic acids to degrade at higher temperatures would be

increased by a long equilibration time. Instead, the same principle was applied to other investigated phenolic acids. For example, at 150 °C, a SHT and DHT of 0 and 90 min were used, respectively, as shown in Figure 3.3. Therefore, the experimental methodology used a SHT of 5 and 0 min at 23 °C and higher temperatures, respectively.
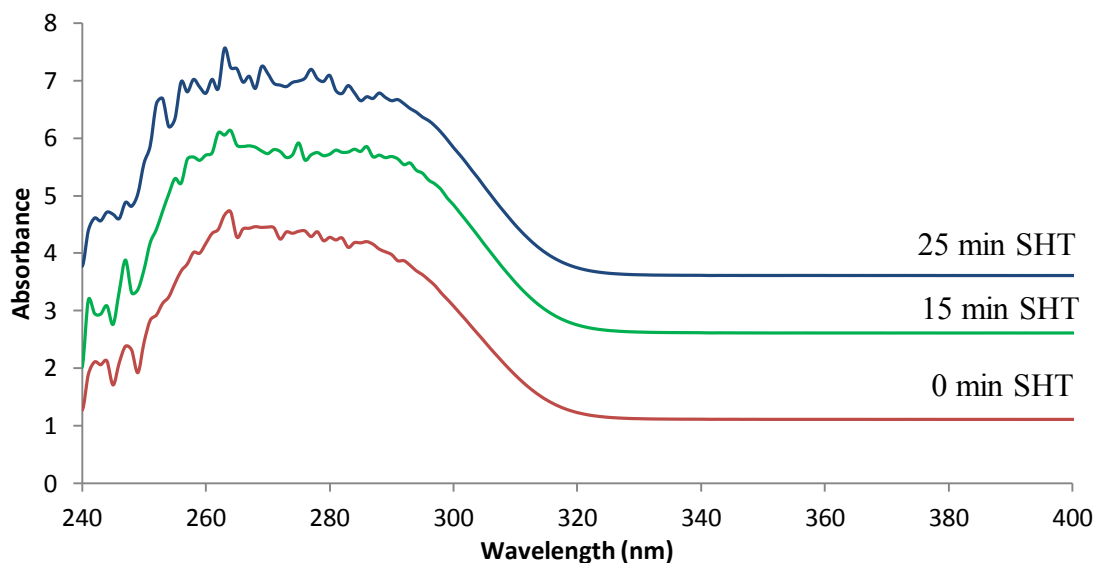
(a)
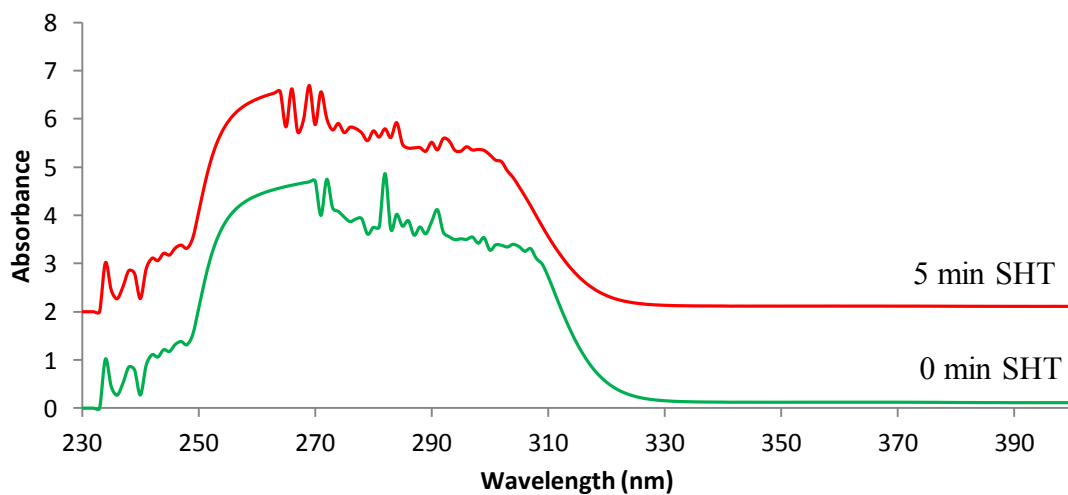
(b)

Figure 3.2 UV spectra of gallic acid solutions obtained after solubility measurements at different static holding times (SHT): 75 °C and 120 bar (a), and 150 °C and 120 bar (b).
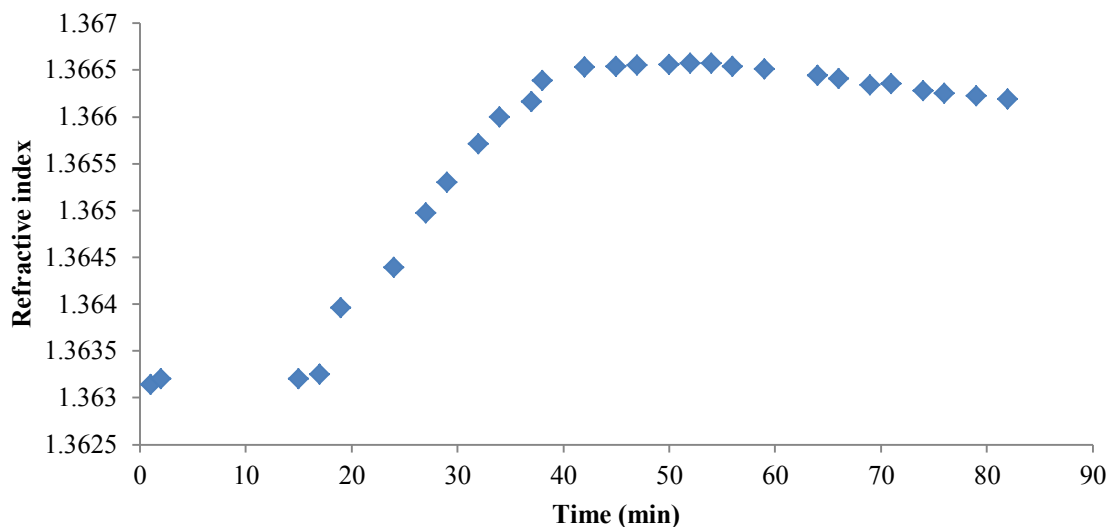
Figure 3.3 Refractive index values of gallic acid solutions collected throughout the solubility experiment at 120 bar, 150°C and low flow rates (0.2 mL/min, water inside the reactor; 0.8 mL/min, water dilution; 5 mL/min, ethanol dilution).

3.3.1.5 Influence of the flow direction

Three different types of water flow direction through the EV were tested by changing configuration of the high pressure equilibrium vessel: horizontal flow, vertical top to bottom flow and vertical bottom to top flow. A horizontal flow direction resulted in the precipitation of the solute at the bottom of the reactor due to gravity and the aqueous solution as a top layer (Figure 3.4). Therefore, it is possible that water can flow through the reactor with minimal contacting or dissolving the solid phenolic acid, which influences the equilibrium state. To avoid this problem, a vertical position of the reactor with water flowing from either the top or the bottom side was tested.

(a)   (b)

Figure 3.4 Horizontal configuration of the reactor to measure phenolic acids solubility in water (a). Picture showing the layers of phenolic acid (upper part) and sand (lower part) inside the reactor after a solubility measurement (b).

The top to bottom flow direction obtained similar values at temperatures lower than 100°C, but higher values than those reported in the literature (Table 3.2). Also, solubility values obtained at temperatures higher than 100°C showed high standard deviations (Table 3.2). These results can be explained as the top to bottom flow inside the EV can favor the exit of a supersaturated solution of phenolic acid crystals. The bottom to top flow direction allowed replication of the solubility values with low standard deviations. With this configuration, the top part of the reactor would be fully saturated with phenolic acid solution while the bottom part would be occupied with the excess amount of phenolic acid and silicon dioxide. Therefore, a vertical bottom to top flow direction was used for the experimental phenolic acid solubility in water determination.

Table 3.2 Experimental and literature data of mole fraction (x) of gallic acid and its standard deviation (SD) in water at different pressures and temperatures.

Temperature (°C)	Mole fraction 10^3 (x±SD)			
	This study		Literature	
	(120 bar)*	(120 bar)**	(Batch, ~1 bar)	(Continuous, ~1.01-3.54 bar)
0.35			0.76±0.01[1]	
14.85			0.96± 0.07[2]	
20.00			1.01[3], 1.2[4], 1.01±0.01[1]	
22.00	1.00±0.08	1.04±0.04		
25.00			1.05±0.02[1],1.63[5], 1.5±0.08[2], 1.22[4], 1.3[3],	1.37±0.07[6]
30.00			1.73[5], 1.96±0.09[2], 1.70[3], 1.28[4], 1.45±0.01[1]	
35.00			2.55[5], 2.26[3], 1.30[4],1.89±0.01[1]	
31.00			2.49±0.02[1], 2.75[5], 2.78±0.12[2], 2.89[3], 1.38[4]	
41.50				2.63±0.03[6]
45.00			3.74[5], 3.79[3], 1.43[4], 3.23±0.05[1]	
50.00	2.64±0.14	2.92±0.07	4.23±0.06[1], 4.18[5], 4.09±0.2[2]	
55.00			5.29[5], 5.41±0.06[1]	
60.00			8.35[5], 7.20±0.06[1]	
61.80				8.77±0.22[6]
65.00			8.63±0.12[1]	
70.00			11.98±0.06[1]	
75.00	10.44±1.92	9.42±0.71	14.24±0.10[1]	
80.00			19.98±0.22[1]	
82.10				21.83±1.58[6]
85.00			26.37±0.21[1]	
90.00			29.86±0.30[1]	
100.00	33.28±2.01	40.09±5.32	34.06[7]	
102.20				53.29±1.58[6]
122.50				95.68±0.52[6]
125.00	39.07±0.30	46.99±1.11		
142.70				232.93±11.50[6]
150.00	49.56±0.15 50.38±0.30[a]	51.49±1.90		

Flow configuration from bottom to top flow direction (*) and from top to bottom flow direction (**) using a flow rate of 0.5 mL/min of water inside the reactor. a: Gallic acid solubility using a water flow rate of 0.2 mL/min inside the reactor.[1] Lu and Lu (2007), [2] Mota et al. (2008), [3] Noubigh et al. (2013), [4] Nouhigh et al. (2008), [5] Daneshfar et al. (2008), [6] Srinivas et al. (2010), [7] Stephen and Stephen (1963).

3.3.1.6 Stability of solid solutes

Degradation of solutes in subcritical water occurs due to thermo-catalytic cracking and oxidation (Sarkar et al., 2014; Alvarez et al., 2014). Therefore, influences of

temperature and oxygen content in water for solubility determination are minimised using a short SHT and degasification of water, respectively. A short SHT minimised cracking of the solute and the small quantity of oxygen in the degassed water could only oxidize a minimum fraction of the large quantity of the solute used. To reduce solute degradation in the present study, water was degassed by ultra-sonication prior to use in solubility experiments, while a substantial amount of solute was loaded into the EV. Colorimetric and HPLC-UV analysis were used to monitor any degradation of a phenolic acid at the experimental conditions used.

To balance accuracy of solubility measurements and cost of manufacturing equilibrium vessel, it is critical to optimize the flow rate. High flow rates results in low residence time, minimizing degradation of phenolic acid. But, it requires a higher amount of phenolic acid with a bigger volume capacity for equilibrium vessel. The optimized flow rates for gallic acid, 2, 4-dihydroxybenzoic acid, and 4-hydroxybenzoic acid solubility measurement at different temperatures are reported in Table 3.3. As solubility increases with temperature, higher amount of ethanol was used at temperatures above 100 ℃ (Table 3.3) to prevent phenolic acid precipitation after cooling. However, due to high solubility and volume capacity of the equilibrium vessel, low flow rates of water were used for the solubility measurement of 3-(4-hydroxyphenyl)-propionic acid at temperatures above 23 °C.

The validation of optimized flow rates was conducted by comparing the solubility value with the ones obtained using lower or higher flow rates with excess amount of phenolic acid. If the solubility results from experiments using different flow rates were consistent, then the flow rates used were considered as validated and the amount of

phenolic acid loaded in the high pressure vessel were adequate. From Table 3.2, the solubility of gallic acid at 150 °C obtained by different flow rate was similar, suggesting the flow rates chosen in the system were adequate.

Table 3.3 Optimized flow rates used in the solubility measurements of phenolic acids.

Compound	Temperature (℃)	Flow rate (mL/min)		
		Pump1	Pump 2	Pump 3
Gallic acid; 4-Hydroxybenzoic acid	23	0.5	0.5	1
	50	0.5	0.5	1
	75	0.5	0.5	1
	100	0.5	0.5	4
	125	0.5	0.5	4
	150	0.4	0.4	5
2,4-Dihydroxybenzoic acid	23	0.5	0.5	1
	50	0.5	0.5	1
3-(4-Hydroxyphenyl)-propionic acid	23	0.5	0.5	1
	50	0.2	0.8	4
	75	0.2	0.8	4
	100	0.2	0.8	4
	125	0.2	0.8	4

*The solvents used for pumps 1, 2 and 3 were water, water and ethanol, respectively.

3.3.2 Solubility data of phenolic acids

Table 3.4 shows that the solubility of 3-(4-hydroxyphenyl)-propionic acid was not influenced by pressure. However, a pressure of 120 bar significantly reduced the solubility of 2,4-dihydroxybenzoic acid at 23 °C, but increased the solubility of 4-hydroxybenzoic acid at 125 and 150 °C, and the solubility of gallic acid at 150 ℃. As observed in Table 3.5, below 100 °C, solubility of phenolic acid increases at all temperatures investigated, but at higher temperatures, solubility of all phenolic acids gradually stabilized, showing a plateau. But, solubility of 2,4-dihydroxybenzoic acid decreased with temperatures over 100 °C due to its degradation as detected by the HPLC-UV analysis of these solutions. From Table 3.4, solubility of gallic acid is in agreement with earlier data reported up to 100 ℃. Slight variations could be attributed to the different methods of measurements and pressure used in the system. However, solubility

values over 100 °C were in disagreement with an early reported study (Srinivas et al., 2010). The high differences of solubility data for the same compound led to errors in one of the experimental methodologies used. A new validation methodology has been developed in our lab that proved the dynamic measurement system used in this study is valid.

The solid-liquid diagram, temperature against mole fraction solubility of phenolic acid was plotted in Figure 3.5, where discontinuities in solubility data were suspected to be a result of polymorphism or solvomorphism of the phenolic acid. The lattice structure change due to pressure or temperature is called polymorphism, and solvomorphism is the change due to solvatation or hydration of the phenolic acid. In Figure 3.5, the different phenolic acid lattice structures were represented by α. The temperature range of the solubility data is limited by the temperature at which there is a transition between more stable forms of the phenolic acid lattice structures producing liquid + α solid phases. For example, in Figure 3.5c, the temperature at which the solubility curves of α1 gallic acid and α2 gallic acid crossed should be the transition temperature. The obtained melting point and enthalpy of fusion of phenolic acids and their mixtures from DSC were compiled in Table 3.5. The thermographs of phenolic acids exhibited solid–solid phase transitions for gallic acid (97 °C) and 2,4-dihydroxybenzoic acid (95 and 152 °C), as shown in Figure 3.6a. The visual observation of the phase changes of these phenolic acids revealed a polymorphism transition between a crystalline form and a plastic form. These results in Gallic acid, 3-(4-hydroxyphenyl) -propionic acid, and 4-hydroxybenzoic acid are reported in Table 3.5. The transition temperature for 2,4-dihydroxybenzoic acid could

not be determined because of the discontinuity of the solubility data due to its degradation.

The presence of solid-solid transition forms for the solubility experiments were confirmed by the DSC analysis of water + phenolic acid mixtures. Thermographs of the aqueous mixtures of gallic acid, 3-(4-hydroxyphenyl)-propionic acid and 4-hydroxybenzoic acid were observed in Figure 3.5 and 3.6b and their transition temperatures were reported in Table 3.5. Figure 3.5 shows that the phase transitions of the solubility data for 4-hydroxybenzoic acid, 3-(4-hydroxyphenyl)-propionic acid and gallic acid in water occurred at 97, 56 and 98 °C, respectively. These data were confirmed by the phase transition temperatures obtained from the DSC analysis (dashed line). The phase transition at 67 °C was not very well detected in the solubility of 4-hydroxybenzoic acid in water due to a 25 °C temperature interval used. For future studies of solute solubility in water, low variations of temperature close to the inflections of the solid-liquid diagram should be used.

The influences of pressure and temperature on the thermos-physical properties of water and phenolic acids are shown in Table 3.1. At 50 bar, the increase of the temperature from 23 to 150 °C decreases the viscosity (η), density (ρ) and relative permittivity (ε_r) of water in 80, 8, and 44%, respectively. Also, increasing the temperature from 25 to 150 °C, the sublimation pressure for phenolic acids increased (Saldaña et al., 2007). Therefore, the main thermos-physical properties that drive the solubility behavior of phenolic acids in SCW are the sublimation pressure of the solid and the viscosity of the water.

Table 3.4 Solubiity of gallic acid, 4-hydroxybenzoic acid, 2,4-dihydroxybenzoic acid and 3-(4-hydroxyphenyl)-propionic acid in water.

T	Mole fraction 10^3 (x±SD)									
	GA				24DA		34HA		4HA	
(°C)	<4 bar	1 bar	50 bar	120 bar	50 bar	120 bar	50 bar	120 bar	50 bar	120 bar
23	-	1.01±0.02	0.67±0.04 c*	1.00±0.09 d	0.94±0.03 b	0.79±0.01 c	2.03±0.07 c	2.53±0.12 c	1.04±0.01 d	1.13±0.08 d
50	4.23 (Lu & Lu, 2007)	2.20±0.02	2.02±0.10 c	2.65±0.14 d	2.83±0.20 b	2.71±0.19 b	13.47±0.09 b	13.71±0.99 b	3.29±0.16 d	3.14±0.13 d
75	14.25 (Lu & Lu, 2007)	13.52±2.8	10.37±0.67 b	10.44±1.93 c	-	-	30.80±1.80 a	29.89±1.60 a	10.42±0.55 c	12.48±0.12 c
100	34.06 (Stephen & Stephen, 1963)	31.59±0.61	34.07±1.77 a	33.29±2.01 b	-	-	29.58±0.48 a	28.85±0.31 a	42.59±0.35 b	39.35±1.51 b
125	95.68 (Srinivas et al., 2010)	-	35.37±0.97 a	39.08±0.31 b	-	-	28.99±0.09 a	27.73±0.78 a	44.92±0.48 a	49.39±0.25 a
150	232.93 (Srinivas et al., 2010)	-	38.24±0.43 a	49.56±0.15 a	-	-	-	-	45.10±0.60 a	50.19±0.97 a

GA: gallic acid, 24DA: 2,4-Dihydroxybenzoic acid ,34HA: 3-(4-hydroxyphenyl) -propionic acid , 4HA: 4-Hydroxybenzoic acid.

* Data with different letter in the same column indicate significant difference at $p<0.05$. Detailed calculation in Appendix A.

Table 3.5 Thermophysical constants of phenolic acids and their aqueous mixtures determined by DSC and solubility measurements.

Solute	T_m (^{o}C)	ΔH_m (J mol^{-1})	T_{tr} (^{o}C)	ΔH_{tr} (J mol^{-1})
Phenolic acid DSC at 1 bar				
GA	263.1	51938	97	937
24DA	228.7	74008	95; 152	252; 2099
34HA	131.9	27534	-	-
4HA	219.2	31961	-	-
H$_2$O + phenolic acid – DSC of the aqueous mixture at 1 bar				
x_{GA}=0.0418	-	-	98	27730
x_{34HA}=0.0318	-	-	56	19658
x_{4HA}=0.0490	-	-	67, 97	4280, 10116

GA: gallic acid, 24DA: 2,4-dihydroxybenzoic acid, 34HA: 3-(4-hydroxyphenyl)-propionic acid and 4HA: 4-hydroxybenzoic acid, MW: molecular weight, T_m: Melting point, T_{tr}: temperature for phase transition, ΔH_m: change of enthalpy at the melting point, ΔH_{tr}: change of enthalpy at the phase transition, x: molar fraction.
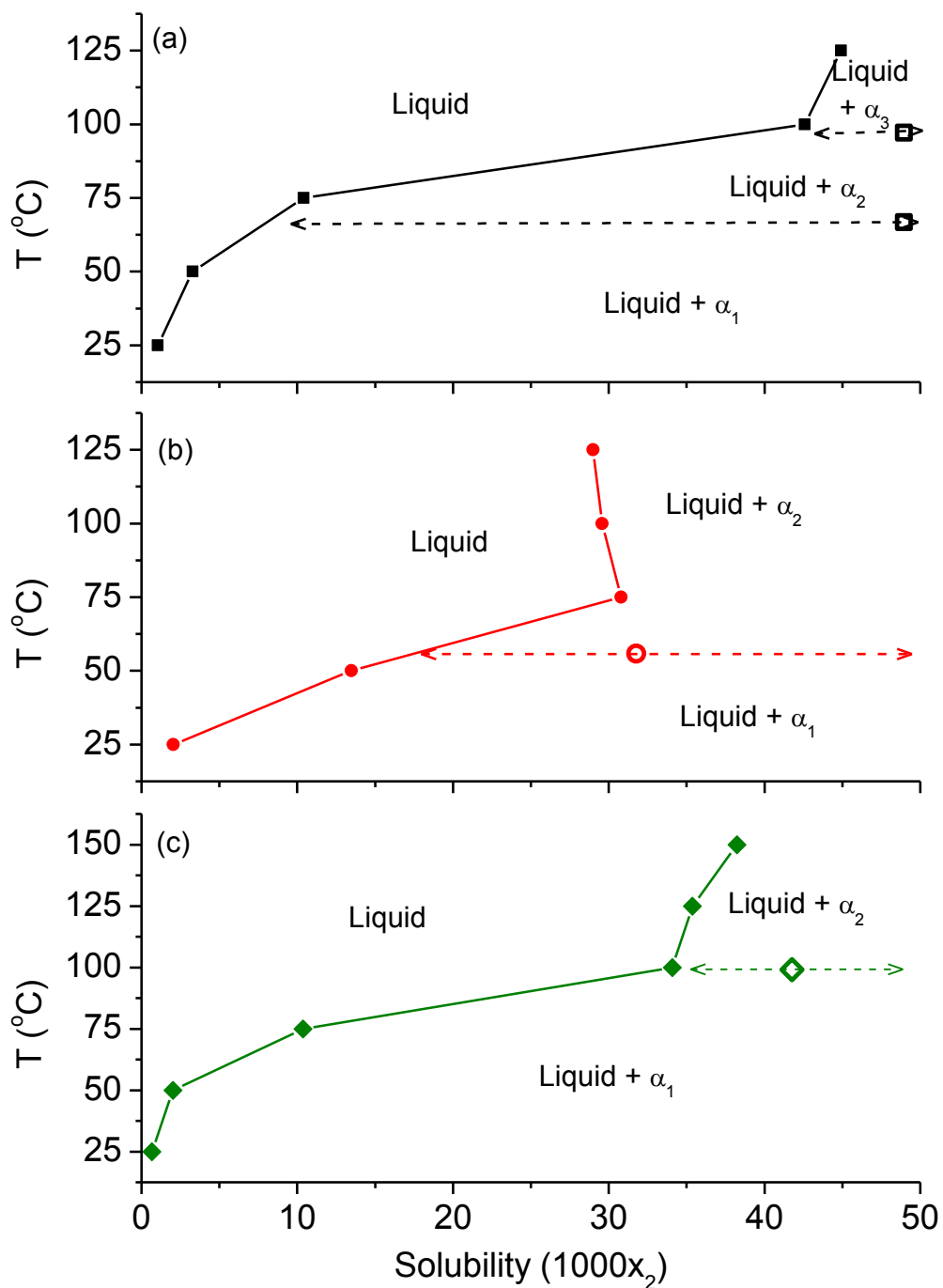
Figure 3.5 Solubility data (solid line and closed symbol) and phase transition temperatures from DSC analysis (open symbol) for 4-hydroxybenzoic acid (a), 3-(4-hydroxyphenyl)-propionic acid (b), and gallic acid (c). Phase transition boundary by DSC measurements (◄-- - ►).
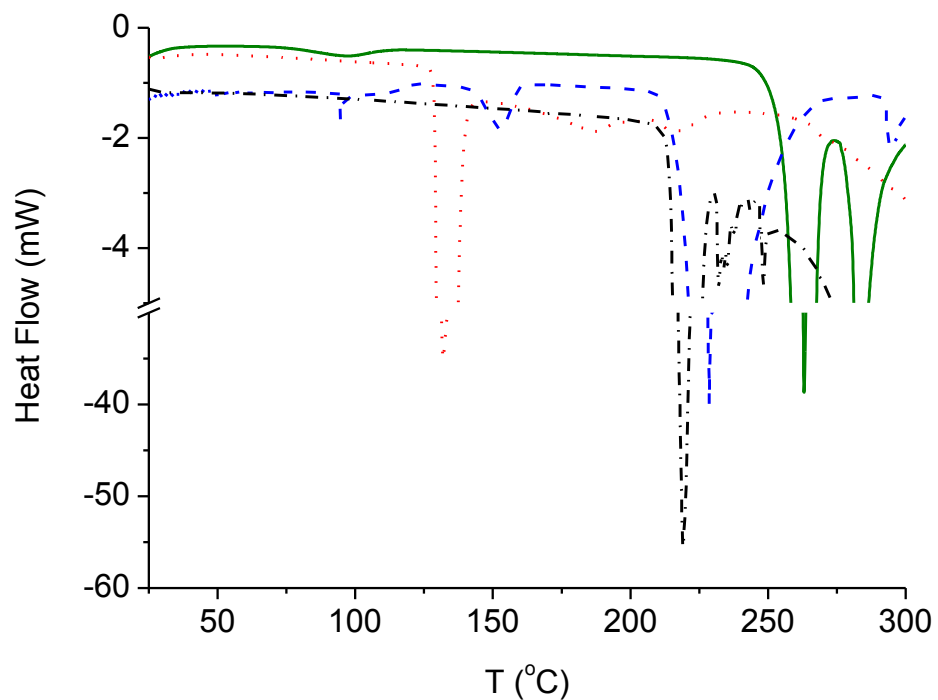
(a)
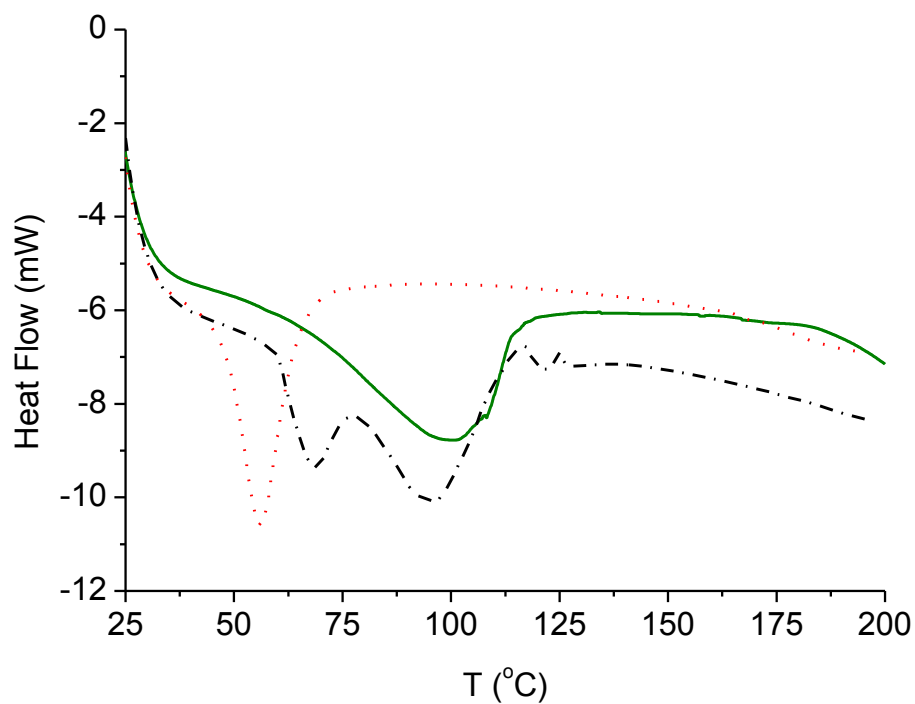
(b)

Figure 3.6 Thermographs of: pure phenolic acids (a) and water + phenolic acid mixtures (b). Gallic acid (solidline), 2,4-dihydroxybenzoic acid (dashed line), 3-(4-hydroxyphenyl)-propionic acid (dotted line), and 4-hydroxybenzoic acid (dashed-dottedline).

3.3.2.1 Conversion of 2, 4-dihydroxybenzoic acid

During solubility measurements of 2, 4-dihydroxybenzoic acid in water over 100 °C produced significant amounts of gas. A similar decarboxylation reaction has been reported for other benzoic acid derivatives in subcritical water (Lindquist & Yang, 2011). The identification of these degraded products was further investigated by HPLC-MS analysis. Based on the HPLC retention time and MS spectra, it is confirmed resorcinol was produced from 2, 4-dihydroxybenzoic acid at temperatures above 75 °C (Figure 3.7a). Therefore, 2, 4-dihydroxybanzoic acid was decomposed into resorcinol and carbon dioxide in water above 75 °C. A study of the conversion of 2, 4-dihydroxybenzoic acid at different temperatures was conducted in a batch system at 50 and 120 bars (Figure 3.7b). The identification of the resulting products was further investigated by HPLC-UV, HPLC-MS and GC-MS analysis. The results confirmed the presence of CO_2 and resorcinol in the gas and liquid phases, respectively. Resorcinol (MW = 110 g mole^{-1}) and 2, 4-dihydroxybenzoic acid (MW = 154 g mole^{-1}) produced m/z values of 109 and 153 in the HPLC-MS spectra, respectively (Figure 3.8). The HPLC-UV spectra for the liquid phase showed two peaks at 7.5 and 23 min, corresponding to resorcinol and 2, 4-dihydroxybenzoic acid, respectively (Figure 3.8a). The resorcinol conversion % (amout of 2, 4-dihydroxybenzoic acid/ amount of original amount of 2,4-dihydroxybenzoic acid) as a function of pressure and temperature was quantified by the HPLC-UV analysis as shown in Figure 3.7b. Higher temperature and pressure significantly promote the decarboxylation reaction, obtaining 100% conversion at 150 ℃ and 120 bar. Then, solubility data for 2, 4-dihydroxybenzoic acid is reliable up to 50 °C as temperatures above 75 °C cause its decarboxylation.
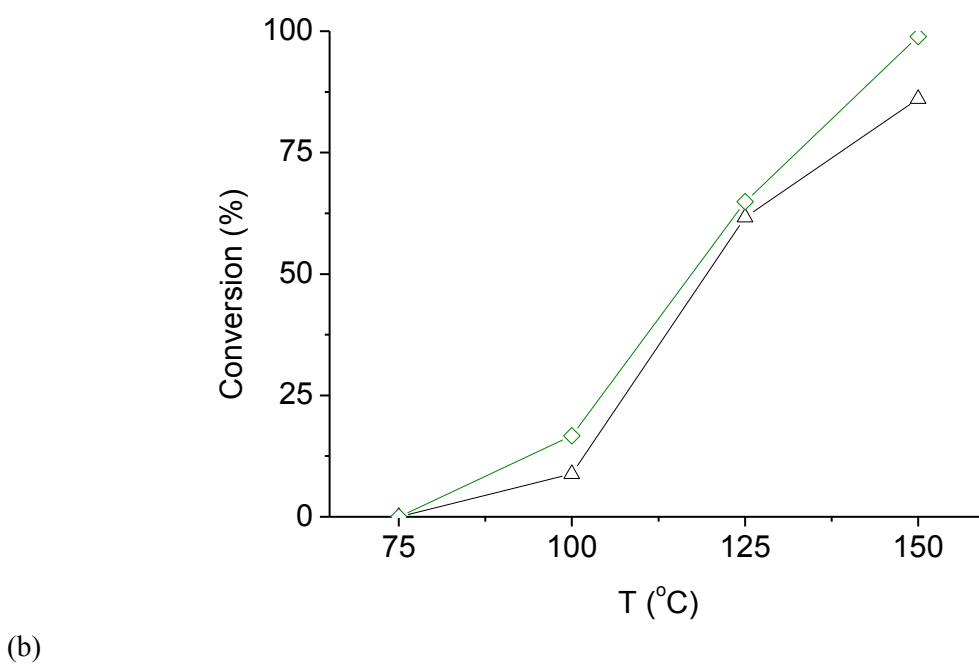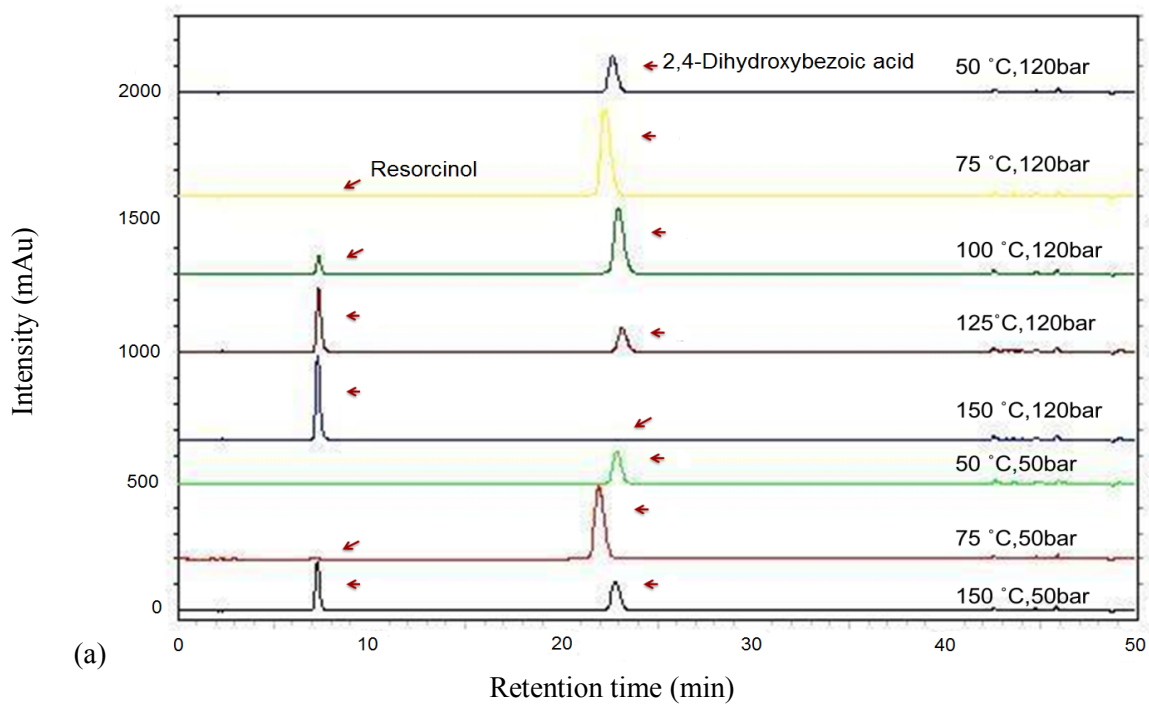
Figure 3.7 Decarboxylation of 2, 4-dihydroxybenzoic acid: (a) HPLC-UV chromatograms for identification of 2,4-dihydroxybenzoic acid and resorcinol. (b) Conversion (%) of resorcinol as a function of temperature at 50 bar (Δ) and 120 bar (◊).
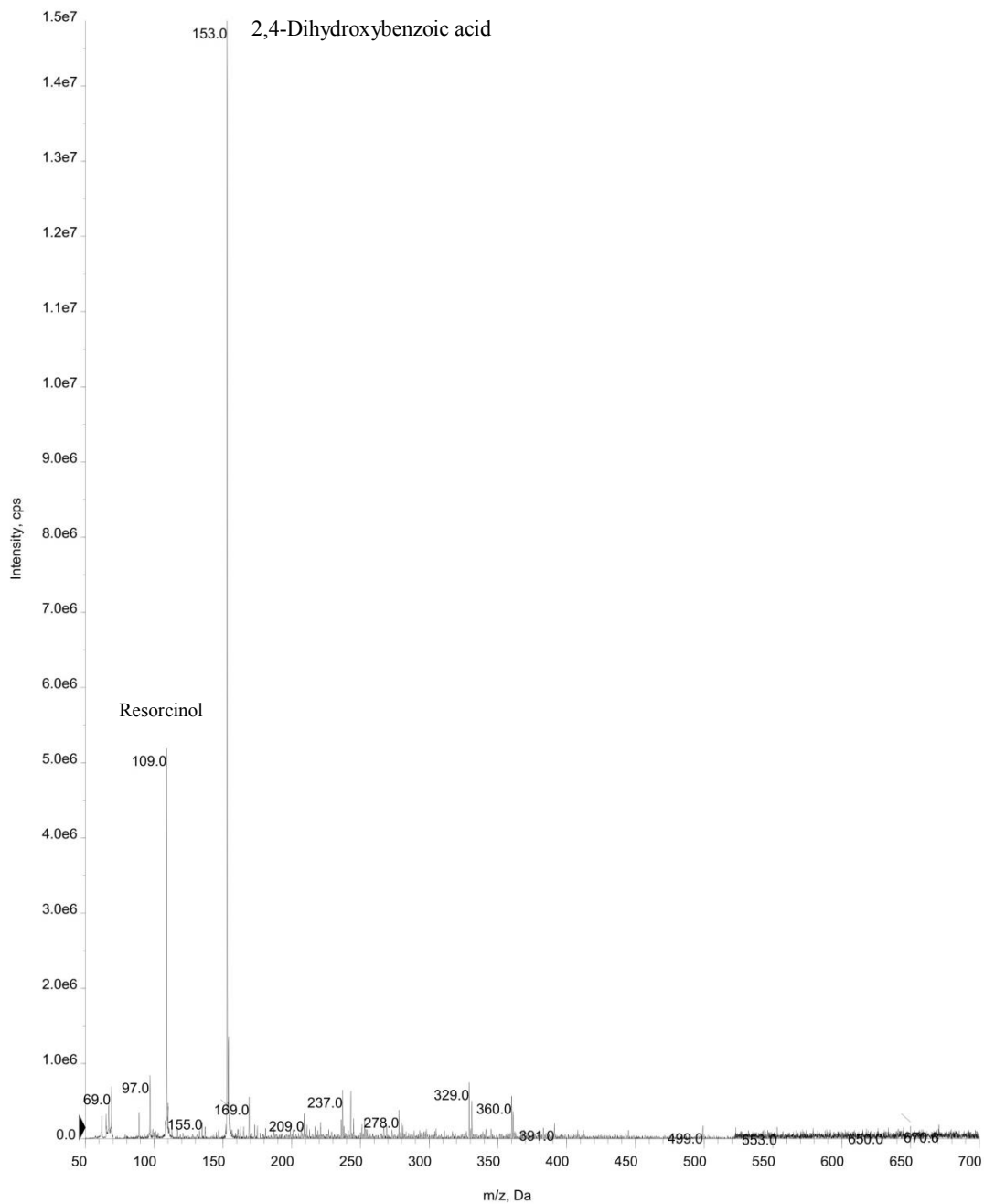
Figure 3.8 Scan mass spectra of liquid products at 150 ℃ and 120 bar, indicating the presence of resorcinol and 2, 4-dihydroxybenzoic acid.

3.4 Conclusions

- A dynamic equilibrium method was developed to determine the solubility of phenolic acids in pressurized water at temperatures from 23 to 150 ℃ under 50 and 120 bar.

92

- Solubility data obtained for gallic acid in water is reliable and more consistent than available literature data.

- Temperature significantly increased the solubility of all phenolic acids studied in water, but the amount of increase gradually decreased after temperature above 100 °C due to change of solvomorphism.

- Number of –OH in the phenolic acid structures studied in this thesis did not influence the solubility of phenolic acid in water.

- Pressure had no significant influence on the solubility of 3-(4-hydroxyphenyl)-propionic acid.A pressure of 120 bar significantly reduced the solubility of 2,4-dihydroxybenzoic acid at 23 ℃ , but increased the solubility of 4-hydroxybenzoic acid at 125 and 150 ℃ , and the solubility of gallic acid at 150 ℃ .

- High pressure (120 bar) and temperature (> 75 °C) promoted the conversion of 2,4-dihydroxybenzoic acid into resorcinol.

3.5 Recommendations

- Manual sample collection in a selected time interval can be replaced by connecting an automatic spectrophotometer to determine equilibrium and absorbance in real time.

- Development of an equilibrium vessel with adjustable sizes can reduce the time and cost of individual vessels with different sizes.

- Measure solubility of other phenolic acids (e.g. caffeic acid) which are commonly present in biomass. Degradation may occur like 2,4-dihydrobenzoic acid.

- It is also necessary to study the stability and solubility of these phenolic acids in subcritical water before an extraction process.

3.6 References

Alberto, M.R., Farias, M.E., de Nadra, M.C.M. 2001. Effect of gallic acid and catechin on *Lactobacillus hilgardii* 5w growth and metabolism of organic compounds. *Journal of Agricultural and Food Chemistry*, **49**(9), 4359-4363.

Alvarez, V.H., Cahyadi, J., Xu, D., Saldaña, M.D.A. 2014. Optimization of phytochemicals production from potato peel using subcritical water: Experimental and dynamic modeling. *The Journal of Supercritical Fluids*, **90**, 8-17.

Alvarez, V.H., Mattedi, S., Iglesias, M., Gonzalez-Olmos, R., Resa, J.M. 2011. Phase equilibria of binary mixtures containing methyl acetate, water, methanol or ethanol at 101.3 kPa. *Physics and Chemistry of Liquids*, **49**(1), 52-71.

Baiano, A., Bevilacqua, L., Terracone, C., Conto, F., Nobile, M.A.d. 2014. Single and interactive effects of process variables on microwave-assisted and conventional extractions of antioxidants from vegetable solid wastes. *Journal of Food Engineering*, **120**, 135-145.

Dada, A.A., Ifesan, B.O.T., Fashakin, J.F. 2013. Antimicrobial and antioxidant properties of selected local spices used in "kunun" beverage in Nigeria. *Acta Scientiarum Polonorum - Technologia Alimentaria*, **12**(4), 373-378.

Daneshfar, A., Ghaziaskar, H.S., Homayoun, N. 2008. Solubility of gallic acid in methanol, ethanol, water, and ethyl acetate. *Journal of Chemical and Engineering Data*, **53**(3), 776-778.

DIADEM public. 2000. The DIPPR information and data evaluation manager. 1.2.0 ed, Thermophysical properties laboratory, Brigham Young University. Provo, UT, USA.

Floriano, W.B., Nascimento, M.A.C. 2004. Dielectric constant and density of water as a function of pressure at constant temperature. *Brazilian Journal of Physics*, **34**(1), 38-41.

Garcia-Perez, E., Noratto, G.D., Garcia-Lara, S., Gutierrez-Uribe, J.A., Mertens-Talcott, S.U. 2013. Micropropagation effect on the anti-carcinogenic activitiy of polyphenolics from Mexican oregano (*Poliomintha glabrescens* Gray) in human colon cancer cells HT-29. *Plant Foods for Human Nutrition*, **68**(2), 155-162.

Gracin, S., Rasmuson, A.C. 2002. Solubility of phenylacetic acid, p-hydroxyphenylacetic acid, p-aminophenylacetic acid, p-hydroxybenzoic acid, and ibuprofen in pure solvents. *Journal of Chemical and Engineering Data*, **47**(6), 1379-1383.

Hunaefi, D., Akumo, D.N., Smetanska, I. 2013. Effect of fermentation on antioxidant properties of red cabbages. *Food Biotechnology*, **27**(1), 66-85.

Kawada, M., Ohno, Y., Ri, Y., Ikoma, T., Yuugetu, H., Asai, T., Watanabe, M., Yasuda, N., Akao, S., Takemura, G., Minatoguchi, S., Gotoh, K., Fujiwara, H., Fukuda, K. 2001. Anti-tumor effect of gallic acid on LL-2 lung cancer cells transplanted in mice. *Anti-Cancer Drugs*, **12**(10), 847-852.

Kayan, B., Yang, Y., Lindquist, E.J., Gizir, A.M. 2010. Solubility of benzoic and salicylic acids in subcritical water at temperatures ranging from (298 to 473) K. *Journal of Chemical and Engineering Data*, **55**(6), 2229-2232.

Lindquist, E., Yang, Y. 2011. Degradation of benzoic acid and its derivatives in subcritical water. *Journal of Chromatography A*, **1218**(15), 2146-2152.

Lu, L.-L., Lu, X.-Y. 2007. Solubilities of gallic acid and its esters in water. *Journal of Chemical and Engineering Data*, **52**(1), 37-39.

Mota, F.L., Queimada, A.J., Pinho, S.P., Macedo, E.A. 2008. Aqueous solubility of some natural phenolic compounds. *Industrial & Engineering Chemistry Research*, **47**(15), 5182-5189.

NIST. 2014. Thermophysical properties of water. *National Institute of Standards and Technology*. Retrived from http://webbook.nist.gov/cgi/fluid.cgi?ID=C7732185& Action=Page.

Noubigh, A., Aydi, A., Mgaidi, A., Abderrabba, M. 2013. Measurement and correlation of the solubility of gallic acid in methanol plus water systems from (293.15 to 318.15) K. *Journal of Molecular Liquids*, **187**, 226-229.

Nouhigh, A., Cherif, M., Provost, E., Abderrabba, M. 2008. Solubility of gallic acid, vanillin, syringic acid, and protocatechuic acid in aqueous sulfate solutions from (293.15 to 318.15) K. *Journal of Chemical and Engineering Data*, **53**(7), 1675-1678.

Queimada, A.J., Mota, F.L., Pinho, S.P., Macedo, E.A. 2009. Solubilities of biologically active phenolic compounds: Measurements and modeling. *Journal of Physical Chemistry B*, **113**(11), 3469-3476.

Saldaña, M.D.A., Alvarez, V.H., Haldar, A. 2012. Solubility and physical properties of sugars in pressurized water. *Journal of Chemical Thermodynamics*, **55**, 115-123.

Saldaña, M.D.A., Tomberli, B., Guigard, S.E., Goldman, S., Gray, C.G., Temelli, F. 2007. Determination of vapor pressure and solubility correlation of phenolic compounds in supercritical CO_2. *The Journal of Supercritical Fluids*, **40**(1), 7-19.

Sarkar, S., Alvarez, V.H., Saldaña, M.D.A. 2014. Relevance of ions in pressurized fluid extraction of carbohydrates and phenolics from barley hull. *Journal of Supercritical Fluids*, **93**, 27-37.

Singh, P.P., Saldaña, M.D.A. 2011. Subcritical water extraction of phenolic compounds from potato peel. *Food Research International*, **44**(8), 2452-2458.

Jin, S.W., Chen, G.L., Du, J.J.M., Wang, L.H., Ren, X., An, T.Y. 2014. Antioxidant properties and principal phenolic compositions of *Cynomorium songaricum* Rupr. *International Journal of Food Properties*, **17**(1), 13-25.

Silva, L.M.R.d., Figueiredo, E.A.T.d., Ricardo, N.M.P.S., Vieira, I.G.P., Figueiredo, R.W.d., Brasil, I.M., Gomes, C.L. 2014. Quantification of bioactive compounds in pulps and by-products of tropical fruits from Brazil. *Food Chemistry*, **143**, 398-404.

Smitha, J., Shylaja, M.D. 2014. Gastric H^+, K^+-ATPase inhibition, and antioxidant properties of selected commonly consumed vegetable sources. *International Journal of Food Properties*, **17**(2), 239-248.

Srinivas, K., King, J.W., Howard, L.R., Monrad, J.K. 2010. Solubility of gallic acid, catechin, and protocatechuic acid in subcritical water from (298.75 to 415.85) K. *Journal of Chemical and Engineering Data*, **55**(9), 3101-3108.

Stephen, H., Stephen, T. 1963. *Solubilities of inorganic and organic compounds* (pp1-350). Pergamon Press: Oxford.

Ho, S.C., Su, M.S., Lin, C.C. 2014. Comparison of peroxynitrite-scavenging capacities of several citrus fruit peels. *International Journal of Food Properties*, **17**(1), 111-124.

Zhong, G., Chen, Z., Min, Y. 2005. Major flavonoids and their antioxidant capacity in grape seeds and skins. *Journal of Southwest Agricultural University*, **27**(1), 64-68.

Chapter 4 : Study on the mechanical, structural and functional characteristics of bioactive films (starch+phenolic acids) produced with subcritical water technology[2]

4.1 Introduction

Growing quantities of plastic bags (plastic rubbish) generated daily from consumers, packaging materials of various industries and mulching film for agricultural applications have thrown a tremendous burden to the environment in the past few decades. It is estimated that one billion ton of plastics have been discarded since 1950s (Mody & Mihu, 2012). Based on a recent report of "Plastic Waste Denominator Study" conducted by Kelleher Environmental in 2012, from 2004 to 2011, about 2.8 million tonnes of plastic waste were disposed in Canada by residential and non-residential sources. Of the total disposed, an estimated 1.9 million tonnes was packaging waste (Kelleher environmental, 2012). Most of the traditional polymers (e.g. low-density polyethylene) commonly used for plastic bags are non-biodegradable, with a very slow degradation rate. A 0.2% weight loss after 10 years of biodegradation for such materials was reported (Shah et al., 2008). Therefore, development of new biodegradable materials that have the same functionalities as traditional plastics can be another alternative to manage these emerging waste-disposal problems worldwide. The production of biodegradable films from renewable and natural polymers, such as gelatin, starch, protein and their combinations has attracted an increasing attention in recent years (Andreuccetti et al., 2012).

Starches have properties, such as nontoxicity, poly-functionality, and high chemical

---

[2]A version of this chapter was submitted to Food Research International

reactivity that make them excellent materials for industrial use (non-food applications). However, the hydrophilic nature of starches is a major constraint that limits the development of starch-based materials. Chemical derivatization, which converts or cross-links the hydrophilic hydroxyl group, has been proposed as alternative to solve this problem and to produce water-resistant materials to prevent degradation. A large variety of additives, such as cellulose nanocrystals (Alves et al., 2015), talc nanoparticles (Lopez et al., 2015), chitosan (Mminh Dang & Rangrong, 2015), coconut oil (Chavez Gutierrez et al., 2014) and treatments like radiation (Ciesla et al., 2015), and photochemical process (Peregrino et al., 2014) have been applied to these natural polymers to alter their native properties (e.g. physical structure, surface morphology, hydrophobicity, and gas permeability) for further applications, such as bioactive packaging materials. Bioactive compounds can be incorporated into the packaging to provide with additional antioxidant or antimicrobial activity (Pyla et al., 2010; Sindhu & Emilia Abraham, 2008).

In this study, an innovative process with subcritical water technology was used to modify and produce potato starch film containing gallic acid and selected phenolic acids. Experimental variables, such as temperature, pressure, glycerol and gallic acid to starch ratio were evaluated to determine the optimum condition for bioactive film production.

4.2 Materials and methods

4.2.1 Materials

Potato starch (83.4 % purity) was provided by AVEBE Co (Edmonton, AB, Canada). Glycerol (> 95% purity, certified ACS grade) was purchased from Fisher Scientific (Ottawa, ON, Canada). Chemicals, such as sodium acetate trihydrate (99%), glacial acetic acid (99.7%), 1,1-Diphenyl-2-pic-ryl-hydrazyl (DPPH) (99.9%), ethanol (>

95%), Folin-Ciocalteau' phenol reagent, sodium carbonate (anhydrous powder), gallic acid (97.5-102.5% titration), trans-ferulic acid (99%), trans-cinnamic acid ($\geq$ 99%), 2,2'-Azino-bis(3-ethylbenzothiazoline-6-sulfonic acid) diammonium salt (HPLC, $\geq$ 98%), potassium persulfate (ACS reagent, $\geq$99%), 2,4,6-Tris(2-pyridyl)-s-triazine ($\geq$ 98%), calcium chloride (96%, anhydrous) and caffeic acid (HPLC, $\geq$ 98%) were acquired from Sigma Aldrich (Oakville, ON, Canada). Purified water from a Milli-Q system (Millipore, Bellerica, MA) was used.

4.2.2 Starch film preparation

4.2.2.1   Preliminary studies

First, preliminary studies (Appendix B. Section B1) were conducted to identify the ideal type of starch (waxy, regular or high amylose) and the water to starch ratio for the formation of starch film. The results showed that regular type of starch with a starch/water ratio equal to 0.5 g/g was able to form a homogeneous film. Then, the influence of different process parameters, such as temperature (75, 100, and 125 ℃), pressure (50, 120 and 190 bar), gallic acid/starch ratio (0, 10, and 20 mg/g) and glycerol/starch ratio (0, 0.5, and 1 g/g) were evaluated using Design Expert Version 6 software. Based on these preliminary studies (Appendix B, Figure B5a-d and Table B.1), the optimum condition (100 °C, 50 bar, 0.5 g glycerol/g starch, 20 mg gallic acid/g starch) was found in terms of both tensile strength and elongation %.

However, to confirm the trend found in the preliminary studies, the second experimental design expanded the range of values of the parameters as follows: temperature (75, 88, 100, 113, 125, and 150 °C), pressure (10, 30, 50, 120, and 190 bar), gallic acid/starch ratio (0, 10, 20, 40, 60, 80, 100, 250, and 400 mg/g) and glycerol/starch

ratio (0, 0.5, 1, 1.5, and 2 g/g). Experiments (Appendix B, Table B.2) were conducted to optimize one parameter at a time. At the end, a final optimum condition for all four parameters was found. In addition to gallic acid, trans-cinnamic acid, trans-ferulic acid and caffeic acid were also tested at the optimum condition.

This experimental design allowed a better understanding about the influence of the four parameters evaluated on the properties of bioactive films produced using subcritical water technology.

4.2.2.2 Film-formation process

Bioactive films were formed using subcritical fluid technology (Aranda Saldaña et al., 2014). The subcritical fluid reaction system is described in the Figure 4.1. Based on the experimental design (Appendix B, Table B.2), known amounts of potato starch, gallic acid, glycerol and water were first preloaded inside the reactor (volume of 270 mL) Then, the loaded reactor was connected to the unit and filled with Milli-Q water using an HPLC pump to eliminate the air inside the reactor, avoiding air bubbles in the final gel solution. Once the reactor was completely filled with water (~260 mL of water), it was sealed by closing all valves. The solution inside the reactor was homogenized with the double helix stirrer for 5 min before heating. The heating process was controlled by a temperature controller, a thermocouple inside the reactor and two band-heaters, which adjust and maintain the temperature of the reactor at set conditions. After reaching the required experimental temperature and pressure, the reactor was kept at this temperature for 10 min (time known as static holding time) for gelatinization and reaction of the starch. The cooling process was performed right after the completion of the static holding time by pouring cold water directly to the closed reactor and collecting the water in a plastic tray,

which brought the reactor temperature to 50 °C in maximum 3 min. Then, the reactor was disconnected from the unit and the viscous solution inside was transferred to a 500 mL Buchner flask and degasified under vacuum for 10 min to eliminate any air bubble trapped inside the gel. It was not suitable to use an ultrasonic bath to degas the starch slurry, as ultrasonic treatment has shown a significant influence on the starch structure (Cheng et al., 2010; Herceg et al., 2010; Luo et al., 2008; Wang et al., 2010b).

For each film, 50 g of degassed solution was transferred to a plastic petri dish with 15 cm diameter and dried in an oven (Model 655G, Fisher Scientific Iso Temp ® oven, Toronto, ON, Canada) at 40°C for 48 h. Dried films were cut, peeled and conditioned at 25 ℃ and 30% RH inside a desiccator that contains a saturated calcium chloride solution for at least 2 days prior to any characterization (Obuz et al., 2001).
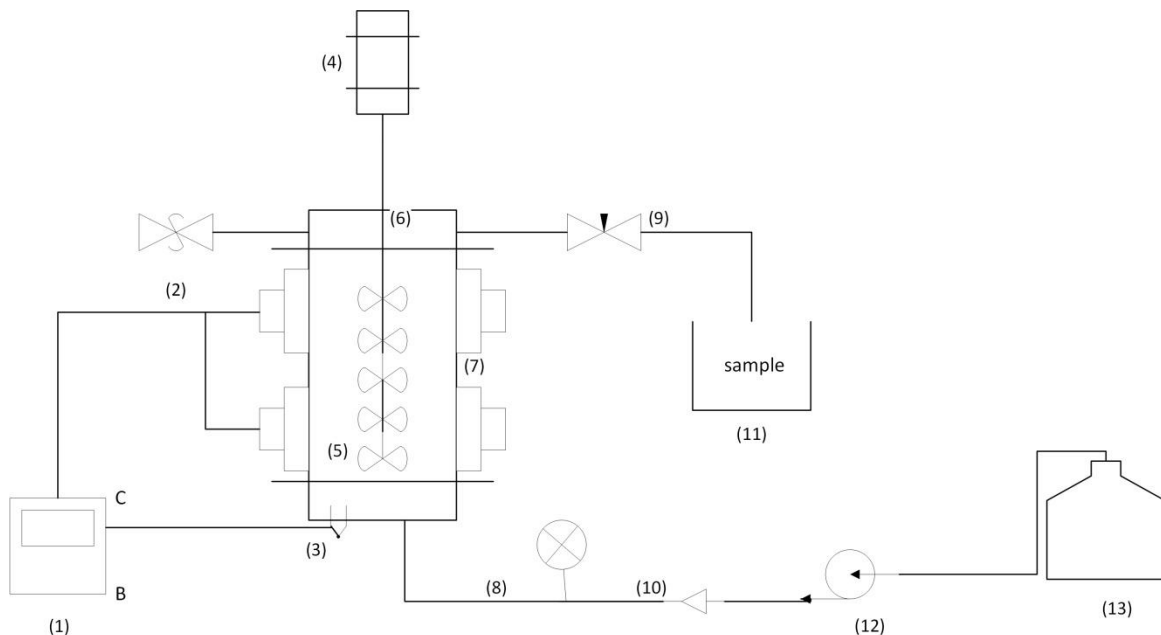
Figure 4.1 Subcritical fluid reaction system operated in batch mode. (1). Temperature controller, (2). Safety valve, (3). Thermocouple, (4). Motor of stirrer driver controlled by the SEPAREX control panel, (5). Double helix stirrer, (6). Reaction vessel, (7). Band heaters, (8). Pressure gauge, (9). Pressure regulator, (10). One-way valve, (11). Solution collector, (12). HPLC pump, and (13). Solvent reservoir.

4.2.3 Film characterization

4.2.3.1 Fourier transform infrared (FTIR) spectroscopy

Absorbance spectra of the film was measured according to the methodology proposed by Qiu et al. (2013) using a Nicolet 8700 Fourier Transform Infrared Spectrometer (Thermo Fisher Scientific Inc, Waltham, MA, USA) equipped with a Smart Speculator for ATR (Attenuated Total Reflection) from 350 to 4000 nm wavelength. The spectra were obtained at a resolution of 4 cm^{-1} with 128 scans.

4.2.3.2 X-Ray diffraction (XRD) and relative crystallinity

X-Ray diffractograms of raw starches and bioactive films were obtained using a Rigaku Geigerflex Powder Diffractometer (Rigaku , Tokyo, Japan) equipped with a cobalt tube, graphite monochromator and scintillation detector operated at 40 kV and 40 mA, scanning speed of 17.7 s/step, step interval of 0.02°, scanning range of 5–72° (Qiu et al., 2013). The relative crystallinities (RC) were measured by the ratio of the relative area of the crystalline peak to total area of the diffractograms, expressed as percentage (%), and calculated by JADE 9.1 software.

4.2.3.3 Film thickness

Film thickness was determined using a hand-held digital micrometer (Model 543-552A, Mitutoyo®, Tokyo, Japan) with a precision of 0.0001 mm. Measurements were carried out at six different film locations and the mean thickness value was used to calculate the permeability, transparency and mechanical properties of the films.

4.2.3.4 Mechanical properties

Films were cut into strip (5cm x 1cm) for tensile strength (TS) and percent elongation at break (E%) test. Tensile strength is calculated by dividing the maximum

load required to break the film by the cross-sectional area (e.g. if the maximum load was 5 N and the cross section was 1 cm^2 based on width and thickness of the cut film, then the tensile strength in this case is 5 MPa).

Percent elongation at break is calculated by dividing the film elongation at rupture by its initial length and multiplying by 100 (e.g. if the initial length of the film strip is 3 cm and the film breaks at 6 cm after applying the pulling force, then the %E is 100% x (6-3)/3=100%). TS and %E were measured on a texture analyzer (5960 Dual Column Tabletop Testing Systems with Instron® Bluehill® Software, Instron, Norwood, MA, USA) according to the ASTM standard method D882. Equilibrated film specimens were mounted between the grips with an initial separation of 30 mm, and the cross-head speed was set at 4 mm/min. The results of tensile strength and percentage of elongation were calculated automatically by the software installed in the texture analyzer. At least, six samples for each type of film were evaluated.

4.2.3.5 Water activity

Dried films were cut in sizes of 1 cm x 1 cm. Then, each film was placed inside a disposable cup designed specifically for this measurement for water activity meter (Aqualab dew point water activity meter 4TE, Pullman, WA, USA) before closing the sample chamber. An infrared beam focused on a tiny mirror inside the water activity meter determines the precise dew point temperature of the sample. That dew point temperature is then translated into a water activity value.

4.2.3.6 Moisture content

Moisture content of films was determined by a gravimetric method (AOAC, 2000). Film samples were cut in 2cm x 2cm square and weighed using an analytical balance

(Mettler Toledo, Mississauga, ON, Canada). Then, samples were placed into pre-weighed and dried aluminium dishes (50 mm diameter x 23 mm deep). The dishes were then placed in a hot air oven (Model 655G, Fisher Scientific IsoTemp® oven, Toronto, ON, Canada) maintained at 105 °C for at least 2 days. After drying, the dishes are transferred into the desiccators for cooling. The weight of the dish containing the dried sample was then recorded. The moisture content (%) is calculated using the following equation:

$$\% \text{ Moisture content} = \frac{(m_A - m_B)}{m_A} \times 100\% \qquad (4.1)$$

where, m_A = weight (g) of the sample before drying, and m_B = weight (g) of the sample after drying.

4.2.3.7 Water solubility

Water solubility (WS) of the film at three different temperatures of 4, 25 and 50 °C were determined using the methodology reported by Sajed et al. (2013). The film samples were cut into square pieces of 4 cm^2 and accurately weighed to record the dried film mass. The films were then placed into a 50 mL centrifuge tube and filled with 50 mL Milli-Q water. The samples were immersed and shaken under constant agitation at 180 rpm for 24 h at a selected temperature. After 24 h, the remaining pieces of the film were filtered and dried using a hot air oven at 105 °C for at least 2 days until a final constant weight was obtained. The percentage of solubility of the film was calculated according to the equation:

$$WS\ (\%) = ((m_0 - m_F)/m_0) \times 100 \qquad (4.2)$$

where m_0 is the weight (g) of dry matter of the film calculated based on the moisture content of the initial film sample and m_F is the final weight (g) of the desiccated undissolved film.

4.2.3.8 Optical properties

4.2.3.8.1 Transparency

A spectrophotometer was used to measure the transparency of bioactive films according to the standard test method of transparency of plastic sheeting (ASTM, 1992). The transparency of the plastic film was determined by measuring the % transmittance of light at 600 nm (T_{600}). The transparency value of the film was calculated by the following equation (Han & Floros, 1997; Nawapat & Thawien, 2013):

$$\text{Transparency value} = -(\log T600)/x \qquad (4.3)$$

where, T600 is the fractional transmittance at 600 nm and x is the film thickness (mm). The greater value represents the lower transparency of the film.

4.2.3.8.2 Color

For color determination of the films, a Hunter Lab colorimeter (CR-400/CR-410, Konica Minolta, Ramsey, NJ, USA) was used to determine the values of L, a, and b. The tests were performed according to the ASTM D2244 method (ASTM, 2011) that uses a D65 illuminant with an opening of 14 mm and a 10° standard observer. The colorimeter was calibrated using a standard white plate (L* = 93.49, a* = −0.25, b* =−0.09). The color measurements were performed by placing the film strips over the colorimeter with at least three points for each sample selected. Total color difference (ΔE), yellowness index (YI), and whiteness index (WI) were calculated similarly to the study reported by Boun and Huxsoll (1991):

$$\Delta E = \sqrt{(L^* - L)^2 + (a^* - a)^2 + (b^* - b)^2} \qquad (4.4)$$

$$YI = 142.86 \, b/L \qquad (4.5)$$

$$WI = 100 - [(100 - L)^2 + a^2 + b^2]^{0.5} \qquad (4.6)$$

where, L^*, a^* and b^* are the color values of the white standard tile and L, a and b are the color parameters of the starch film samples.

4.2.3.8.3 Gloss

Gloss of both sides of the bioactive films was measured at 60° angle, according to the ASTM standard D523 method (ASTM, 1999), which uses a flat surface gloss metre (GM 268, M&I instruments, Mississauga, ON, Canada). Measurements were performed in triplicate for each sample and three films of each formulation were evaluated. All results are expressed as gloss units (GU), relative to a highly polished surface of black glass standard with a value near to 100.

4.2.3.9 Contact angle

Contact angle measurements were carried out using a Dynamic Contact Angle and Tension Analysis instrument (FTA200, First Ten Angstroms, Inc. Portsmouth, VA, USA) at room temperature following the methodology described by He et al. (2013) with minor modifications. A 3 µL droplet of distilled water was placed on both sides of the surface of the starch film and water contact angle was immediately recorded. The value was obtained 5 s after the droplet contacted the surface. Each data point of contact angle was the mean of at least four measurements taken at random points on the film sample.

4.2.3.10 Scanning electron microscopy

Scanning electron microscopy (SEM) was used to investigate the surface morphology of pure phenolic acids, starches, and surfaces and fractures of bioactive films

using the JEOL 6301F Field Emission Scanning Electron Microscope (JEOL CANADA INC, Montreal, QC, Canada). Film samples were cut into strips, frozen in liquid nitrogen and then fractured. Samples were mounted on circular aluminium stubs with double sticky tape and then coated with 20 nm of gold examined and photographed.

4.2.3.11 Determination of antioxidant activity

For this analysis, 0.2 g of each film sample cut into pieces of approximately 0.5 x 0.5 cm was extracted with 8 mL of an ethanol+water mixture (1:1 v/v ratio) under constant stirring for 24 h. Then, the film+solvent mixture was centrifuged at 5000 rpm, 4°C for 10 min and the supernatant was used for the antioxidant activity measurement using the Ferric ion reducing antioxidant power (FRAP), 2,2- azinobis (3-ethyl-benzothiazoline-6-sulfonic acid) (ABTS) and 2,2- diphenyl-1-picrylhydrazyl (DPPH) radical scavenging capacity assays.

For accurate quantification and further comparison of methods, a standard curve was prepared using various concentrations of Trolox (6-hydroxy-2, 5, 7, 8-tetramethylchroman-2-carboxylic acid), a vitamin E analogue. The antioxidant activity of phenolic acid extracted from the film was converted to trolox equivalent antioxidant activity (TEAC) by comparing the corresponding percentage of absorbance reduction to the trolox concentration–response curve and expressed as the mass of Trolox, which produces the same percentage of absorbance reduction as the sample solution (Appendix B, Figure B1). The TEAC of the solutions was determined. All determinations were carried out three times using a spectrophotometer (Genova, Barioworld Scientific, Essex, UK).

4.2.3.11.1 Ferric Reducing Antioxidant Potential (FRAP) Assay

The ferric reducing power of gallic acid in the film extracts was determined using a modified version of the FRAP assay (Benzie & Strain, 1996). This method is based on the reduction, at low pH, of a colorless ferric complex (Fe^{3+}-tripyridyltriazine) to a blue-colored ferrous complex (Fe^{2+}-tripyridyltriazine) by the action of electron-donating antioxidants. The reduction is monitored by measuring the change of absorbance at 593 nm. The working FRAP reagent was prepared daily by mixing 300 mM acetate buffer, pH 3.6, with 10 mM TPTZ (2,4,6-tri(2-pyridyl)-s-triazine) in 40 mM hydrochloric acid and 20 mM ferric chloride in 10:1:1 volume ratio.

A standard curve was prepared using various concentrations of trolox. One hundred microliters of sample solutions and 300 μL of Milli-Q water were added to 3 mL of freshly prepared FRAP reagent. The reaction mixture was incubated for 30 min at 37 °C in a water bath. Then, absorbance of the samples was measured at 593 nm. A sample blank with ethanol + water mixture (1:1 v/v) was also used. The difference between sample absorbance and blank absorbance was calculated and used to determine the FRAP value. All measurements were done in triplicate.

4.2.3.11.2 Inhibition of ABTS$^{+\bullet}$ assay

The free radical scavenging capacity of film extract was also studied using the ABTS radical cation decolorization assay (Re et al., 1999), which is based on the reduction of ABTS+• radicals by antioxidants. The ABTS was dissolved in deionized water to a 7 mM concentration. The ABTS radical cation (ABTS$^{+\bullet}$) was produced by reacting ABTS solution with 2.45 mM potassium persulfate, allowing the mixture to stand in the dark at room temperature for 16 h before use. For this study, the ABTS+•

solution was diluted in Milli-Q water to an absorbance of 0.7 at 734 nm. An appropriate solvent blank reading was taken. After the addition of 100 μL of ethanolic extract solutions to 3 mL of ABTS+• solution, the absorbance reading was taken at 30 °C and 15 min after the initial mixing. All solutions were used the same day they were prepared, and all determinations were carried out in triplicate. The percentage of inhibition of ABTS+• was calculated using the following equation:

$$\text{Inhibition ABTS (\%)} = 100(A_0-A_1)/A_0 \qquad (4.7)$$

where, A_0 is the absorbance of the blank and A_1 is the sample absorbance.

Based on the standard curve of trolox, a valid reading can be generated only when the inhibition value is between 14 to 93%, lower or higher than this range resulted in inaccurate values. Therefore, appropriate dilutions for each sample solution were performed to ensure valid results.

4.2.3.11.3 Inhibition of DPPH assay

Inhibition of 1,1-Diphenyl-2-pic-ryl-hydrazyl (DPPH) assay (Blois, 1958; Eklund et al., 2005) was used to analyze the antioxidant activity of dissolved film solutions. To use this inhibition DPPH assay, the pH of the sample solution should be between 5 and 6.5. Otherwise, a buffer is needed to adjust the pH. As the pH of all dissolved film solutions were around 4, acetic acid buffer (0.1 M, pH 5.5) solution was added to adjust the pH of sample to 5.5. First, 0.1 mL of sample solution was mixed with 0.9 mL of buffer and 2 mL of the DPPH solution. The blank contained 0.1 mL of ethanol +water mixture (1:1 v/v), 0.9 mL of buffer and 2 mL of the DPPH solution. Then, the mixture was vortexed for 5s and stored in a dark place for 2 h based on preliminary experiments. Finally, all samples were measured for absorbance at wavelength of 517 nm in a

spectrophotometer (Genova, Barioworld Scientific, Essex, UK) using plastic cuvettes. All measurements were performed in triplicate and the results were calculated based on the following equation:

$$\text{Inhibition DPPH (\%)} = 100\,(A_0 - A_1)\,/A_0 \qquad (4.8)$$

where A_0 is the absorbance of the blank and A_1 is the sample absorbance

Based on the standard curve of trolox, a valid reading can be generated only when the inhibition values are between 14 to 84%. Therefore, appropriated dilutions for each sample solution were performed to ensure valid results.

4.2.3.12 Total phenolic content assay

Total phenolic content was determined following the methodology by described in Chapter 3, Section 3.2.2.5 with minor modifications. The absorbances were then compared with the standard curve of gallic acid solutions to quantify the total phenolic content. Total phenolic content was expressed as milligrams of gallic acid equivalents per gram of film. All measurements were performed in triplicate.

4.2.3.13 Antimicrobial test

The disc-diffusion assay was carried out according to methodologies reported in the literature (Ali-Shtayeh et al., 1998; Jeng-Leun et al., 2001). Films were tested for their inhibition against *Escherichia coli* AW1.7 and *Bacillus subtilis* FAD 110, which were kindly provided by Dr. Ganzle's microbiology lab. Each microbial culture was grown at 37 °C in Lysogeny broth (LB) broth for 18 h with shaking of 120 rpm. Cell numbers were adjusted to 10^{-4} CFU/mL with 0.1% peptone water prior to their use. Each culture was uniformly streaked on LB agar. A starch film square (2 cm x 2 cm) was then placed on the agar. Due to the hydrophobicity of the film, a sterilized glass plate (2 cm x 2 cm)

was used to keep the film in with the surface of agar. The agar plate was incubated at 37°C for 18 h and the clear zone formed around the film disc on the media was recorded. A control of starch film without gallic acid was run in parallel. Analyses were performed three times for each strain.

4.2.3.14 Water vapor permeability

Water vapor permeability (WVP) of the films was determined according to the ASTM E96-00 method (ASTM, 2000). Payne-permeation cups (1003, Sheen instruments, Cypress, CA, USA) with a 10 cm^2 exposure surface were used where 13.5 g anhydrous calcium chloride (0% RH) was added and a 1.0 cm headspace from anhydrous calcium chloride to the opening of the cup was left. The test films were sealed on top of the permeation cups. These cups were then placed in a desiccator containing saturated sodium chloride solution (75% RH) and kept at 22˚C. The cups were weighed at 24 h intervals over a 7-day period. The weight of cups were recorded to the nearest 0.0001 g and plotted as a function of time. The slope of each line was calculated by linear regression ($R^2 \geq 0.99$). The measured WVP of the films was determined using the following equation (Bonilla et al., 2013):

$$WVP = (WVTR* H)/\Delta P \qquad (4.9)$$

where, WVTR is the water vapor transmission rate (g m^{-2} h^{-1}) through a film, calculated from the slope of the straight line divided by the exposed film area (m^2), H is the mean film thickness (mm), and ΔP is the partial water vapor pressure difference (Pa) across the two sides of the film. For each type of film, WVP measurements were replicated three times.

111

4.2.3.15 High-performance liquid chromatography (HPLC)

Degradation of phenolic acids during heating was examined following the methodology reported by Singh and Saldaña (2011) using a Shimadzu Scientific HPLC system (Shimadzu Scientific Instruments Inc., Columbia, MD, USA). Methodology is described in Chapter 3, Section 3.2.2.6.

4.2.4 Statistical analysis

Minitab statistical software (version 17, Minitab Inc, State College, PA, USA) was used to conduct the analysis of variance (ANOVA) between data values and Tukey's pairwise test was used to identify significant difference at $p < 0.05$ between means of each sample.

4.3 Results and discussion

The following section discussed the influence of four parameters (i.e. gallic acid/starch ratio, temperature, glycerol/starch ratio and pressure) on the structural, mechanical, physical, optical, morphological and antioxidant properties of the starch bioactive films. In the end, films with different phenolic acid were produced under the optimum condition obtained and their properties were also evaluated.

4.3.1 Effect of gallic acid/starch ratio on the properties of starch films

4.3.1.1 Structural properties of starch films with different gallic acid/starch ratio

Fourier transform infrared spectroscopy was used to characterize the presence of specific chemical groups and interactions of polymers (e.g. PVA/xylan composite, and chitosan/wheat starch) (Wang et al., 2014). The FTIR spectra of pure potato starch, gallic acids and films produced with different concentration of gallic acid are depicted in Figure. 4.2. In the spectrum of native potato starch (Figure 4.2a), there are several

discernible peaks at 1058, 1160, 1180 and 1201 cm^{-1}, which are attributed to the C-O bond stretching (Goheen & Wool, 1991). Additional characteristic peaks at 993, 919, 848, 757, and 696 cm^{-1} are due to the entire anhydroglucose ring stretching vibrations (Qiu et al., 2013). The extremely broad band between 3000 and 3600 cm^{-1} and the peak at 2910 cm^{-1} correspond to OH and CH stretching, respectively, while the peak at 1648 cm^{-1} corresponds to δ (OH) bending of water (Mano et al., 2003).

In polysaccharides and polyol systems, hydrogen bonding changes are of great importance. Furthermore, in the FTIR spectra, the most direct method to distinguish the molecular interaction is to monitor the band shifts of certain functional groups (e.g. C=C, -OH) (Liu et al., 2013). In addition, the interaction occurring in a specific system can be uniquely reflected by changes of the spectral peaks wavelength numbers (Yin et al., 1999). As observed in FTIR of starch films (Figures 4.2c), in the characteristic range of potato starch, various new peaks appeared around wavelengths of 980, 1186, and 1303 cm^{-1}, indicating that new interactions were formed after heat treatment as well as after the addition of gallic acid and glycerol. Compared to the FTIR of pure gallic acid (Figure 4.2b), in the range of wavelengths of 1544 to 1687 cm^{-1}, three new peaks were found at wavelengths of 1511, 1608 and 1687 cm^{-1} when gallic acid/starch ratio was higher than 40 mg/g, confirming that the new interactions with starch involved the aromatic C=C bending in gallic acid (Figure 4.2 c).
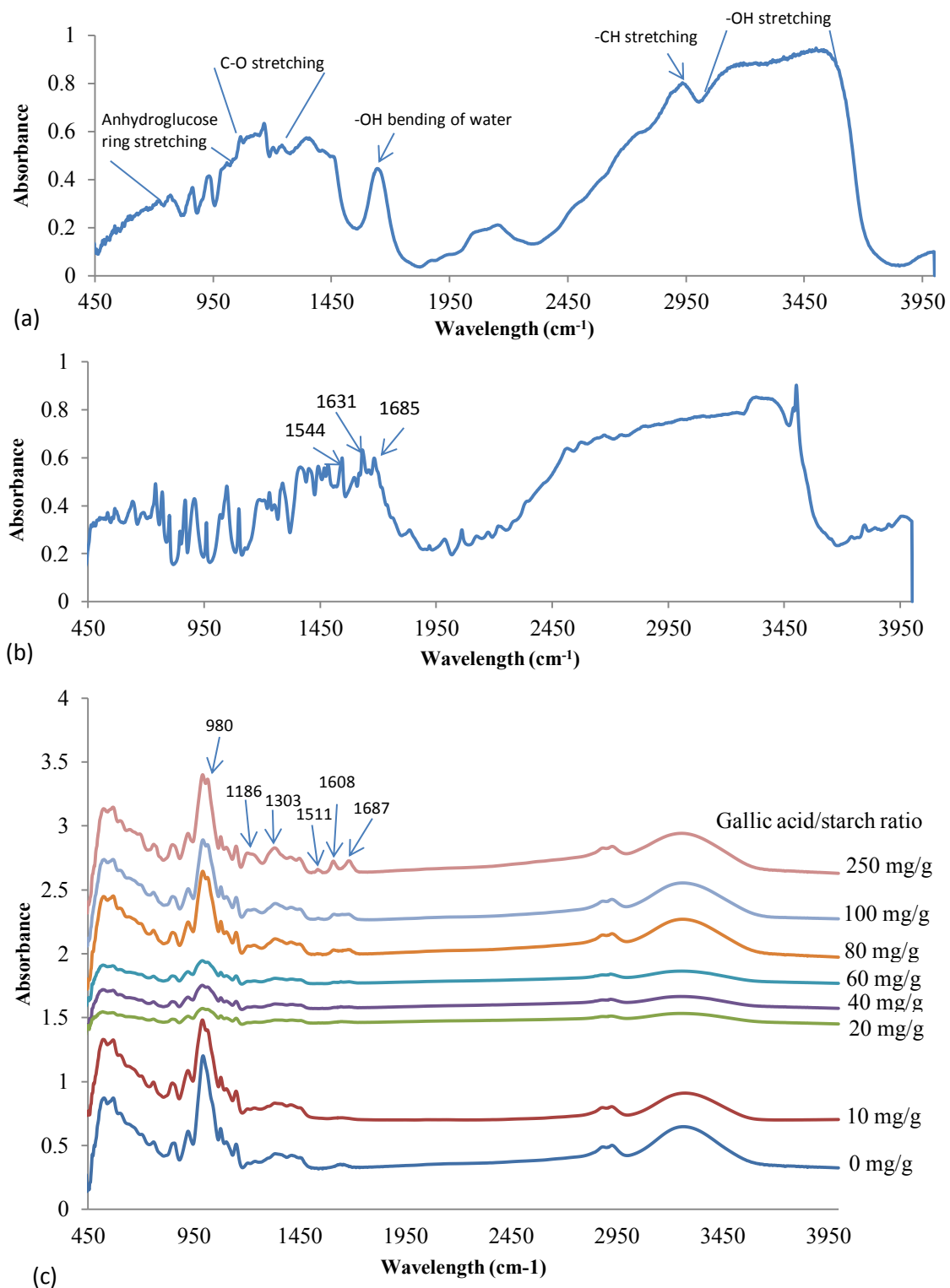
Figure 4.2 FTIR spectra of native potato starch (a), pure gallic acid (b) and bioactive films (c) added with different concentrations of gallic acid at constant glycerol/starch ratio of 0.5 g/g, pressure of 50 bar, and temperature of 100 °C.

According to the X-ray diffraction curves, the crystal structure of starch can be divided into four types, including A, B, C and V type. Of these A (cereal), B (potato and banana), and C-type (peas and beans) are the crystal structures of natural starches, and V type is crystalline and typical of the complexes formed by amylose and lipids (Belgacem & Gandini, 2008).

The crystalline pattern and relative crystallinity (%) of potato starch used in this thesis are shown in Figure 4.3a, which displayed typical B-type X-ray diffraction patterns at 2θ with the first peak around $5.5°$, the second peak near $17°$, and the third peak around $22°$. A small peak around $20°$ was also found, indicating V-type crystallinity that results from interactions of granular monoacyl lipids with single amylose helices, as isolated starch generally has only trace quantities of bound lipids (~0.1%). The XRD pattern and relative crystallinity (11.4%) for potato starch used in this study was typical and consistent with earlier reports (Gani et al., 2014; Guo et al., 2014). The X-ray diffraction pattern of starch is influenced by its origin, environmental growing conditions (e.g. ambient temperature) (Huang et al., 2007a), additives like alcohols and fatty acids, but mainly by the chain length (CL) of amylopectin (A-type CL (23-29 glucose molecules); B-type CL (30-44 glucose molecules)). Starches having CL between 23 and 29 glucose molecules exhibit A, B or C-type patterns (Sajilata et al., 2006). The influences of experimental parameters such as gallic acid/starch ratio on the XRD pattern and relative crystallinity (%) of bioactive films were not studied before. The XRD diffractogram of formulated films and are shown in Figures 4.3b. It is clear that bioactive films produced from starch have different XRD patterns compared to the native potato starch. From Figure 4.3b, the predominant type of crystallinity changed from B type in native starch to

V-type with the addition of gallic acid. Although there is no significant change in the relative crystallinity until the highest gallic acid ratio (250 mg/g) was used, the change in crystalline type indicates new interactions, or reactions between starch and additives (e.g. gallic acid) that occurred during film production.
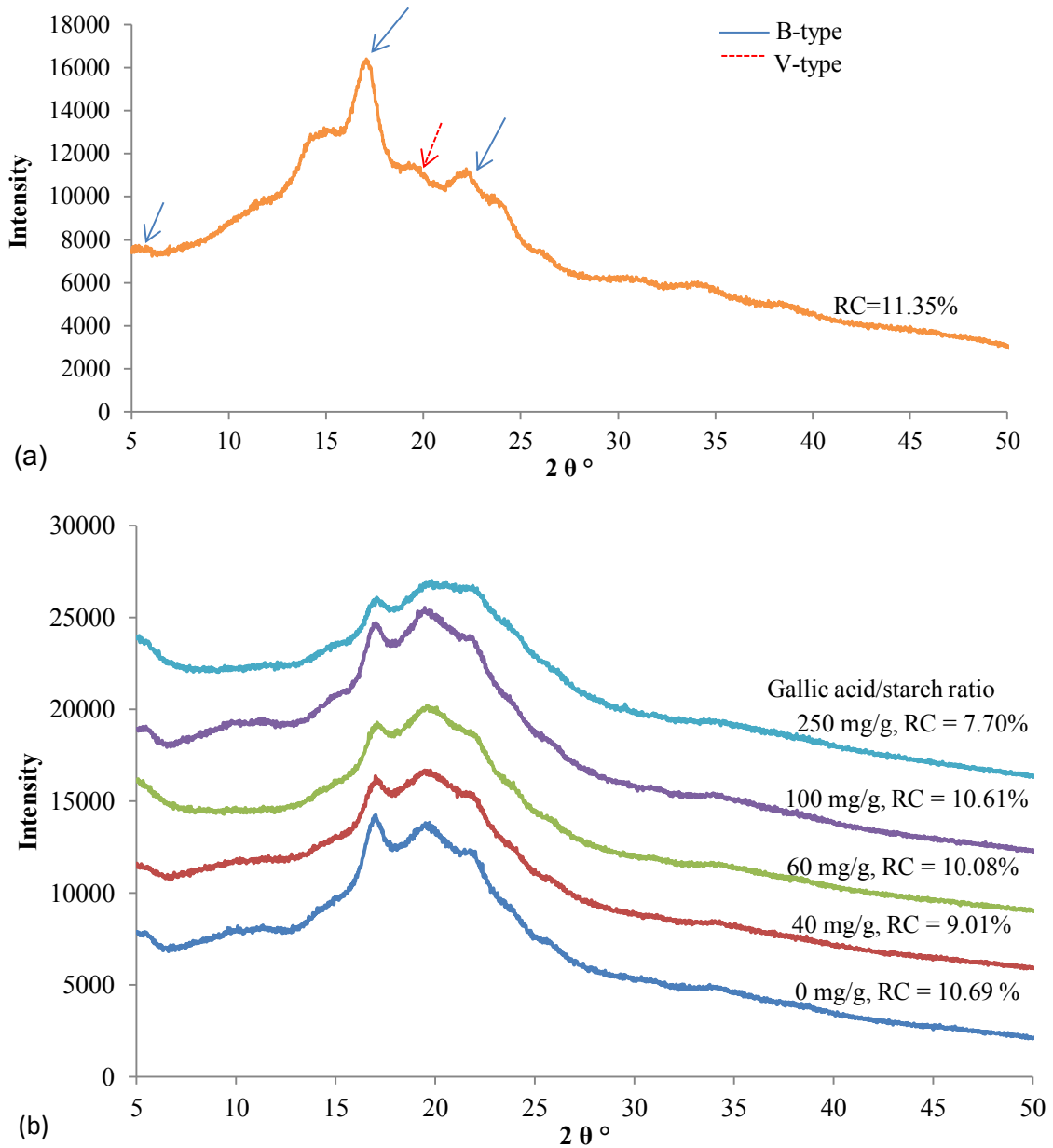
Figure 4.3 XRD and relative crystallinity (RC, %) of unmodified native potato starch (a) and bioactive films (b) added with different concentrations of gallic acid at constant glycerol/starch ratio of 0.5 g/g, pressure of 50 bar, and temperature of 100 °C.

4.3.1.2 Mechanical properties of starch films with different gallic acid/starch ratio

Based on the preliminary study (Appendix B, Section B2), an initial experimental condition (temperature=100 °C, pressure=50 bar, and glycerol/starch ratio=0.5 g/g) was selected to evaluate the effect of different gallic acid concentrations added into the film forming solution to determine the optimum concentration of gallic acid that leads to the best mechanical properties of tensile strength and elongation. Modification of bioactive starch films with gallic acid/starch ratio from 10 to 60 mg/g resulted in films with tensile strength of 5.9-7.25 MPa (Figure 4.4). On the other hand, film elongation decreased significantly when modified with 20 to 40 mg gallic acid/g starch. However, with the addition of higher concentrations of gallic acid from 60 to 100 mg/g, elongation increased. Sun et al. (2014) preparing chitosan/gallic acid films also showed the same trend, TS increase 13 to 23 MPa when increased from gallic acid addition increased from 0 g to 0.5g/100g solution. Accordingly, the addition of a higher concentration (1.5 g/100g) of gallic acid led to a significantly decrease of TS of the chitosan film (9 MPa). In their study, the elongation % of film decrease from 33 % to 11% after addition of gallic acid. They concluded the reason for the highest TS among the films after adding a relatively lowe dose of gallic acid was due to the formation of intermolecular hydrogen bonding between the NH_3^+ of the chitosan backbone and the OH^- of gallic acid (Sun et al., 2011).

Therefore, high TS of films formed by starch and glycerol could also be attributed to the hydrogen bonding between the –OH on stach backbone and the –OH of gallic acid. In addition, this trend suggests that a low concentration of gallic acid may induce anti-plasticizer effect, which was described by Seow et al. (1999) as an enhancement of the glass transition temperature of a material by addition of low concentration of low-

molecular mass (e.g. water, glycerol), which increased the order, compactness, rigidity and brittleness of polymeric system.

However, further addition of plasticizer beyond a critical limit decreases this anti-plasticizer effect. In case of starch film, antiplastizicier effect starts to increase the rigidity and reduce the flexibility of film, and then the plasticized film gets even stiffer than the non-plasticized starch film (Chang et al., 2006). One explanation for anti-plasticization effect is that when a low concentration of gallic acid is used with starch solution, gallic acid binds starch molecules tightly and occupies the sites initially taken by water molecule and therefore reduces the mobility of starch fragments in the solution, forming a rigid film (Mali et al., 2008). These results led to the conclusion that gallic acid can be cross-linked to starch, and also can act as a plasticizer when added at high concentrations. A similar trend on film mechanical properties was reported by Rachtanapun and Tongdeesoontorn (2009), when 400 mg of gallic acid was added to a rice flour/cassava starch blended film at 80 °C. Although their film obtained with 400 mg gallic acid and sorbitol as plasticizer had a similar tensile strength (6-8 MPa), when compared with 40 mg gallic acid/g starch obtained at subcritical condition. However, the film elongation % was 10-15%, significantly lower than films prepared in this thesis (40-76%). Based on these properties, 40 mg gallic acid/g starch was selected as the optimal ratio for both mechanical properties of tensile strength and elongation %.

(a)   **(b)**
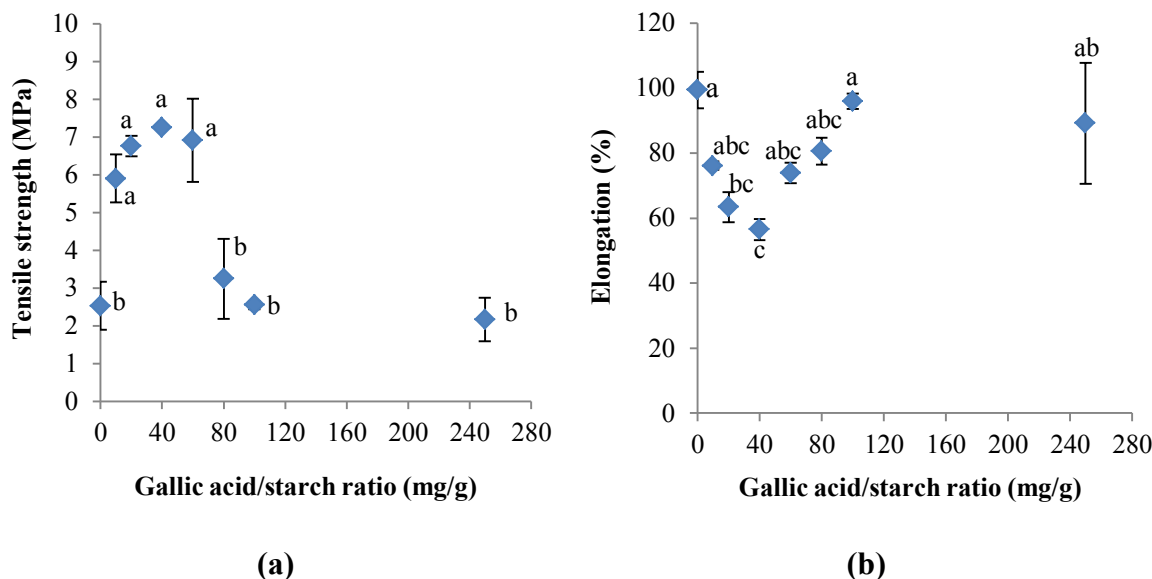
Figure 4.4 Tensile stress (a) and elongation percentage (%) (b) of bioactive films added with different concentration of gallic acid, at glycerol/starch ratio of 0.5 g/g, pressure of 50 bar, and temperature of 100 °C. Data followed by the same letter are not significantly different at $p > 0.05$. Value of each data point is reported in Table B.3 in Appendix B.

4.3.1.3 Water activity, moisture content and water solubility of starch films with different gallic acid/starch ratio

Water activity (a_w) measures the availability of water that can take part in any chemical reaction (Feng et al., 2015), while moisture content indicates the overall water content in the sample. High moisture content does not guarantee higher water activity as the water could be bound and difficult to be used in the reaction. It is known that a_w is one of the basic properties of a food that exerts major influence on microbial survival and growth (Beuchat et al., 2013; Farakos et al., 2013), the reduction of water activity of food below 0.85 can reduce most bacterial growth. Water activity and moisture content of bioactive films with different concentrations of gallic acid are shown in Figures 4.5. There is no significant influence of gallic acid/starch ratios on the water activity of films (Table B.4 in Appendix B). Moisture content of starch film with 20, 40 and 250 mg gallic

119

acid /g starch were significantly lower by ~4% than films without gallic acid. Among the

moisture content of films with gallic acid, there is no significant difference between the

moisture content of films with gallic acid/starch ratio from 10 to 100 mg/g. The moisture

content of film with 250 mg gallic acid/g starch was significantly lower by~5% than the

one with 80 mg gallic acid/g starch, which can be due to the structure changes (formation

of V type crystalline) found in XRD results.

| (a) | (b) |
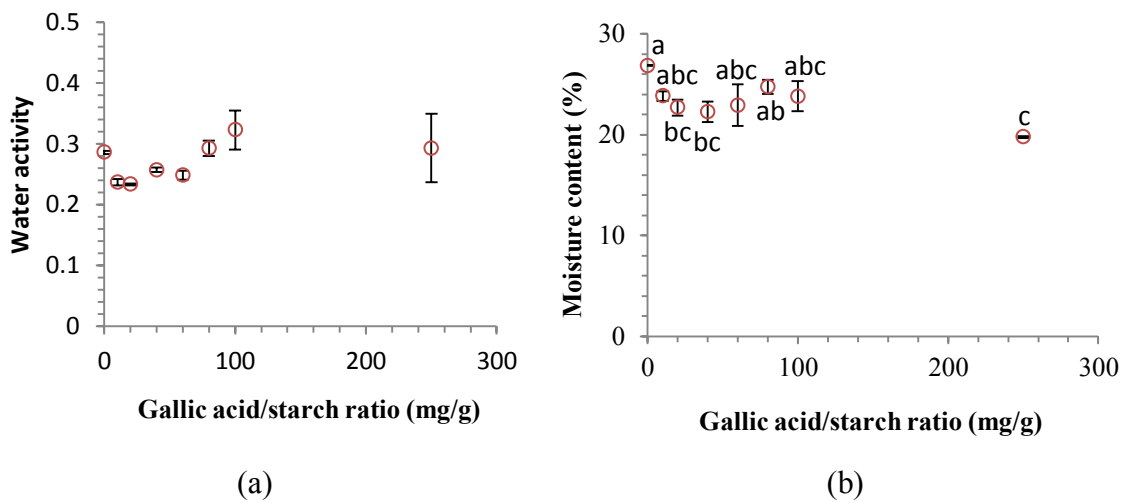
Figure 4.5 Water activity (a) and moisture content (b) of bioactive films added with different amounts of gallic acid at constant glycerol/starch ratio of 0.5 g/g, pressure of 50 bar, and temperature of 100 °C. Data followed by the same letter are not significantly different at p>0.05. Value of each data point is shown in Table B.4 in Appendix B. No significant difference found in water activity.

Water solubility of films is an important factor when choosing a film for specific

applications. When water resistance and integrity are required for packaging food

products with high moisture contents at different storage temperatures, water solubility is

a challenge (Goksu et al., 2007). The water solubility of bioactive starch films with

different concentration of gallic acid at three different temperatures are shown in Figure

4.6. Generally, the effects of additives (e.g. zein, phenolic acids) on the solubility of films

depend on the inherent hydrophilicity and hydrophobicity of additives (Kavoosi, Dadfar,

& Purfard, 2013). The use of hydrophilic compounds such as ascorbic acid (Soon-Do, 2014), and phenolic acid increase solubility of film in water, whereas hydrophobic compounds such as zein (a protein from maize) make the surface of film water-proof and less soluble (Takahashi et al., 2002). Takahashi et al. (2002) was able to produce a zein-carboxymethyl starch conjugate film, which was almost insoluble in hot water from 50 to 90 °C for the time period tested (15 min).

In this study, solubility of films with different amounts of gallic acid in water followed this trend, that is increasing the amount of gallic acid added increased the hydrophilicity of the film and therefore increase its solubility in water (Figure 4.6). A significant increase of ~14% on solubility of the film at all temperatures investigated was only found when 250 mg/g gallic acid was added.
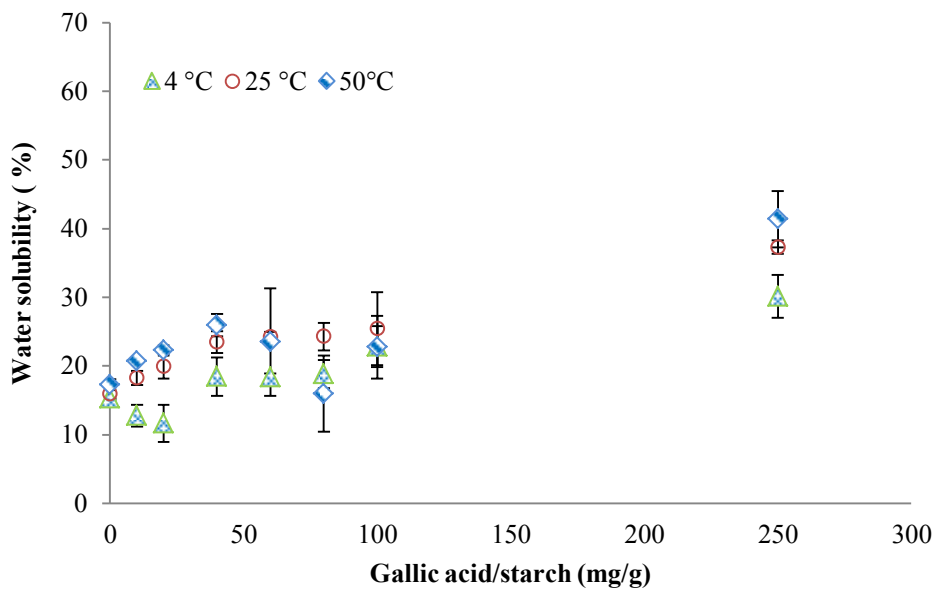
Figure 4.6 Solubility of bioactive films added with different amounts of gallic acid in water at 4, 25 and 50 °C at a constant glycerol/starch ratio of 0.5 g/g, pressure of 50 bar, temperature of 100 ℃ . Tukey's test results in Table B.5 in Appendix B.

4.3.1.4 Optical and morphological properties of starch films with different gallic acid/starch ratio

Figure 4.7 shows WI of bioactive starch films, containing various amounts of gallic acid. Besides, the addition of gallic acid had no significant influence on total color difference (ΔE) and yellowness index (YI) (Table B.6 in Appendix B). In general, the transparency is affected by various factors, including the thickness of the film, and concentration of additives (Bangyekan et al., 2006). Color and translucency are also important when using as packaging materials (Ibrahim et al., 2014). More transparent films can be made with the addition of gallic acid at 100 mg/g or higher as low transparency value means high transparency. However, due to large variation in the translucency values of films, there is no significant difference found among films (Table B.7 in Appendix B). In terms of whiteness index, a significant reduction was found only with gallic acid/starch ratio around 40 mg/g. In general, the color of films with gallic acid added was less white.
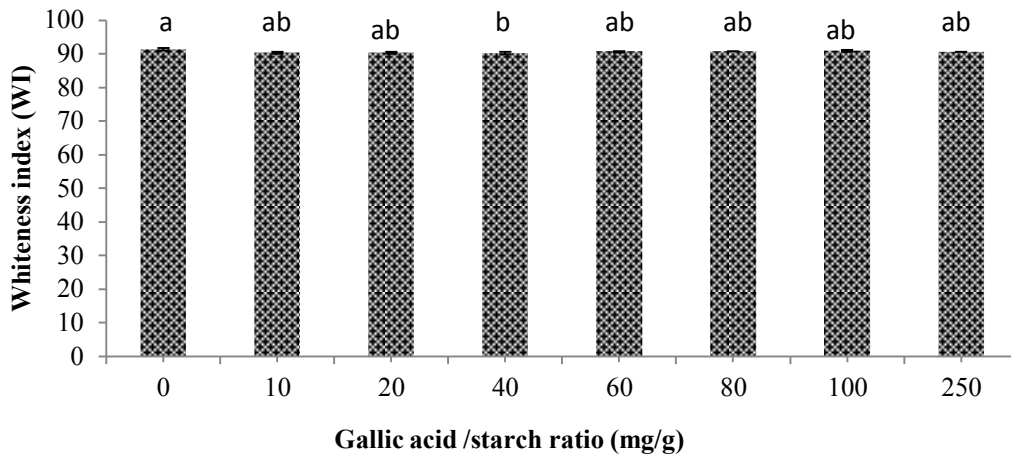
Figure 4.7 Whiteness index of bioactive films added with different amounts of gallic acid at constant glycerol/starch of 0.5 g/g, pressure of 50 bar, and temperature of 100 °C Data followed by the same letter are not significantly different at p>0.05. Value of each data point is shown in Table B. 6 in Appendix B.

A better understanding of the surface of bioactive films can help design and adjust its application in the industry. In this study, differences on the surface texture were visually observed and therefore, contact angle and gloss on both sides of the film were measured. Results from SEM of the films also confirmed the difference between the top and bottom sides of the films and several layers were observed in the cross section of the films. Gloss of film is related to the smoothness of the film surface. Studies (Bitencourt et al., 2014; Jiménez et al., 2012a) suggested that starch films tend to crystallize during film formation and the crystals near the film surface could reduce its smoothness, decreasing the gloss. A study conducted by Jiménez et al. (2012b) also indicated that crystals are heterogeneously distributed, resulting in a different degree of roughness in the different surface zones.

The shape and surface of potato starch and the other phenolic acids used are shown in Figure 4.8a-b. Potato starch has an oval shape and smooth surface with different sizes of starch granules. Gallic acids showed a stick like shape. The shapes of these raw materials changed and exerted different appearances after forming the bioactive films (Figure 4.8c-g). With the addition of gallic acid /starch ratio from 10 to 250 mg/g, the surface as well as the cross section of bioactive films became more homogeneous and smoother, with less bumps (incompletely gelatinized starch granules)(Figure 4.8c-f). However, phase separation and recrystallization of gallic acid could occur if high concentrations (400 mg/g) were added (Figure 4.8 g2).
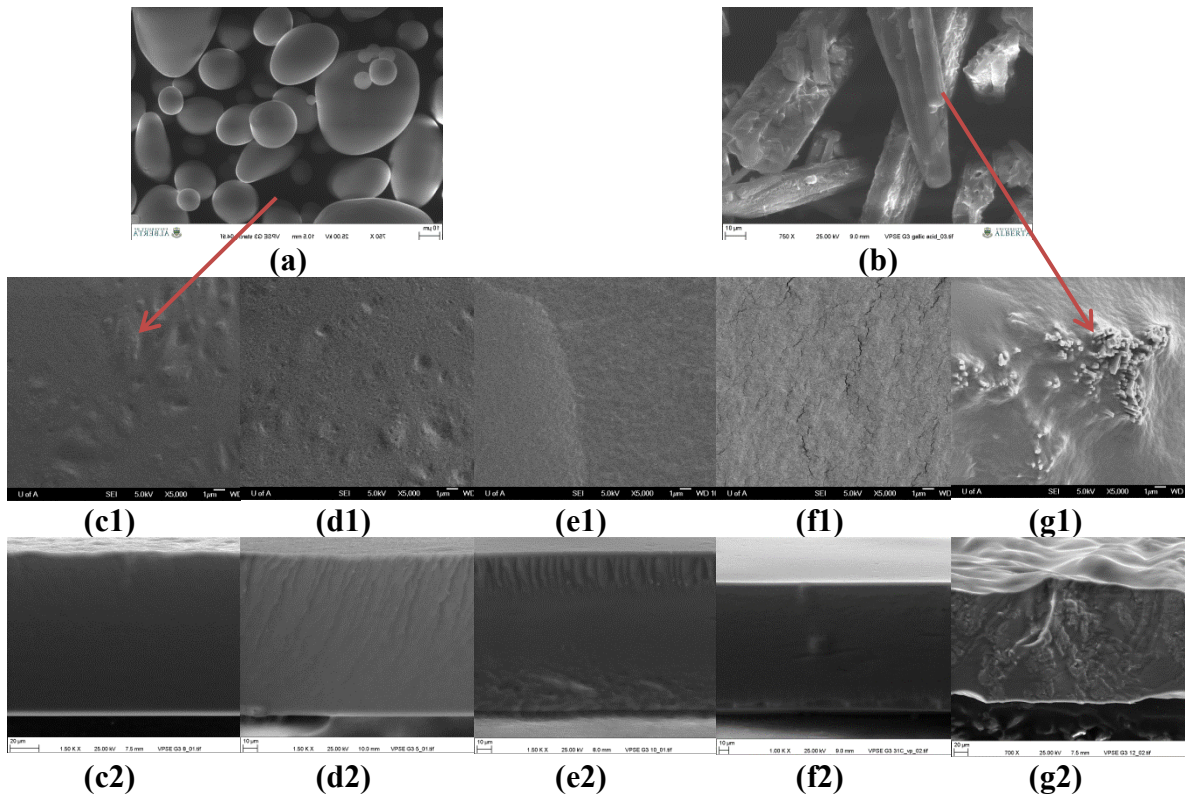
Figure 4.8 SEM images of pure native potato starch (a), gallic acid (b) and bioactive films added with different amounts of gallic acid (c:0, d:40, e:100, f:250, g:400 mg/g starch) at constant glycerol/starch ratio of 0.5 g/g, pressure of 50 bar, and temperature of 100 °C. (a-b: surface images captured without coating at 750 magnification under VP mode; c1-g1: surface image captured with gold coating at 5000 magnification, c2-g2: cross section images captured without coating at 1000 magnification under VP mode).

The roughness of films with different gallic acid/starch ratio also reflected on the gloss value of the surface of films measured (Figure 4.9). As gloss value indicates the roughness of the surface, film with smoother surface will have a higher gloss value (Yonehara et al., 2004). With the addition of gallic acid, the gloss of both sides of the film increased and the difference is reduced significantly at high concentrations of gallic acid where the film became smoother (Figure 4.9a). Similar gloss value (73 GU) was also obtained in a study that used corn starch (2% w/w water), glycerol (0.25g/g starch) and stearic acid (0.15g/g starch) to form a film at 95 °C for 30 min (Jiméneza et. al., 2011). On the other hand, the contact angle measurement provides a quantitative way to

124

characterize wettability of starch films. An increase in contact angle with water suggests an improvement of the hydrophobic character of the film surface (Muscat et al., 2013). In Figure 4.9b, no significant difference in the contact angle on both sides of the formulated starch film was observed. Also, the addition of gallic acid had no influence on the contact angle. High contact angles ($\theta > 70°$) indicate a hydrophobic surface and low contact angles ($\theta < 20°$) indicate a hydrophilic surface (Tang & Jiang, 2007).

Therefore, surfaces on both sides of the films formed in this study were considered as hydrophobic, which was attributed to the crosslinking of gallic acid to starch molecules through hydrogen bonding and reduce the availability of -OH groups on starch molecule with water. However, from the solubility data discussed in Section 4.3.2.4, the hydrophobicity of the film surface cannot be maintained for more than 24 h as ~24% of the film was dissolved in 24 h, which indicated the bonding in the film between starch and additives (e.g. gallic acid and glycerol) were not stable and can be interrupted during the time. Therefore, applying stronger crosslinking agent and/or adding hydrophobic substances (e.g. zein, fatty acids) during film formulation could be used to improve the hydrophobicity of starch film permanently.
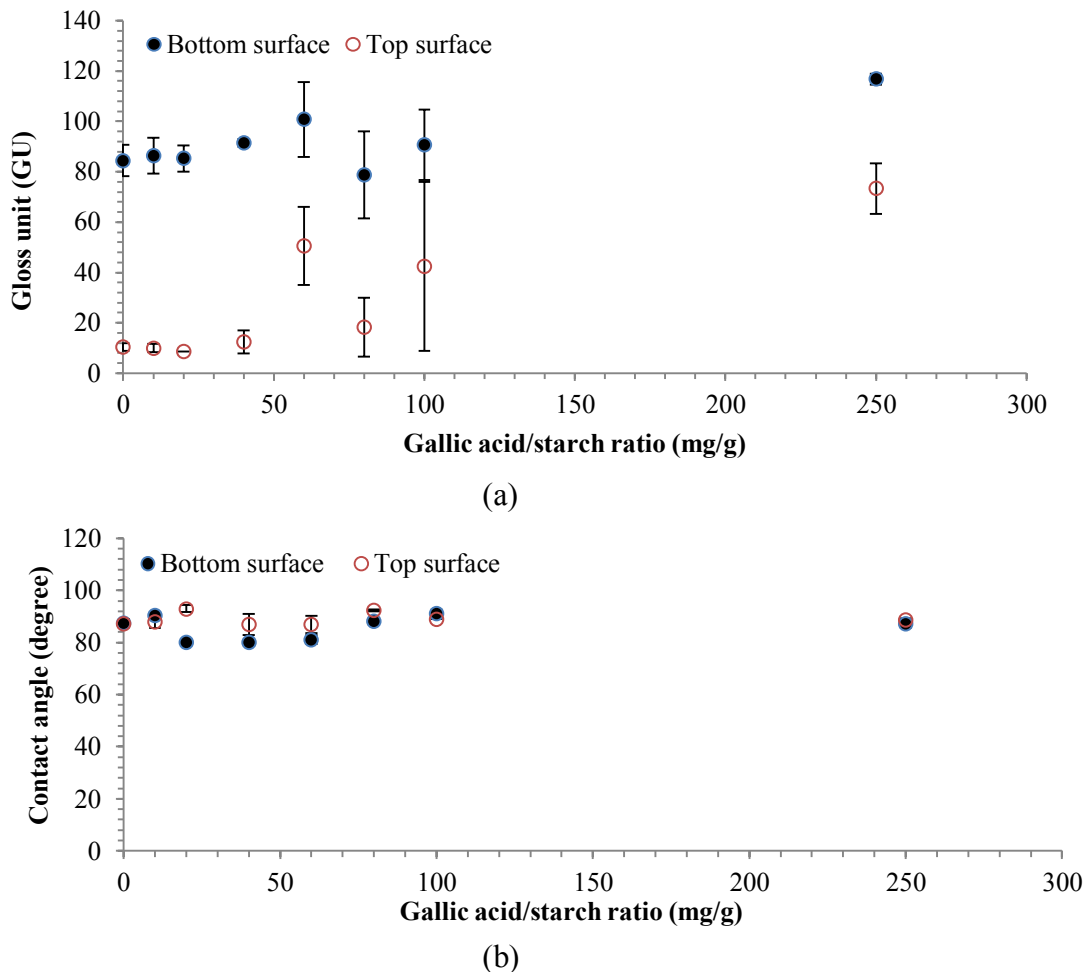
Figure 4.9 Gloss measurements at 60 ° (a) and contact angle (b) for both sides of bioactive films added with different amounts of gallic acid at constant glycerol/starch ratio of 0.5 g/g, pressure of 50 bar, temperature of 100 °C (Bottom surface: smooth part of the film, and top surface: rough part of the film). Tukey's test results in Table B.7-8 in Appendix B.

4.3.1.5 Antioxidant capacity and total phenolic content of starch films with different gallic acid/starch ratio

Antioxidant capacity of bioactive films were determined by analysing the film dissolving solution (ethanol: water =1:1 v/v) by three different techniques, ABTS, DPPH, and FRAP. These techniques are widely used in the literature for determination of antioxidant activity of edible films, and thermoplastic films (Baheiraei et al., 2014;

Blanco-Pascual et al., 2014; Bremer Boaventura et al., 2013; Ruiz-Navajas et al., 2013; Samsudin et al., 2014; Vidhu & Philip, 2015). The final antioxidant capacity for each analysis was converted to trolox equivalent antioxidant capacity (TEAC) for comparison. TEAC value and total phenolic acid content of films incorporated with different amounts of gallic acid are shown in Figure 4.10. As expected, TEAC value as well as total phenolic content released from films increased significantly along with the higher gallic acid/starch ratio added to the film. The releasing amount of gallic acid from film into the dissolving ethanol/water moisture were proportional (~50%) to the amount of gallic acid added into the films (Figure 4.10d). As the dissolving process has been performed for 24h, free or weakly bounded gallic acid was released to the solution. Therefore, the remaining 50% gallic acid can be physically trapped beneath the film network which requires a longer dissolving time to release, or it can be chemically crosslinked to the starch molecules through covalent bonds, like condensation reaction between the –OH of the gallic acid with the -OH of the starch within the presence of a catalyst, subcritical water. However, variations were found among these three different techniques, DPPH provided a lower TEAC value, while ABTS provided a higher value compared to FRAP.
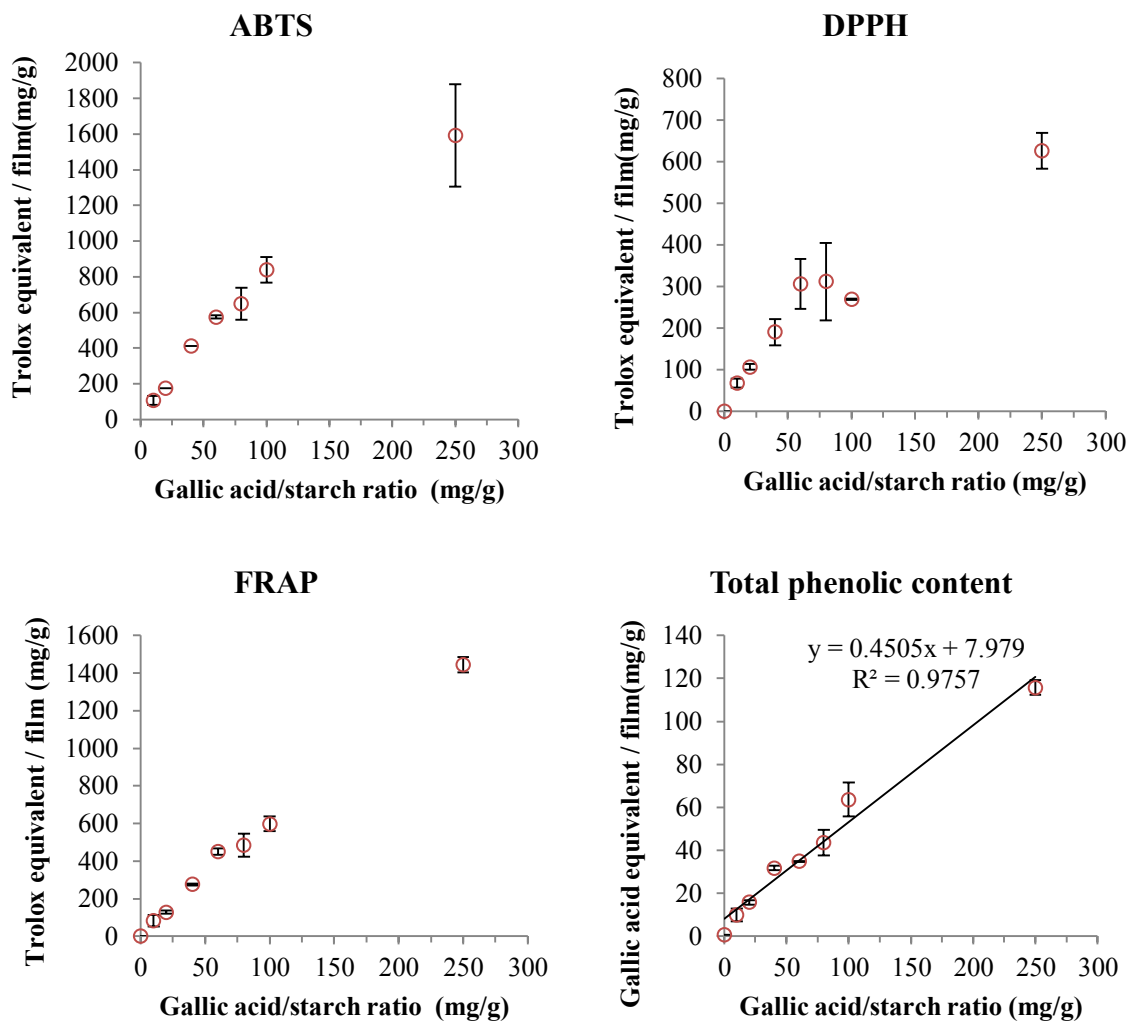
Figure 4.10 Antioxidant activity and total phenolic content of bioactive films added with different concentrations of gallic acid at constant glycerol/starch ratio of 0.5 g/g, pressure of 50 bar, temperature of 100 °C. Tukey's test results are shown in Table B.9 in Appendix B.

4.3.2 Effect of temperature on the properties of starch films

4.3.2.1 Structural properties of starch films obtained at different temperatures

Increasing the temperature during film formation could reduce the intensity of interactions between starch molecules, gallic acid and glycerol. As shown in Figure 4.11, the intensity of peaks around a wavelength of 970 cm^{-1}, which is related to entire anhydroglucose ring stretching vibrations in starch, was significantly reduced after

128

heating at temperatures above 100 °C (Figure 4.11), suggesting the loss of interactions by depolymerization.
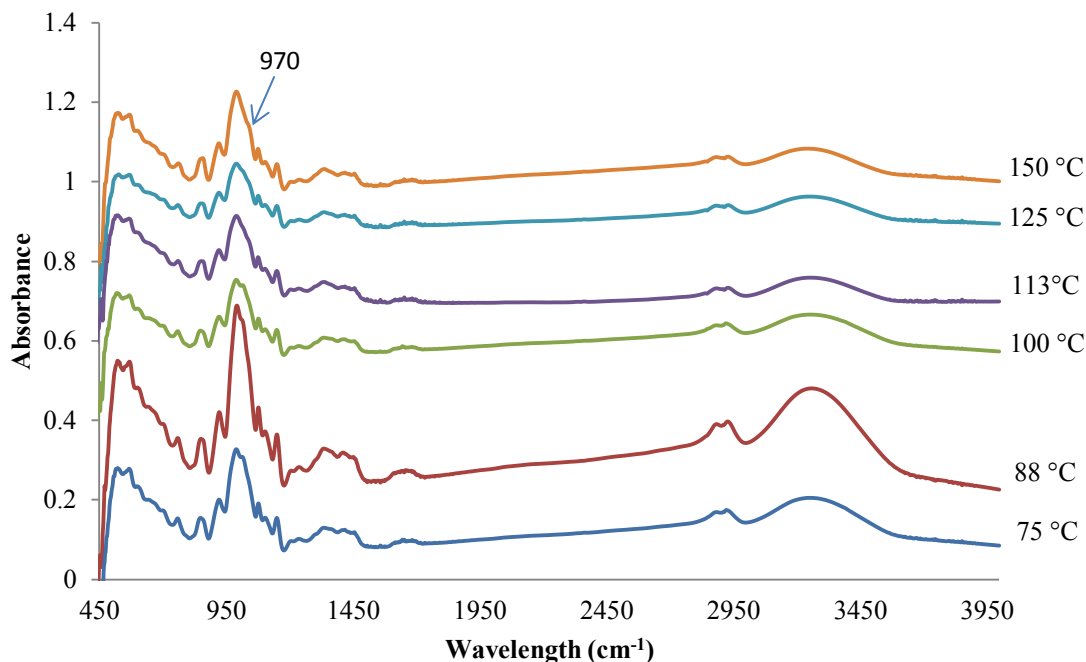
Figure 4.11 FTIR of bioactive films produced at different temperatures and constant glycerol/starch ratio of 0.5 g/g, gallic acid/starch ratio of 40 mg/g, and pressure of 50 bar.

The influence of temperature on the XRD and RC (%) of bioactive films was more severe at 150 °C. From Figure 4.12, different types of peaks were observed as well as high RC (%) values (increase of ~6%), which results from hydrolysis of starch induced by high temperature. New crystalline types were formed when starch molecules depolymerized to different chain lengths. As the gelatinization temperature of potato starch is around 69 °C, the peak of the film produced at 75 °C of a higher temperature showed a broad peak area compared to native starch, indicating rupture of starch granules during gelatinization, which exposed the −OH groups on starch for further crosslinking with gallic acid and glycerol.
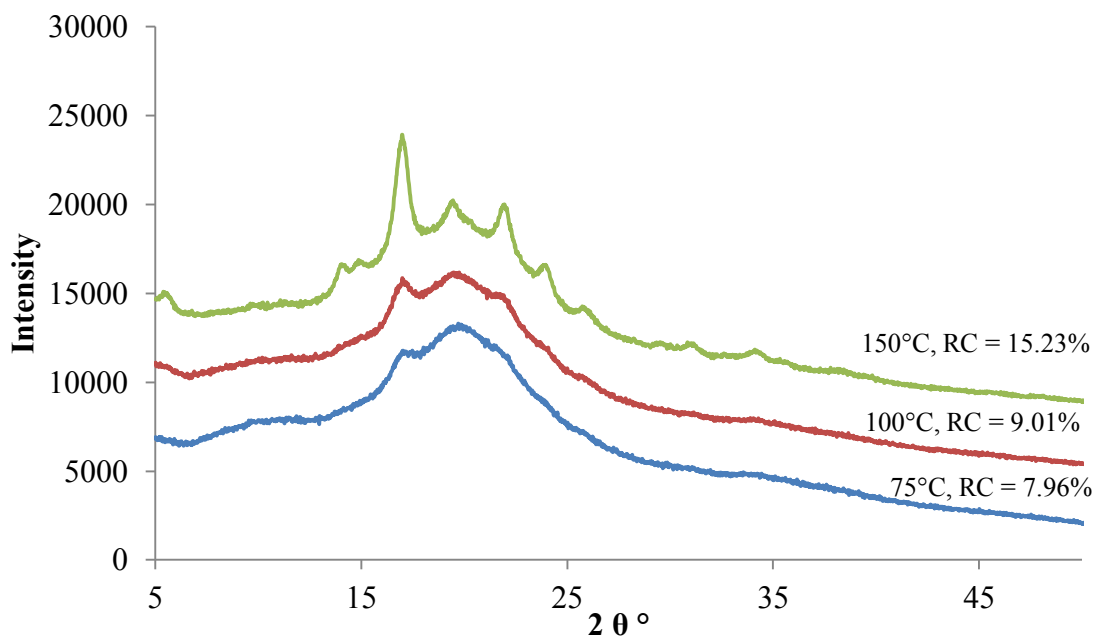
Figure 4.12 XRD and relative crystallinity (RC, %) of bioactive films produced at different temperatures and constant glycerol/starch ratio of 0.5 g/g, gallic acid/starch ratio of 40 mg/g, and pressure of 50 bar.

4.3.2.2 Mechanical properties of starch films obtained at different temperatures

As reaction kinetics in water, especially subcritical water is enhanced by increasing temperature (Rogalinski et al., 2008). With increasing temperature, more interactions between starch molecules and gallic acid, or other acids could have accelerated hydrolysis reaction or depolymerization. The effect of temperature on tensile strength and elongation of bioactive films is shown in Figure 4.13. With an increasing curing temperature, TS significantly increased from 75 to 100 °C, but then significantly decreased after 100 °C. On the other hand, %E significantly decreased with an increasing temperature. As the heating time of 10 min was kept constant for all experiments, the changes in TS and E (%) could be due to different degree of gelatinization as well as hydrolysis of amylose and amylopectin induced by different temperatures applied. High temperature causes a more severe hydrolysis on starch molecules, which reduces the

130

chain length that is essential for the formation of strong association between amylose and amylopectin (Fujio et al., 1995). During this overheating condition (above gelatinization temperature of starch), free amylose and amylopectin of the starch granules are leached out with water, causing serious deformation and rupture. Shorter chain length can also create less space for mobility of a plasticizer and reduce the flexibility of film. In this study, a temperature around 100 °C provided the best mechanical properties and therefore, it was selected as the optimum temperature for bioactive film production.

(a)   (b)
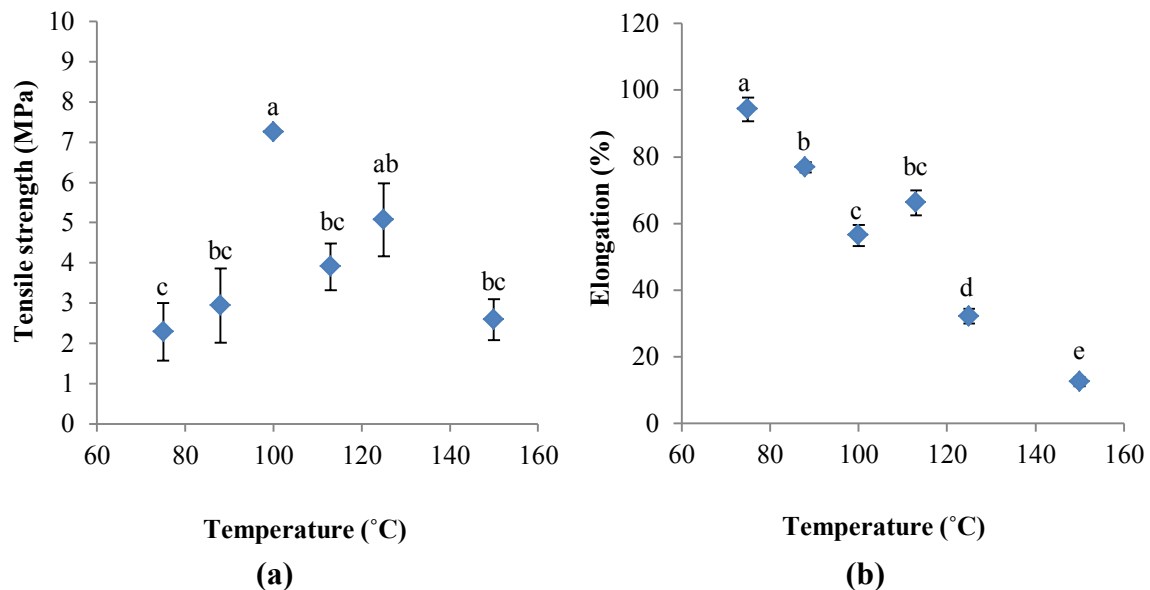
Figure 4.13 Tensile stress (a) and elongation percentage (%) (b) of bioactive films produced at different temperatures and constant glycerol/starch ratio of 0.5 g/g, gallic acid/starch ratio of 40 mg/g, and pressure of 50 bar. Data followed by the same letter are not significantly different at p>0.05.Value of each data point is reported in Table B.3 in Appendix B.

4.3.2.3 Water activity, moisture content and water solubility of starch films obtained at different temperatures

Water activity of films significantly increased from 0.25 to 0.33 when heating temperature increase to 88 °C, but there is no significant different in water activity of

131

films treated at other temperatures. The water activities of films formed at temperatures other than 88 °C were around 0.25 to 0.27 (Table B.4. in Appendix B). The moisture contents of films formed at different heating temperatures were all around 22-27%. Significant difference ($p < 0.05$) in moisture content of films was only found between films heated at 100 °C (22%) and 150 °C (27%) (Table B.4. in Appendix B). Depolymerization of starch molecules with an increase of temperature (>100 °C) also facilitated the dissolution of films in water. Significantly higher solubility of films in water were found at 4, 25 and 50 °C, which suggest the integrity of bioactive films produced at 150 °C cannot be maintained when dissolving at these three temperatures, which further confirmed the depolymerization of starch induced by heating temperature (Figure 4.14).
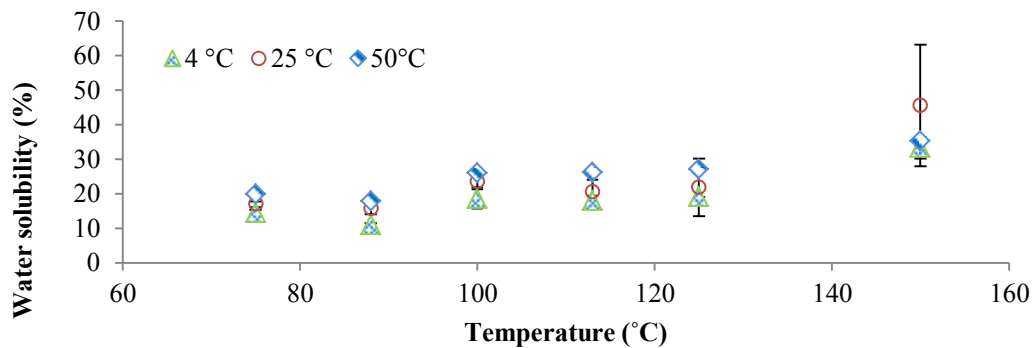
Figure 4.14 Solubility of bioactive films produced at different temperatures in water at 4, 25 and 50 °C at a constant glycerol/starch ratio of 0.5 g/g, gallic acid/starch ratio of 40 mg/g, and pressure of 50 bar. Tukey's test results in Table B.5 in Appendix B.

4.3.2.4 Optical and morphological properties of starch films obtained at different temperatures

Figure 4.15 indicates the influence of temperature on the color and transparency of films. Significant increase on total color difference and yellow index of films produced at

132

150 °C (Figure 4.15a). In addition, a significant reduction of whiteness index of film was only found in films produced at 150 °C (Figure 4.15b). Therefore, the film produced at 150 °C was more yellow and less white compared to films produced at other temperatures. The influence of depolymerization at 150 °C also affects the translucency of film (Figure 4.15c-d). The translucency value of films showed a large variation from 5 to 45 and no significant difference was found with other temperature in transparency value, which indicated film produced at 150 °C was not homogeneous (some parts were transparent, while other parts were opaque) and confirmed by visual observation.
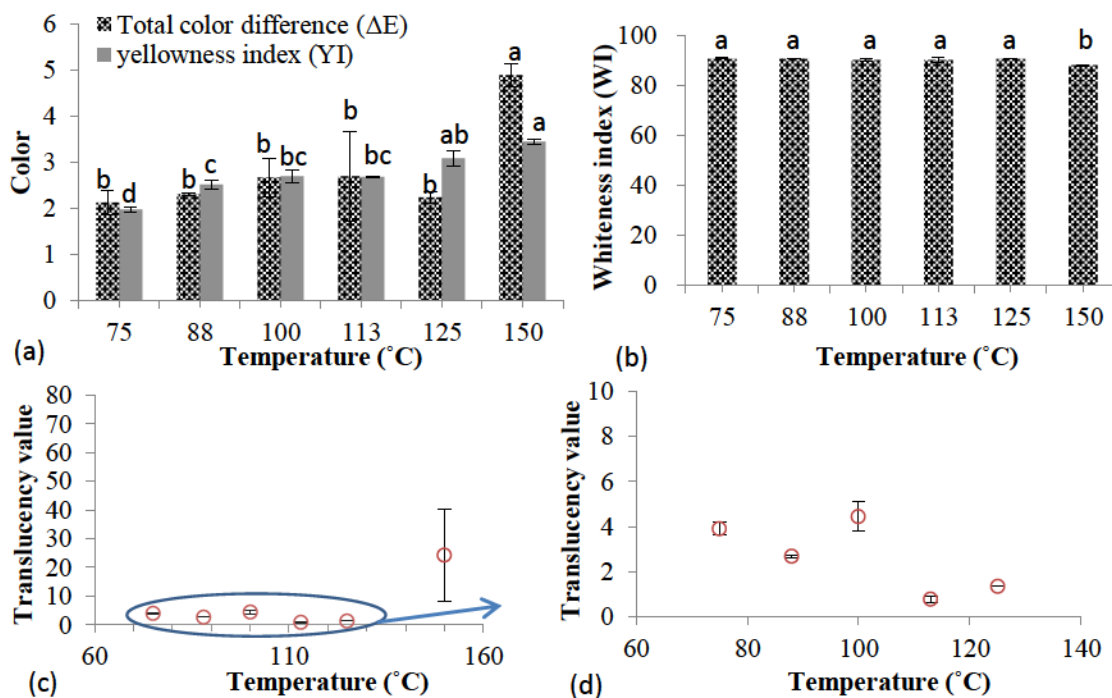
Figure 4.15 Total color difference (ΔE) and yellow index (YI)(a), whiteness (WI) (b) and translucency values (c-d) of bioactive films produced at different temperatures at constant glycerol/starch ratio of 0.5 g/g, gallic acid /starch of 40 mg/g, and pressure of 50 bar. Data followed by the same letter are not significantly different at p>0.05. Value of each data point is shown in Table B.6-7 in Appendix B. No significant difference found in translucency results.

Sufficient heating is necessary for the rupture of starch granules and the production of homogenized films and smooth surface of the film. In terms of contact angle, a

133

temperature of 150 °C significantly increased the contact angle value of the top surface of film, while significantly decrease the bottom one (Figure 4.16b). Significant differences on gloss of films produced at different temperatures were observed in Figures 4.16a. A film produced at the optimum temperature of 100 °C had the highest gloss unit on both sides of the film. In addition, there was no significant difference in the gloss on both sides of the film produced at 113 °C, which suggests homogenized gel formation during gelatinization and uniformed association between starch molecules during retrogradation of the film. This homogenised structure formed at 113 °C could also be responsible the increase on elongation % of the film found in Figure 4.13b. As shown in Figure 4.17, the film surface produced at 75 °C had lots of pits and bumps, which are from incompletely gelatinization of starch granules. However, at 150 °C, depolymerisation occurred, resulting in a porous film surface (Figure 4.17c1), which was consistent with findings of other studies (Liu & Zhao, 1990; Menchavez et al., 2014). In their studies, sponge-like structure on the starch granule were observed after heating potato or corn starch at temperatures from 80 to 100 °C for 5 min, which suggest higher temperatures resulted in further swelling and melting and led to strong deformation of the granules. However, the less porous structure was observed in the cross section, which suggesting the interaction inside the film still strong enough to hold the network from falling apart. As during the drying process of the film, water evaporated from the gel matrix and reduced the distance between starch moles to re-associate. However, depolymerized starch molecules has a short chain-length and could only formed a network with limited size, which cannot fill the space left by water molecules. This phenomenon can be reduced inside the film, as due to gravity, gel from the top layers can fill the space among the lower layer network

134

(Figure 4.17 c2). However, there is nothing to fill the space on the top layer of the gel network created during drying, and resulted in the porous structure seen in Figure 4.17 c1. Therefore, temperature is essential for the formation of homogeneous film structure by controlling the degree of gelatinization as well as depolymerization of starch molecules.

(a)

(b)
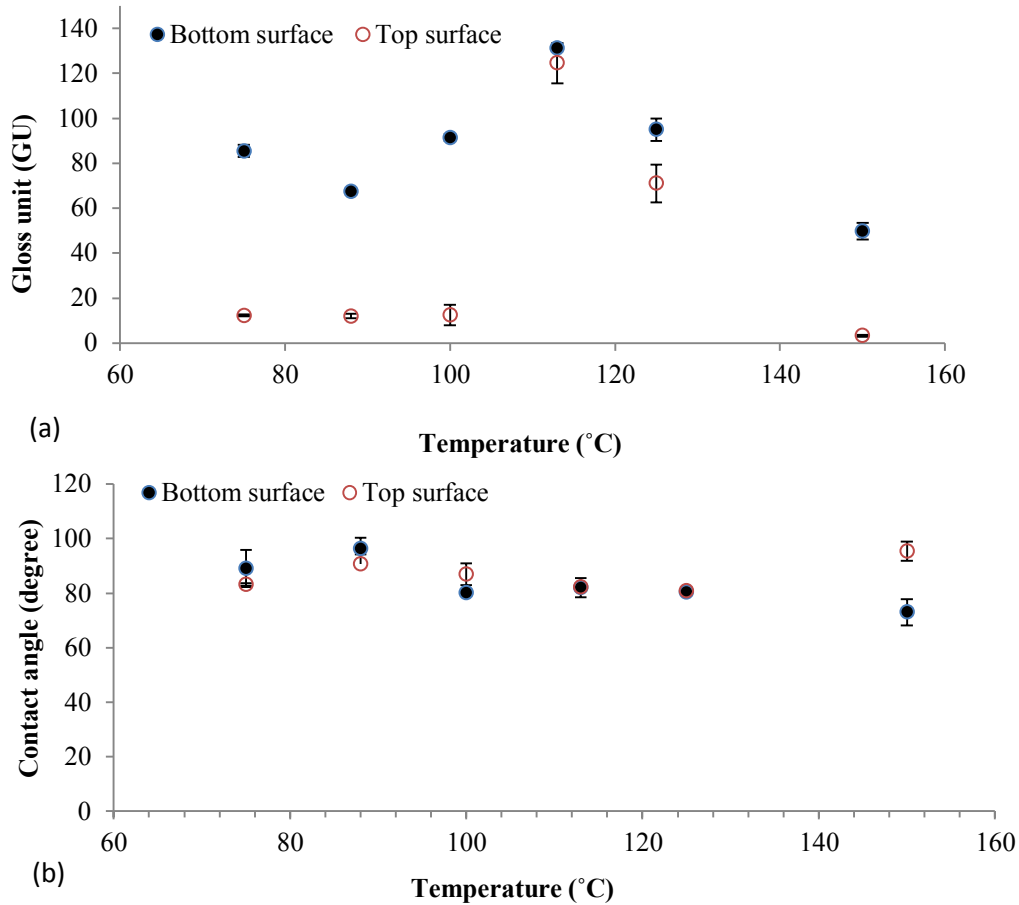
Figure 4.16 Gloss measurements at 60° (a) and contact angle (b) for both sides of bioactive films produced at different temperatures with glycerol/starch ratio of 0.5 g/g, gallic acid /starch ratio of 40 mg/g, pressure of 50 bar. (Bottom surface: smooth part of the film, and top surface: rough part of the film). Tukey's test results in Table B.7-8 in Appendix B.

135
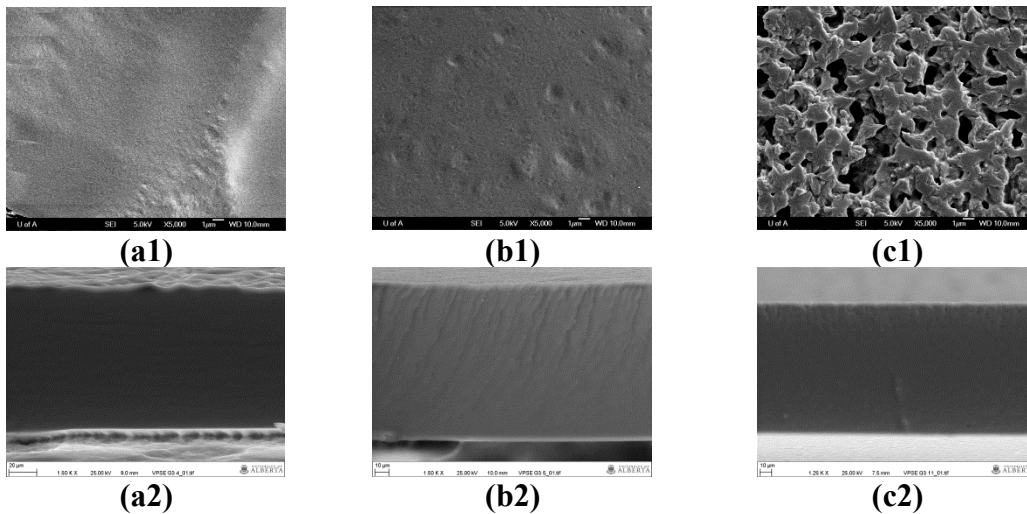
Figure 4.17 SEM images of bioactive films produced at different temperatures (a: 75, b: 100, c: 150 °C) with glycerol/starch ratio of 0.5 g/g, gallic acid/starch ratio of 40 mg/g, pressure of 50 bar. (a1-c1: surface images captured with gold coating at 5000 magnification, a2-c2: cross section images captured without coating at 1500 magnification under VP mode).

4.3.2.5 Antioxidant capacity and total phenolic content of starch films obtained at different temperatures

As shown in Figure 4.18, the film produced at 100 °C had a significant higher antioxidant activity and total phenolic acid released compared to the one produced at 150°C, which further demonstrate the benefit of homogenized gel on the distribution of phenolic acid in the film. As discussed in the above Section 4.3.2.4, the influence of depolymerisation at high temperature was reflected mainly on the surface of the film. Gallic acid from the top layers started to disassociate from the starch molecules during the depolymerisation as confirmed by FTIR and start to accumulate in the lower gel network due to gravity. Therefore, the availability of gallic acid on the surface of the film was reduced and when dissolving this structure in ethanol+water mixture, less gallic acid can be released and resulted in a lower total phenolic content and antioxidant activity.

136

However, gallic acid incorporated in a homogenized gel formed at 100 °C was evenly distributed in the film and give more accessibility to be released.
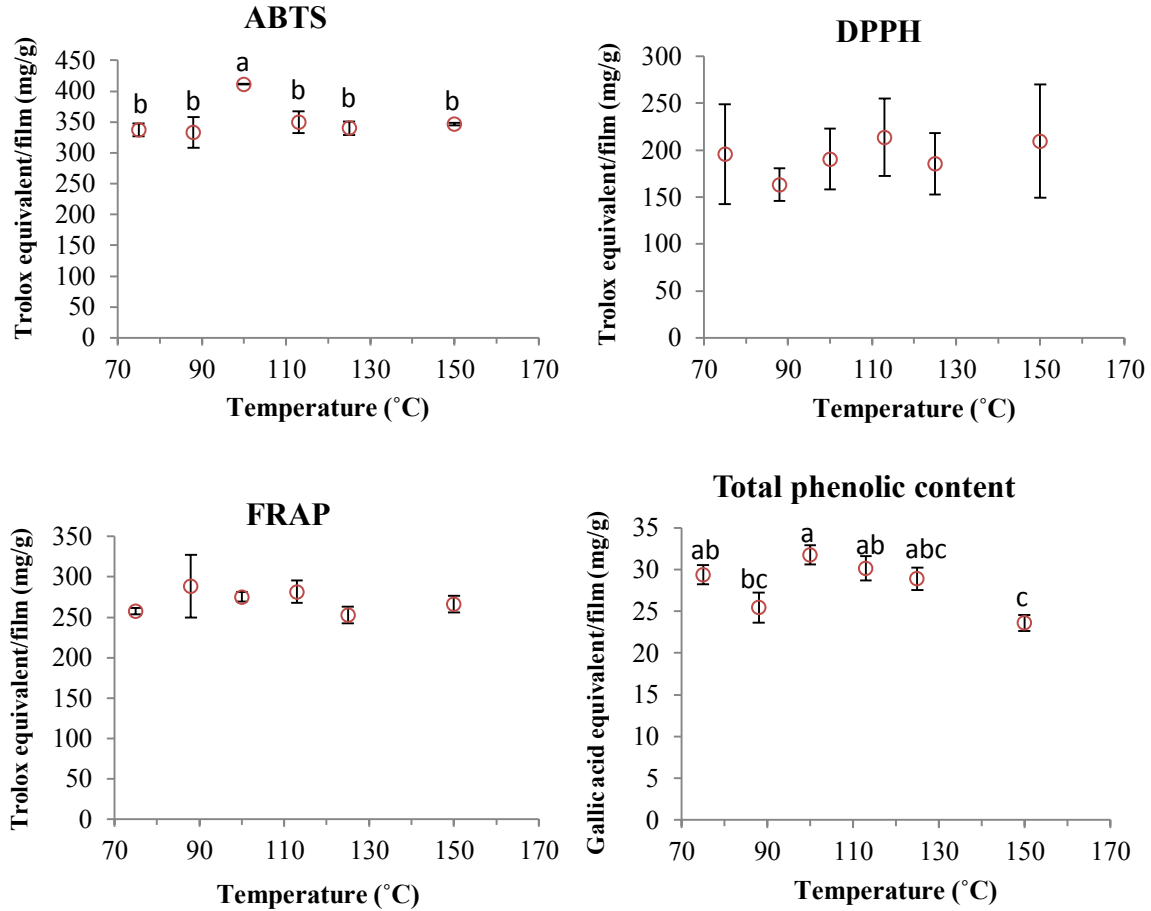
Figure 4.18 Antioxidant activity and total phenolic content of bioactive films produced at different temperatures and constant glycerol/starch ratio of 0.5 g/g, gallic acid/starch ratio of 40 mg/g, pressure of 50 bar. Data followed by the same letter are not significantly different at p>0.05. Value of each data point is shown in Table B.9 in Appendix B. No significant difference found in FRAP and DPPH results.

4.3.3 Effect of glycerol/starch ratio on the properties of starch films

4.3.3.1 Structural properties of starch films with different glycerol acid/starch ratio

The effect of glycerol can be analyzed by comparing the spectra of glycerol-containing films to the control without glycerol. As shown in Figures 4.19a-b, the main

137

peaks located at 1022 and 1100 cm^{-1} of glycerol have shifted to lower wavelength numbers of 1016 and 1076 cm^{-1} for the films, indicating that the addition of glycerol promoted hydrogen bonding interactions among gallic acid, starch and glycerol. However, from the mechanical properties data, if the interaction was too strong, higher than 1.5 g glycerol/g starch, the film had a very poor tensile strength and elongation %. Therefore, if the intensity of the peak at 1022 cm^{-1} is higher than the peak at 985 cm^{-1}, the mechanical properties of the film can be compromised.
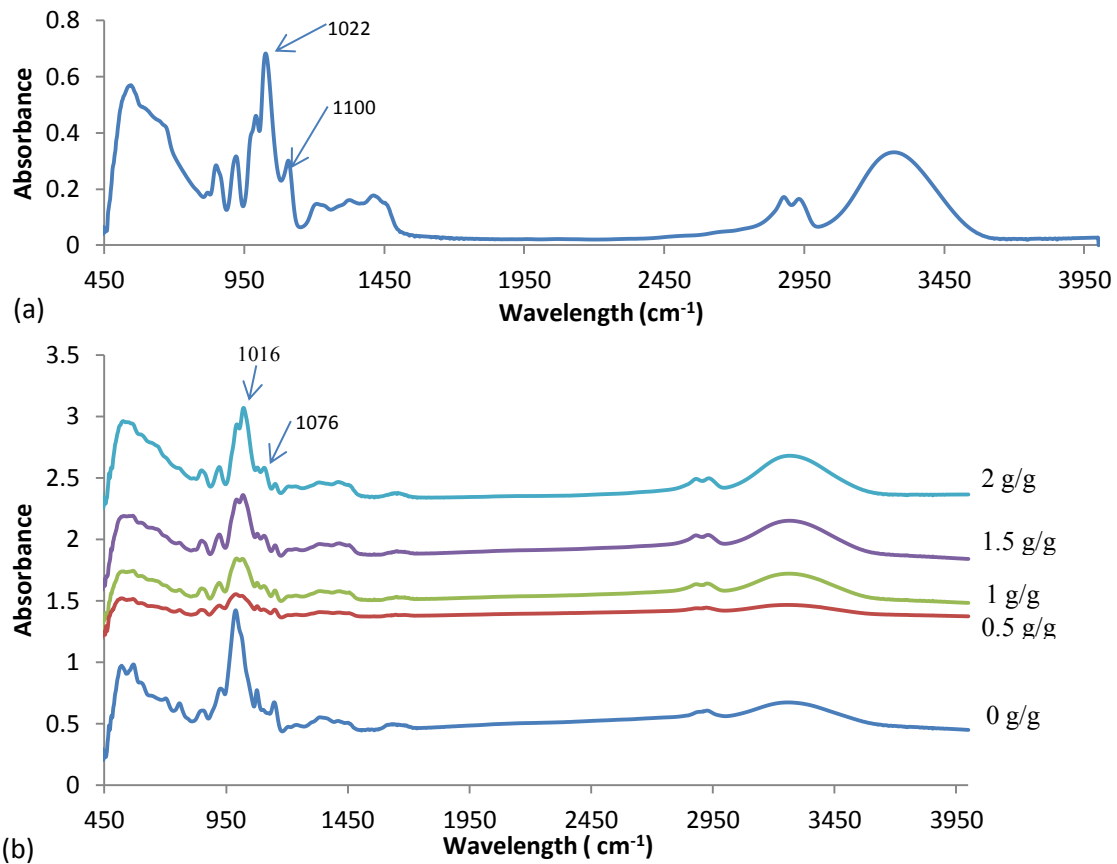
Figure 4.19 FTIR spectra of pure glycerol (a) and bioactive films (b) added with different concentrations of glycerol at constant gallic acid/starch ratio of 40 mg, temperature of 100°C, and pressure of 50 bar.

The XRD of films with different glycerol concentration was shown in Figure 4.20. The signature peak (17°) for B-type crystalline was reduced as glycerol/starch ratio

138

increased. On the contrary, the peak intensity around (20°) for V type crystalline was significantly increased, which suggest the transformation of crystalline type inside the film. It is known that a crystal complex could be formed between glycerol and amylose (Ayala et al., 2014; Goderis et al., 2014), which might account for the changes in crystalline patterns. The complex might alter the association between amylose and amylopectin, and the formation of hydrogen-bonding between glycerol or gallic acid and amylose or amylopectin that occurs in the amorphous phase, generating starch with a more amorphous structure (Qiu et al., 2013). Furthermore, disruption of native crystalline structure during gelatinization and re-crystallization during drying stage (Hu et al., 2009) might be responsible for the changes in crystalline patterns. Even without the use of gallic acid or glycerol, the crystalline patterns differed to that of native starch (Figure 4.3a).
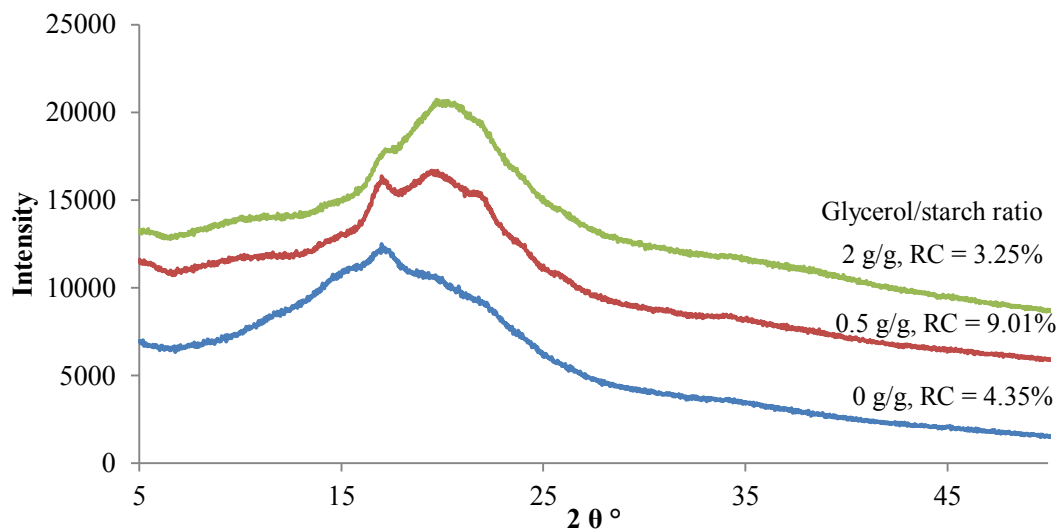
Figure 4.20 XRD and relative crystallinity (RC, %) of bioactive films added with different concentrations of glycerol at constant gallic acid/starch ratio of 40 mg/g, temperature of 100 °C, and pressure of 50 bar.

139

4.3.3.2 Mechanical properties of starch films with different glycerol acid/starch ratio

Plasticizers, such as sorbitol, and glycerol, are low molecular weight compounds with several hydroxyl groups. Therefore, they can easily penetrate inside starch granule and increase the free volume of the amorphous phase and reduce interactions between the starch polymer chains (Myllarinen et al., 2002). The effect of adding glycerol on the tensile strength and elongation of bioactive films is shown in Figure 4.21.

Bioactive films without the use of glycerol became brittle (E% close to 0), but very strong with TS around 52 MPa. With an increase in glycerol concentration, TS decreased significantly and E% increased significantly from 0 to 60%. Since plasticizers reduce the intermolecular interactions and increase the amount of hydrogen bonding. Polar groups (−OH) of the plasticizer are believed to form polymer–plasticizer hydrogen bonds, replacing polymer–polymer interactions and hence leading to lower values for tensile strength, which have been found in glycerol cross-linked gliadin-based film (Soares & Soldi, 2010).

Optimum concentration of plasticizers in the mixture can be critical to exert and maintain the plasticiser effect (Godbillot et al., 2006; Pushpadass & Hanna, 2009). Films with more glycerol (≥1.5 g/g in this thesis) had a sticky texture and were very breakable. In other studies (Cerqueira et al., 2012; Saiah et al., 2009), the amount of plasticizer (e.g. glycerol) added into polysaccharides (e.g. galactomannan, wheat flour) film–forming preparations varies between 10 and 60% by weight of the polysaccharide. Although gallic acid can also act as a plasticizer, 40 mg gallic acid/g starch (4% w/w) was used in this study, which is lower than the percentage (10-60%) required，exerting plasticization

effect. Therefore, 0.5 g glycerol/g starch was chosen as the optimum ratio to evaluate the

mechanical properties (Figure 4.21).

(a)

(b)

(c)
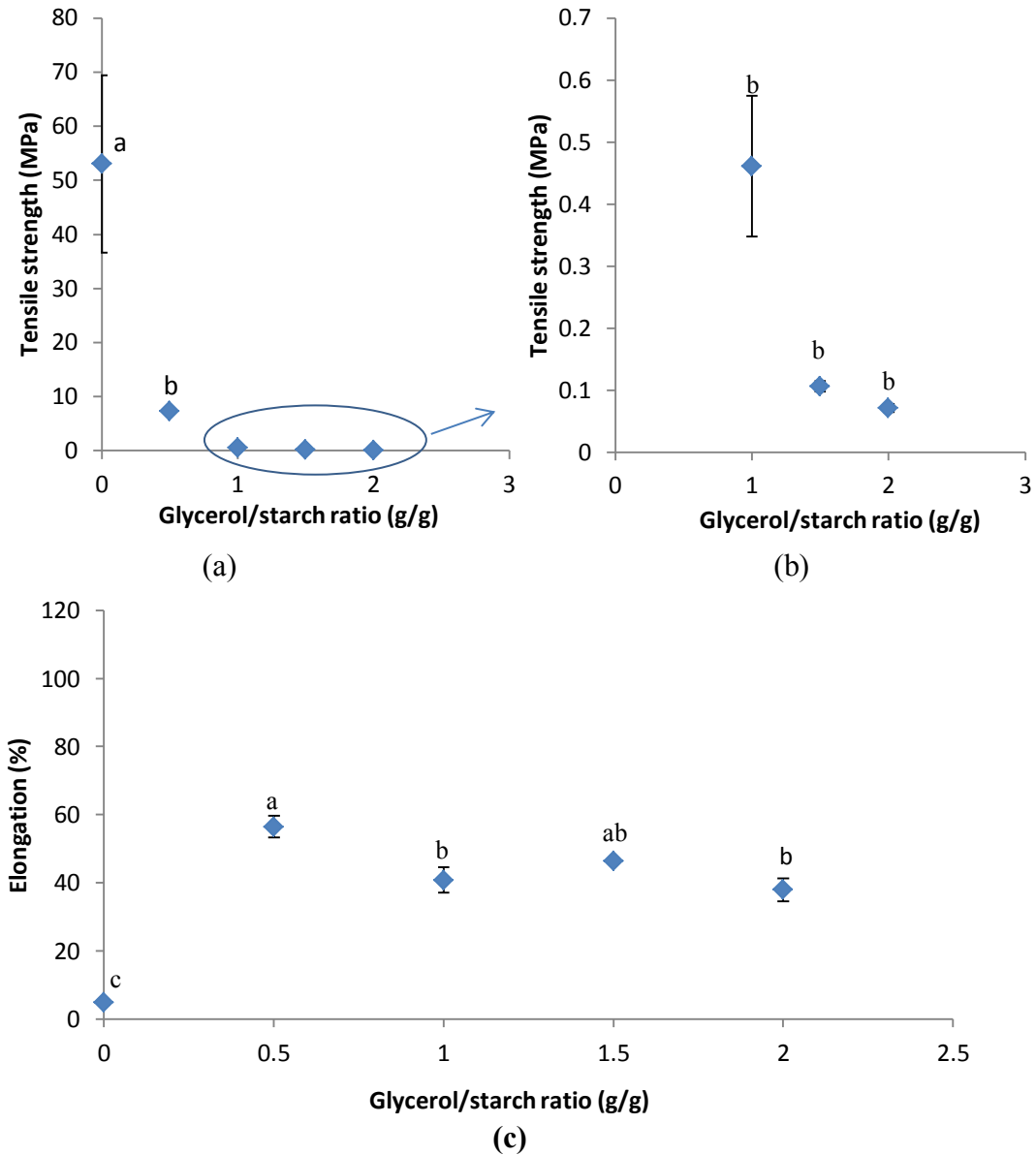
Figure 4.21 Tensile stress (a and b) and elongation percentage (%) (c) of bioactive films added with different concentrations of glycerol at constant gallic acid/starch ratio of 40 mg/g, temperature of 100 °C, and pressure of 50 bar. Data followed by the same letter are not significantly at $p > 0.05$. Value of each data point is shown in Table B.3 in Appendix B.

4.3.3.3 Water activity, moisture content and water solubility of starch films with different glycerol/starch ratio

In addition, all films had a mean water activity lower than 0.35. The influence of glycerol on moisture content was significant, which is consistent with the findings earlier reported by Valencia et al. (2014). These authors found that a glycerol/starch ratio of 0.5 resulted in a moisture content around 17% versus 22% in this study (Figure 4.22b). Without glycerol, films had the lowest moisture content (~6%) (Figure 4.22), suggesting that more free water was present and glycerol trapped water through hydrogen bonding due to the hydrophilic character of glycerol (Galdeano et al., 2009; Huang et al., 2007b).

(a)   (b)
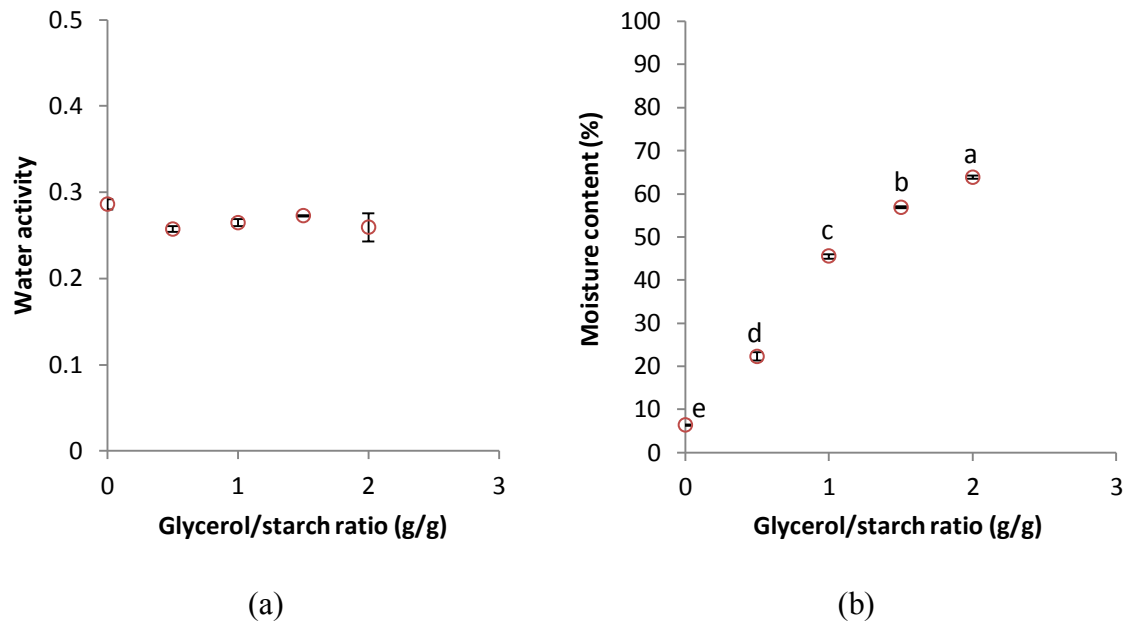
Figure 4.22 Water activity (a) and moisture content (b) of bioactive films added with different concentrations of glycerol at constant gallic acid /starch ratio of 40 mg/g, temperature of 100 °C, and pressure of 50 bar. Data followed by the same letter are not significantly different at $p > 0.05$. Value of each data point is shown in Table B.4 in Appendix B. No significant difference found in water activity).

In addition, when a hydrophilic additive (glycerol) was added at 0.5 g glycerol/g starch resulted in a significantly higher (~13%) solubility of film than any other ratio

used (Figure 4.23). The solubility of the film without glycerol was the lowest (~5-11%) at all three temperatures investigated. Also, when the glycerol/starch ratio was higher than 0.5 g/g, the formation of V-type crystalline between glycerol and amylose as confirmed by XRD resulted in soft and sticky texture films, preventing the dissolution of films into water as the hydration sites on starch were occupied by glycerol.
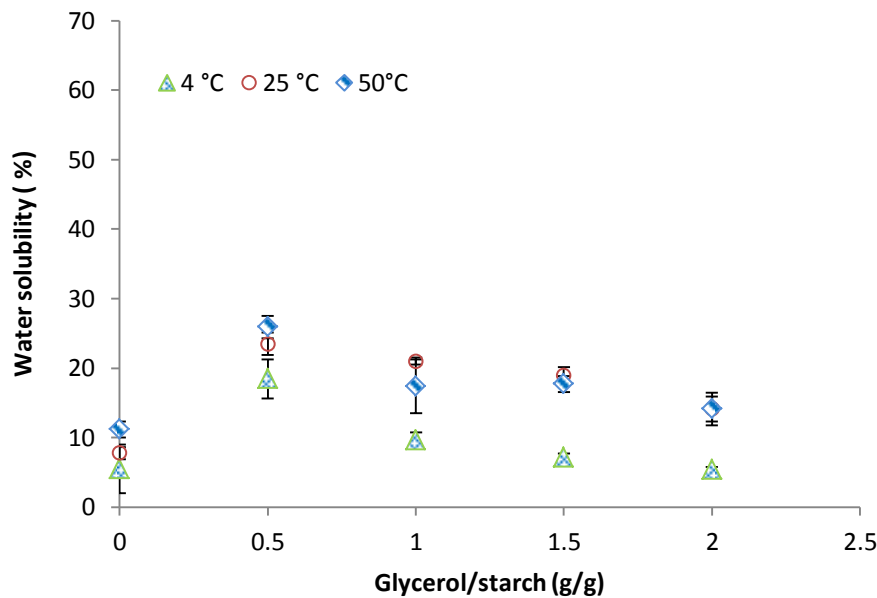
Figure 4.23 Solubility of bioactive films added with different concentrations of glycerol (with gallic acid /starch ratio of 40 mg/g, temperature of 100 °C, pressure 50 bar) in water at 4, 25 and 50 °C. Tukey's test results in Table B.5 in Appendix B.

4.3.3.4 Optical and morphological properties of starch films with different glycerol/starch ratio

There is no significant difference on the color and translucency values of films added with glycerol/starch ratio from 0 to 1.5 mg/g (Table B.7 in Appendix B). Significantly increases on total color difference and translucency value were found only with films added with 2g glycerol/g starch. In addition, the whiteness index of film with 2g glycerol/ g starch was significantly lower compared to other films with lower glycerol

143

amount. These changes found at film with 2g glycerol/g starch were similar to the one formed at 150 °C (section 4.3.2.4), except the yellowness index in this case was not changed. Therefore, high glycerol can also induce a similar effect on the color as depolymerization of starch induced by higher temperature heating (150 °C). High concentration of glycerol prevents hydration of starch granule during gelatinization and resulted in incomplete swollen of starch. Also, the V-type crystalline formed by glycerol and amylose (confirmed by XRD) reduced the association between starch molecule and increase the volume between amylose and amylopectin, which created a similar porous structure as depolymerized starch chains in film produced at 150 °C. However, during the drying process, glycerol was not evaporated completely as water and allows them to fill the pore or space in the film and re-associated. Therefore, the surface texture resulted from high concentration of glycerol was not the same as the one induced by high temperature depolymerization. The distinguishing color of the films with 2g glycerol/g starch was mainly from the incompletely gelatinized starch granule and the color of glycerol.

Films without the addition of glycerol had no gloss value due to its brittle texture, being difficult to obtain the required size of sample for analysis. SEM images in Figure 4.24 also suggest the plasticizing and anti-plasticizing effects. From the cross section of films, films without glycerol are more compact, while films with glycerol are more swollen. A significant difference was observed when a glycerol amount of 2g/g starch was used, as excess glycerol prevent the water uptake of starch, resulting in incomplete gelatinization, which reflected on these large pits and bumps on the film surfaces.
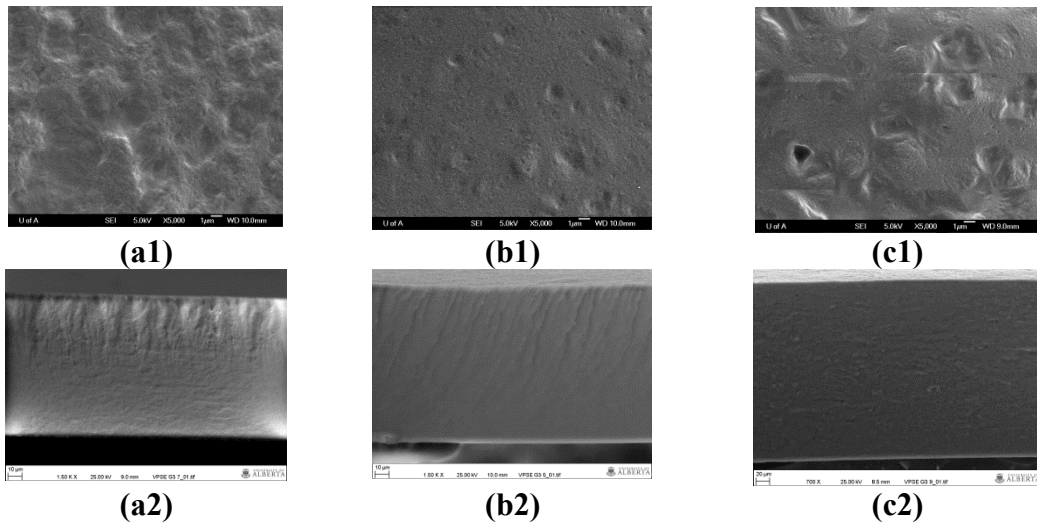
Figure 4.24 SEM image of bioactive films added with different concentrations of glycerol (a: 0, b: 0.5, c: 2 g/g) at a constant gallic acid /starch ratio of 40 mg/g, temperature of 100 °C, pressure of 50 bar. (a1-c1: surface images captured with gold coating at 5000 magnification, a2-c2: cross section images captured without coating at 1500 magnification under VP mode)

Results reported in Figure 4.25 showed that increasing glycerol concentration significantly decreased the initial contact angle from ~ 80° for a film with 0.5 g glycerol/g starch to ~ 46° for a film with 2 g glycerol/g starch, following the same trend found for using tapioca starch (Chang et al., 2006). These results showed that the surface hydrophobicity of potato starch bioactive films decreased with the increase of glycerol concentration, which can be ascribed to the hydrophilic character of glycerol (Ahmadi et al., 2012; Carneiro-da-Cunha et al., 2009). A similar trend was also shown in data of gloss, but the difference between each side of the film was also reduced with an increase in glycerol content.

145
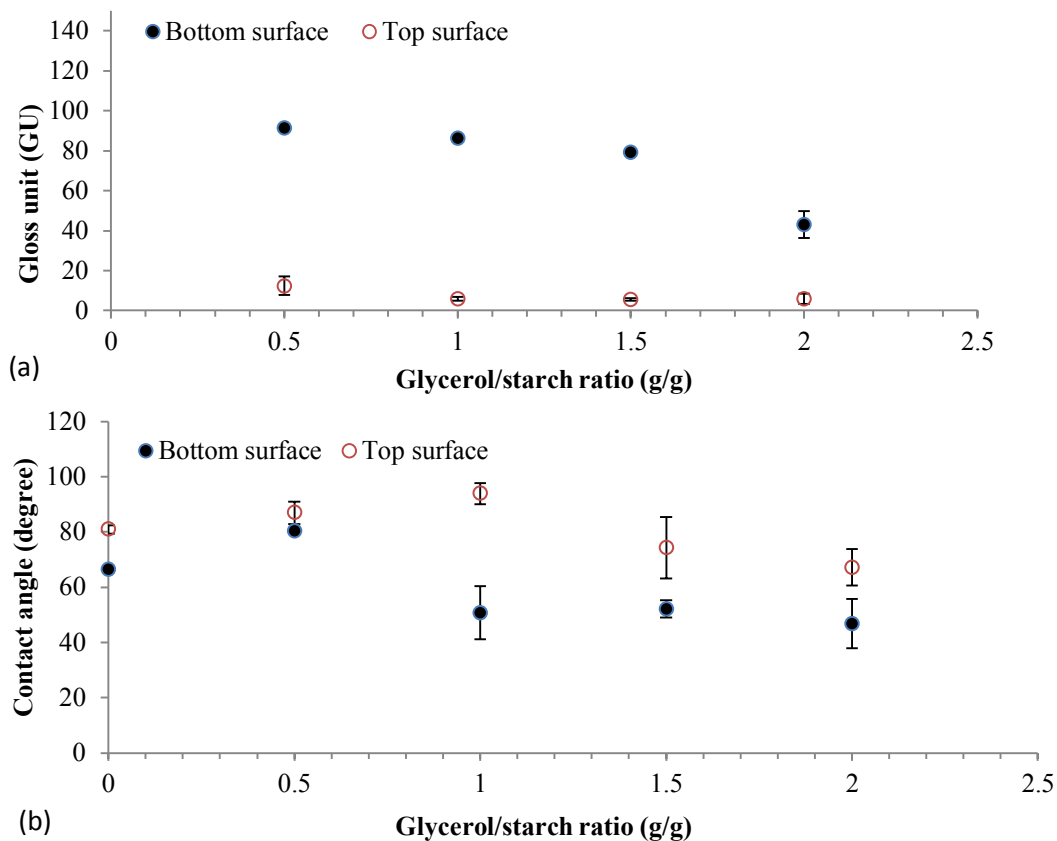
Figure 4.25 Gloss measurements at 60 °(a) and contact angle (b) for both sides of bioactive films added with different concentrations of glycerol and constant gallic acid /starch ratio of 40 mg/g, temperature of 100 °C, pressure of 50 bar. Bottom surface: smooth part of the film, and top surface: rough part of the film). Tukey's test results in Table B.7-8 in Appendix B.

4.3.3.5 Antioxidant capacity and total phenolic content of starch films with different glycerol/starch ratio

From the water solubility results in Section 4.3.3.3, it was confirmed the decreased water solubility after increased glycerol/starch ratio from 0.5 to 2 g/g, which suggest less component was released from the film into water. Although the antioxidant activity and total phenolic content was conducted with ethanol+water solution to maximize the gallic acid extraction from the film, a similar reduction was found. But the highest antioxidant activity and total phenolic content were from the filmed without glycerol (Figure 4.26),

146

which has the lowest water solubility (Section 4.3.3.3). A possible mechanism for this behavior could be that with a suitable amount of glycerol, crosslinking between starch and gallic acid can be promoted, without glycerol or with excess glycerol, gallic acid was weakly bonded, which can be easily released when dissolving in water or ethanol solution. The lower water solubility of film without glycerol was due to the highly compact structure between starch molecules, while for films with excess glycerol was due to ungelatinized starch granules. But, in both cases, the soluble part was mainly from gallic acid and few starch. On the other hand, with suitable amount of glycerol (0.5 g/g), starch granules were properly gelatinized and gallic acid was distributed in the film. In this case, the soluble part has lower amount of gallic acid, but more starch molecules.
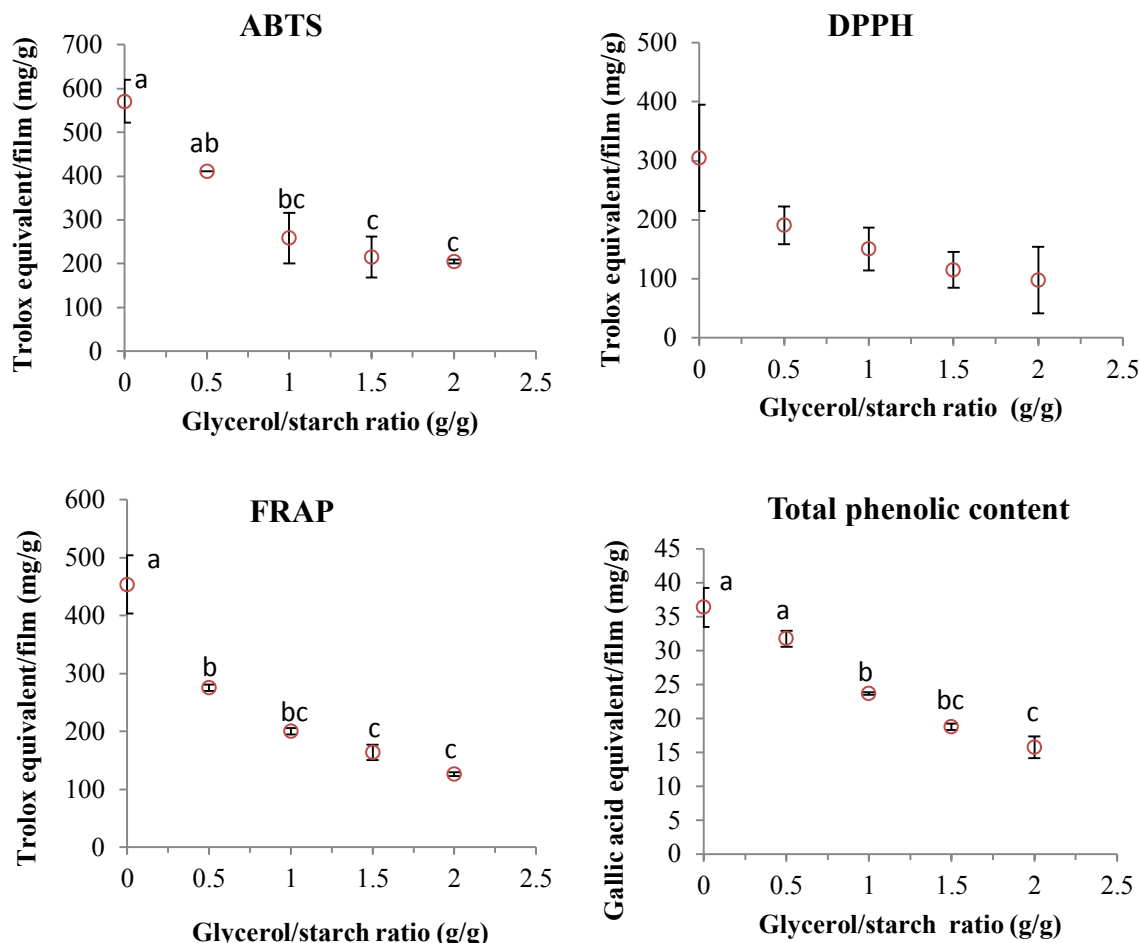
Figure 4.26 Antioxidant activity and total phenolic content of bioactive film added with different concentrations of glycerol, gallic acid /starch ratio of 40 mg/g, temperature of 100 °C, pressure 50 bar. Data followed by the same letter are not significantly different at p>0.05, value of each data point is shown in Table B.9 in Appendix B. No significant difference found in DPPH results.

4.3.4 Effect of pressure on the properties of starch films

4.3.4.1 Structural properties of starch films produced at different pressures

No significant influence of pressure on FTIR of starch films was observed in terms of formation of new interactions between gallic acid, glycerol and starch molecules (Figure B.7, Appendix B). From the XRD results in Figure 4.27, pressure had no significant influence on the crystalline pattern and relative crystallinity of bioactive films. But, at a high pressure of 190 bar, the peak intensity for B-type crystalline was higher

148

than the one for V-type (Figure 4.27). In addition, the relative crystallinity % at 190 bar was slightly higher by ~1.3-2.8% than lower pressures, which suggest more B-type crystalline was formed under 190 bar. Pressure promoted interactions between starch molecules. During gelatinization, high pressure facilitates the rupture of starch granules, allowing more crystalline formation during the cooling process (Menchavez et al., 2014).
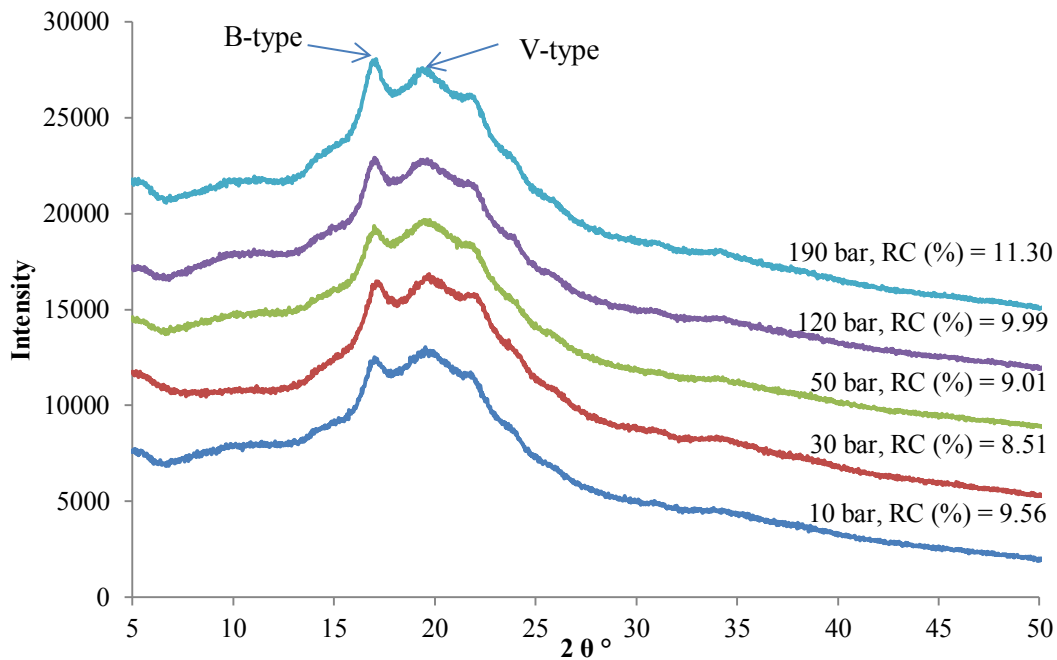
Figure 4.27 XRD and relative crystallinity (RC, %) of bioactive films produced at different pressures and constant glycerol/starch ratio of 0.5 g/g, gallic acid/starch ratio of 40 mg/g, and temperature of 100 °C.

4.3.4.2 Mechanical properties of starch films produced at different pressures

Gelatinization of potato starch was the major reaction occurring inside the high-pressure reactor. With the use of heat, water is able to penetrate into the starch granule and functions as a plasticizer, resulting in irreversible swelling and breakage of granule structure (Wang et al., 2010a). The effect of pressure on the tensile strength and elongation of bioactive films was shown in Figure 4.28. Pressure used in this study (20 to 190 bar) had no significant influence on the TS of film. Some studies (Blaszczak et al.,

2007; Kawai et al., 2007; Stute et al., 1996; Vallons & Arendt, 2009) suggested that high hydrostatic pressure (HHP) treatment can facilitate gelatinization of starch even at room temperature to produce gelatinized starch with no difference compared to heat-treated starches (heated above the gelatinization temperature of starch, e.g. 75 °C for potato starch). However, the range of pressure applied in HHP is high (500 to 6000 bar), and its influence on lowering starch gelatinization temperature was only observed at pressures higher than 600 bar (Qiu et al., 2014), which is higher than the pressures used in this study (up to 190 bar). Menchavez et al. (2014) used low pressures of 1-2 bar, suggesting that under the same heating temperature, the pressurised cooking is effective to produce highly swollen starch granules as compared with the one without applying any pressure. Highly swollen starch exposes more sites on the starch molecules to other additives such as glycerol and gallic acid as well as to other starch molecules to re-associate with them stronger. A significant reduction on the E% of the film was found when a pressure of 50 bar was used, higher or lower pressure than 50 bar had no significant influence on the elongation of films (~70%). As the association between amylose and amylopectin became stronger under pressure, it was difficult for the plasticizer glycerol to create a space and provide flexibility to the films. Thus, 30 bar was selected as the optimum pressure to obtain reasonable mechanical properties.

(a)   **(b)**
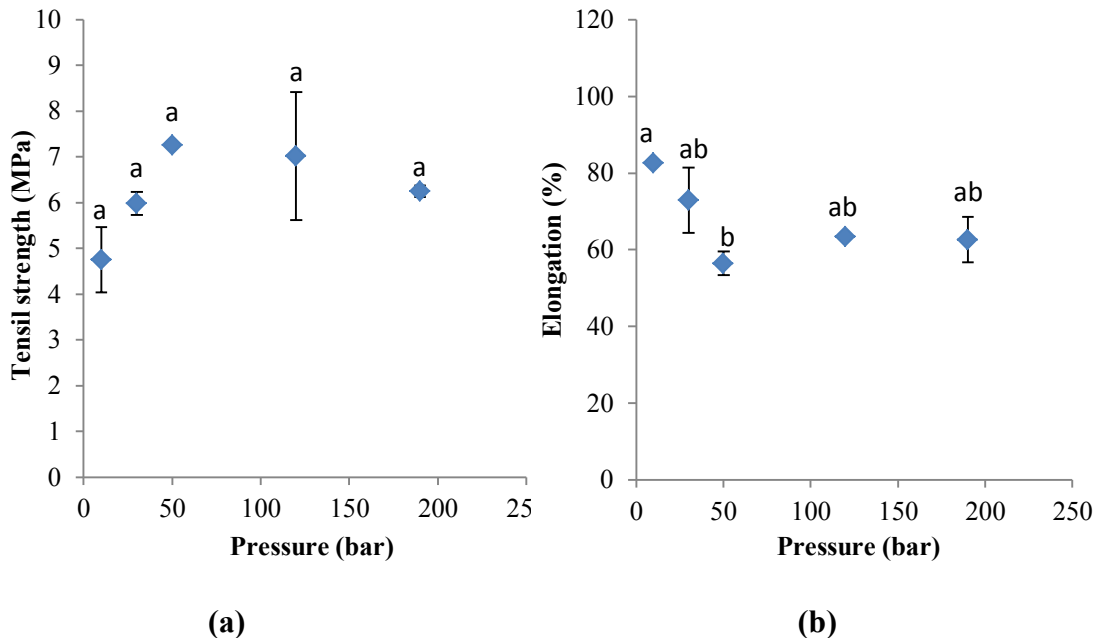
Figure 4.28 Tensile stress (a) and elongation percentage (%) (b) of bioactive films produced at different pressures and constant glycerol/starch ratio of 0.5 g/g, gallic acid/starch ratio of 40 mg/g, temperature of 100 °C. Data followed by the same letter are not significantly different at $p > 0.05$. Value of each data point is shown in Table B.3 in Appendix B.

4.3.4.3 Other properties of starch films produced at different pressures

In terms of other properties measured, no significant difference was found in water activity, moisture content, water solubility, color, translucency, gloss, antioxidant capacity and total phenolic content of bioactive films produced at different pressures (Table 4-9, Appendix B). Differences were only found on the contact angle as well as the SEM image of bioactive films. Like found in other parameters discussed above, the bottom surface of the film had a significantly higher gloss value (90 to 99 GU), compare to the top surface (76 to 85 GU), which indicated the bottom surface was smoother (Figure 4.29 a). However, the surface with high gloss tends to have slightly lower (18%) contact angle at 30 bar and 120 bar. Possible mechanism could be that smooth surface creates a high gloss surface, but also increase the number of –OH on the surface, which

151

increase the accessibility of these –OH to water and form hydrogen bonding and reflect a lower contact angle value. The gloss value of bottom surface were significantly higher (by ~88 GU) than the top surface of films at all pressures , which indicate the significant difference on the roughness of surface caused by the evaporation of water. However, this difference texture did not significantly influence the contact angle value, suggest the gel network still intact and after water left during drying, the association between starch molecules and glycerol were strong enough to exert hydrophobicity on both sides of surfaces.

(a)

(b)
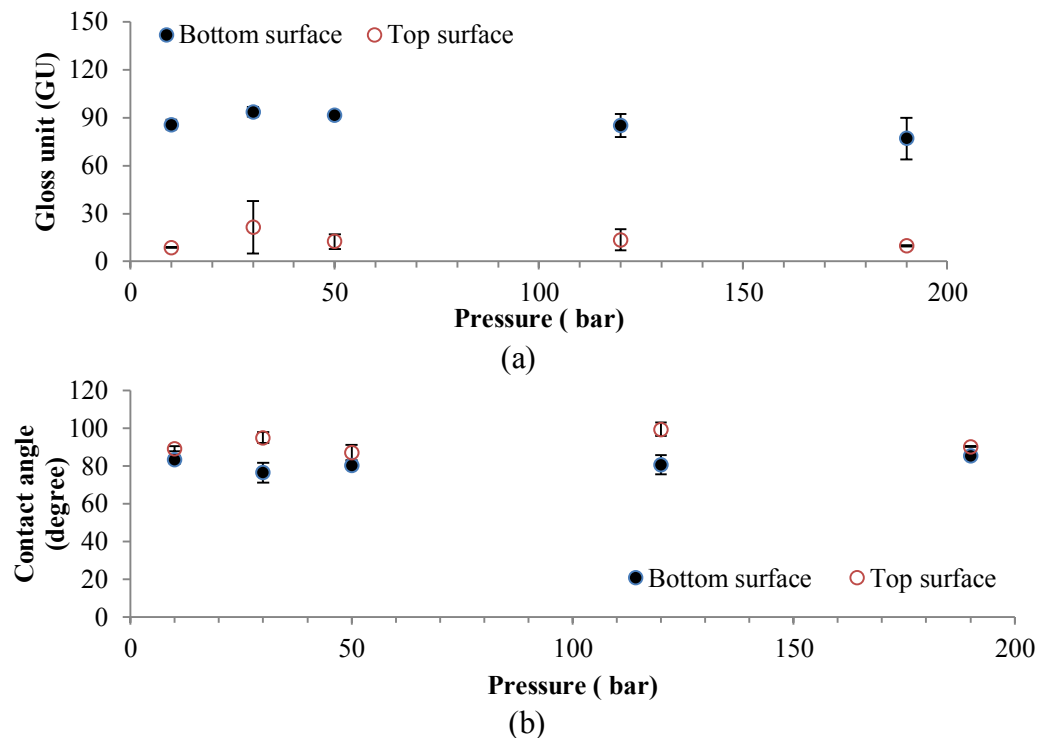
Figure 4.29 Gloss measurements at 60° (a) and contact angle (b) for both sides of bioactive films produced at different pressures and constant glycerol/starch ratio of 0.5 g/g, gallic acid/starch ratio of 40 mg/g, of 100 °C (Bottom surface: smooth part of the film, and top surface: rough part of the film). Tukey's test results in Table B.7-8 in Appendix B.

From the SEM images (Figure 4.30), films formed under high pressures show a smoother surface and more homogenized cross section. The surface of film produced at

152

10 bar still had few bump and bit representing the incompletely gelatinized starch granule (Figure 30a1), which were significantly reduced on the film produced at higher pressure (30 to 190 bar). Other studies (Menchavez et al., 2014; Noranizan et al., 2010; Srikaeo et al., 2006) found similar mud like structure of starch granules in wheat, sago, tapioca and potato starch treated in an autoclave system with temperature around 120 °C for 1h. Based on their conclusions, this change in granule structure meant sufficiently deformation, which allowed more amylopectin to be leached out. Therefore, in this study, same degree of gelatinization can be achieved with a high pressure (>30 bar) at 100 °C for 10 min.

(a1)　　**(b1)**　　**(c1)**　　**(d1)**　　**(e1)**

(a2)　　**(b2)**　　**(c2)**　　**(d2)**　　**(e2)**
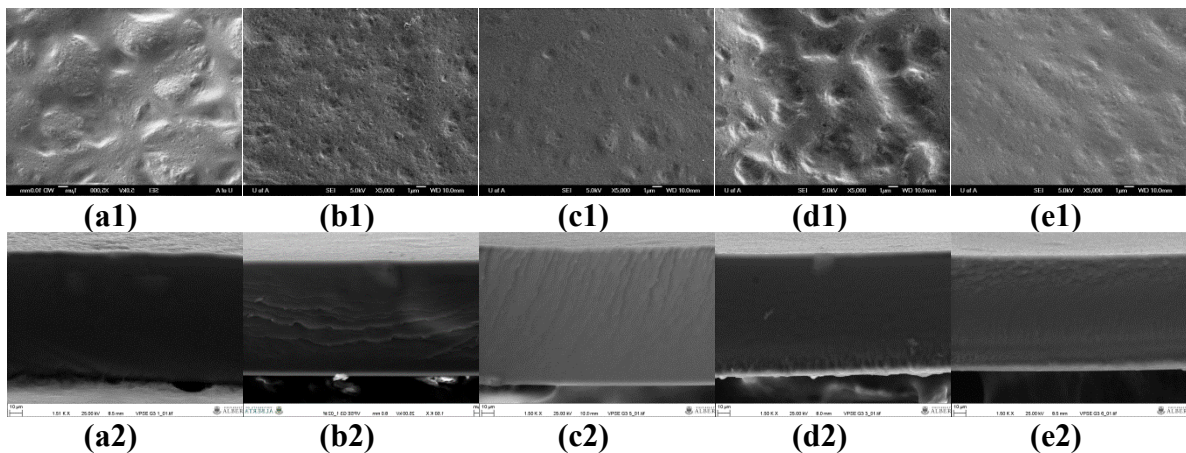
Figure 4.30 SEM images of bioactive film produced at different pressures (a:10 bar,b:30 bar,c:50 bar,d:120 bar, e: 190 bar) with glycerol/starch ratio of 0.5 g/g, gallic acid /starch ratio of 40 mg/g, temperature of 100 °C. (a1-e1: surface image captured with gold coating at 5000 magnification, a2-e2: cross section image captured without coating at 1500 magnification under VP mode)

4.3.5 Effect of different phenolic acids on the properties of starch films

　　The optimum condition for balanced mechanical properties of starch gallic acid film was found with 40 mg gallic acid/ g starch, 0.5 g glycerol/g starch, 100 °C and 30 bar. To expand the application this formula, instead of gallic acid, caffeic acid, ferulic

acid and cinnamic acid was added to the film separately. The influences of these phenolic acids on the properties of starch film were discussed below.

4.3.5.1 Structural properties of starch films with different phenolic acids

As the structures of phenolic acids are not the same, different FTIR patterns of phenolic acids are expected. From Figure 4.31 a-c, different FTIR patterns among phenolic acids were found in the range of wavelengths between 450 and 1700 cm^{-1}. But, after incorporating these phenolic acids into the film, the FTIR spectra (Figure 4.31d) of their films were all similar. An additional peak was found in the film added with trans-ferulic acid and gallic acid (Figure 4.31d). The peak of ferulic acid at wavelength of 1511 cm^{-1} had been shifted slightly to 1513 cm^{-1} after being added to the film under optimum condition. There was no additional peak was found in the film added with trans-cinnamic acid and caffeic acid, suggesting that the interaction of these two phenolic acids with glycerol and starch molecules was relatively low (Figure 4.31d). One explanation could be that the concentration of glycerol (0.5 g/g starch) in the film is significantly higher than the concentration of phenolic acid (40 mg/g starch) incorporated and the interactions between these phenolic acids and starch were not significant enough to be detected by FTIR. Also, it can be concluded that under the optimum condition used in this study, the influence derived from the structural difference among the structure of selected phenolic acids was minimized, as the FTIR results for films with different phenolic acids were similar.
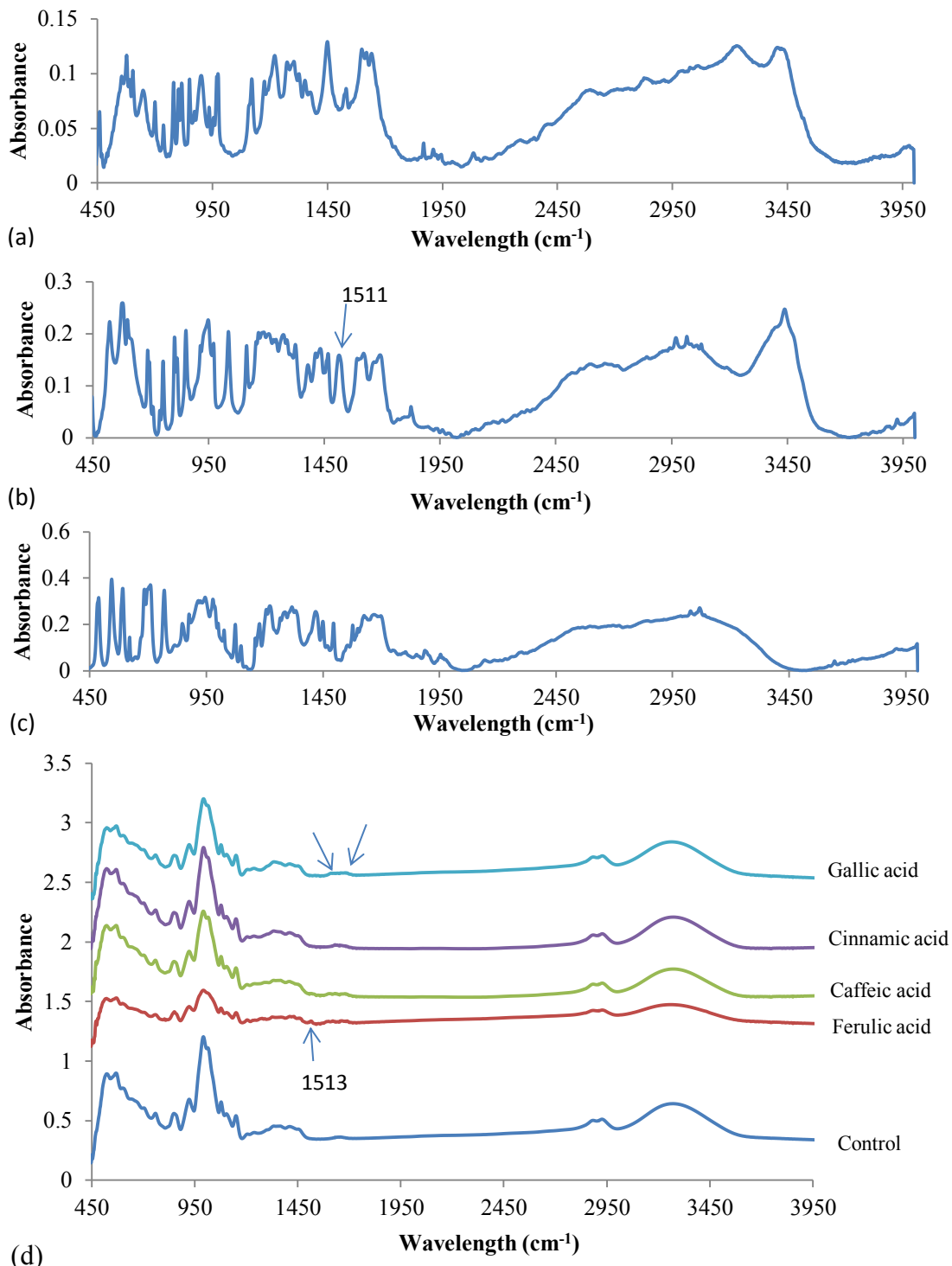
Figure 4.31 FTIR of Pure caffeic acid (a), pure trans-ferulic acid (b), pure trans-cinnamic acid (c) and bioactive films (d) produced with different phenolic acids at optimal conditions (phenolic acid/starch ratio of 40 mg/g, temperature of 100 °C, glycerol/starch ratio of 0.5 g/g and pressure of 30 bar).

A different XRD pattern was observed in the film produced using trans-cinnamic acid (Figure 4.32). The major peak (18.5°) of cinnamic acid film was belong to A-type crystalline of starch, However, the intensity of the peak in normal starch is around 16000, but in films formed with the use of cinnamic acid , the peak intensity is around 80000. This change could be due to formation of a modified A-type crystalline under this optimum processing condition. That was validated by visual observation of the film where small homogenized particles were formed after gelatinization, resulting in a gel-like suspension, which was different from the other experiments. However, after the cooling and drying process, this suspension still formed integral and uniform films.
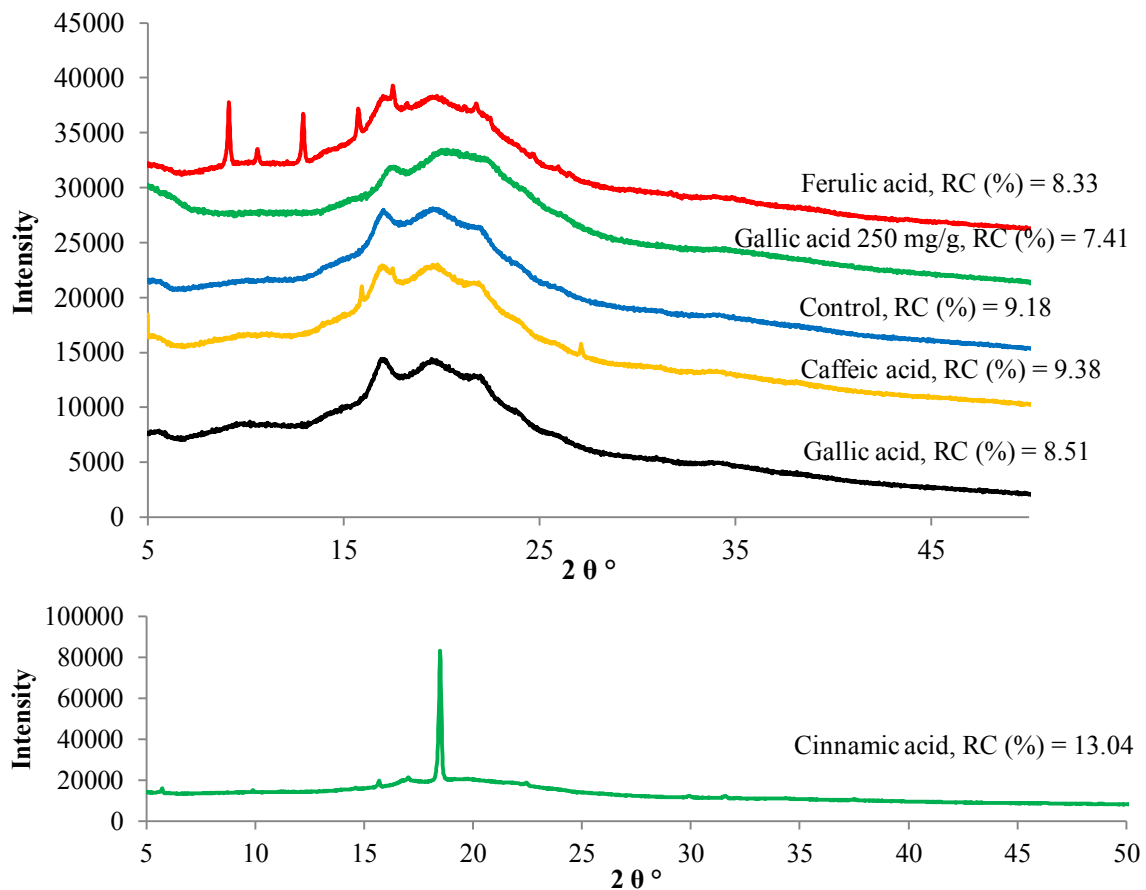
Figure 4.32 XRD and relative crystallinity (RC, %) of bioactive films produced at optimal conditions (phenolic acid/starch ratio of 40 mg/g, temperature of 100 °C, pressure of 30 bar, and glycerol/starch ratio of 0.5g/g) with different phenolic acids.

156

4.3.5.2   Mechanical properties of starch films with different phenolic acids

After optimizing the four process parameters (temperature, pressure, gallic acid/starch ratio, and glycerol/starch ratio), gallic acid was replaced with three other phenolic acids and bioactive films with different phenolic acids were formed under optimum condition (100 °C, 30 bar, 40 mg phenolic acid/g starch, and 0.5 g glycerol/g starch). Since this optimum condition was produced based on gallic acid, it would be necessary to optimize processing conditions for the other phenolic acids used. The effect of adding phenolic acids on the tensile strength and elongation of bioactive films is shown in Figure 4.33. The control film had no phenolic acid, but was produced under the same optimum processing conditions. It was found that there is no significant difference in E% between the control and the other bioactive films. In terms of TS, films added with gallic acid had significant higher TS values compared to other phenolic acids. However, films with 250 mg/g of gallic acid had a significant lower TS value compared to the control.

The structure of hydrocinnamic acid derivatives differed from hydrobenzoic acid derivatives and the number and position of hydroxyl and methoxy groups can cause different interactions with starches (Zhu et al., 2008). From the study of Zhu et al. (2008), trans-cinnamic acid without a hydroxyl group on the aromatic ring produced the highest pasting viscosity among all hydrocinnamic acid derivatives. In general, their functional groups could interact with amylose and amylopectin through hydrogen bonding and van de Waals forces. Therefore, experimental parameter optimization for hydrobenzoic acid derivative bioactive films may not be suitable for hydrocinnamic acid derivative bioactive films.

157
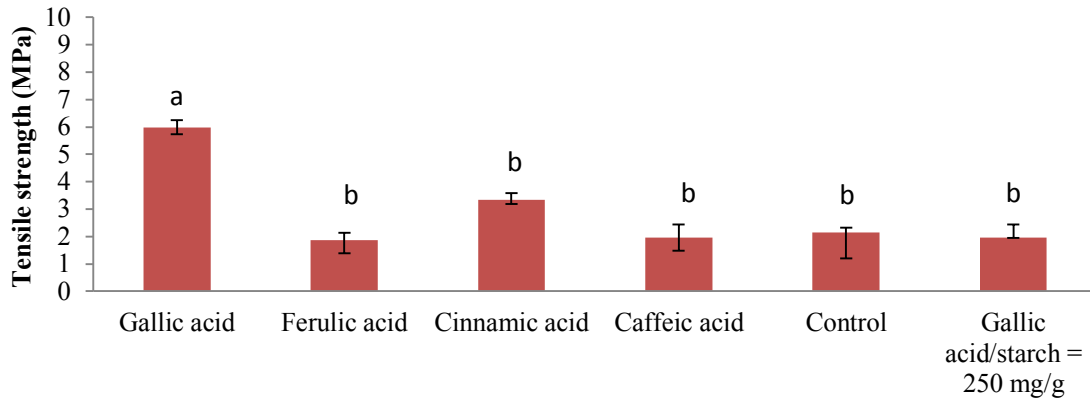
(a)
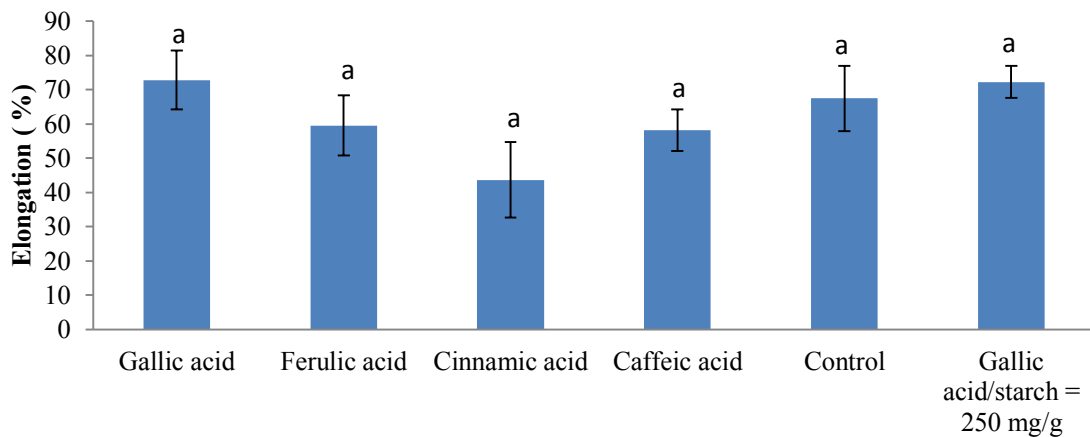
(b)

Figure 4.33 Tensile stress (a) and elongation percentage (%) (b) of bioactive films produced with different phenolic acids at optimal conditions (phenolic acid/starch ratio of 40 mg/g, glycerol/starch ratio of 0.5g/g, temperature of 100 °C, and pressure of 30 bar). Data followed by the same letter are not significantly different at $p > 0.05$. Value of each data point is shown in Table B.3 in Appendix B.

4.3.5.3 Water activity and moisture content and water solubility of starch films with different phenolic acids

Compared to the control, addition of different phenolic acids under optimum conditions can significantly reduce the moisture content of films, except for the one with cinnamic acid. Also, the degree of reduction depends on the amount of phenolic acid used, as a significant reduction of 4% was found after increasing gallic acid/starch ratio to 250 mg/g from 40 mg/g (Figure 4.34). No significant difference was found in water

activity of films with different phenolic acids (Table B.4 in Appendix B). But these values were higher than that of the control (9%). Compared to the control, addition of different phenolic acids had no significant influence on the solubility of the film in water at 4, 25 and 50 °C (Table B.5 in Appendix B). But the film with 250 mg gallic acid/g stach has twice the solubility as the control at all three temperatures. Although no significant difference was found on solubility of films at all three temperature, but solubility of film in water at 25 and 50 °C were slightly higher (~7%) compared to films stored at 4 °C, as the solubility generally increased along with temperature.
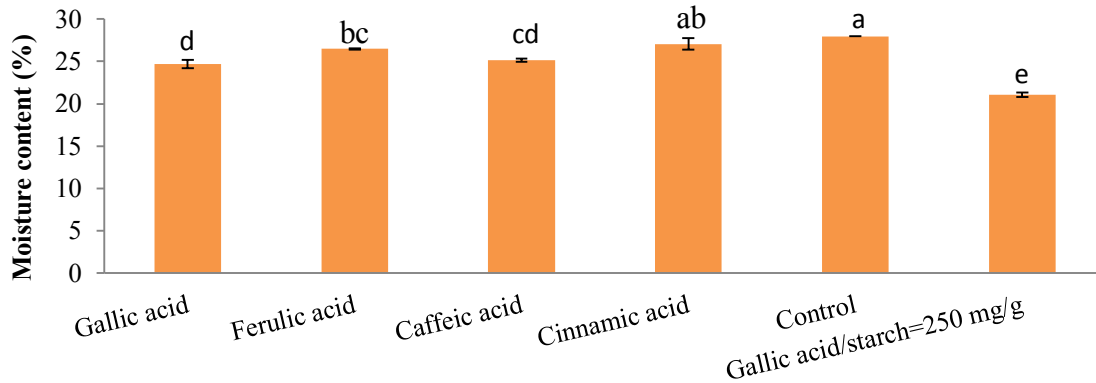
Figure 4.34 Moisture content of bioactive films produced with different phenolic acids at optimal conditions: phenolic acid/starch ratio of 40 mg/g, temperature of 100 °C, glycerol/starch ratio of 0.5 g/g, and pressure of 30 bar. Data followed by the same letter are not significantly different at p>0.05. Value of each data point is shown in Table B.4 in Appendix B.

4.3.5.4 Optical and morphological properties of starch films with different phenolic

acids

There was no significant difference among other phenolic acids compared to the control in terms of the ΔE and WI value, but a film with 250 mg gallic acid/g starch had a significant increase in the YI (3.39) compared to the control (YI=2.3) (Table B.6, Appendix B). However, films with trans-ferulic, and trans-cinnamic acids were less

transparent compared to the films with gallic acid (Figure 4.35), suggesting different degree of cross-linking can vary depending on the structure or –OH groups on the aromatic rings and the optimum condition for gallic acid may not be ideal for hydrocinnamic acid derivatives.
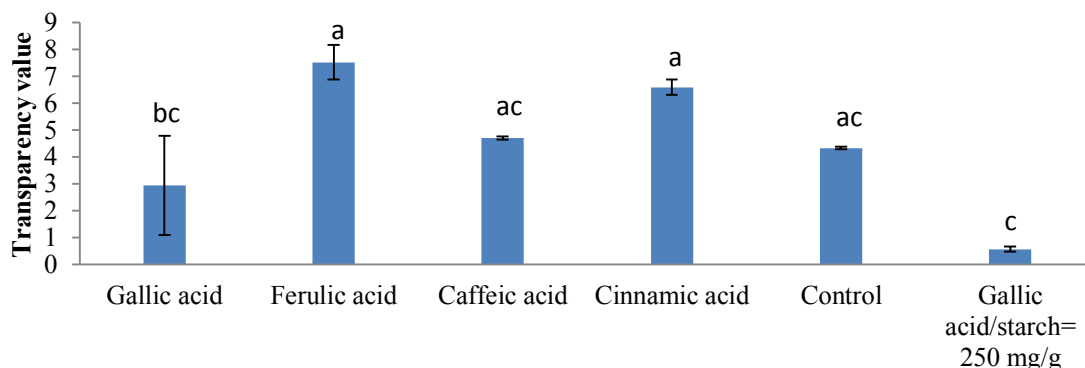
Figure 4.35 Translucency of bioactive films produced with different phenolic acids at optimal conditions: phenolic acids/starch ratio of 40 mg/g, temperature of 100 °C, pressure of 30 bar, and glycerol/starch ratio of 0.5 g/g. Data followed by the same letter are not significantly different at p>0.05. Value of each data point is shown in Table B. 7 in Appendix B.

In terms of contact angle and gloss of the film, the addition of phenolic acid in general had no significant influence in these two properties (Figure 4.36). Significant increase in gloss was observed only with gallic acid at 250 mg/g. Incorporation of trans-cinnamic acid induced reduction in the contact angle of the top surface of the film. Gallic acid had the highest solubility in water among all four phenolic acids studied, which allowed more gallic acid to interact with starch molecules. As observed in Figure 4.37, recrystallized phenolic acid crystals were formed inside as well as on the surface of the film added with trans-ferulic acid, trans-cinnamic acid and caffeic acid. Compared to the control, under the optimum condition, films with gallic acid had a smoother texture on

both cross section and surface, which suggest gallic acid promoted the gelatinization of starch.

Native starch is considered a hydrophilic material that absorbs moisture from the air, which usually has a contact angle value around 40° (Namazi et al., 2011). Contact angle (~100°) and gloss of film (~80 GU) without gallic acid produced at optimum conditions are significantly higher than other starch films with contact angle around 17-95° and gloss about 30 GU (Huang et al., 2014; Ortega-Toro et al., 2014; Seyedi et al., 2014; Winkler et al., 2014), indicating the benefit of subcritical water in modifying starch hydrophobicity.
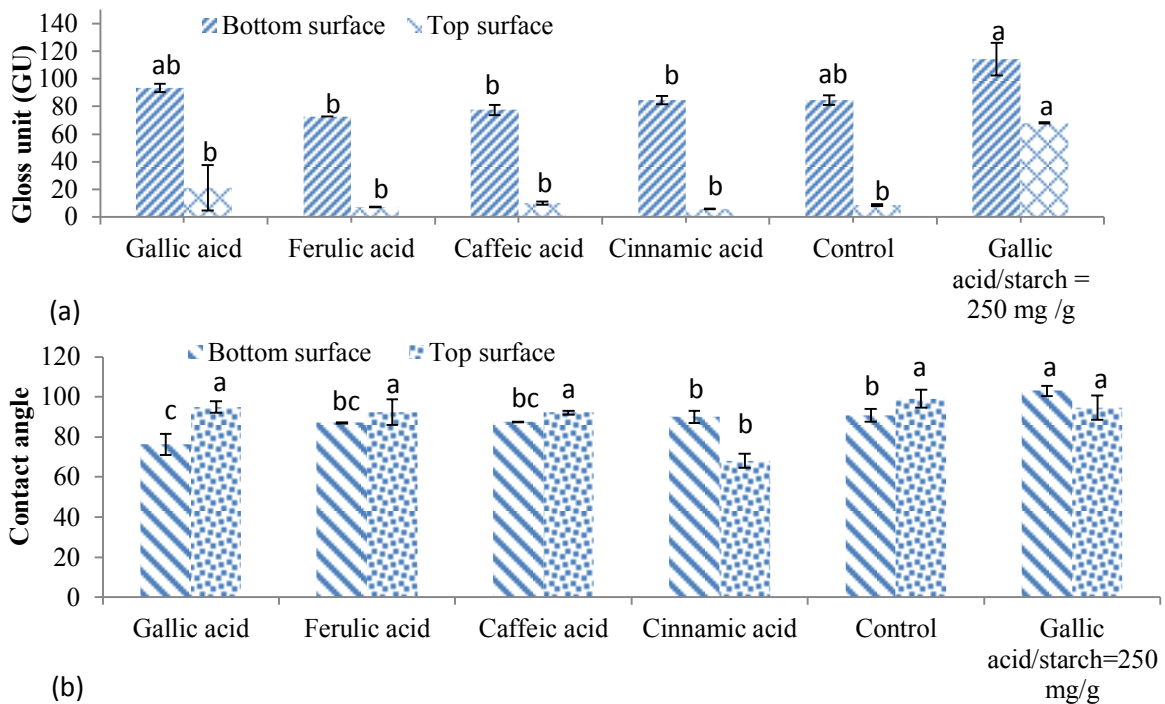
Figure 4.36 Gloss measurements at 60 °(a) and contact angle (b) for both sides of bioactive films produced at optimal conditions: phenolic acid/starch ratio of 40 mg/g, temperature of 100 °C, pressure of 30 bar, glycerol/starch ratio of 0.5 g/g) with different phenolic acids. (Bottom surface: smooth part of the film, and top surface: rough part of the film). Data followed by the same letter are not significantly different at p>0.05. Value of each data point is shown in Table B.7-8 in Appendix B.

161
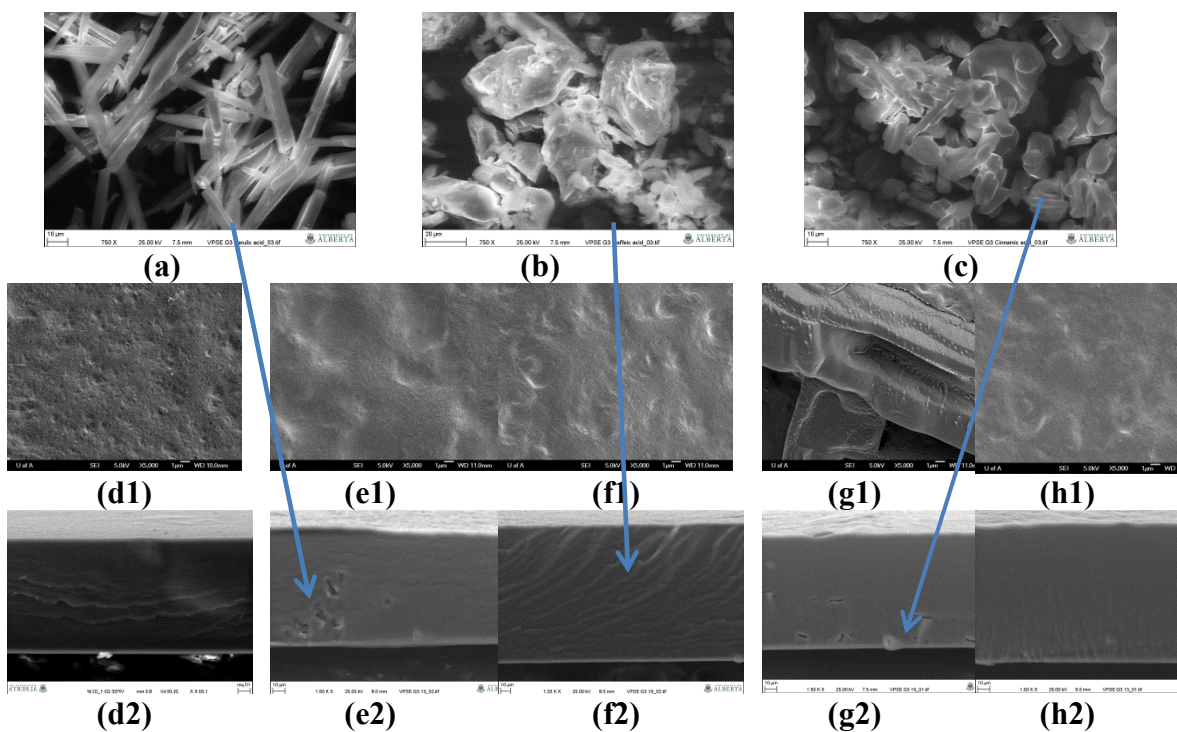
Figure 4.37 SEM images of ferulic acid (a), caffeic acid (b), and cinnamic acid (c) and bioactive films produced at optimal conditions (phenolic acid/starch ratio of 40 mg/g, temperature of 100 °C, pressure of 30 bar, glycerol/starch ratio of 0.5 g/g with different phenolic acids (d: gallic acid, e: ferulic acid, f: caffeic acid, g: cinnamic acid, h: without phenolics). (a-c: surface images captured without coating at 750 magnification under VP mode, d1-h1: surface image captured with gold coating at 5000 magnification, d2-h2: cross section image captured without coating at 1000 magnification under VP mode).

4.3.5.5 Antioxidant capacity and total phenolic content of starch films with different phenolic acids

In terms of other phenolic acids, gallic acid had significantly higher antioxidant capacity and total phenolic content, followed by caffeic acid and trans-ferulic acid. Antioxidant capacity and total phenolic content of trans-cinnamic acid films were not possible to determine by the methodology used in this study (Figure 4.38). However, HPLC analysis confirmed the existence of cinnamic acid in film dissolving solution with a similar concentration to trans-ferulic acid (Table B.9 in Appendix B).

162

Antioxidant activity

Total phenolic content
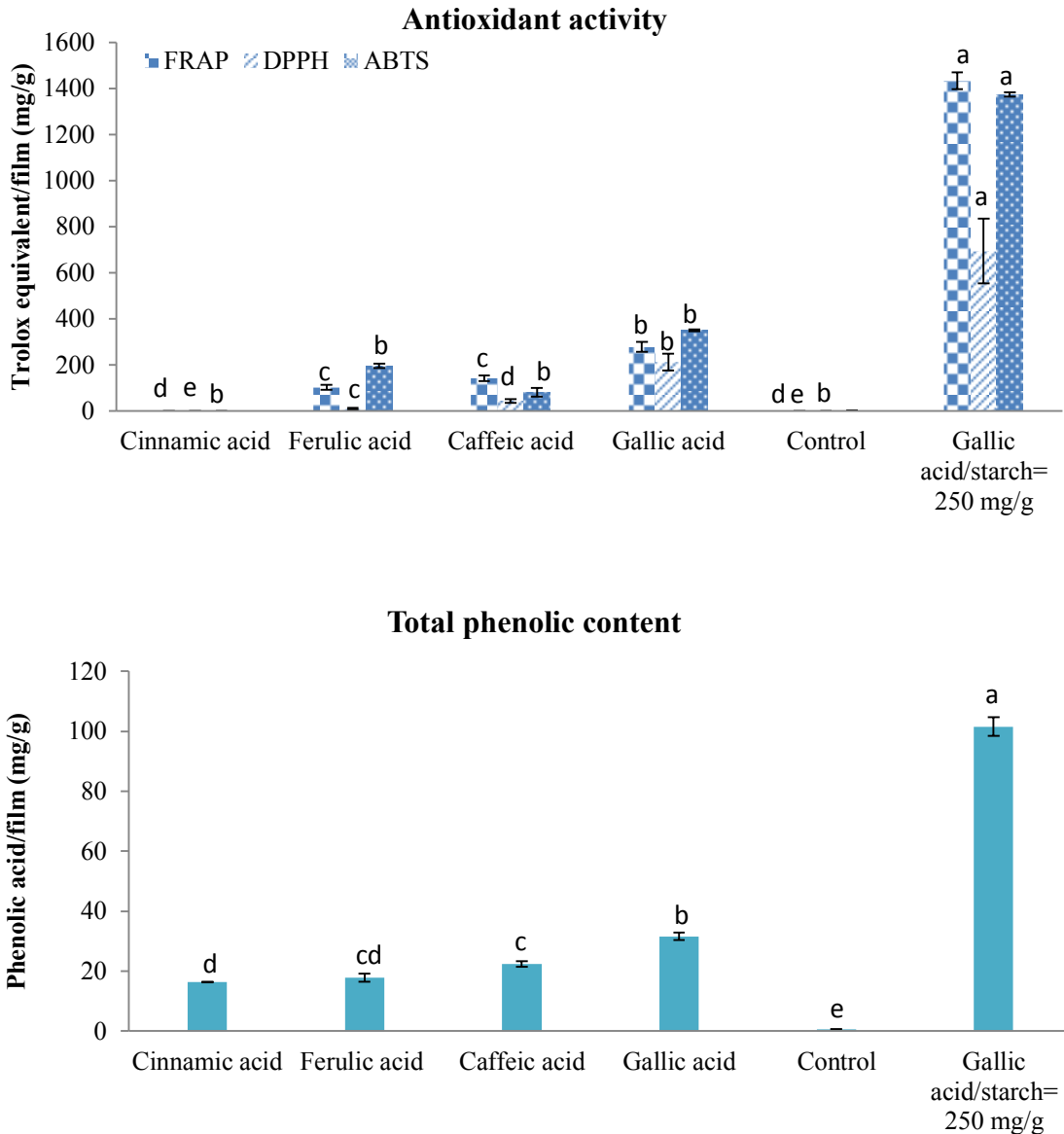
Figure 4.38 Antioxidant activity and total phenolic content of bioactive film produced at optimal conditions: phenolic acids/starch of 40 mg/g, temperature of 100 °C, pressure of 30 bar, glycerol/starch ratio of 0.5 g/g. Data followed by the same letter are not significantly different at $p>0.05$. Value of each data point is shown in Table B.9 in Appendix B.

4.3.5.6 Antimicrobial activity of starch films with different phenolic acids

An attempt was made to determine the antimicrobial activity of starch films formed under optimum condition. For the antimicrobial test, the inhibition zone was not observed in all the films produced for both strains, which means the absolute amount of gallic acid

163

released from the selected size of film onto agar was not adequate to exert an inhibition zone for two strains of *Escherichia coli* AW1.7 and *Bacillus subtilis* FAD 110 before they died naturally from lack of nutrients.

From the study by Corrales et al. (2009), the particle release of antimicrobials from the film directly depended on the nature, structure and features of the film polymer as well as the medium contacted with the film, as strong antimicrobial activity of grape seed extract observed in disc diffusion test was not found in real meat products. Therefore, it may be possible to change to other mediums or solutions where more phenolic acids can be released from the film to inhibit the growth of microorganisms. Due to the hydrophobic nature of films produced in this thesis, films were not able to completely attach to the LB agar without glass cover.

Also, increase the amount of phenolic acids can be alternatives to improve antimicrobial properties of the film. Although the aqueous solubility of gallic acid (14.7g/L) is higher compared to that of trans-cinnamic acid (0.23 g/L), trans-ferulic acid (0.78 g/L), and caffeic acid (0.98 g/L) at room temperature (Mota et al., 2008). The antimicrobial activity of gallic acid based on minimum inhibition concentration (MIC) is at least two times lower than the other three phenolic acids used (Table 2.1 in Chapter 2) (Sanchez-Maldonado et al., 2011). Therefore, less amount of phenolic acid with higher antimicrobial activity is needed to exert same antimicrobial activity of inhibition of growth of microorganism. However, from the SEM images in Figure 4.37, recrystallization of cinnamic acid, caffeic and ferulic acid inside and on the surface of the films were observed, which suggested that the amount added (40 mg/g) was excess.

Another alternative to improve the antimicrobial activity is to use other natural antimicrobials for film production and test their effectiveness, such as tannic acid (Pyla et al., 2010), natural extract from plant (e.g. grape seed extract) (Kanmani & Rhim, 2014), essential oils (Ghasemlou et al., 2013; Kavoosi et al., 2014). However, the interactions between starch and these antimicrobials are complicated and it is necessary to balance the mechanical properties as well as other physical properties with functional properties like antimicrobial and antioxidant activity.

In addition, in this study, color change on films with gallic acid added was visually observed as it became darker when gallic acid concentration in the film increased (Figure 4.39). This color change was not observed in the film without gallic acid or added with other phenolic acids, which may suggest that a metabolite was produced by either of these two strains from gallic acid. Also, visual observation found in the same film studied, only the part covered by the glass turned did not turn black, which indicated this reaction could be aerobic.
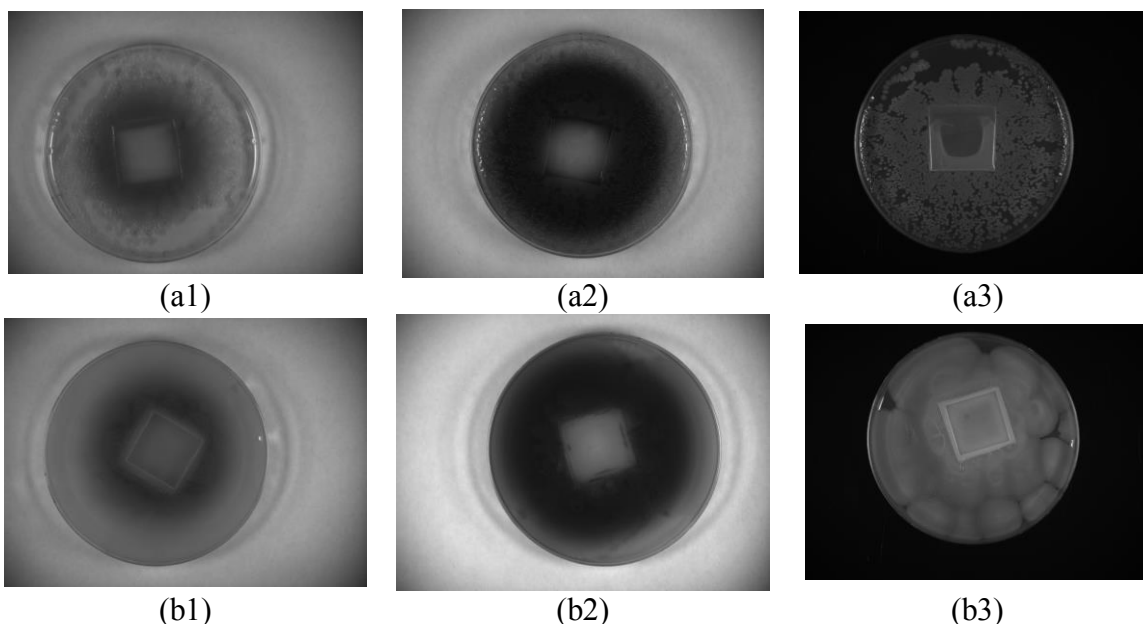
Figure 4.39 Antimicribial results of bioactive films with different concentration of gallic acid on *Ecoli* AW1.7 (a1-a3) and *Bacillus subtilis* FAD 110 (b1-b3). Experimental condition for a1 and b1: gallic acid/starch ratio of 40 mg/g, temperature of 100 ℃ , pressure of 30 bar, glycerol/starch ratio of 0.5g/g; for a2 and b2: gallic acid/starch ratio of 250 mg/g, temperature of 100 °C, pressure of 30 bar, glycerol/starch ratio of 0.5g/g; for a3 and b3: without gallic acid, temperature of 100 °C, pressure of 30 bar, glycerol/starch ratio of 0.5g/g.

4.3.6 Water vapor permeability of optimum starch films

When a starch film is used as a packaging material to cover food products, consumers expect the film to protect the food inside within specific shelf-life. In terms of the chemical composition and structure of the film, characteristics of the product, and the storage conditions, an efficient starch film should provide excellent barrier properties against gas, water vapor, and aroma (Fontes et al., 2011). Water vapour permeability (WVP) values relate the final application of a film in contact with food systems and they must be as low as possible to avoid water transfer (Ma et al., 2008). Data obtained in this study concluded that there is no significant difference between the optimum film with and without gallic acid (Figure 4.40). However, the WVP (~1 to $1.1*10^{-3}$ g.mm/m^2.h.Pa)

166

of films produced in this thesis were significantly lower compared to films of pea (6-6.7x10^{-3} g.mm/m^2.h.Pa), potato (6.1-7.2x10^{-3} g.mm/m^2.h.Pa) and cassava starch (5.4-6.8x10^{-3} g.mm/m^2.h.Pa) films (Al-Hassan & Norziah, 2012; Cano et al., 2014). These films in literature were also produced with glycerol with even lower concentration (0.25 g glycerol/g starch), therefore, the low water vapor permeability of films obtained in this thesis can be attributed to several reasons. First, many studies (Arvanitoyannis et al., 1998; Bourtoom et al., 2006; McHugh et al., 1993) had suggested the addition of hydrophilic compounds like glycerol, sorbitol or protein increase the water vapor permeability of films by absorbing water from the environment.

Although films formed in this these contain 0.5 g glycerol/g starch, the water permeability of film with and without gallic acid were significantly lower, which indicate a strong network was formed in the film under optimum subcritical water condition and reduce the driving force (diffusion coefficient) for water to pass through the film. It could be also related the hydrophobic surface of the films confirmed in contact angle results, which further reduce the interaction of films with water molecules from the environment. Also, films produced in this thesis had a thickness around 0.14mm, which were relatively thicker than the ones generally obtained in the literature (around 0.007 to 0.08 mm). Therefore, water vapor needs more time and stronger driving force to passing through the film, which resulted in a lower water vapor permeability of the film produced in this thesis. The measurement of water vapor permeability of optimum film with and without gallic acid further confirmed the benefit of subcritical water in the formation of a highly crosslinked gel network, which exerted significant improvement in gas barrier properties.

167

Future study can examine other gas, like oxygen and may use films produced in this thesis as oxygen scavenger to prevent oxidation of food.
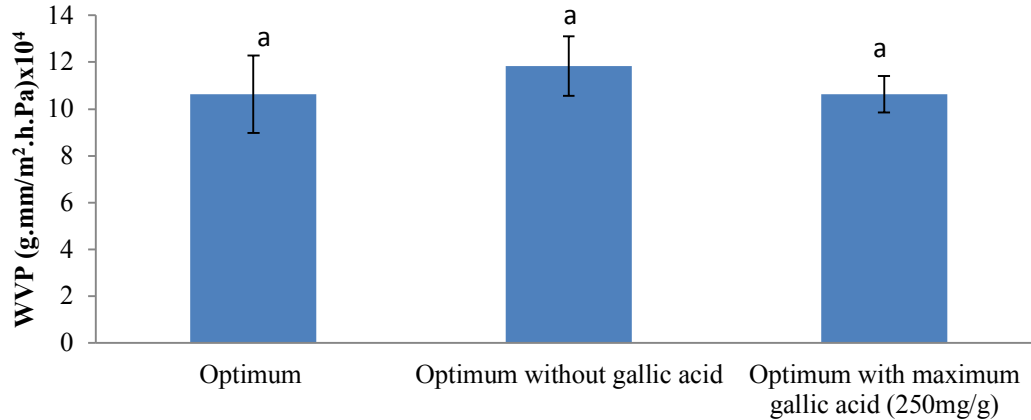
Figure 4.40 Water vapor permeability (WVP) of bioactive films produced at optimum conditions: gallic acid/starch ratio of 40 mg/g, temperature of 100 °C, pressure of 30 bar, glycerol/starch ratio of 0.5 g/g. Data followed by the same letter are not significantly different at p>0.05. Value of each data point is shown in Table B.10 in Appendix B.

4.4 Conclusions

The properties of the film formed in this thesis confirmed the advantages of using subcritical water to form a cross-linked network. Four experimental process parameters (temperature, pressure, gallic acid/starch ratio, and glycerol/starch ratio) were evaluated and optimized to obtain bioactive films with certain characteristics (Table 4.1) at 100 °C, 30 bar, 0.5 g glycerol/g starch and 40 mg gallic acid/g starch. The maximum ratio of gallic acid/starch added without phase separation in the film was 250 mg/g. This film had better mechanical properties when produced at 50 bar.

4.4.1 Influence of gallic acid/starch ratio

- The Influence of gallic acid was mainly from its interaction of –OH groups on the aromatic ring with starch to promote formation of V- type crystalline and promote a smooth and homogenous surface film.

- Gallic acid also acted as a plasticizer in terms of mechanical properties. Higher or lower concentrations than 10 - 60 mg/g starch resulted in low tensile strength. With the addition of more than 60 mg gallic acid/g starch, the elongation of the film improved.

- The addition of gallic acid had minor influence on the water activity and moisture content of the films. Also, gradually improved the transparency of the films.

- Adding gallic acid also improved the gloss of the films on both sides, but no significant influence on the hydrophobicity and water permeability of films were observed.

4.4.2 Influence of temperature

- Temperature is essential for the formation of homogeneous film structures by controlling the degree of gelatinization and depolymerization of starch molecules.

- The elongation % of films decreased with an increase of heating temperature. But, the tensile strength of films decreased at lower or higher temperatures than 100°C.

- Temperature had no influence on the water activity and moisture content of films.

- Severe depolymerization was only observed at 150 °C, resulting in a reduction of the intensity of intermolecular bonds of starch chains, which increased the water solubility of films.

4.4.3 Influence of glycerol/starch ratio

- Glycerol, a plasticizer, was essential for elongation of films. Also it associated with amylose and formed V–type crystalline in the film. However, an excess of glycerol (>1.5 g/g starch) not only compromised the mechanical properties significantly, but also reduced the hydrophobicity, release of phenolics and the gloss of the film.

4.4.4 Influence of pressure

- Pressure applied (10 to 190 bar) had no significant influence on the modification of starch surface in terms of water activity, moisture content, water solubility, color, translucency, gloss, antioxidant capacity and total phenolic content of bioactive films. But, it had a slightly influence to facilitate rupture of starch to obtain a homogeneous gel.

- Only at a pressure of 190 bar, a slightly increase of B-type crystalline was observed from the XRD spectra.

4.4.5 Influence of different phenolic acids

- Due to the low aqueous solubility of caffeic, ferulic and cinammic acid, their influence on the antimicrobial activity against two strains was no significant.

- Formation of a modified A-type crystalline of starch was observed in the film prepared with cinnamic acid, which needs further study to confirm its configuration.

Table 4.1 Main characteristics of bioactive films.

Parameter	Control	Optimum	Maximum gallic acid
Temperature (˚C)	100	100	100
Pressure (bar)	30	30	**50**
Gallic acid/starch ratio (mg/g)	**0**	**40**	**250**
Glycerol/starch ratio (g/g)	0.5	0.5	0.5
Property			
Tensile stress (MPa)	2.15±0.96	5.98±0.25	2.16±0.58
Elongation (%)	67.46±9.57	72.85±8.52	89.23±18.62
Contact angle (top surface)	90.84±4.40	76.44±5.26	87.26±1.64
Contact angle (bottom surface)	99.09±3.26	94.96±2.87	88.68±0.47
Moisture content (%)	27.98±0.00	24.69±0.49	19.77±0.08
Color (YI)	2.30±0.59	2.79±0.10	2.45±0.717
Color (WI)	90.58±0.41	90.64±0.38	90.55±0.06
Gloss (top surface)	84.66±3.41	93.46±2.96	116.83±2.12
Gloss (bottom surface)	8.66±0.65	21.25±16.38	73.3±9.99
Translucency	4.33±0.049	2.94±1.84	0.75±0.16
Water activity	0.33±0.029	0.26±0.033	0.29±0.056
Water solubility (4 ˚C)	14.02±2.59	17.62 ±5.13	30.13±3.12
Water solubility (25 ˚C)	14.85±3.51	20.72 ±1.05	37.32±0.94
Water solubility (50 ˚C)	8.89±2.50	23.56±1.59	41.36±4.13
Water vapor permeability $(g.mm/m^2.h.Pa)x10^4$	11.83±1.26	10.63±1.65	10.63±0.77
Total phenolic content	0.61±0.017	31.56±1.27	115.81±3.45
Antioxidant activity (FRAP) (mg Trolox equivalent/g film)	0.94±0.14	227.93±22.34	1432.24±36.91

4.5 Recommendations

- Perform chemical crosslinking by adding a crosslinking agent, such as polyvinyl alcohol, or glutaraldehyde to crosslink phenolic acids to natural polymers like starch, or cellulose.

- Adding hydrophobic natural compounds (e.g. zein) to change the hydrophobicity of the film to be water proof, expanding film applications.

- Modify the experimental system to perform semi-continuous production of bioactive films in laboratory and industrial scale.

- Examine the antimicrobial activity using other microorganisms (e.g. fungi). Instead of using the disc-diffusion assay, use Log reduction assay to quantify the antimicrobial activity of bioactive films.

- Determine the chain-length of the depolymerized starch at each experimental condition to better understand the effect of pH, temperature and pressure on the starch modification.

- Incorporate other antimicrobial compounds such as tannic acid, or ascorbic acid to improve the antimicrobial activity.

- Use bioactive films produced in this thesis in real food systems, like wrap a beef with this film and evaluate shelf-life of the meat.

- Measure kinetic release of phenolic acids from the films into different solutions of water, ethanol, or their mixtures.

- Measure oxygen permeability of the film.

- Incorporate more gallic acid by lowering the pH of the solution to increase the antimicrobial activity of the film.

4.6 References

Ahmadi, R., Kalbasi-Ashtari, A., Oromiehie, A., Yarmand, M.S., Jahandideh, F. 2012. Development and characterization of a novel biodegradable edible film obtained from psyllium seed (*Plantago ovata Forsk*). *Journal of Food Engineering*, **109**(4), 745-751.

Al-Hassan, A.A., Norziah, M.H. 2012. Starch-gelatin edible films: Water vapor permeability and mechanical properties as affected by plasticizers. *Food Hydrocolloids*, **26**(1), 108-117.

Ali-Shtayeh, M.S., Yaghmour, R.M.R., Faidi, Y.R., Salem, K., Al-Nuri, M.A. 1998. Antimicrobial activity of 20 plants used in folkloric medicine in the Palestinian area. *Journal of Ethnopharmacology*, **60**(3), 265-271.

Alves, J.S., Dos Reis, K.C., Menezes, E.G.T., Pereira, F.V., Pereira, J. 2015. Effect of cellulose nanocrystals and gelatin in corn starch plasticized films. *Carbohydrate polymers*, **115**, 215-22.

Andreuccetti, C., Carvalho, R.A., Galicia-Garcia, T., Martinez-Bustos, F., Gonzalez-Nunez, R., Grosso, C.R.F. 2012. Functional properties of gelatin-based films containing Yucca schidigera extract produced via casting, extrusion and blown extrusion processes: A preliminary study. *Journal of Food Engineering*, **113**(1), 33-40.

AOAC International. 2000. Official Methods of Analysis.17[th]ed. *AOAC International*, Gaithersbersburg, MD.

Aranda Saldaña, M.D., Alvarez, V.H., Vasanthan, T. (2014). PCT/CA2014/000432, WO 2014 186864 A1. Modification of starches and production of new biopolymers using subcritical water technology.

Arvanitoyannis, I., Nakayama, A., Aiba, S. 1998. Edible films made from hydroxypropyl starch and gelatin and plasticized by polyols and water. *Carbohydrate Polymers*, **36**(2-3), 105-119.

ASTM D1746-92, 1992.Standard test method for transparency of plastic sheeting, *ASTM International*, West Conshohocken, PA,

ASTM E96-00, 2000. Standard test methods for water vapor transmission of materials, *ASTM International*, West Conshohocken, PA.

ASTM D2244-11.2011. Standard practice for calculation of color tolerances and color differences from instrumentally measured color coordinates, *ASTM International*, West Conshohocken, PA,

ASTM D523-89. 1999, Standard test method for specular gloss, *ASTM International*, West Conshohocken, PA.

ASTM D882-12. 2012. Standard test method for tensile properties of thin plastic sheeting, *ASTM International*, West Conshohocken, PA.

Ayala, G., Vargas, R.A., Agudelo, A.C. 2014. Influence of glycerol and temperature on the rheological properties of potato starch solutions. *International Agrophysics*, **28**(3), 261-268.

Baheiraei, N., Yeganeh, H., Ai, J., Gharibi, R., Azami, M., Faghihi, F. 2014. Synthesis, characterization and antioxidant activity of a novel electroactive and biodegradable polyurethane for cardiac tissue engineering application. *Materials science & engineering. C, Materials for biological applications*, **44**, 24-37.

Bangyekan, C., Aht-Ong, D., Srikulkit, K. 2006. Preparation and properties evaluation of chitosan-coated cassava starch films. *Carbohydrate Polymers*, **63**(1), 61-71.

Belgacem, M.N., Gandini, A. 2008. Monomers, Polymers and Composites from Renewable Resources, Elsevier.

Benzie, I.F.F., Strain, J.J. 1996. The ferric reducing ability of plasma (FRAP) as a measure of "antioxidant power": The FRAP assay. *Analytical Biochemistry*, **239**(1), 70-76.

Beuchat, L.R., Komitopoulou, E., Beckers, H., Betts, R.P., Bourdichon, F., Fanning, S., Joosten, H.M., Ter Kuile, B.H. 2013. Low-water activity foods: Increased concern as vehicles of foodborne pathogens. *Journal of Food Protection*, **76**(1), 150-172.

Bitencourt, C.M., Favaro-Trindade, C.S., Sobral, P.J.A., Carvalho, R.A. 2014. Gelatin-based films additivated with curcuma ethanol extract: Antioxidant activity and physical properties of films. *Food Hydrocolloids*, **40**, 145-152.

Blanco-Pascual, N., Montero, M.P., Gomez-Guillen, M.C. 2014. Antioxidant film development from unrefined extracts of brown seaweeds Laminaria digitata and Ascophyllum nodosum. *Food Hydrocolloids*, **37**, 100-110.

Blaszczak, W., Fornal, J., Kiseleva, V.I., Yuryev, V.P., Sergeev, A.I., Sadowska, J. 2007. Effect of high pressure on thermal, structural and osmotic properties of waxy maize and Hylon VII starch blends. *Carbohydrate Polymers*, **68**(3), 387-396.

Blois, M.S. 1958. Antioxidant determinations by the use of a stable free radical. *Nature*, **181**(4617), 1199-1200.

Bonilla, J., Talon, E., Atares, L., Vargas, M., Chiralt, A. 2013. Effect of the incorporation of antioxidants on physicochemical and antioxidant properties of wheat starch-chitosan films. *Journal of Food Engineering*, **118**(3), 271-278.

Boun, H.R., Huxsoll, C.C. 1991. Control of Minimally Processed Carrot (*Daucus carota*) Surface Discoloration Caused by Abrasion Peeling. *Journal of Food Science*, **56**(2), 416-418.

Bourtoom, T., Chinnan, M.S., Jantawat, P., Sanguandeekul, R. 2006. Effect of plasticizer type and concentration on the properties of edible film from water-soluble fish proteins in surimi wash-water. *Food Science and Technology International*, **12**(2), 119-126.

Bremer Boaventura, B.C., Negrao Murakami, A.N., Prudencio, E.S., Maraschin, M., Murakami, F.S., Amante, E.R., de Mello Castanho Amboni, R.D. 2013. Enhancement of bioactive compounds content and antioxidant activity of aqueous extract of mate (*Ilex paraguariensis* A. St. Hil.) through freeze concentration technology. *Food Research International*, **53**(2), 686-692.

Cano, A., Jiménez, A., Cháfer, M., Gónzalez, C., Chiralt, A. 2014. Effect of amylose: Amylopectin ratio and rice bran addition on starch films properties. *Carbohydrate Polymers*, **111**(0), 543-555.

Carneiro-da-Cunha, M.G., Cerqueira, M.A., Souza, B.W.S., Souza, M.P., Teixeira, J.A., Vicente, A.A. 2009. Physical properties of edible coatings and films made with a polysaccharide from *Anacardium occidentale* L. *Journal of Food Engineering*, **95**(3), 379-385.

Cerqueira, M.A., Souza, B.W.S., Teixeira, J.A., Vicente, A.A. 2012. Effect of glycerol and corn oil on physicochemical properties of polysaccharide films - A comparative study. *Food Hydrocolloids*, **27**(1), 175-184.

Chang, Y.P., Karim, A.A., Seow, C.C. 2006. Interactive plasticizing-antiplasticizing effects of water and glycerol on the tensile properties of tapioca starch films. *Food Hydrocolloids*, **20**(1), 1-8.

Chavez Gutierrez, M., del Carmen Nunez-Santiago, M., Andrea Romero-Bastida, C., Martinez-Bustos, F. 2014. Effects of coconut oil concentration as a plasticizer and Yucca schidigera extract as a surfactant in the preparation of extruded corn starch films. *Starch-Starke*, **66**(11-12), 1079-1088.

Cheng, W., Chen, J., Liu, D., Ye, X., Ke, F. 2010. Impact of ultrasonic treatment on properties of starch film-forming dispersion and the resulting films. *Carbohydrate Polymers*, **81**(3), 707-711.

Ciesla, K., Sartowska, B., Krolak, E. 2015. SEM studies of the structure of the gels prepared from untreated and radiation modified potato starch. *Radiation Physics and Chemistry*, **106**, 289-302.

Corrales, M., Han, J.H., Tauscher, B. 2009. Antimicrobial properties of grape seed extracts and their effectiveness after incorporation into pea starch films. *International Journal of Food Science and Technology*, **44**(2), 425-433.

Eklund, P.C., Langvik, O.K., Warna, J.P., Salmi, T.O., Willfor, S.M., Sjoholm, R.E. 2005. Chemical studies on antioxidant mechanisms and free radical scavenging properties of lignans. *Organic & Biomolecular Chemistry*, **3**(18), 3336-3347.

Farakos, S.M.S., Frank, J.F., Schaffner, D.W. 2013. Modeling the influence of temperature, water activity and water mobility on the persistence of Salmonella in low-moisture foods. *International Journal of Food Microbiology*, **166**(2), 280-293.

Feng, L., Wei, Z., Rui-Jin, Y., Yali, T., Wendy, K. 2015. Survival of *salmonella enterica* in skim milk powder with different water activity and water mobility. *Food Control*, **47**, 1-6.

Fontes, L.C.B., Ramos, K.K., Sivi, T.C., Queiroz, F.P.C. 2011. Biodegradable edible films from renewable sources-potential for their application in fried foods. *American Journal of Food Technology*, **6**(7), 555-567.

Fujio, Y., Igura, N., Hayakawa, I. 1995. Depolymerization of molten-moisturized-starch molecules by shearing force under high-temperature. *Starch-Starke*, **47**(4), 143-145.

Galdeano, M.C., Grossmann, M.V.E., Mali, S., Bello-Perez, L.A., Garcia, M.A., Zamudio-Flores, P.B. 2009. Effects of production process and plasticizers on stability of films and sheets of oat starch. *Materials Science & Engineering C-Biomimetic and Supramolecular Systems*, **29**(2), 492-498.

Gani, A., Nazia, S., Rather, S.A., Wani, S.M., Shah, A., Bashir, M., Masoodi, F.A., Gani, A. 2014. Effect of gamma-irradiation on granule structure and physicochemical properties of starch extracted from two types of potatoes grown in Jammu & Kashmir, India. *Lwt-Food Science and Technology*, **58**(1), 239-246.

Ghasemlou, M., Aliheidari, N., Fahmi, R., Shojaee-Aliabadi, S., Keshavarz, B., Cran, M.J., Khaksar, R. 2013. Physical, mechanical and barrier properties of corn starch films incorporated with plant essential oils. *Carbohydrate Polymers*, **98**(1), 1117-1126.

Godbillot, L., Dole, P., Joly, C., Roge, B., Mathlouthi, M. 2006. Analysis of water binding in starch plasticized films. *Food Chemistry*, **96**(3), 380-386.

Goderis, B., Putseys, J.A., Gommes, C.J., Bosmans, G.M., Delcour, J.A. 2014. The structure and thermal stability of amylose-lipid complexes: A case study on amylose-glycerol monostearate. *Crystal Growth & Design*, **14**(7), 3221-3233.

Goheen, S.M., Wool, R.P. 1991. Degradation of polyethylene–starch blends in soil. *Journal of Applied Polymer Science*, **42**(10), 2691-2701.

Goksu, E.I., Karamanlioglu, M., Bakir, U., Yilmaz, L., Yilmazer, U. 2007. Production and characterization of films from cotton stalk xylan. *Journal of Agricultural and Food Chemistry*, **55**(26), 10685-10691.

Guo, J.J., Kang, H.Q., Feng, X., Lian, X.J., Li, L. 2014. The interaction of sweet potato amylose/amylopectin and KCl during drying. *Food Hydrocolloids*, **41**, 325-331.

Han, J.H., Floros, J.D. 1997. Casting antimicrobial packaging films and measuring their physical properties and antimicrobial activity. *Journal of Plastic Film & Sheeting*, **13**(4), 287-298.

He, G.J., Liu, Q., Thompson, M.R. 2013. Characterization of structure and properties of thermoplastic potato starch film surface cross-linked by UV irradiation. *Starch-Starke*, **65**(3-4), 304-311.

Herceg, I.L., Jambrak, A.R., Subaric, D., Brncic, M., Brncic, S.R., Badanjak, M., Tripalo, B., Jezek, D., Novotni, D., Herceg, Z. 2010. Texture and pasting properties of ultrasonically treated corn starch. *Czech Journal of Food Sciences*, **28**(2), 83-93.

Huang, C., Zhu, J., Chen, L., Li, L., Li, X. 2014. Structural changes and plasticizer migration of starch-based food packaging material contacting with milk during microwave heating. *Food Control*, **36**(1), 55-62.

Huang, J.R., Schols, H.A., van Soest, J.J.G., Jin, Z.Y., Sulmann, E., Voragen, A.G.J. 2007a. Physicochemical properties and amylopectin chain profiles of cowpea, chickpea and yellow pea starches. *Food Chemistry*, **101**(4), 1338-1345.

Huang, Z.Q., Lu, J.P., Li, X.H., Tong, Z.F. 2007b. Effect of mechanical activation on physico-chemical properties and structure of cassava starch. *Carbohydrate Polymers*, **68**(1), 128-135.

Hu, G.F., Chen, J.Y., Gao, J.P. 2009. Preparation and characteristics of oxidized potato starch films. *Carbohydrate Polymers*, **76**(2), 291-298.

Ibrahim, H., Farag, M., Megahed, H., Mehanny, S. 2014. Characteristics of starch-based biodegradable composites reinforced with date palm and flax fibers. *Carbohydrate Polymers*, **101**(0), 11-19.

Jeng-Leun, M., Chiu-Ping, C., Pao-Chuan, H. 2001. Antimicrobial effect of extracts from Chinese chive, cinnamon, and corni fructus. *Journal of Agricultural and Food Chemistry*, **49**(1), 183-188.

Jiménez, A., Talens, P., Chiralt, A. 2011. Effect of saturated and unsaturated fatty acids on structural and optical properties of corn starch-glycerol based films. In *Proceedings of 11th International Congress on Engineering and Food,* 2, 871-972.

Jiménez, A., Fabra, M.J., Talens, P., Chiralt, A. 2012a. Effect of sodium caseinate on properties and ageing behaviour of corn starch based films. *Food Hydrocolloids*, **29**(2), 265-271.

Jiménez, A., Fabra, M.J., Talens, P., Chiralt, A. 2012b. Effect of re-crystallization on tensile, optical and water vapour barrier properties of corn starch films containing fatty acids. *Food Hydrocolloids*, **26**(1), 302-310.

Kanmani, P., Rhim, J.-W. 2014. Antimicrobial and physical-mechanical properties of agar-based films incorporated with grapefruit seed extract. *Carbohydrate Polymers*, **102**, 708-716.

Kavoosi, G., Rahmatollahi, A., Dadfar, S.M.M., Purfard, A.M. 2014. Effects of essential oil on the water binding capacity, physico-mechanical properties, antioxidant and antibacterial activity of gelatin films. *LWT-Food Science and Technology*, **57**(2), 556-561.

Kawai, K., Fukami, K., Yamamoto, K. 2007. Effects of treatment pressure, holding time, and starch content on gelatinization and retrogradation properties of potato starch-water mixtures treated with high hydrostatic pressure. *Carbohydrate Polymers*, **69**(3), 590-596.

Kelleher Environmental. 2012. Plastic waste denominator study for Canada- Executive summary. Retrived from http://www.plastics.ca/_files/file.php?fileid=itemrnvQpa HgBD&filename=file_Kell_Disposal_Report_31_MAR_2012_Revised.pdf, 7 pp.

Liu, H.H., Raju, A., Guo, Q.P., Benu, A. 2013. Preparation and characterization of glycerol plasticized (high-amylose) starch-chitosan films. *Journal of Food Engineering*, **116**(2), 588-597.

Liu, J.M., Zhao, S.L. 1990. Scanning electron-microscope study on gelatinization of starch granules in excess water. *Starch-Starke*, **42**(3), 96-98.

Lopez, O.V., Castillo, L.A., Garcia, M.A., Villar, M.A., Barbosa, S.E. 2015. Food packaging bags based on thermoplastic corn starch reinforced with talc nanoparticles. *Food Hydrocolloids*, **43**, 18-24.

Luo, Z.G., Fu, X., He, X.W., Luo, F.X., Gao, Q.Y., Yu, S.J. 2008. Effect of ultrasonic treatment on the physicochemical properties of maize starches differing in amylose content. *Starch-Starke*, **60**(11), 646-653.

Ma, X., Chang, P.R., Yu, J. 2008. Properties of biodegradable thermoplastic pea starch/carboxymethyl cellulose and pea starch/microcrystalline cellulose composites. *Carbohydrate Polymers*, **72**(3), 369-375.

Mali, S., Grossmann, M.V.E., Garcia, M.A., Martino, M.N., Zaritzky, N.E. 2008. Antiplasticizing effect of glycerol and sorbitol on the properties of cassava starch films. *Brazilian Journal of Food Technology*, **11**(3), 194-200.

Mano, J.F., Koniarova, D., Reis, R.L. 2003. Thermal properties of thermoplastic starch/synthetic polymer blends with potential biomedical applicability. *Journal of Materials Science-Materials in Medicine*, **14**(2), 127-135.

McHugh, T.H., Avenabustillos, R., Krochta, J.M. 1993. Hydrophilic edible films - modified procedure for water-vapor permeability and explanation of thickness effects. *Journal of Food Science*, **58**(4), 899-903.

Menchavez, R.L., Adavan, C.R.M., Calgas, J.M. 2014. Starch consolidation of red clay-based ceramic slurry inside a pressure-cooking system. *Materials Research-Ibero-American Journal of Materials*, **17**(1), 157-167.

Mminh Dang, K., Rangrong, Y. 2015. Development of thermoplastic starch blown film by incorporating plasticized chitosan. *Carbohydrate Polymers*, **115**, 575-581.

Mody, P., Mihu, S.R. 2012. Curses of Plastic on Environment. *Journal of Asian Research Consortium*, **2**(1), 55-60.

Mota, F.L., Queimada, A.J., Pinho, S.P., Macedo, E.A. 2008. Aqueous solubility of some natural phenolic compounds. *Industrial & Engineering Chemistry Research*, **47**(15), 5182-5189.

Muscat, D., Adhikari, R., McKnight, S., Guo, Q., Adhikari, B. 2013. The physicochemical characteristics and hydrophobicity of high amylose starch-glycerol films in the presence of three natural waxes. *Journal of Food Engineering*, **119**(2), 205-219.

Myllarinen, P., Partanen, R., Seppala, J., Forssell, P. 2002. Effect of glycerol on behaviour of amylose and amylopectin films. *Carbohydrate Polymers*, **50**(4), 355-361.

Namazi, H., Fathi, F., Dadkhah, A. 2011. Hydrophobically modified starch using long-chain fatty acids for preparation of nanosized starch particles. *Scientia Iranica*, **18**(3), 439-445.

Nawapat, D., Thawien, W. 2013. Effect of UV-treatment on the properties of biodegradable rice starch films. *International Food Research Journal*, **20**(3), 1313-1322.

Noranizan, M.A., Dzulkifly, M.H., Russly, A.R. 2010. Effect of heat treatment on the physico-chemical properties of starch from different botanical sources. *International Food Research Journal*, **17**(1), 127-135.

Obuz, E., Herald, T.J., Rausch, K. 2001. Characterization of extruded plant protein and petroleum-based packaging sheets. *Cereal Chemistry*, **78**(1), 97-100.

Ortega-Toro, R., Jiménez, A., Talens, P., Chiralt, A. 2014. Effect of the incorporation of surfactants on the physical properties of corn starch films. *Food Hydrocolloids*, **38**, 66-75.

Peregrino, P.P., Sales, M.J.A., da Silva, M.F.P., Soler, M.A.G., da Silva, L.F.L., Moreira, S.G.C., Paterno, L.G. 2014. Thermal and electrical properties of starch-graphene oxide nanocomposites improved by photochemical treatment. *Carbohydrate Polymers*, **106**, 305-311.

Pushpadass, H.A., Hanna, M.A. 2009. Age-induced changes in the microstructure and selected properties of extruded starch films plasticized with glycerol and stearic acid. *Industrial & Engineering Chemistry Research*, **48**(18), 8457-8463.

Pyla, R., Kim, T.-J., Silva, J.L., Jung, Y.-S. 2010. Enhanced antimicrobial activity of starch-based film impregnated with thermally processed tannic acid, a strong antioxidant. *International Journal of Food Microbiology*, **137**(2-3), 154-160.

Qiu, L.P., Hu, F., Peng, Y.L. 2013. Structural and mechanical characteristics of film using modified corn starch by the same two chemical processes used in different sequences. *Carbohydrate Polymers*, **91**(2), 590-596.

Qiu, S., Li, Y.Y., Chen, H., Liu, Y., Yin, L.J. 2014. Effects of high-pressure homogenization on thermal and electrical properties of wheat starch. *Journal of Food Engineering*, **128**, 53-59.

Rachtanapun, P., Tongdeesoontorn, W. 2009. Effect of antioxidants on properties of rice flour/cassava starch film blends plasticized with sorbitol. *Kasetsart Journal, Natural Sciences*, **43**(5), 252-258.

Re, R., Pellegrini, N., Proteggente, A., Pannala, A., Yang, M., Rice-Evans, C. 1999. Antioxidant activity applying an improved ABTS radical cation decolorization assay. *Free Radical Biology and Medicine*, **26**(9-10), 1231-1237.

Rogalinski, T., Liu, K., Albrecht, T., Brunner, G. 2008. Hydrolysis kinetics of biopolymers in subcritical water. *Journal of Supercritical Fluids*, **46**(3), 335-341.

Ruiz-Navajas, Y., Viuda-Martos, M., Sendra, E., Perez-Alvarez, J.A., Fernandez-Lopez, J. 2013. In vitro antibacterial and antioxidant properties of chitosan edible films incorporated with *Thymus moroderi* or *Thymus piperella* essential oils. *Food Control*, **30**(2), 386-392.

Saiah, R., Sreekumar, P.A., Leblanc, N., Saiter, J.M. 2009. Structure and thermal stability of thermoplastic films based on wheat flour modified by monoglyceride. *Industrial Crops and Products*, **29**(1), 241-247.

Sajilata, M.G., Singhal, R.S., Kulkarni, P.R. 2006. Resistant starch - a review. *Comprehensive Reviews in Food Science and Food Safety*, **5**(1), 1-17.

Sajed, H., Sahebkar, A., & Iranshahi, M. 2013. *Zataria multiflora Boiss*. (Shirazi thyme)—An ancient condiment with modern pharmaceutical uses. *Journal of Ethnopharmacology*, 145(3), 686-698.

Samsudin, H., Soto-Valdez, H., Auras, R. 2014. Poly(lactic acid) film incorporated with marigold flower extract (*Tagetes erecta*) intended for fatty-food application. *Food Control*, **46**, 55-66.

Sanchez-Maldonado, A.F., Schieber, A., Ganzle, M.G. 2011. Structure-function relationships of the antibacterial activity of phenolic acids and their metabolism by lactic acid bacteria. *Journal of Applied Microbiology*, **111**(5), 1176-1184.

Seow, C.C., Cheah, P.B., Chang, Y.P. 1999. Antiplasticization by water in reduced-moisture food systems. *Journal of Food Science*, **64**(4), 576-581.

Seyedi, S., Koocheki, A., Mohebbi, M., Zahedi, Y. 2014. *Lepidium perfoliatum* seed gum: a new source of carbohydrate to make a biodegradable film. *Carbohydrate Polymers*, **101**, 349-358.

Shah, A.A., Hasan, F., Hameed, A., Ahmed, S. 2008. Biological degradation of plastics: A comprehensive review. *Biotechnology Advances*, **26**(3), 246-65.

Sindhu, M., Emilia Abraham, T. 2008. Characterisation of ferulic acid incorporated starch-chitosan blend films. *Food Hydrocolloids*, **22**(5), 826-835.

Singh, P.P., Saldaña, M.D.A. 2011. Subcritical water extraction of phenolic compounds from potato peel. *Food Research International*, **44**(8), 2452-2458.

Soares, R.M.D., Soldi, V. 2010. The influence of different cross-linking reactions and glycerol addition on thermal and mechanical properties of biodegradable gliadin-based film. *Materials Science & Engineering C-Materials for Biological Applications*, **30**(5), 691-698.

Soon-Do, Y. 2014. Cross-linked potato starch-based blend films using ascorbic acid as a plasticizer. *Journal of Agricultural and Food Chemistry*, **62**(8), 1755-1764.

Srikaeo, K., Furst, J.E., Ashton, J.F., Hosken, R.W. 2006. Microstructural changes of starch in cooked wheat grains as affected by cooking temperatures and times. *LWT-Food Science and Technology*, **39**(5), 528-533.

Stute, R., Klingler, R.W., Boguslawski, S., Eshtiaghi, M.N., Knorr, D. 1996. Effects of high pressures treatment on starches. *Starch-Starke*, **48**(11-12), 399-408.

Sun, Y., Liu, Y., Li, Y., Lv, M., Li, P., Xu, H., Wang, L. 2011. Preparation and characterization of novel curdlan/chitosan blending membranes for antibacterial applications. *Carbohydrate Polymers*, **84**(3), 952-959.

Sun, X.X., Wang, Z., Kadouh, H., Zhou, K. 2014. The antimicrobial, mechanical, physical and structural properties of chitosan-gallic acid films. *LWT -- Food Science and Technology*, **57**(1), 83-89.

Takahashi, K., Ogata, A., Yang, W.H., Hattori, M. 2002. Increased hydrophobicity of carboxymethyl starch film by conjugation with zein. *Bioscience Biotechnology and Biochemistry*, **66**(6), 1276-1280.

Tang, C.H., Jiang, Y. 2007. Modulation of mechanical and surface hydrophobic properties of food protein films by transglutaminase treatment. *Food Research International*, **40**(4), 504-509.

Valencia, G.A., Agudelo Henao, A.C., Vargas Zapata, R.A. 2014. Influence of glycerol content on the electrical properties of potato starch films. *Starch/Starke*, **66**(3/4), 260-266.

Vallons, K.J.R., Arendt, E.K. 2009. Effects of high pressure and temperature on the structural and rheological properties of sorghum starch. *Innovative Food Science & Emerging Technologies*, **10**(4), 449-456.

Vidhu, V.K., Philip, D. 2015. Biogenic synthesis of SnO_2 nanoparticles: Evaluation of antibacterial and antioxidant activities. *Spectrochimica Acta Part A-Molecular and Biomolecular Spectroscopy*, **134**, 372-379.

Wang, L., Xie, B., Shi, J., Xue, S., Deng, Q., Wei, Y., Tian, B. 2010a. Physicochemical properties and structure of starches from Chinese rice cultivars. *Food Hydrocolloids*, **24**(2-3), 208-216.

Wang, M., Luo, Z., Tu, Y., Dong, S., Pei, Z. 2010b. Effect of ultrasonic treatment on the granular properties of maize starches. *Modern Food Science and Technology*, **26**(5), 448-450.

Wang, S.Y., Ren, J.L., Kong, W.Q., Gao, C.D., Liu, C.F., Peng, F., Sun, R.C. 2014. Influence of urea and glycerol on functional properties of biodegradable PVA/xylan composite films. *Cellulose*, **21**(1), 495-505.

Winkler, H., Vorwerg, W., Rihm, R. 2014. Thermal and mechanical properties of fatty acid starch esters. *Carbohydrate Polymers*, **102**, 941-949.

Yin, Y.J., Yao, K.D., Cheng, G.X., Ma, J.B. 1999. Properties of polyelectrolyte complex films of chitosan and gelatin. *Polymer International*, **48**(6), 429-432.

Yonehara, M., Matsui, T., Kihara, K., Isono, H., Kijima, A., Sugibayashi, T. 2004. Experimental relationships between surface roughness, glossiness and color of chromatic colored metals. *Materials Transactions*, **45**(4), 1027-1032.

Zhu, F., Cai, Y.Z., Sun, M., Corke, H. 2008. Effect of phenolic compounds on the pasting and textural properties of wheat starch. *Starch/Staerke*, **60**(11), 609-616.

Chapter 5: Formation of starch bioactive gels under subcritical water media

5.1 Introduction

Recently, the term hydrogel has been defined as two- or multi-component system consisting of a three-dimensional network structure obtained from synthetic and/or natural polymers, which can absorb and retain a significant amount of water (Ahmed, 2013). The most important characteristic of a hydrogel is its ability to absorb water through hydrophilic functional groups attached to its polymeric backbone, while resisting to be dissolved by its cross-linked network chains (Zhang et al., 2006). A continuous polymerization on the macromolecular chains results in an increasing size of the branched part, which leads to a decreased solubility (Gulrez & Al-Assaf, 2011). Therefore, hydrogels have superior swelling and absorbing capacity compared to traditional absorbents, such as sponge, cotton, and wood pulp. Hydrogels are widely used in many fields, such as in hygienic products, like baby diapers, sanitary napkin, female tampon (Huang et al., 2012), horticulture (e.g. carriers for solid matrix priming of carrot seeds) (Olszewski et al., 2012), sealing (e.g. self-adhering hemostatic sealing pad) (Lewis et al., 2014), drug delivery systems (Belscak-Cvitanovic et al., 2015; Lima-Tenorio et al., 2015), wound healing (Dogan et al., 2014; Pinho et al., 2014), dye removal (Saber-Samandari et al., 2014) and coal dewatering (Kabiri et al., 2011).

Hydrogels can be produced from both synthetic and natural polymers through mainly two pathways: physical and chemical methods. Hydrogels formed through physical method (e.g. ionic interaction, crystallization, stereocomplex formation between L-lactic acid and D-lactic acid) are held together by molecular entanglement, or

secondary forces including ionic, hydrogen bonding or hydrophobic interaction, all of which are reversible and can be disrupted by changes in physical condition or application of stress (Hennink & van Nostrum, 2012). On the other hand, hydrogels formed through chemical modification (e.g. grafting, cross-linking and condensation) resulted in a permanent network covalently cross-linked, as covalent bonds are stronger and more stable than hydrogen bonds (Hennink & van Nostrum, 2012). Although chemical modification leads to a more stable hydrogel, its major concern is the toxicity of the crosslinking agent (e.g. glycolaldehyde) left in the hydrogels, which has to be removed before any final application. Therefore, in recent years, there has been increasing interest in physically crosslinked hydrogels (e.g. hydrophobic modification with chitosan) or non-toxic chemical methods such as gamma irradiation and electron beam (Lam et al., 2015) or UV induced polymerization (Omer et al., 2015; Xing et al., 2014). In this study, a new modification method was evaluated for the formation of bioactive loaded hydrogel from a natural polymer. The objectives of this study were to form potato starch based bioactive gels loaded with phenolic acids under subcritical water media and evaluate their physical, structural and functional properties. Due to the non-toxicity and biodegradable nature of this hydrogel, it can be potentially used in a variety of applications, such as wound healing pad, waste water absorbent, and drug or nutraceutical carrier in food and pharmaceutical industry.

5.2 Materials and methods

5.2.1 Materials

Materials used were the same as the ones described in Chapter 4, Section 4.2.1.

5.2.2 Methods

5.2.2.1   Formation of hydrogel

Hydrogels were prepared following the same procedure of starch bioactive film described in the materials and methods Section 4.2.2.2 in Chapter 4, with modification in the drying method. Gel samples obtained from the SCW reaction unit were first frozen at −18 °C overnight, and then freeze dried using a freeze dry system (Labconco, Kansas City, MO, USA) over a 48 h period at a vacuum pressure of 8.8 Pa with a collector temperature of −44 °C. All experiments were done at least in duplicate.

5.2.2.2   Characterization of starch based bioactive gels

5.2.2.2.1   Apparent bulk density

Density of a hydrogel is calculated based on the following equation:

$$\rho = \frac{m}{V} \qquad (5.1)$$

where, ρ is the density of hydrogel (g/cm^3), m is the mass (g) and V is the volume (cm^3) of the hydrogel calculated based on its dimensions measured.

5.2.2.2.2   Porosity measurement

For porosity determination, the solvent replacement method was used (Yin et al., 2007b). Dried hydrogels (1.5 cm in diameter x 1 cm height) were immersed in 45 mL absolute ethanol for 24 h and weighed after blotting excess ethanol on the surface with a paper towel. The porosity (%) was calculated using the following equation:

$$Porosity\ (\%) = \frac{(m_2 - m_1)}{\rho V} \times 100 \qquad (5.2)$$

where, m_1 and m_2 are the masses (g) of the hydrogel before and after immersion in ethanol, respectively, ρ is the density of absolute ethanol (0.789 g/cm^3) and V is the volume (cm^3) of the hydrogel.

5.2.2.2.3 Measurement of the equilibrium swelling degree in water

The equilibrium swelling degree of the porous bioactive gel was determined following the gravimetric method reported by (Shi et al., 2011). Briefly, dried samples were cut into cylinder shapes with a diameter of 2cm and a height of 1 cm, then immersed in 50 mL Milli-Q water at room temperature for 24 h until reaching swelling equilibrium. The swollen samples were then filtered to remove unabsorbed water with a cheese cloth and drained for 10 min to remove excess water. The equilibrium swelling degree (Q_{eq}, g/g) was determined according to the following equation:

$$Q_{eq} = \frac{m_s - m_d}{m_d} \tag{5.3}$$

where, m_d is the mass of dried sample (g) and m_s is the mass of swollen hydrogel (g).

5.2.2.2.4 Scanning electron microscope

Refer to materials and methods Section 4.2.3.10 in Chapter 4.

5.2.2.2.5 Fourier transform infrared (FTIR) spectroscopy

Refer to materials and methods Section 4.2.3.1 in Chapter 4.

5.2.2.2.6 High-performance liquid chromatography (HPLC)

Refer to materials and method in Section 4.2.3.15 in Chapter 4.

5.2.2.2.7 Total phenolic content released from the bioactive gels

Dried hydrogels (1.5 cm in diameter x 1 cm height) were immersed in 45 mL absolute ethanol at room temperature for 24 h. Then, 10 mL of the solution was stored

and used for the analysis of total phenolic content using the same methodology described in Section 3.2.2.5 in Chapter 3. Total phenolic content was expressed as milligrams of gallic acid equivalents per gram of hydrogel. All measurements were performed at least in duplicate.

5.3 Results and discussion

Bioactive gels formed were evaluated based on their physical structure (density, porosity) and functional properties (swelling degree and total phenolic content released). The influences of experiment parameters (gallic acid/starch ratio, temperature, glycerol/starch ratio and pressure) on these properties of hydrogels were discussed.

5.3.1 Effect of gallic acid/starch ratio on properties of bioactive gels

A proposed mechanism for potato starch hydrogel formation is shown in Figure 5.1. The main interactions among gallic acid, glycerol and amylose and amylopectin were through hydrogen bonding. With the assistant of heat and pressure under excess water, amylose and amylopectin leached out from the starch granule and started reassociation among them, which later formed the gel network. Glycerol and gallic acid are both small molecules that have three –OH groups, which allow them to associate with starch backbone through hydrogen bonding.

187
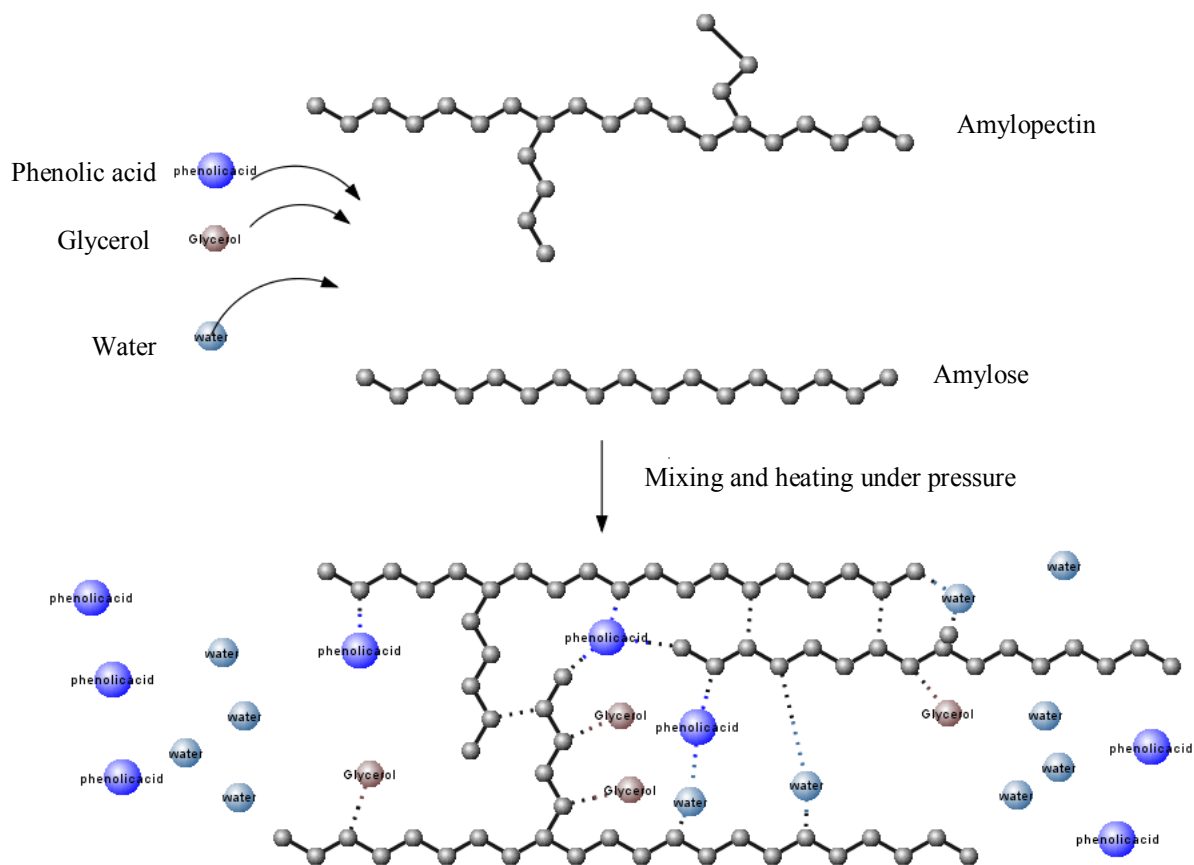
Figure 5.1 Proposed mechanism for gallic acid, glycerol and starch molecules interaction during hydrogel formation.

These interactions were confirmed by FTIR (Figure 5.2). For the FTIR results of potato starch (Figure 4.2), there is only one absorbance at wavelength of 1648 cm^{-1}in the band of 1500 to 1700 cm^{-1} which represents –OH of water. Four major absorbances (wavelengths of 1544, 1596, 1631 and 1685 cm^{-1}) were found in pure gallic acid (Figure 4.14), but no peak was found in glycerol (Figure 4.17) in this range of wavelengths. The new peaks around wavelengths of 1537, 1608 and 1681 cm^{-1} (Figure 5.2) suggest new interactions through hydrogen bonding between gallic acid and starch molecules. However, the peak around wavelength 1537 cm^{-1} differs from the peak of 1511 cm^{-1} found in the starch film (Figure 4.15), which suggests that peak (1537 cm^{-1}) of the bioactive gels were influenced by the removal of water during freeze drying.
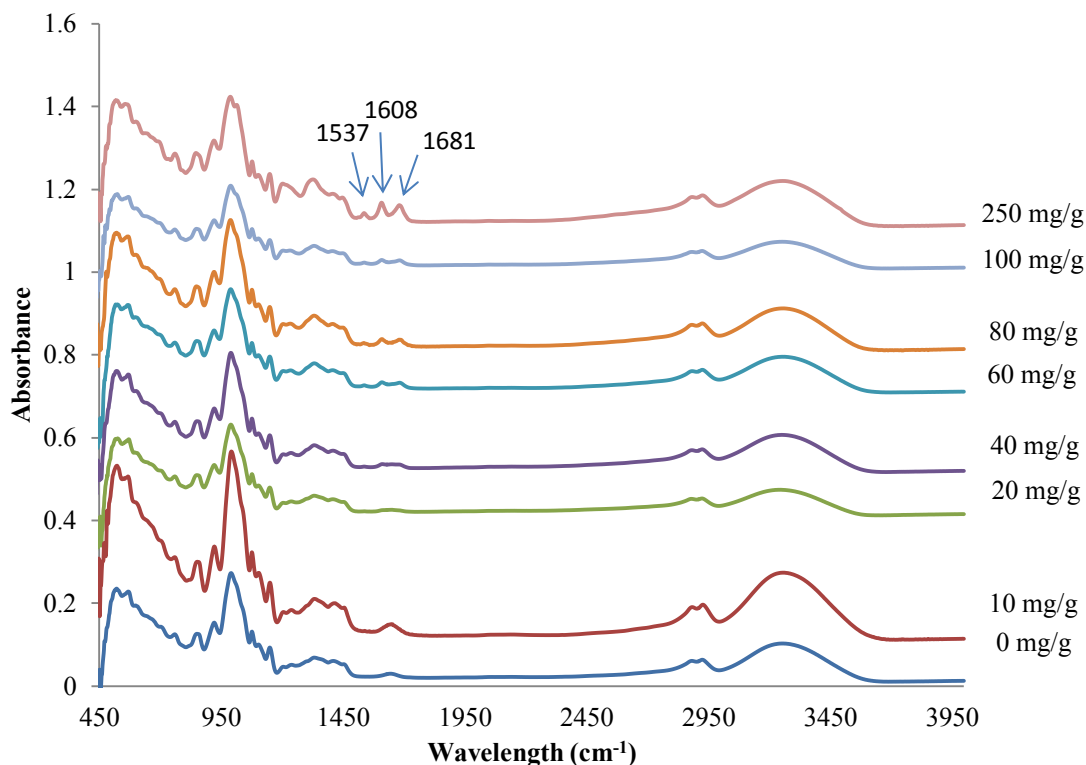
Figure 5.2 FTIR of bioactive gels added with different amounts of gallic acid at a constant glycerol/gallic acid ratio of 0.5 g/g, pressure of 50 bar and temperature of 100 ℃.

In addition, a high content of gallic acid (>100 mg/g) may cause problems during gelatinization and drying. During gelatinization, an excess of gallic acid could occupy the site for water to hydrate limiting the accessibility of starch to water, therefore resulted in incomplete swollen of starch granule and prevent a formation of a strong network. On the other hand, pH of the solution decreased with more gallic acid, which accelerated acid depolymerization of starch, resulting in a short chain polymer that can be dissolved in water. During the freeze drying process, free water was removed from the gel matrix, releasing compounds, such as phenolic acids that dissolved in water. In terms of high concentrations of gallic acid, gels with 100 and 250 mg gallic acid/g starch, the recrystallization of excess gallic acid from water could have also blocked or compromised the association between starch molecules, resulting in a fragile network

189

filled with gallic acid crystals and broken pieces of starch gel (Figure 5.3c). By comparing SEM images of pure gallic acid (Figure 5.3a) and potato starch (Figure 5.3 b), it can be confirmed that the stick part of the feeler was gallic acid and round head of the feeler was starch. The SEM images in Figure 5.4 showed that bioactive gels with high concentration of gallic acid tend to form lots of feeler-like structure on the surface of bioactive gels, which are gallic acid crystals covered by potato starch. Bioactive gels without the addition of gallic acid (Figure 5.4a1-a2) have a smoother surface than the ones with gallic acid (Figure 5.4b-c). For these fragile hydrogels with 100 and 250 mg gallic acid/g starch, density, porosity as well as swelling degree were difficult to measure. Therefore, only total phenolic content of gels with 100 and 250 mg gallic acid/g starch were determined.
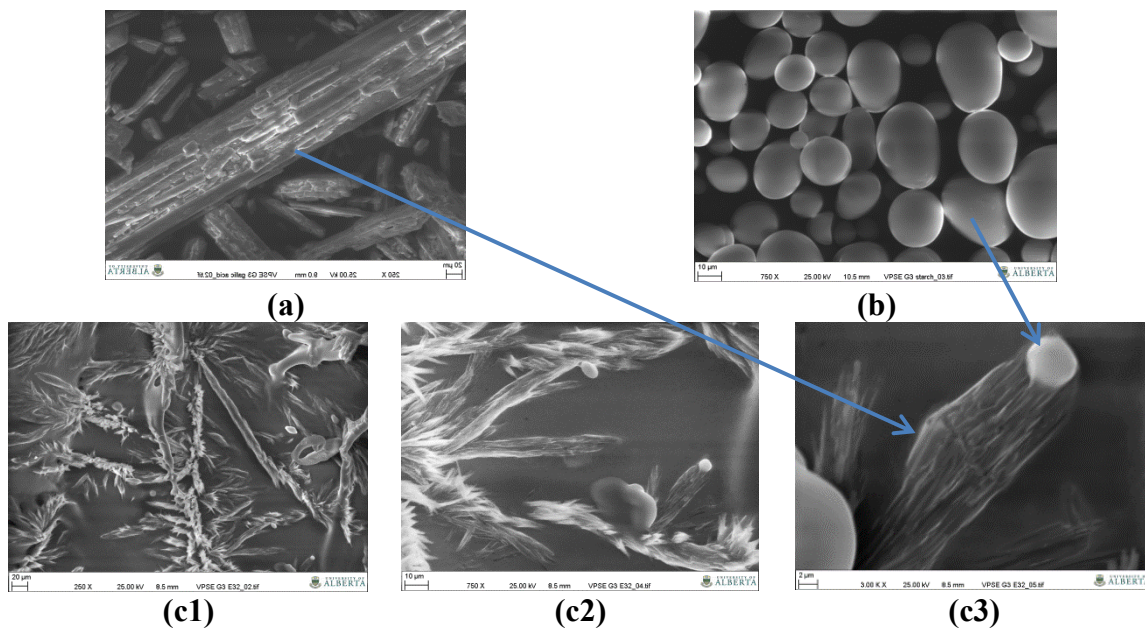
Figure 5.3 SEM images of pure gallic acid (a), native potato starch (b), gel formed with 400mg gallic acid/g starch, glycerol/starch ratio of 0.5 g/g, pressure of 50 bar, and temperature of 100 ℃ (c1-c3: surface image captured without coating at 250 X , 750X and 3000 X magnification under VP mode, respectively)

| (a1) | (b1) | (c1) |
| (a2) | (b2) | (c2) |
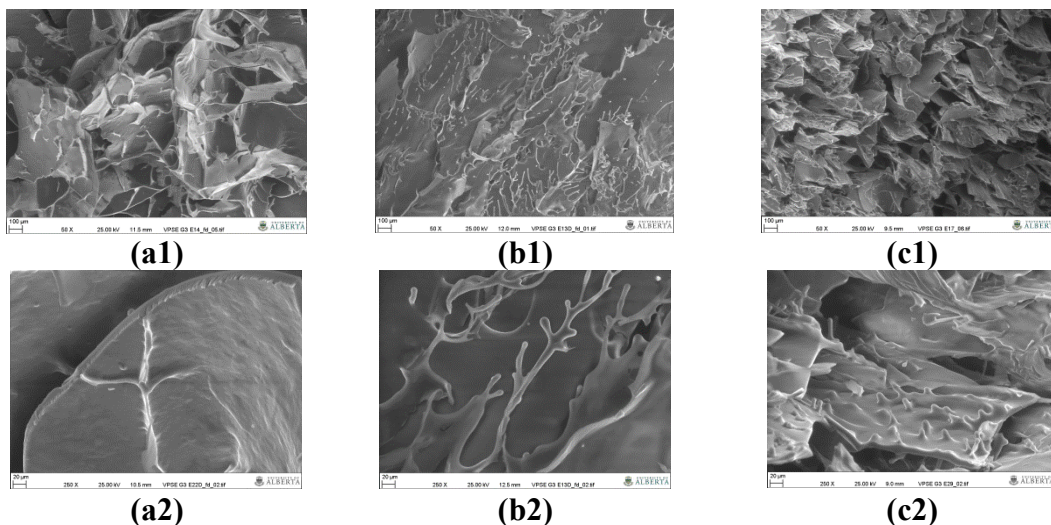
Figure 5.4 SEM images of bioactive gels added with different concentrations of gallic acid (a:0, b:40, c:100 mg/g starch) at constant glycerol/starch ratio of 0.5 g/g, pressure of 50 bar, and temperature of 100 °C (a1-c1: surface image captured without coating at 50 X magnification under VP mode, a2-c2: surface image captured without coating at 250 X magnification under VP mode)

Properties of bioactive gels incorporated with different concentrations of gallic acid are shown in Figure 5.5a-d. There is no significant influence of gallic acid on the density of hydrogels (Figure 5.5a). The bulk density of the hydrogels formed in this study was around 0.1g/cm^3,which was significantly lower than other hydrogels made of acrylamide (0.85 to 1.64 g/cm^3) (Mahdavinia et al., 2009), poly(acrylamide-co-acrylic acid (0.32-1.29 g/cm^3) (Gemeinhart et al., 2000), N-isopropylacrylamide (1.02-1.847) (Chern et al., 2004) but similar to those silica aerogels (0.01 to 0.1 g/cm^3) (Sun et al., 2014).

In terms of porosity, there is no significant influence of gallic acid on the porosity (%) of hydrogel (Figure 5.5c). Hydrogels obtained in this study also had 35-85 % porosity, which were high enough to compete with the one made from poly(acrylic acid-co-acrylamide)/O-carboxymethyl chitosan (62-83%) by chemical crosslinking (Yin et al., 2007a).

Significant decreases in the swelling degree (%) was observed with an increase of gallic acid amount, which indicated that the hydrogen bondings were formed between

191

starch molecules, but were weaker due to the interference of gallic acid. The hydrogel formed in this study had a swelling degree of approximately around 10, which was relatively low compared to other chemically crosslinked hydrogels with a swelling degree around 80 (hydrogels crosslinked by glutaraldehyde with chitosan) (Yin et al., 2007a), 7-24 for hydrogels crosslinked by N,N Methylenebisacrylamide with N-isopropylacrylamide (Chern et al., 2004) and 200-1000 for starch-g-poly (acrylic acid-co-sodium acrylate) hydrogel formed through free radical polymerization (Zhang et al., 2006). During the water absorption process for swelling degree determination, water first penetrates the matrix and hydrates hydrophilic groups and hydrophobic groups (total bound water) (de Moura et al., 2005; Zhang et al., 2006). As these hydrophilic and hydrophobic sites have been taken, the network imbibes additional water (free water) due to the osmotic driving forces of the polymeric network chains toward infinite dilution, but this swelling is restricted by the physical or chemically linked gel network. Eventually, the hydrogel reaches an equilibrium swelling capacity where all the pores or void spaces were filled with free water (Hoffman, 2002).

High porosity but low swelling degree indicates that the pore cannot retain water through hydrogen bonding, the site for hydrogen bonding was occupied, the surface is hydrophobic, or the film is partially dissolved and start to release compounds while immersing water. Based on equation 5.3, if the mass of a swollen gel is reduced, the swelling degree is also reduced. Therefore, in this study the stability of swollen hydrogel in water was low compared to chemically cross-linked hydrogels.

Addition of gallic acid resulted in three main effects on the structure of the bioactive gels: a) acted as a cross-linking agent to promote stronger associations between

starch and water molecules, b) modified the wall of the pores as more feeler was formed, and c) reduced the chain-length of starch molecules through acid depolymerization and decreased the strength of gel network.

In terms of functionality of bioactive gels, a linear trend was found between the ratio of gallic acid/starch and the ratio of phenolic acid/gel released in water (Figure 5.5d) for 24 h, which indicated that the treatment did not degrade phenolic acids like in other sever chemical modifications such as gamma rays (Zhao et al., 2015) and electron beams (Ajji et al., 2008). Therefore, hydrogels obtained in this study can be used as phenolic acid carrier.
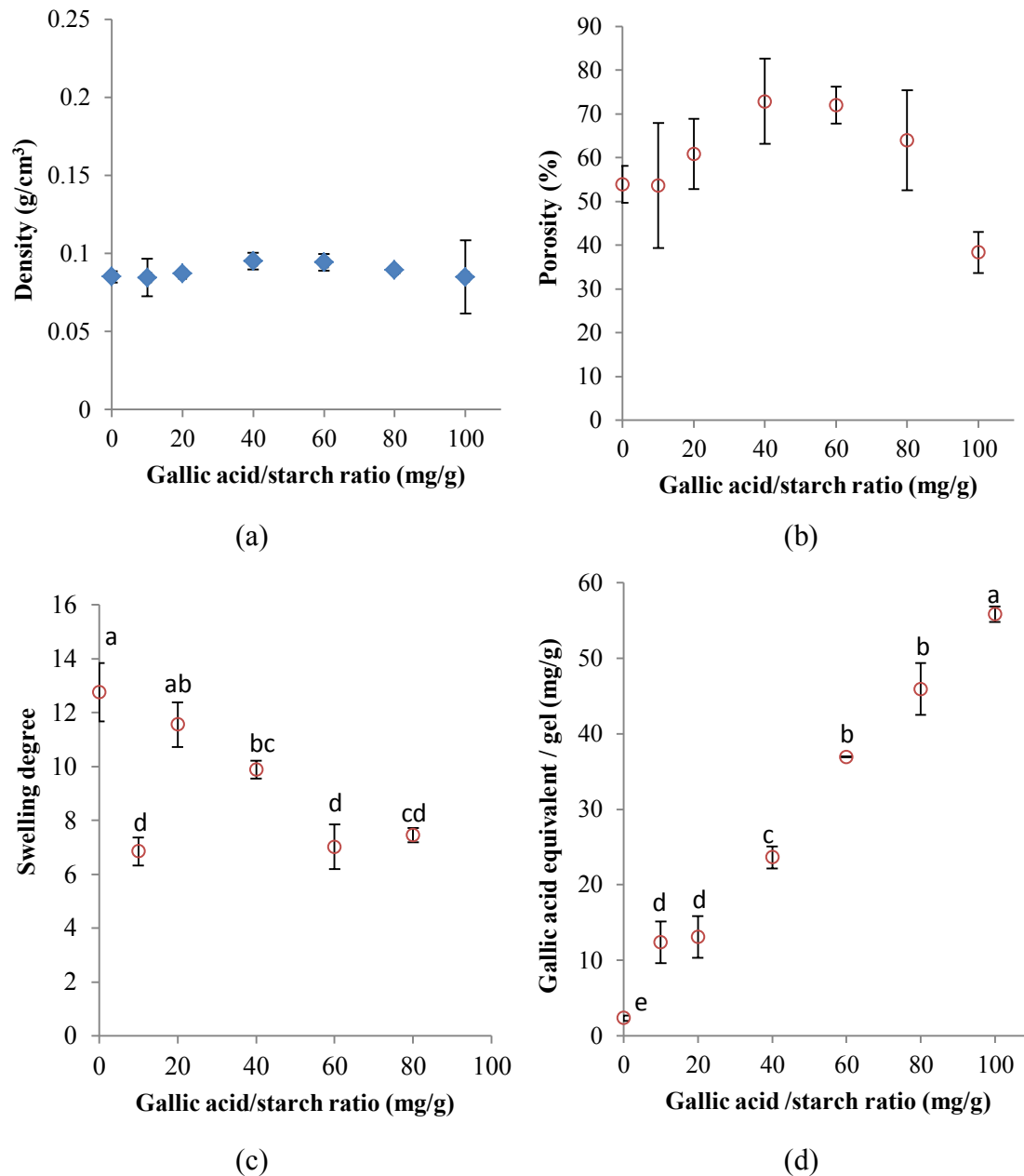
Figure 5.5 Density (a), porosity (b), swelling degree (c), total phenolic content (d) of bioactive gels obtained with glycerol/starch ratio of 0.5 g/g, pressure of 50 bar, temperature of 100 °C and different amounts of gallic acid. Data with the same letter are not significantly different at p>0.05. Values of each data point are shown in Table C.1 in Appendix C. No significant difference was found in density and porosity results.

Overall, 40 mg gallic acid/g starch was considered to be the optimum ratio which gives a hydrogel with density of 0.095 g/cm³, porosity of 72.7% and swelling degree of 9.88.

5.3.2 Effect of temperature on properties of bioactive gels

There was no significant influence of reaction temperature on swelling degree, porosity (%), density and total phenolic content of bioactive gels (Figure 5.6). But, gels formed at 150 °C cannot hold integrity after freeze drying.

(a)

(b)

(c)

(d)
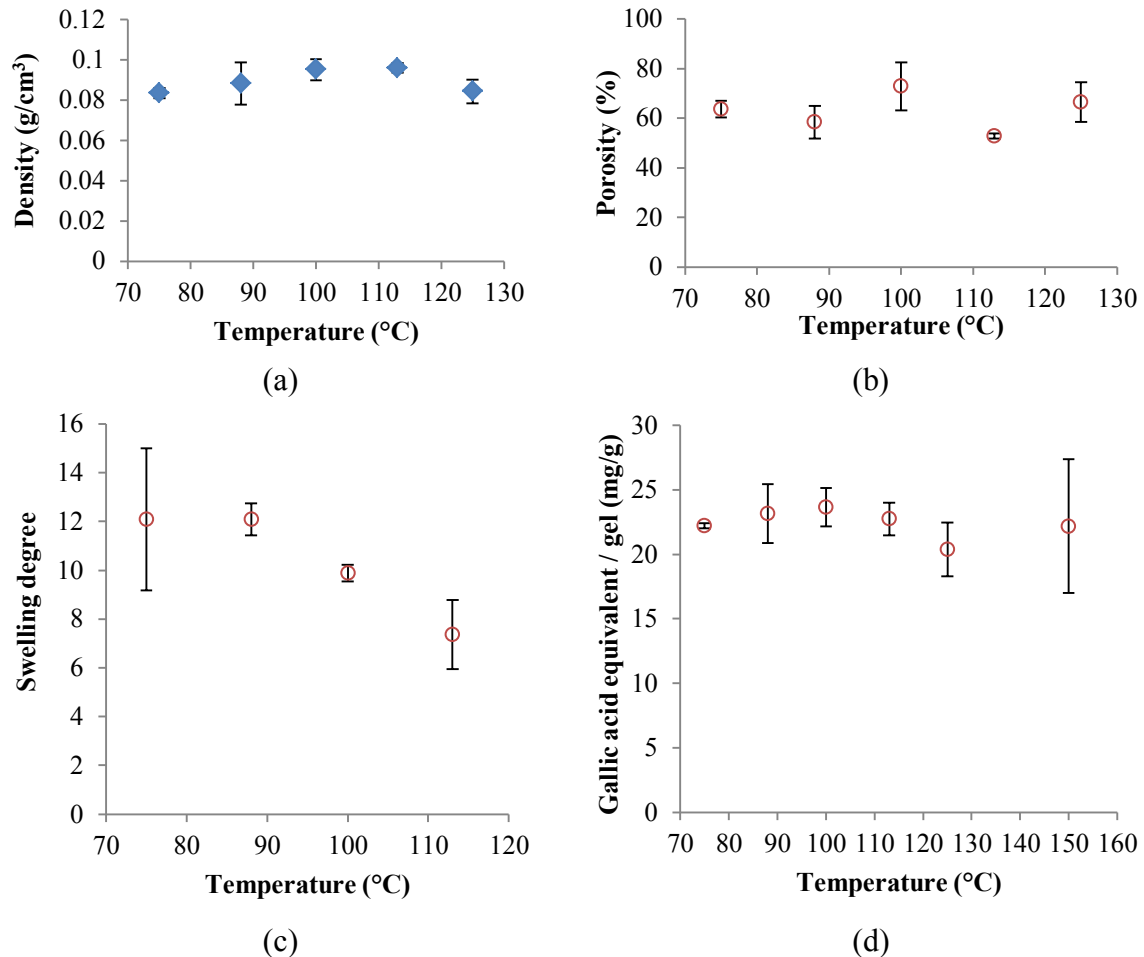
Figure 5.6 Density (a), porosity (b), swelling degree (c), total phenolic content (d) of bioactive gels bioactive gels produced at different temperatures with glycerol/gallic acid ratio of 0.5 g/g, gallic acid /starch ratio of 40 mg/g and pressure of 50 bar. Data with the same letter are not significantly different at p>0.05. Values of each data point are shown in Table C.1 in Appendix C. No significant difference was found in the above results.

From the SEM images (Figure 5.7), the wall of the pores for the gels produced at 150 °C became thinner and more fragile due to weak associations between starch molecules of shorter chain lengths. But, films (Chapter 4) formed at 150 °C were very

strong and intact, which suggest the remaining 20% moisture in the film help the association of starch molecule during oven drying.
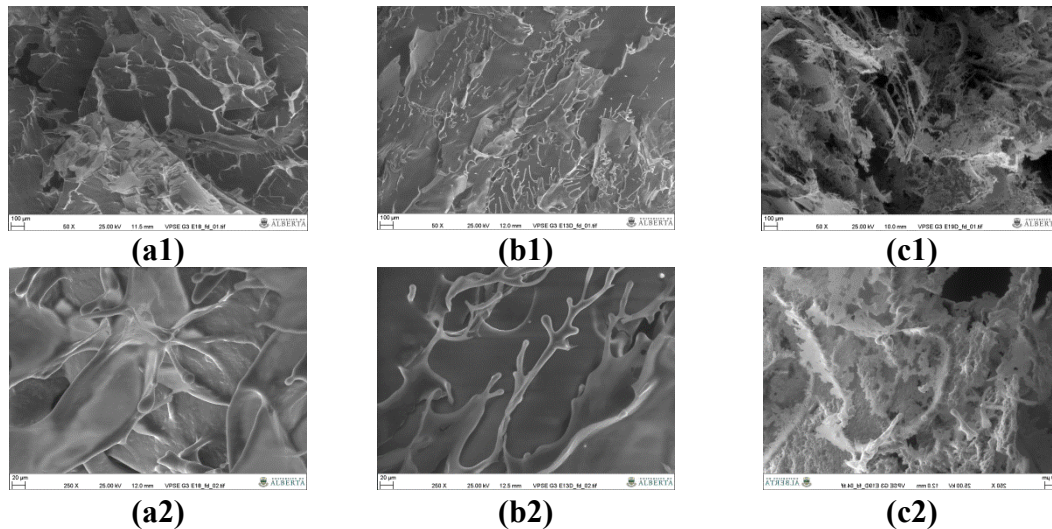
Figure 5.7 SEM images of bioactive gels produced at different temperatures (a: 75, b: 100, c: 150 °C) constant glycerol/starch ratio of 0.5 g/g, gallic acid/starch ratio of 40 mg/g and pressure of 50 bar. (a1-c1: surface image captured without coating at 50 X magnification under VP mode, a2-c2: surface image captured without coating at 250 X magnification under VP mode)

In general, the heating temperatures used for starch based hydrogels are around 80 ℃ (Lanthong et al., 2006; Omidian et al., 2007; Qunyi & Ganwei, 2005; Talaat et al., 2008), which is above the temperature for starch gelatinization. High temperature (>140 °C) under low pH condition (1.8-3.2) can reduce the degree of polymerization of potato, corn and wheat starches (Igura et al., 1997; Shuttleworth et al., 2011).

Therefore, adding gallic acid to produce bioactive gels under high temperatures (>125 °C) facilitated depolymerization of starch molecules, lowering its capacity to retain water and reducing its swelling degree. The fragile gel structure formed at 150 °C made the gel network unstable, as large standard deviations on gallic acid release/gel were found compared to gels produced at lower temperatures, which suggested an optimum temperature is needed to form a strong and stable network to absorb water while releasing

196

bioactive compounds. From the FTIR results (Figure 5. 8), it was found that a peak around 1037 cm^{-1} start to separate from the big peak around 989 cm^{-1}, which can be related to the formation of new C-H from depolymerisation. Thus, temperature did not influence the pore formation inside hydrogel, but influence the strength of gel network through depolymerization. Therefore, 100 °C was chosen as the optimum to form a stronger network.
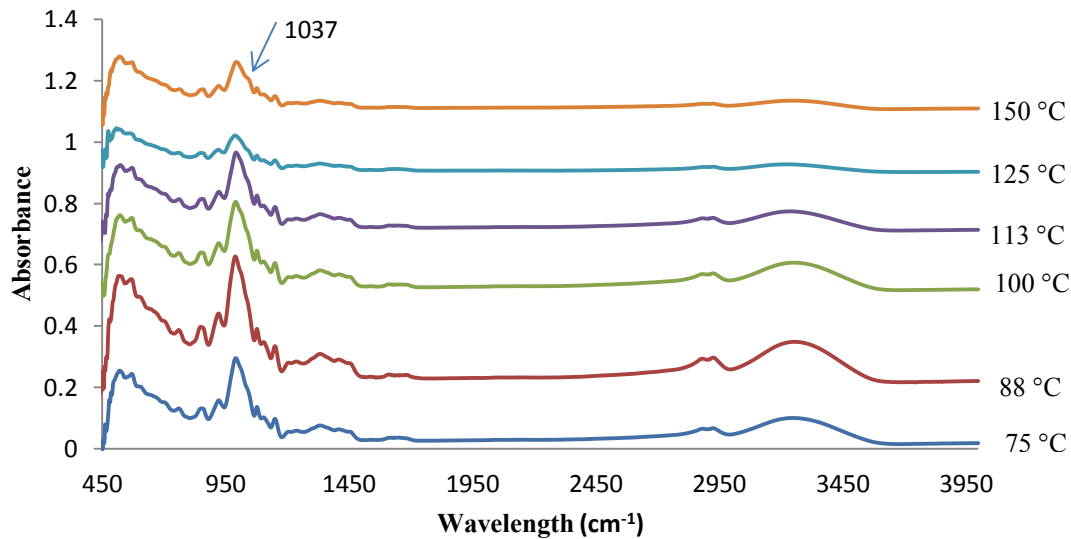
Figure 5.8 FTIR of bioactive gels produced at different temperatures with constant glycerol/gallic acid ratio of 0.5 g/g, gallic acid/starch ratio of 40 mg/g and pressure of 50 bar.

5.3.3 Effect of glycerol/starch ratio on properties of bioactive gels

As the freezing point of glycerol+water mixtures decreases from -0.3 to -42.5 °C with an increase in the percentage of glycerol from 3 to 64.7% present in the gel (Lane, 1925), glycerol in bioactive gels in this thesis cannot be completely removed during the freeze drying process. Due to the hydrophilic nature of glycerol, the surfaces of bioactive gels produced with more than 1 g glycerol/g starch were moister compared to gels with 0.5 g/g or without glycerol. Density and porosity (%) of bioactive gels are shown in Figure 5.9a-b, a significant increase in density and a decrease of porosity were found

when glycerol/starch ratio was > 1 g/g, which suggested that fewer pores are formed (Mahdavinia et al., 2009). Starch gels with more porous structure can increase the contact between water and surface as well as create more space to hold water, resulting in a higher water absorbance capacity (Zhang et al., 2006).

A bioactive gel was still formed without glycerol but had a significant low density (0.05 g/cm^3) and a high porosity (55.8%) indicating that more pores were formed inside. But, the gel lost its integrity after immersing in water for swelling degree determination. Therefore, glycerol could have acted as a crosslinking agent in the gel network to form hydrogen bonding and helped hold the structure during rehydration or swelling. Concentration of glycerol added (>0.5 g/g) were higher than that of gallic acid (40 mg/g), indicating gallic acid alone is not enough to form a strong gel network. However, chemically cross-linked glycerol polyacrylic acid hydrogel showed a swelling degree in water around 250 (Lee et al., 2011), which was much higher than the one formed in this thesis, suggesting superior stability of the hydrogel due to the presence of covalent bonds instead of hydrogen bonds.

In terms of total phenolic content released after 24 h (Figure 5.9d), gallic acid releasing amount increased with 0.5 g glycerol/g starch, but decreased after adding more than 0.5 g glycerol/g starch in the gel, which is consistent to the trend found in a study that used kappa carrageenan and pregelatinized starch based hydrogel loaded with miconazole (Lefnaoui & Moulai-Mostefa, 2014). In their study, they found that glycerol (65-70% in weight) increased the solubility of drug and promoted its release into water, but increasing the concentration of glycerol over 70% (in weight), a reduction by 7% on the release amount of drug was observed. In this study, glycerol/starch ratio over 1g/g

resulted in a low porosity network preventing the contact between water and gallic acid, which significantly reduced the release of the phenolic acid.
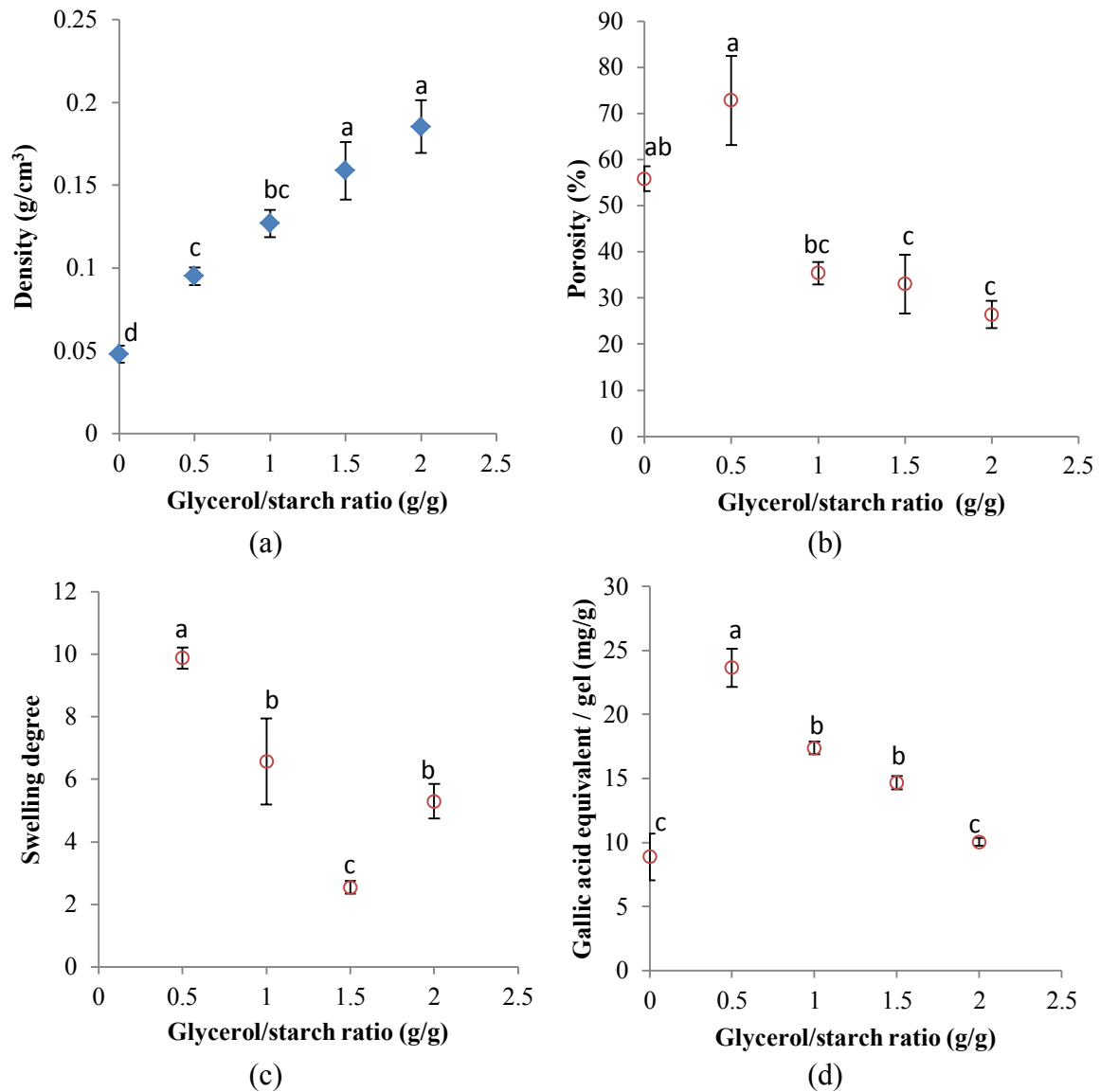
Figure 5.9 Density (a), porosity (b), swelling degree (c), total phenolic content (d) of bioactive gels added with different amounts of glycerol and constant gallic acid /starch ratio of 40 mg/g, temperature of 100 °C and pressure of 50 bar. Data with the same letter are not significantly different at p>0.05. Values of each data point are shown in Table C.1 in Appendix C.

From the SEM images in Figure 5.8, it was confirmed that high concentrations of glycerol resulted in fewer pores where starch molecules were clotted together, restricting the rehydration of hydrogel during swelling. Similar results were reported for starch film

in chapter 4, Figures 4.17-4.18. The FTIR spetra (Figure 5.11) indicated that absorption at 1022, and 1099 cm^{-1} of pure glycerol started to shift to 1020 and 1079 cm^{-1}, respectively, which indicated interactions among gallic acid, starch and glycerol through hydrogen bonds.

Thus, optimum glycerol/starch ratio was 0.5 g/g in terms of physical structure (density, and porosity) and functionality (gallic acid releasing capacity, and swelling degree).
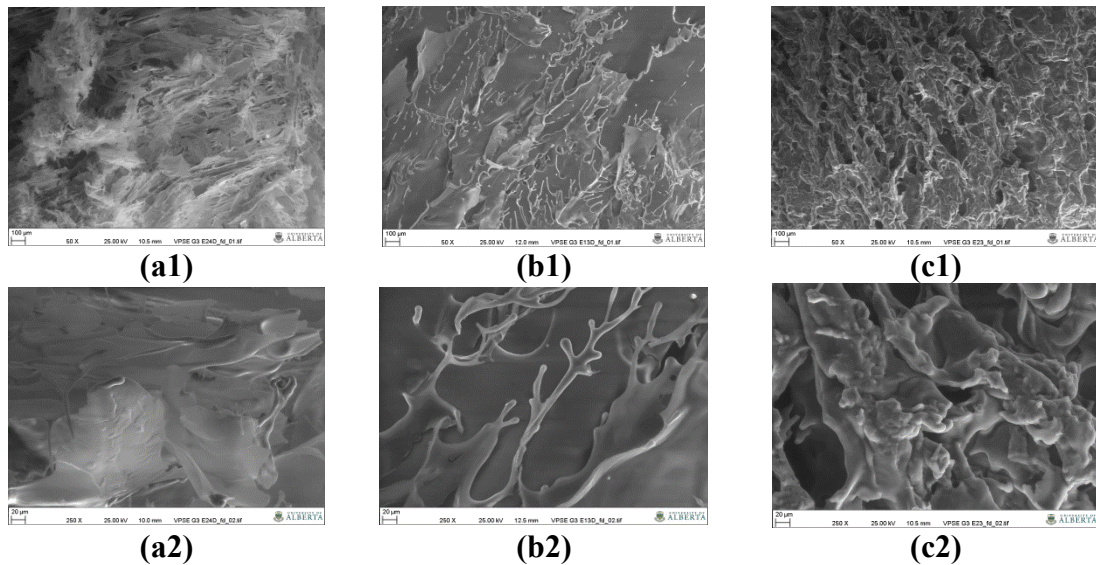
Figure 5.10 SEM images of bioactive gels added with different concentrations of glycerol (a: 0, b: 0.5, c: 2 g/g) at constant gallic acid/starch ratio of 40 mg/g, temperature of 100 ℃ and pressure of 50 bar. (a1-c1: surface images captured without coating at 50 X magnification under VP mode, a2-c2: surface images captured without coating at 250 X magnification under VP mode)
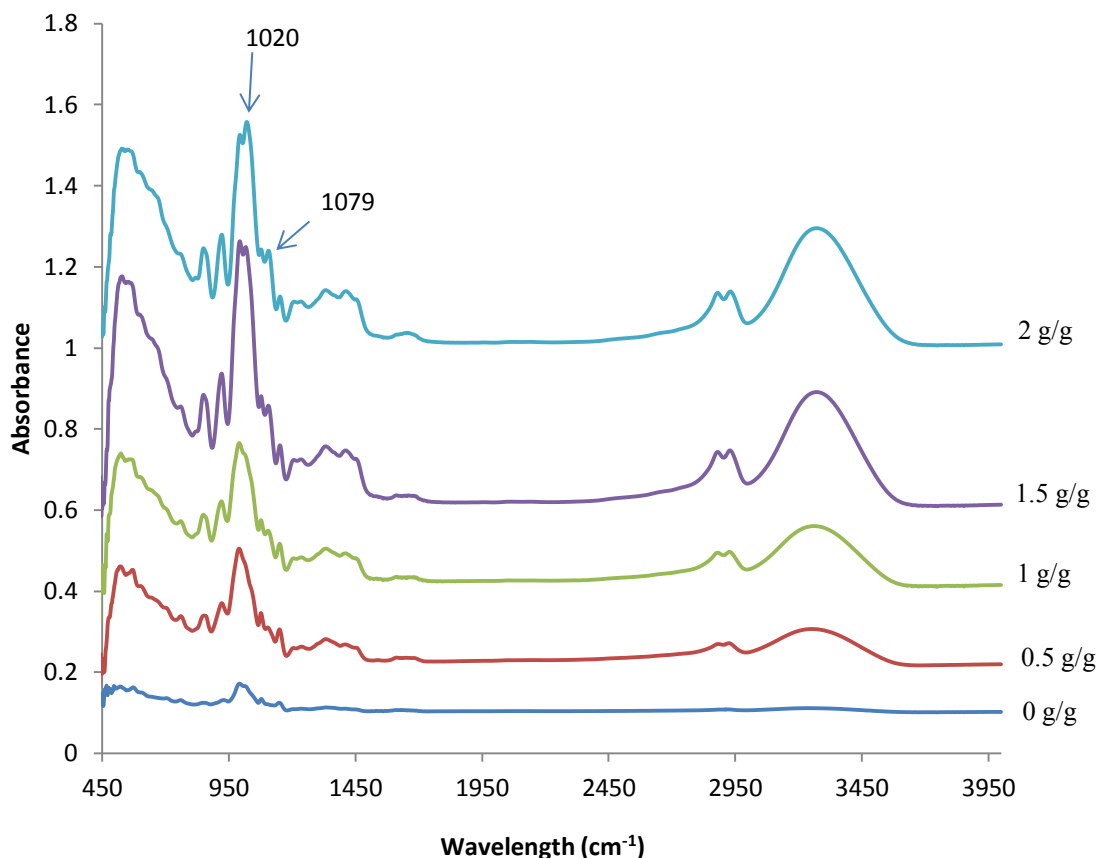
Figure 5.11 FTIR spectra of bioactive gels with different concentrations of glycerol at constant gallic acid/starch ratio of 40 mg/g, temperature of 100 ℃ and pressure of 50 bar.

5.3.4 Effect of pressure on properties of bioactive gels

Properties of bioactive gels produced at different pressures indicated no significant influence of pressure on density, porosity and total phenolic content released (Figure 5.12a-b). But, the swelling degree (Figure 5.12c) of the bioactive gel formed at 190 bar was significantly lower than the one at 10 bar, which indicated that the stability of the bioactive gel was significantly reduced. High pressure facilitated gelatinization and produced a more homogenized gel when 20% water was presented in the bioactive film (Section 4.3.3.4, Chapter 4). Association among starch molecules, glycerol and gallic acid became stronger under high pressure. However, for bioactive gels, after freeze drying, water was completely removed, resulting in a weaker porous structure. From the

201

SEM images in Figure 5.13, low pressures of 10 and 30 bar seem to form more uniformed pores than at a high pressure (> 50 bar). In terms of the FTIR spectra and total phenolic content released, there is no significant difference among different pressures used. Therefore, the influence of pressure on bioactive gels was not significant compared to the other parameters (gallic acid/starch ratio, glycerol/starch ratio and temperature). Based on the SEM images, 10 or 30 bar can be chosen as the optimum pressure due to the higher stability after swelling and homogenized porous structure
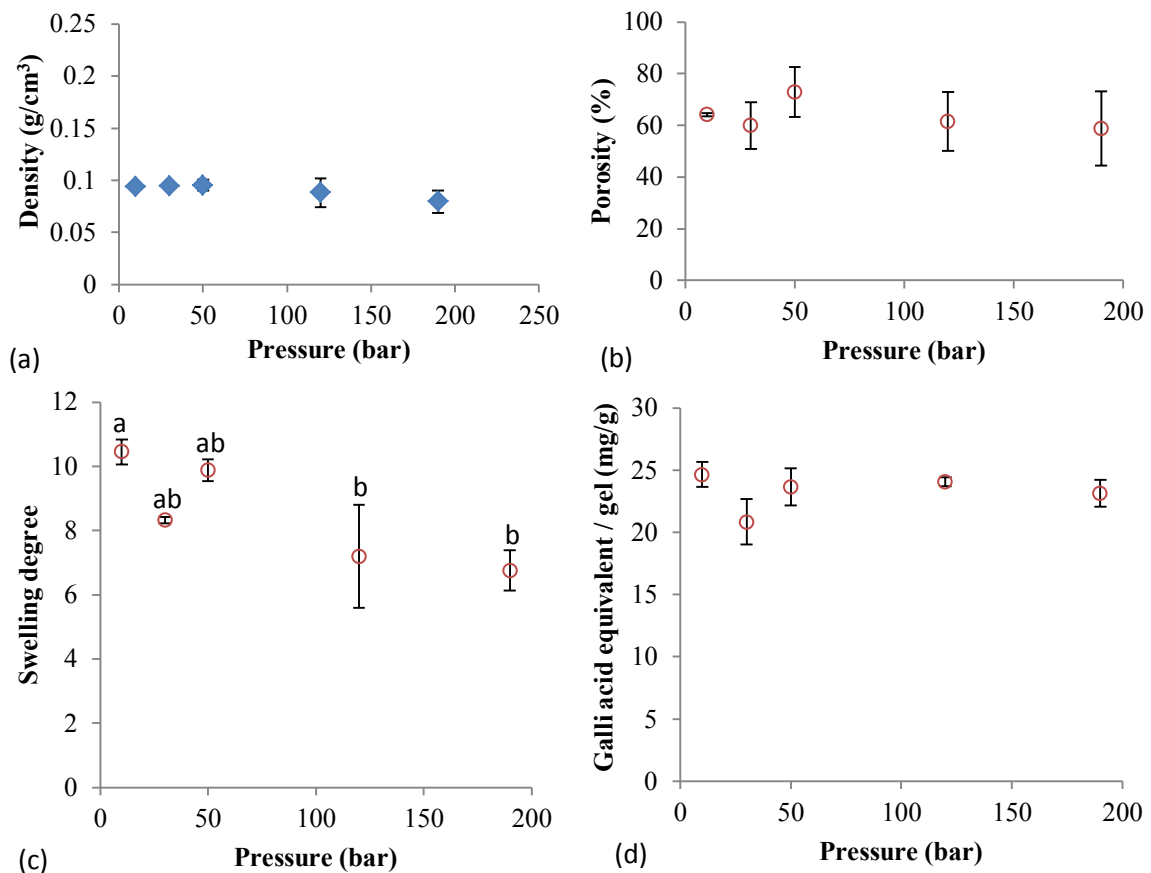
Figure 5.12 Density (a), porosity (b), swelling degree (c), total phenolic content (d) of bioactive gels produced at different pressures and constant glycerol/starch ratio of 0.5 g/g, gallic acid/starch ratio of 40 mg/g, and temperature of 100 ℃ . Data with the same letter are not significantly different at p>0.05. Values of each data point are shown in Table C.1 in Appendix C. No significant difference was found in density, porosity and total phenolic content results.

(a1)　　　**(b1)**　　　**(c1)**　　　**(d1)**　　　**(e1)**

(a2)　　　**(b2)**　　　**(c2)**　　　**(d2)**　　　**(e2)**
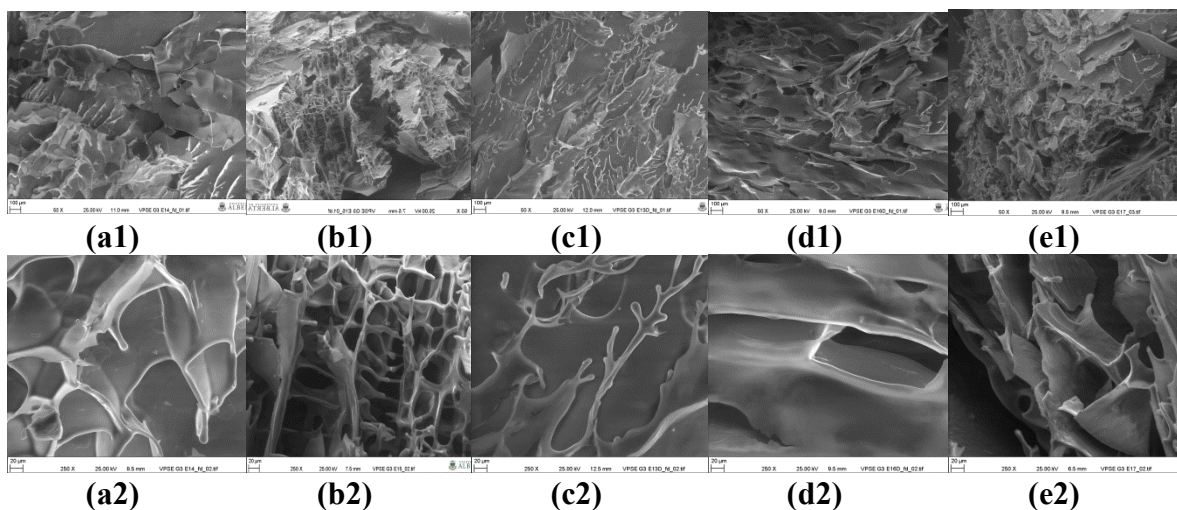
Figure 5.13 SEM images of bioactive gels produced at different pressures (a:10 bar, b:30 bar, c:50 bar, d:120 bar, e: 190 bar) with constant glycerol/starch ratio of 0.5 g/g, gallic acid /starch ratio of 40 mg/g, and temperature of 100 °C. (a1-e1: surface image captured without coating at 50 X magnification under VP mode, a2-e2: surface image captured without coating at 250 X magnification under VP mode)
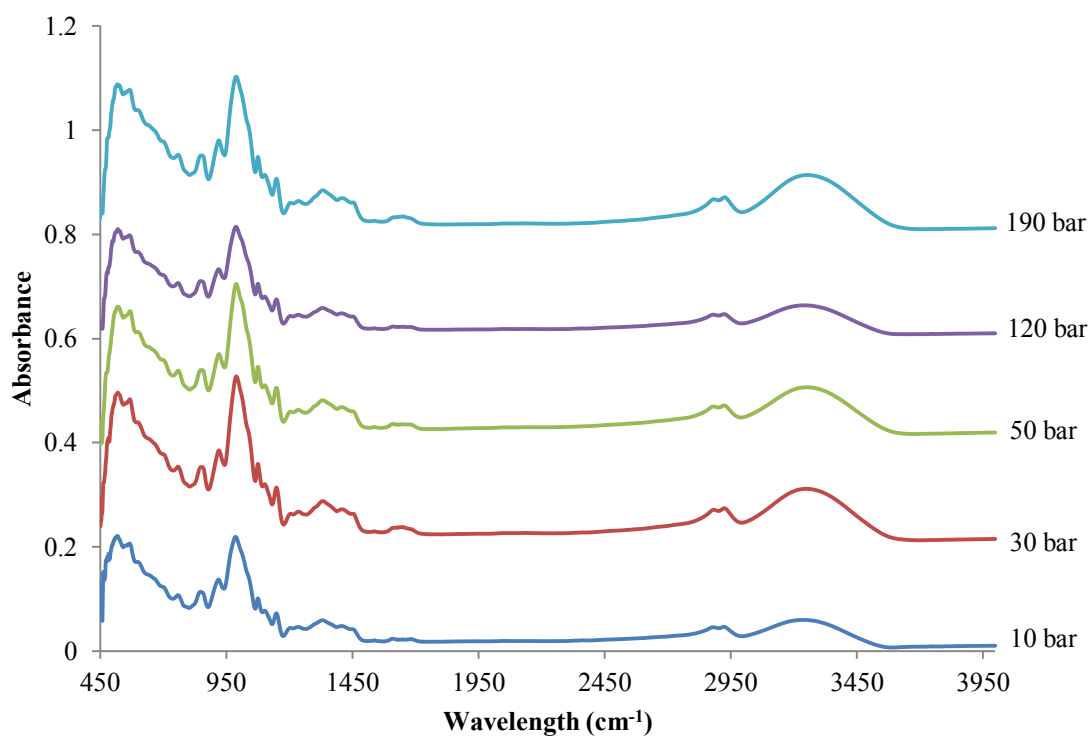
Figure 5.14 FTIR spectra of bioactive gels obtained at different pressures and constant glycerol/gallic acid ratio of 0.5 g/g, gallic acid/starch ratio of 40 mg/g, and temperature of 100 °C.

5.3.5 Effect of different phenolic acids on properties of bioactive gels

Phenolic acids used in this thesis can be divided into two groups: hydrobenzoic acids (gallic acid) and hydrocinnamic acids (cinnamic acid, caffeic acid and ferulic acid). The basic structures are shown in Figure 5.15 where hydrocinnamic acids have an additional C=C double bond than hydrobenzoic acids.

| Gallic acid | Cinnamic acid | Caffeic acid | Ferulic acid |
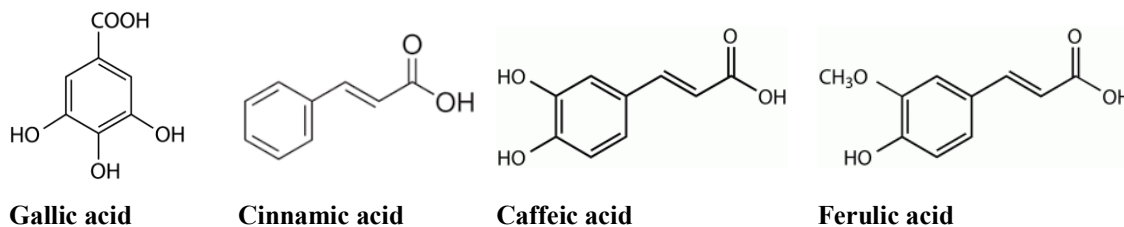
Figure 5.15 Structure of phenolic acids used to obtain bioactive gels.

The use of a specific phenolic acid with a defined structure had no significant influence on the density, porosity and swelling degree of bioactive gels formed compared to the control (Figure 5.16a-c). All bioactive gels including the control without any phenolic acid had densities around 0.1 g/cm^3 (Figure 5.16a). Based on the total phenolic content results in Figure 5.16d, phenolic acids incorporated in the gels can be released, providing functional properties (e.g. antioxidant activity) compared to the control. However, during total phenolic content analysis, cinnamic acid was not identified by our methodology (Section 3.2.2.5, Chapter 3), but HPLC was able to quantify the amount of cinnamic acid released.
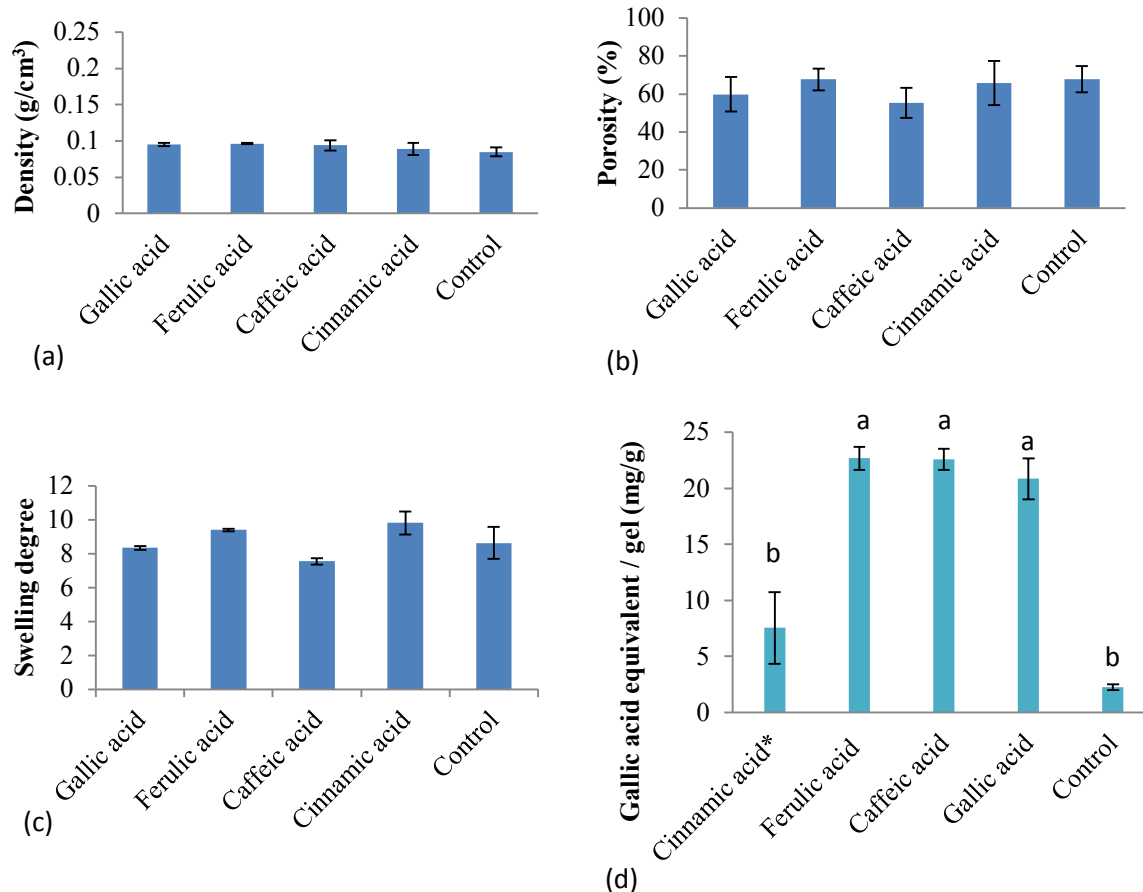
Figure 5.16 Density (a), porosity (b), swelling degree (c), total phenolic content (d) of bioactive gels obtained at optimal conditions: phenolic acids/starch ratio of 40 mg/g, temperature of 100 °C, pressure of 30 bar and glycerol/starch ratio of 0.5 g/g. Data with the same letter are not significantly different at $p>0.05$. Values of each data point are shown in Table C.1 in Appendix C. No significant difference was found in density, porosity and swelling degree results.*Total phenolic content for cinnamic acid measured by HPLC.

Differences were observed on surface morphology (Figure 5.17). That could be attributed to the number of –OH groups on the aromatic ring. Gallic acid and caffeic acid had at least 2 hydroxyl groups, facilitating more interactions with amylose/amylopectin through hydrogen bonds and van der Waals forces as it was confirmed by FTIR Figure 5.18. In another study, the peak viscosity of wheat starch after heating at 95 °C for 7.5 min significantly increased after incorporation of the same phenolic acid selected in this thesis, which confirmed the interactions formed between phenolic acid and starch

molecules (Zhu et al., 2008). These interactions could be stronger after freeze drying, which removes the interference of water between them and formed a stronger network, reducing the pore size and preventing the penetration of water, resulting in a low porosity % and swelling degree.

From the SEM images of bioactive gels showed in Figure 5.17, different porous structures with different phenolic acids are observed. Gels with gallic acid (5.17a) and caffeic acid (5.17c) were more porous, but the pore shape was different. Caffeic acid bioactive gel exhibited a sheet-like layer that was supported by stick-like poles, while the pores in gallic acid gel were similar to a honeycomb, probably due to the presence of one C=C bond in the caffeic acid. These differences in the structure of bioactive gels could also be due to different degree of retrogradation during cooling. The degree of retrogradation may be governed by various factors such as pH, botanical origin, and temperature (Bao et al., 2007; Hirashima et al., 2005; Kawai et al., 2007). Zhu et al. (2008) confirmed a decrease in the pH of wheat starch solution with the same phenolic acids used in this thesis, leading to different degree of retrogradation. It was reported that at a constant water content of 34%, the rate of retrogradation varied depending on the botanical origin, like potato starch showed the highest ($\sim$0.17 h^{-1}) followed by waxy maize ($\sim$0.12 h^{-1}) and wheat starch was the slowest ($\sim$0.05 h^{-1}) (Ottenhof et al., 2005). Many phenolic compounds tend to be in their hydrated forms through hydrogen bonding via their hydroxyl group. Upon gelatinization, phenolic compounds start to hydrate, thus reduce the availability of water to starch gelatinization.

(a1)   **(b1)**   **(c1)**   **(d1)**   **(e1)**

(a2)   **(b2)**   **(c2)**   **(d2)**   **(e2)**
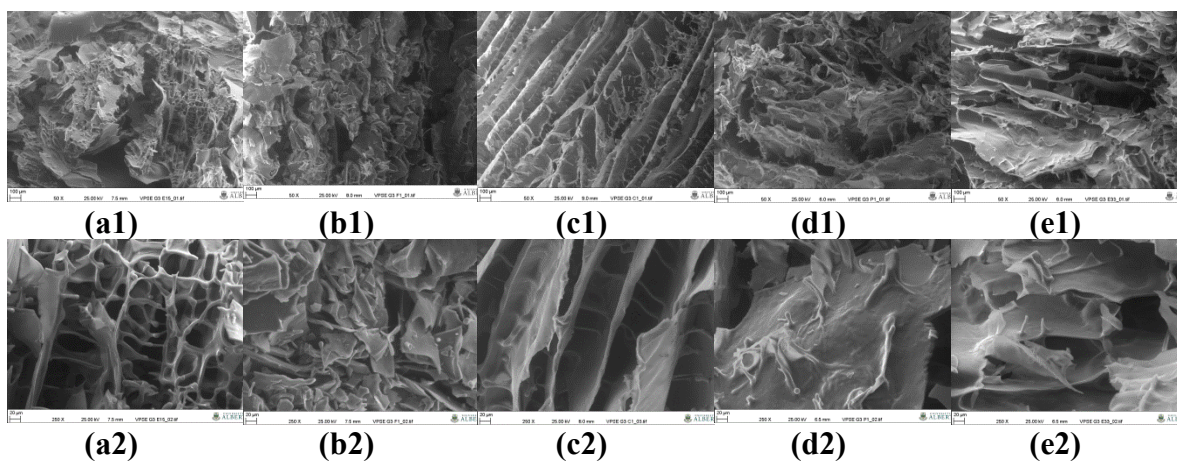
Figure 5.17 SEM images of bioactive gel produced at optimal conditions (phenolic acids /starch ratio of 40 mg/g, temperature of 100 °C, pressure of 30 bar, glycerol/starch ratio of 0.5 g/g) with different phenolic acid (a: gallic acid, b: ferulic acid, c: caffeic acid,d: cinnamic acid, e: without phenolics (control)). (a1-e1: surface images captured without coating at 50 X magnification under VP mode, a2-e2: surface images captured without coating at 250 X magnification under VP mode).
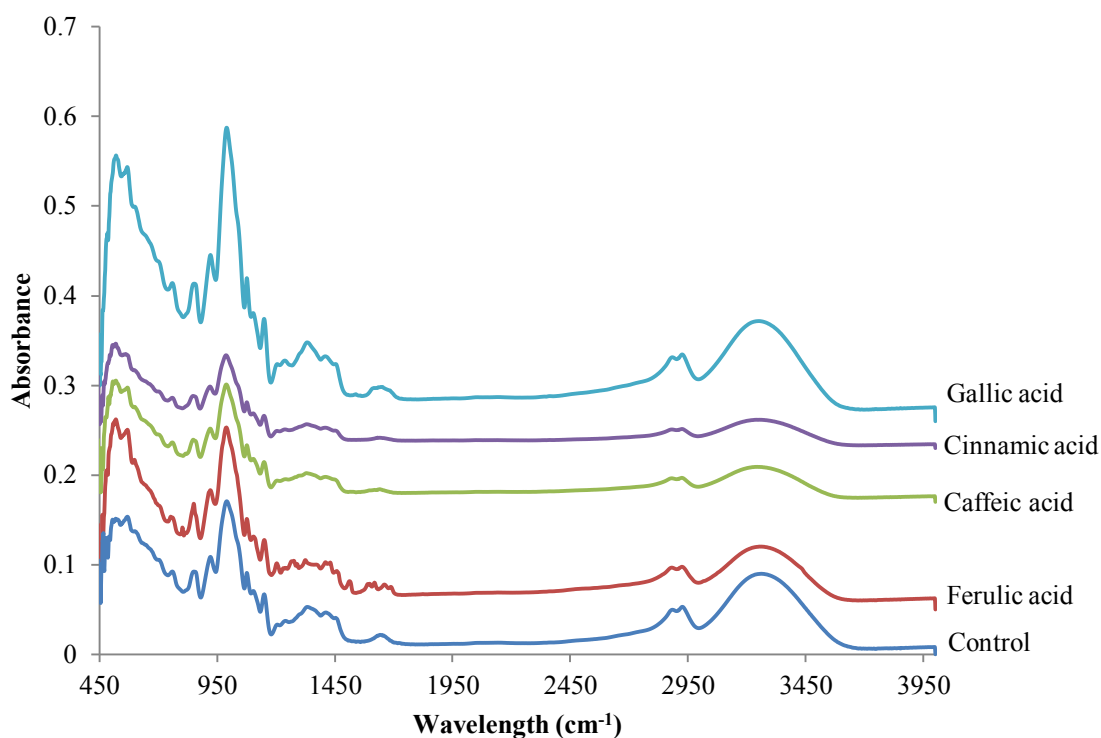
Figure 5.18 FTIR of bioactive gel produced at optimal conditions (phenolic acid/starch ratio of 40 mg/g, temperature of 100 °C, pressure of 30 bar, and glycerol/starch ratio of 0.5 g/g) with different phenolic acids.

5.4 Conclusions

- Experimental conditions used in this study allowed the formation of hydrogels loaded with phenolic acids, which has a density of $0.1 g/cm^{-1}$ and a porosity of 60%.

- Optimum condition for bioactive starch hydrogel was 40 mg gallic acid/g starch, 0.5 g glycerol/g starch, temperature of 100 °C and pressure of 10 or 30 bar.

- The swelling degree of hydrogels formed in this study were around 10, which allowed to absorb 10 times more water than its own weight, however, this value was low compared to chemically cross-linked hydrogels, which had a swelling degree of 250-1000.

- The addition of phenolic acid provided antioxidant activity functionality to the hydrogel.

- The number of the –OH groups on the additives and the presence of C=C bonds can be critical for the pore formation and shape, respectively.

- Among the four experimental parameters evaluated in this study, gallic acid/starch and glycerol/starch ratios played the most significant role in the formation of stable and integral network of bioactive gels.

- Without glycerol, the hydrogel can be easily reversed to gel solution using water. Therefore, low density hydrogel without glycerol may be used as portable or disposable gels.

- Potential applications of hydrogels obtained in this thesis can be to manufacture functional food/feed for pets. Also, the porous hydrogels can be loaded with functional ingredients using supercritical CO_2. Besides, the shape of hydrogel can

be manipulated through the use of molds during drying, resulting in a variety of shapes to fulfill the market gaps. Besides, new application of hydrogel (powder) might also mimic the benefit of dietary fiber.

| (a) | (b) | (c) | (d) | (e) |
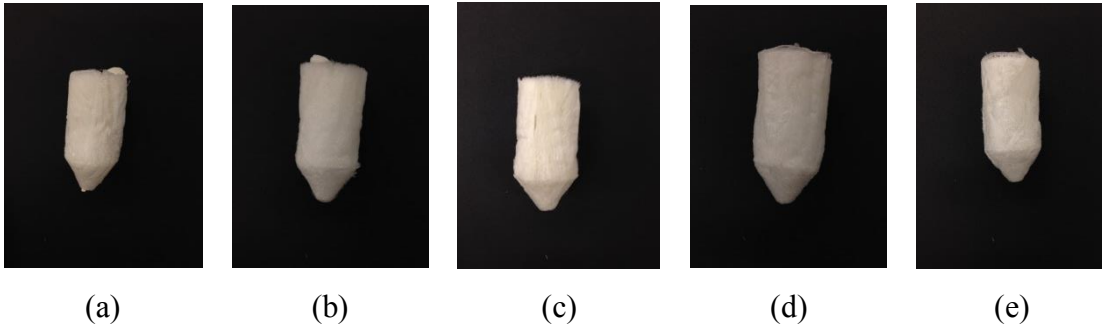
Figure 5.19 Bioactive gels produced at optimal conditions (phenolic acid/starch ratio of 40 mg/g, temperature of 100 °C, pressure of 30 bar, and glycerol/starch ratio of 0.5 g/g) with different phenolic acids: (a) Gallic acid, (b) Cinnamic acid, (c) Caffeic acid, (d) Ferulic acid, and (e) Control.

5.5 Recommendations

- Future studies should measure the pore size, and pore volume using nitrogen Brunauer-Emmett-Teller adsorption and desorption isotherms.

- Texture of bioactive gels should be measured by strip extensiometry, ring extensiometry, compression test or bulge test.

- Results on the properties of bioactive gels obtained with the use of different phenolic acids suggest the potential use of caffeic acid to provide a uniform 3D network. Caffeic acid also demonstrated a better antimicrobial and antioxidant activity than gallic acid. Furthermore, hydrogels with caffeic acid can be used in biomedical or pharmaceutical applications.

5.6 References

Ahmed, E. M. 2013. Hydrogel: Preparation, characterization, and applications. *Journal of Advanced Research*, http://dx.doi.org/10.1016/j.jare.2013.07.006, In press.

Ajji, Z., Mirjaliji, G., Alkhatab, A., Dada, H. 2008. Use of electron beam for the production of hydrogel dressings. *Radiation Physics and Chemistry*, **77**(2), 200-202.

Bao, J.S., Shen, Y., Jin, L. 2007. Determination of thermal and retrogradation properties of rice starch using near-infrared spectroscopy. *Journal of Cereal Science*, **46**(1), 75-81.

Belscak-Cvitanovic, A., Komes, D., Karlovic, S., Djakovic, S., Spoljaric, I., Mrsic, G., Jezek, D. 2015. Improving the controlled delivery formulations of caffeine in alginate hydrogel beads combined with pectin, carrageenan, chitosan and psyllium. *Food Chemistry*, **167**, 378-386.

Chern, J.M., Lee, W.F., Hsieh, M.Y. 2004. Preparation and swelling characterization of poly (n-isopropylacrylamide)-based porous hydrogels. *Journal of Applied Polymer Science*, **92**(6), 3651-3658.

de Moura, M.R., Guilherme, M.R., Campese, G.M., Radovanovic, E., Rubira, A.F., Muniz, E.C. 2005. Porous alginate-Ca^{2+} hydrogels interpenetrated with PNIPAAm networks: Interrelationship between compressive stress and pore morphology. *European Polymer Journal*, **41**(12), 2845-2852.

Dogan, A., Demirci, S., Caglayan, A.B., Kilic, E., Gunal, M.Y., Uslu, U., Cumbul, A., Sahin, F. 2014. Sodium pentaborate pentahydrate and pluronic containing hydrogel increases cutaneous wound healing in vitro and in vivo. *Biological trace element research*, **162**(1-3), 72-9.

Gemeinhart, R.A., Park, H., Park, K. 2000. Pore structure of superporous hydrogels. *Polymers for Advanced Technologies*, **11**(8-12), 617-625.

Hennink, W.E., van Nostrum, C.F. 2012. Novel crosslinking methods to design hydrogels. *Advanced Drug Delivery Reviews*, **64**, 223-236.

Hirashima, M., Takahashi, R., Nishinari, K. 2005. Effects of adding acids before and after gelatinization on the viscoelasticity of cornstarch pastes. *Food Hydrocolloids*, **19**(5), 909-914.

Hoffman, A.S. 2002. Hydrogels for biomedical applications. *Advanced Drug Delivery Reviews*, **54**(1), 3-12.

Huang, Y.W., Zeng, M., Ren, J., Wang, J., Fan, L.R., Xu, Q.Y. 2012. Preparation and swelling properties of graphene oxide/poly(acrylic acid-co-acrylamide) super-absorbent hydrogel nanocomposites. *Colloids and Surfaces a-Physicochemical and Engineering Aspects*, **401**, 97-106.

Igura, N., Hayakawa, I., Fujio, Y. 1997. Effect of longer heating time on depolymerization of low moisturized starches. *Starch - Stärke*, **49**(1), 2-5.

Kabiri, K., Omidian, H., Zohuriaan-Mehr, M.J., Doroudiani, S. 2011. Superabsorbent hydrogel composites and nanocomposites: A review. *Polymer Composites*, **32**(2), 277-289.

Kawai, K., Fukami, K., Yamamoto, K. 2007. State diagram of potato starch-water mixtures treated with high hydrostatic pressure. *Carbohydrate Polymers*, **67**(4), 530-535.

Lam, Y.L., Muniyandy, S., Kamaruddin, H., Mansor, A., Janarthanan, P. 2015. Radiation cross-linked carboxymethyl sago pulp hydrogels loaded with ciprofloxacin: Influence of irradiation on gel fraction, entrapped drug and in vitro release. *Radiation Physics and Chemistry*, **106**, 213-222.

Lane, L.B. 1925. Freezing points of glycerol and its aqueous solutions. *Industrial and Engineering Chemistry*, **17**, 924-924.

Lanthong, P., Nuisin, R., Kiatkamjornwong, S. 2006. Graft copolymerization, characterization, and degradation of cassava starch-g-acrylamide/itaconic acid superabsorbents. *Carbohydrate Polymers*, **66**(2), 229-245.

Lee, A.L.S., Ordeñez, G., Chakraborty, S. 2011. Novel glycerol cross-linked poly (acrylic acid) hydrogel for encapsulation and release of benzocaine. *Philippino Science Letters*, **4**(2), 81-87.

Lefnaoui, S., Moulai-Mostefa, N. 2014. Investigation and optimization of formulation factors of a hydrogel network based on kappa carrageenan–pregelatinized starch blend using an experimental design. *Colloids and Surfaces A: Physicochemical and Engineering Aspects*, **458**(0), 117-125.

Lewis, K.M., Spazierer, D., Slezak, P., Baumgartner, B., Regenbogen, J., Gulle, H. 2014. Swelling, sealing, and hemostatic ability of a novel biomaterial: A polyethylene glycol-coated collagen pad. *Journal of Biomaterials Applications*, **29**(5), 780-788.

Lima-Tenorio, M.K., Tenorio-Neto, E.T., Guilherme, M.R., Garcia, F.P., Nakamura, C.V., Pineda, E.A.G., Rubira, A.F. 2015. Water transport properties through starch-based hydrogel nanocomposites responding to both pH and a remote magnetic field. *Chemical Engineering Journal*, **259**, 620-629.

Mahdavinia, G.R., Mousavi, S.B., Karimi, F., Marandi, G.B., Garabaghi, H., Shahabvand, S. 2009. Synthesis of porous poly(acrylamide) hydrogels using calcium carbonate and its application for slow release of potassium nitrate. *Express Polymer Letters*, **3**(5), 279-285.

Olszewski, M.W., Goldsmith, R.S., Guthrie, E.K., Young, C.A. 2012. Use of sieved compost plus hydrogel for solid matrix priming of carrot seeds. *Compost Science & Utilization*, **20**(1), 5-10.

Omer, R.A., Hughes, A., Hama, J.R., Wang, W., Tai, H. 2015. Hydrogels from dextran and soybean oil by UV photo-polymerization. *Journal of Applied Polymer Science*, **132**(6), 41446-41446.

Omidian, H., Park, K., Rocca, J.G. 2007. Recent developments in superporous hydrogels. *Journal of Pharmacy and Pharmacology*, **59**(3), 317-327.

Ottenhof, M.A., Hill, S.E., Farhat, I.A. 2005. Comparative study of the retrogradation of intermediate water content waxy maize, wheat, and potato starches. *Journal of Agricultural and Food Chemistry*, **53**(3), 631-638.

Pinho, E., Grootveld, M., Soares, G., Henriques, M. 2014. Cyclodextrin-based hydrogels toward improved wound dressings. *Critical Reviews in Biotechnology*, **34**(4), 328-37.

Qunyi, T., Ganwei, Z. 2005. Rapid synthesis of a superabsorbent from a saponified starch and acrylonitrile/AMPS graft copolymers. *Carbohydrate Polymers*, **62**(1), 74-79.

Saber-Samandari, S., Gulcan, H.O., Saber-Samandari, S., Gazi, M. 2014. Efficient removal of anionic and cationic dyes from an aqueous solution using pullulan-graft-polyacrylamide porous hydrogel. *Water Air and Soil Pollution*, **225**(11).

Shi, X.N., Wang, W.B., Wang, A.Q. 2011. Effect of surfactant on porosity and swelling behaviors of guar gum-g-poly(sodium acrylate-co-styrene)/attapulgite superabsorbent hydrogels. *Colloids and Surfaces B-Biointerfaces*, **88**(1), 279-286.

Shuttleworth, P.S., Budarin, V., Clark, J.H. 2011. Thermal investigation of 'molten starch'. *Journal of Thermal Analysis and Calorimetry*, **105**(2), 577-581.

Sun, T., Zhuo, Q., Liu, X., Sun, Z.P., Wu, Z.J., Fan, H.Y. 2014. Hydrophobic silica aerogel reinforced with carbon nanotube for oils removal. *Journal of Porous Materials*, **21**(6), 967-973.

Gulrez, S.K.H., Al-Assaf, S., Glyn, O.P. 2011. Hydrogels: Methods of preparation, characterisation and applications. in: *Progress in Molecular and Environmental Bioengineering – From Analysis and Modeling to Technology Applications*, (Eds.) A. Carpi, InTech Croatia, pp 118-150.

Talaat, H.A., Sorour, M.H., Aboulnour, A.G., Shaalan, H.F., Ahmed, E.M., Awad, A.M., Ahmed, M.A. 2008. Development of a multi-component fertilizing hydrogel with relevant techno-economic indicators. *American-Eurasian Journal of Agricultural and Environmental Science*, **3**(5), 764-770.

Xing, L.-B., Hou, S.-F., Zhou, J., Li, S., Zhu, T., Li, Z., Si, W., Zhuo, S. 2014. UV-assisted photoreduction of graphene oxide into hydrogels: High-rate capacitive performance in supercapacitor. *Journal of Physical Chemistry C*, **118**(45), 25924-25930.

Yin, L., Fei, L., Cui, F., Tang, C., Yin, C. 2007a. Superporous hydrogels containing poly(acrylic acid-co-acrylamide)/O-carboxymethyl chitosan interpenetrating polymer networks. *Biomaterials*, **28**(6), 1258-1266.

Yin, L.C., Fei, L.K., Cui, F.Y., Tang, C., Yin, C.H. 2007b. Superporous hydrogels containing poly(acrylic acid-co-acrylamide)/O-carboxymethyl chitosan interpenetrating polymer networks. *Biomaterials*, **28**(6), 1258-1266.

Zhang, J.P., Wang, L., Wang, A.Q. 2006. Preparation and swelling behavior of fast-swelling superabsorbent hydrogels based on starch-g-poly (acrylic acid-co-sodium acrylate). *Macromolecular Materials and Engineering*, **291**(6), 612-620.

Zhao, L., Gwon, H.-J., Lim, Y.-M., Nho, Y.-C., Kim, S.Y. 2015. Gamma ray-induced synthesis of hyaluronic acid/chondroitin sulfate-based hydrogels for biomedical applications. *Radiation Physics and Chemistry*, **106**, 404-412.

Zhu, F., Cai, Y.Z., Sun, M., Corke, H. 2008. Effect of phenolic compounds on the pasting and textural properties of wheat starch. *Starch-Starke*, **60**(11), 609-616.

Chapter 6: Conclusions and Recommendations

6.1 Conclusions

The first part of this thesis examined the solubility and dissolving capacity of phenolic acids in water under different temperatures and pressures, and the second part focused on the interactions between phenolic acids and potato starch, which allowed the development of two potato starch based products, bioactive film and gel, following the optimization of four parameters (gallic acid/starch ratio, glycerol/starch ratio, temperature and pressure). The following conclusions are based on the major findings of this research:

6.1.1 Solubility of phenolic acid in pressurized water

- New solubility data of selected phenolic acids (gallic, 2,4-dihydroxybenzoic, 3-(4-hydroxyphenyl)-propionic and 4-hydroxybenzoic acids) in subcritical water was obtained using a dynamic high pressure equilibrium method.

- Temperature had the most significant effect on the solubility of selected phenolic acids in water while the effect of pressure was insignificant.

- Pressure promoted the conversion of 2,4-dihydroxybezoic acid to resorcinol in subcritical water and 100% conversion was achieved at 150 °C and 120 bar.

- The solubility of phenolic acids in water was mainly influenced by phenolic properties of sublimation pressure, polymorphism and water viscosity.

6.1.2 Bioactive films made of starch and phenolic acids

- Bioactive films with a cross-linked network were obtained in this thesis using subcritical water technology.

214

- The optimized condition based on the four parameters evaluated, which produced a film with improved mechanical and functional properties were 100°C, 30 bar, 0.5 g glycerol/g starch and 40 mg gallic acid/g starch.

- Influence of gallic acid was mainly from the interactions of its –OH group of the aromatic ring with starch, promoting the formation of V- type crystalline with starch that resulted in a more yellow, transparent, smooth and homogenous film compare to the control.

- The maximum ratio of gallic acid/starch added without phase separation in the film was 250 mg/g. This film had better mechanical properties when produced at 50 bar.

- Gallic acid also acted as a plasticizer at 10 to 60 mg/g starch, resulting in a film with high tensile strength. But, elongation increased after adding more than 60 mg gallic acid/g starch.

- Temperature was essential for a homogeneous film structure by controlling the degree of gelatinization and depolymerization of starch molecules. The film elongation % decreased with an increase on the heating temperature. Severe depolymerization was only observed at 150 °C, resulting in the reduction of intermolecular bonds between starch chains and increasing of the water solubility of the resulted films.

- Glycerol formed V –type crystalline with amylose inside the film and acted as a plasticizer, which is essential for the tensile strength and elongation % of films. However, an excess of glycerol (>1.5 g/g starch) not only compromised the

mechanical properties significantly, but also reduced the hydrophobicity, water solubility, release of antioxidant and the gloss of the film.

- Pressure had a minor influence on the modification of starch surface morphology, but facilitated the rupture of starch during gelatinization.

- The optimum condition may not be ideal when using other phenolic acids, as the aqueous solubility of the three phenolic acids investigated in this thesis is relatively lower than that of gallic acid.

- Bioactive films produced in this thesis can be potentially used as functional packaging materials or edible films for food applications.

6.1.3 Bioactive gels made of starch and phenolic acids

- The optimum condition for bioactive starch hydrogel in terms of porosity, density and swelling degree was 40 mg gallic acid/g starch, 0.5 g glycerol/g starch, temperature of 100°C and pressure of 10 or 30 bar, which allowed the formation of hydrogels with a density of 0.1 g/cm^3, swelling degree of 10 and porosity of 60%.

- Among the four experimental parameters evaluated in this study, gallic acid/starch and glycerol/starch ratios were significant, contributing to the formation of stable and integral network of bioactive gels.

- Due to the relatively low swelling degree, hydrogels obtained in this thesis may not be suitable to use as a superabsorbent hydrogel, but it can be used as a functional food or flavor carrier due to the "green" process applied.

6.2 Recommendations

The following recommendations are for further studies derived from this research:

216

6.2.1 Solubility of phenolic acid in water

- Improve the dynamic system for solubility measurement in terms of on-line sample analysis and the use of adjustable equilibrium vessel to reduce experimental time.

- Measure the solubility of hydrocinnamic acids, such as caffeic acid and cinnmaic acid in subcritical water

6.2.2 Bioactive films made of starch and phenolic acids

- Improve the properties of films by incorporating other functional additives (e.g. chitosan, zein, etc).

- To boost the antimicrobial activity of the films, incorporate more phenolic acids. Then, improve their release amount from the film to the product.

6.2.3 Bioactive gels made of starch and phenolic acids

- Further characterize the mechanical properties of hydrogels using a texture analyser.

- Future study should explore the antimicrobial and antioxidant activity of starch hydrogel with the use of caffeic acid. As this research demonstrated its use resulted in uniform pore size distribution (SEM analysis).

APPENDIX A: Solubility of phenolic acids in water

A.1 Calculation of total phenolic content

The refractive index of water+ethanol mixtures varied depending on the amount of ethanol added. For each experiment, the mixing ratio is fixed and the refractive index change depended only on the amount of phenolic acid dissolved. Methodology for total phenolic content quantification was is described in Chapter 3, Section 3.2.4.1. Standard curves and quantification of phenolic acid of sample collected required to use the same reagents, which should be prepared and used for only one month. The calculation was performed using a liner equation (Figure A.1). Results were calculated on the basis of the standard curves.
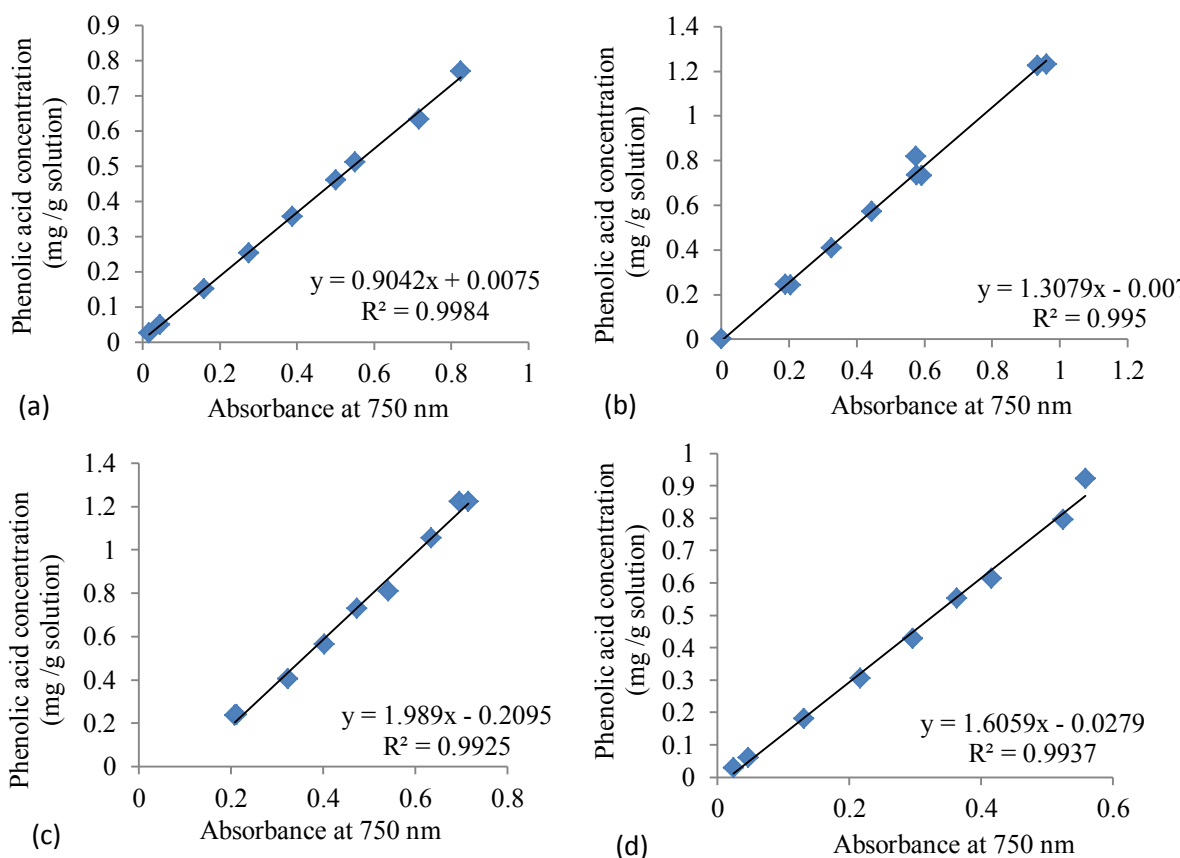
Figure A.1 Standard curves for total phenolic content of phenolic acid (a) Gallic acid; (b) 2,4-Dihydroxybenzoic acid; (c) 4-Hidroxybenzoic acid; (d) 3-(4-Hydroxyphenyl) propionic acid.

To obtain valid readings from the spectrophotometer (absorbances from 0.2 to 0.8) and within the range of the standard curve, samples needed to be properly diluted with ethanol. As the concentration of phenolic acid in each sample is different, two trials were made for each sample to determine the proper dilution factor (DF_1).

Quantification of phenolic acids in sample:

For example:

The concentration (C_1) of gallic acid in the diluted sample can be calculated using the linear equation of from the standard curve of gallic acid (Figure A1a):

$$y = 0.9042x + 0.0075 \qquad\qquad\qquad (A.1)$$

where, y is the concentration of the phenolic acid (C_1) in the sample, and x is the absorbance of the phenolic acid in the solution at 750 nm.

When x=0.428,

Then, y=0.9042*0. 428+0.0075

C_1=0.39449 mg gallic acid/g solution

To obtain the concentration (C_2) of gallic acid before the dilution for the analysis, multiply by DF_1, if sample was diluted 10 times the volume, then DF_1=10,

$$C_2 = C_1 \text{ x } DF_1 \qquad\qquad\qquad (A.2)$$

C_2 =3.9449 mg gallic acid/g solution

But, before cooling, the saturated solution coming out from the reaction vessel needed to be diluted to prevent recrystallization of gallic acid in the tube of the reactor from the solution. Therefore, to obtain the initial concentration (C_s) of saturated gallic acid solution, another dilution factor (DF_2) needed to be considered, which calculated based on the following equation:

$$DF_2 = F_t / F_i \qquad\qquad (A.3)$$

where, F_t is the sum of flow rates from each pump, and F_i is the initial flow rate of water that flew through the saturated vessel fully packed with pure gallic acid.

So, if DF_2 is 10,

Then, C_s=39.449 mg gallic acid/g solution, which was the solubility of gallic acid in water at this temperature.

To compare with other literature data, the solubility of phenolic acid in water should be also expressed as mole fraction (x_i) using Equation (3.1) in Chapter 3, Section 3.2.3. For example the solubility of gallic acid at 23 °C is 10 mg/g water,

then

$$\text{Mole fraction } x_i = \frac{1}{1+\dfrac{MW_i}{S * MW_w}} = \frac{1}{1+\dfrac{170\ g/mole}{10\ mg/g * 18\ g/mole}} = \frac{1}{1+\dfrac{170g}{180mg}} = 0.0010577$$

Detailed absorbance, dilution factors for each phenolic acid under different temperatures and pressures are shown in Table A.1. ANOVA test results for the influence of temperature and pressure are shown in Table A.2 and A.3, respectively.

Table A.1 Data and coefficients used to calculate solubility of phenolic acid under in water different temperatures and pressures

Temperature (℃)	Pressure (Bar)	Absorbance at 750 nm		DF$_1$	DF$_2$	Solubility (mg phenolic acid /g water)		Average*
		1	1			1	2	
4-Hydroxybenzoic acid								
23	120	0.655	0.775	3	4	8.00	9.31	8.66d
50	120	0.381	0.344	15	4	25.16	23.18	24.17d
75	120	0.448	0.459	20	10	96.02	97.92	96.97c
100	120	1.029	1.122	30	10	301.72	326.90	314.31b
125	120	1.014	1.025	40	10	396.58	400.82	398.70a
150	120	0.548	0.523	50	14.5	413.67	397.24	405.46a
23	50	0.661	0.652	3	4	8.07	7.97	8.02d
50	50	0.361	0.407	15	4	24.09	26.59	25.34d
75	50	0.388	0.340	20	10	85.11	76.49	80.80c
100	50	1.165	1.186	30	10	338.40	344.32	341.36b
125	50	0.926	0.904	40	10	364.89	356.85	360.87a
150	50	0.478	0.462	50	14.5	367.52	357.38	362.45a
3-(4-Hydroxyphenyl)propionic acid								
23	120	0.688	0.766	8	4	22.30	24.56	23.43c
50	120	0.575	0.679	50	4	118.94	137.70	128.32b
75	120	0.581	0.512	20	25	300.07	268.77	284.42a
100	120	0.530	0.517	20	25	277.30	271.24	274.27a
125	120	0.388	0.416	60	10	255.72	270.91	263.31a
23	50	0.545	0.589	8	4	18.18	19.43	18.81c
50	50	0.610	0.619	50	4	125.23	126.90	126.06b
75	50	0.605	0.527	20	25	311.09	275.74	293.41a
100	50	0.550	0.529	20	25	286.15	276.73	281.44a
125	50	0.423	0.427	60	10	274.71	276.45	275.58a
2,4-Dihydroxybenzoic acid								
23	120	0.387	0.379	4	4	6.79	6.69	6.74a
50	120	0.261	0.217	20	4	24.88	21.67	23.27b
23	50	0.458	0.490	4	4	7.83	8.29	8.06a
50	50	0.278	0.229	20	4	26.08	22.58	24.33b

* Letter assigned indicates significant difference ($p < 0.05$) under the same pressure for each phenolic acid, based on Tukey's test.

Table A.1 continued. Data and coefficients used to calculate solubility of phenolic acid under in water different temperatures and pressures

Temperature (℃)	Pressure (Bar)	Absorbance at 750 nm		DF₁	DF₂	Solubility (mg phenolic acid /g water)		Average*
		1	2			1	2	
Gallic acid								
23	120	0.487	0.396	5	4	10.32	8.66	9.49d
50	120	0.245	0.283	20	4	23.71	26.46	25.08d
75	120	0.141	0.244	40	10	81.11	118.33	99.72c
100	120	0.395	0.339	80	10	345.76	305.12	325.44b
125	120	0.444	0.453	80	10	381.18	387.49	384.34b
150	120	0.333	0.336	90	14.5	491.30	494.45	492.87a
23	50	0.286	0.246	5	4	6.67	5.94	6.30c
50	50	0.194	0.168	20	4	20.04	18.18	19.11c
75	50	0.173	0.209	40	10	92.59	105.43	99.01b
100	50	0.353	0.403	80	10	315.44	351.30	333.37a
125	50	0.382	0.410	80	10	336.68	356.34	346.51a
150	50	0.232	0.239	90	14.5	371.39	380.16	375.78a

* Letter assigned indicates significant difference ($p < 0.05$) under the same pressure for each phenolic acid, based on Tukey's test.

A.2 ANOVA analysis

Table A.2 ANOVA analysis to evaluate the influence of temperature on the solubility of phenolic acid in water under different pressureS.

Compound	Pressure (bar)		df	Sum of Squares	Mean Square	F-value	p-value
					Solubility (mg/g)		
Gallic acid	120	Between groups	5	418622	83724.4	324.38	**0.000**
		Within groups	6	159	258.1		
		Total	11	420170			
	50	Between groups	5	301045	60209.1	376.80	**0.000**
		Within groups	6	959	159.8		
		Total	11	302004			
4-Hydroxybenzoic acid	120	Between groups	5	345034	69006.8	888.90	**0.000**
		Within groups	6	466	77.6		
		Total	11	345500			
	50	Between groups	5	307499	61499.8	2607.02	**0.000**
		Within groups	6	142	23.6		
		Total	11	307640			
3-(4-Hydroxyphenyl)pro pionic acid	120	Between groups	4	105656	26414.1	164.67	**0.000**
		Within groups	5	802	160.4		
		Total	9	106458			
	50	Between groups	4	118729	29682.1	220.59	**0.000**
		Within groups	5	673	134.6		
		Total	9	119401			
2,4-Dihydroxybenzoic acid	120	Between groups	2	9627.00	4813.50	335.08	**0.000**
		Within groups	3	43.10	14.37		
		Total	5	9670.10			
	50	Between groups	2	3719.5	1859.75	46.94	**0.005**
		Within groups	3	118.9	39.62		
		Total	5	3838.4			

Table A.3 ANOVA analysis to evaluate the influence of pressure on the solubility of phenolic acid in water under different temperatures.

Compound	Temperature (°C)		df	Solubility (mg/g) Sum of Squares	Mean Square	F-value	p-value
Gallic acid	23	Between groups	1	10.138	10.1383	12.38	0.072
		Within groups	2	1.637	0.8187		
		Total	3	11.776			
	50	Between groups	1	35.691	35.961	12.94	0.069
		Within groups	2	5.515	2.758		
		Total	3	41.206			
	75	Between groups	1	0.510	0.510	0.00	0.974
		Within groups	2	774.976	387.488		
		Total	3	775.486			
	100	Between groups	1	62.86	62.86	0.09	0.797
		Within groups	2	1468.85	734.42		
		Total	3	1531.71			
	125	Between groups	1	1430.8	1430.8	13.43	0.067
		Within groups	2	213.0	106.5		
		Total	3	1643.8			
	150	Between groups	1	13711.9	13711.9	632.07	**0.002**
		Within groups	2	43.4	21.7		
		Total	3	13755.3			
2,4-Dihydroxybenzoic acid	23	Between groups	1	1.7413	1.74130	31.10	**0.031**
		Within groups	2	0.1120	0.05598		
		Total	3	1.8533			
	50	Between groups	1	1.125	1.125	0.20	0.699
		Within groups	2	11.297	5.649		
		Total	3	12.422			

Table A.3 continued. ANOVA analysis to evaluate the influence of pressure on the solubility of phenolic acid in water under different temperatures.

| Compound | Temperature (°C) | | df | Solubility (mg/g) | | F-value | p-value |
				Sum of Squares	Mean Square		
4-Hydroxybenzoic acid	23	Between groups	1	0.4031	0.4031	0.94	0.435
		Within groups	2	0.8591	0.4295		
		Total	3	1.2622			
	50	Between groups	1	1.367	1.367	0.54	0.541
		Within groups	2	5.107	2.554		
		Total	3	6.474			
	75	Between groups	1	261.42	261.42	13.40	0.067
		Within groups	2	39.01	19.51		
		Total	3	300.43			
	100	Between groups	1	731.9	731.9	4.37	0.172
		Within groups	2	334.6	167.3		
		Total	3	1066.5			
	125	Between groups	1	1431.02	1431.02	69.37	**0.014**
		Within groups	2	41.26	20.63		
		Total	3	1472.28			
	150	Between groups	1	1849.6	1849.6	19.84	**0.047**
		Within groups	2	186.5	93.24		
		Total	3	2036.1			
3-(4-Hydroxyphenyl) propionic acid	23	Between groups	1	21.385	21.385	12.8	0.070
		Within groups	2	3.341	1.671		
		Total	3	24.726			
	50	Between groups	1	5.109	5.109	0.06	0.833
		Within groups	2	177.327	88.664		
		Total	3	182.436			
	75	Between groups	1	80.80	80.80	0.14	0.740
		Within groups	2	1114.61	557.31		
		Total	3	1195.41			
	100	Between groups	1	51.47	51.47	1.64	0.329
		Within groups	2	62.73	31.37		
		Total	3	114.2			
	125	Between groups	1	150.4	150.44	2.58	0.250
		Within groups	2	116.8	58.4		
		Total	3	267.2			

APPENDIX B: Bioactive films

B.1 Preliminary study
a) First set of preliminary experiments

1) Objective: produce corn starch and barley starch films using a water bath.

Raw material: high amylose corn starch, regular corn starch, waxy corn starch, high amylose barley starch, regular barley starch, waxy barley starch, glycerol, milli Q water.

Experimental design

1. 1.1g of barley starch was added into 50 g milli Q water
2. The solution was then put in magnetic stirrer and stirring for 10 mins.
3. Heating up to 80°C in water bath and continue heating for 15 mins.
4. Remove from the heater and 0.46g(12 drops) of glycerol was then added into the solution and keep stirring for another 5 mins, temperature should be maintain at 80 °C.
5. 20 gram of the solution was then pour into a 10 cm petri dish and all the sample were duplicate.
6. All the samples were then store at 25°C for drying.
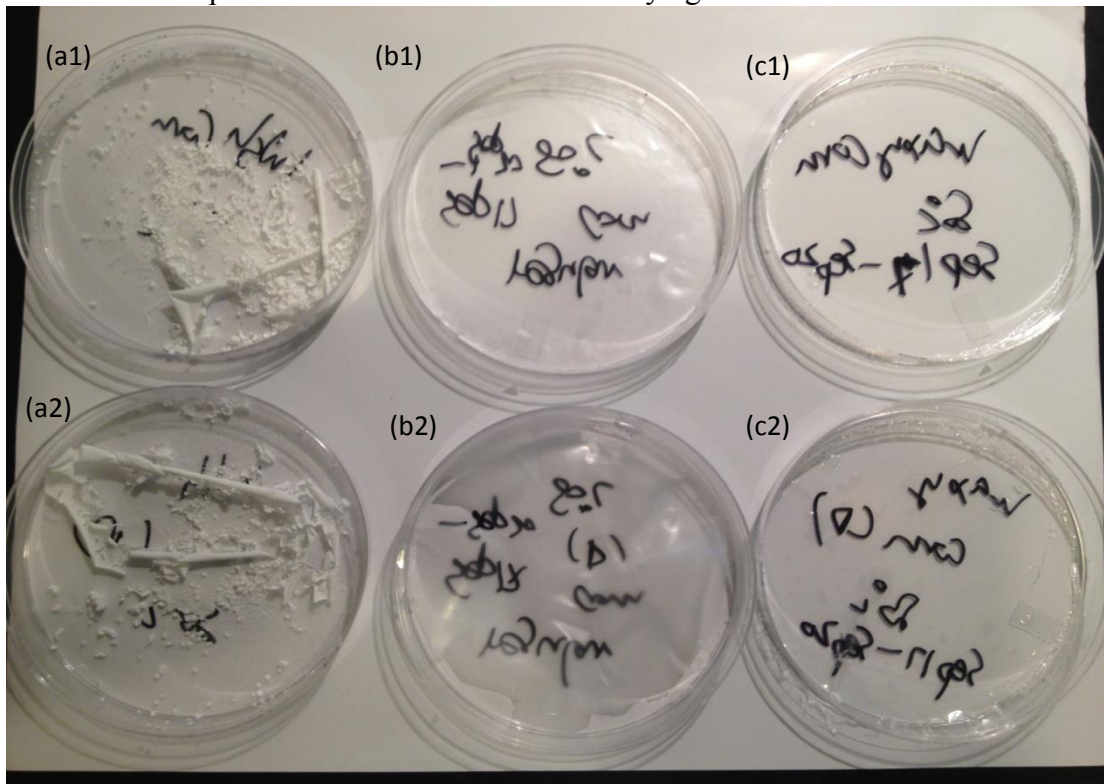
Figure B.1 Digital image of solution-cast barley starch films with different amylose percentage content: (a1) high amylose corn starch film, (b1) regular corn starch film, (c1) waxy corn starch film, (a2), (b2), (c2) are their duplicate, respectively.
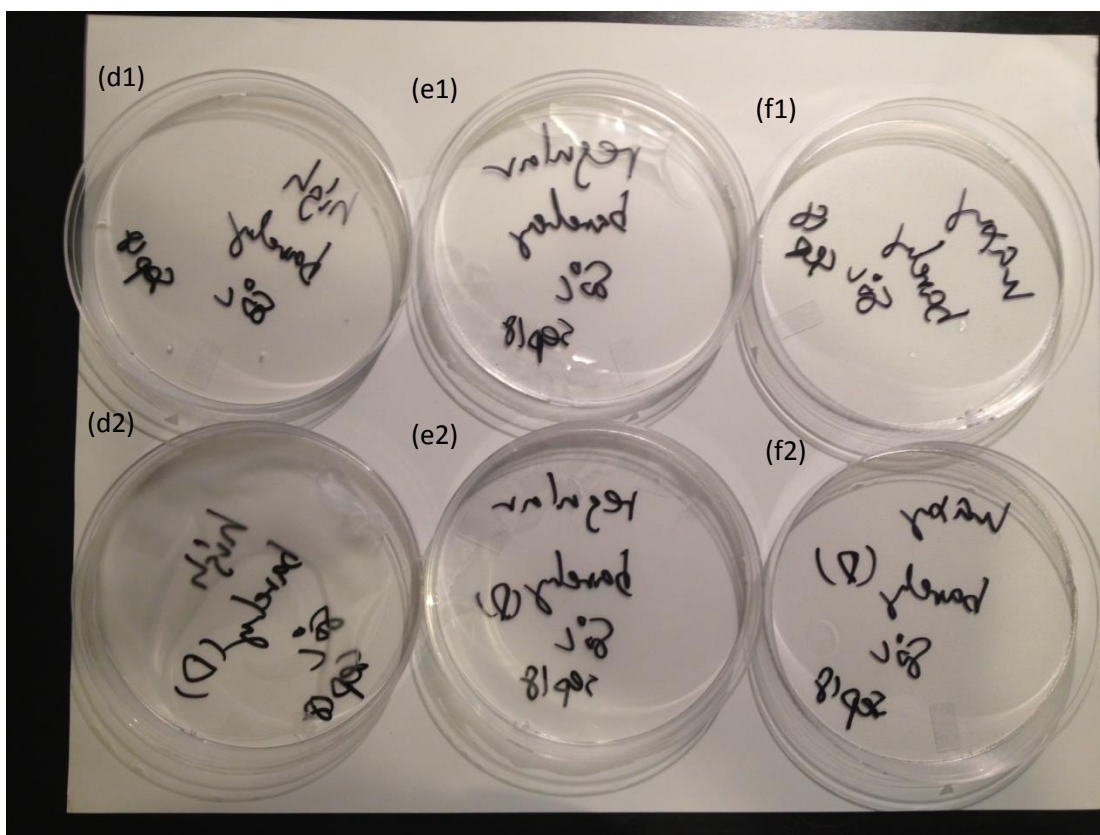
Figure B.2 Digital image of solution-cast barley starch films with different amylose percentage content: (d) high amylose barley starch film, (e) regular barley starch film, (f) waxy barley starch film, (d2), (e2), (f2) are their duplicate, respectively.

2) **Objective:** produce starch films using less water to reduce drying time.

Raw material: high amylose barley starch, regular corn starch, glycerol, milli Q water.
Experimental design:
1. Formula: A) 1.1g of starch was added into 12.5 g milli Q water.
   B) 1.1g of starch was added into 25 g milli Q water.
   C) 1.1g of starch was added into 37.5 g milli Q water.
2. The solution was then put onto a magnetic stirrer and stirring for 5 min.
3. Heating up to 80°C in water bath and continue heating for 15 min.
4. Remove from the heater and 10drops（0.42）of glycerol was then added into the solution and kept stirring for another 5 min, temperature should be maintained at 80 °C.
5. ~13 gram of the solution was then pour into a 10cm petri dish, all sample were performed in duplicate, except the 25% one.
6. All the samples were then store at 35°C for drying.
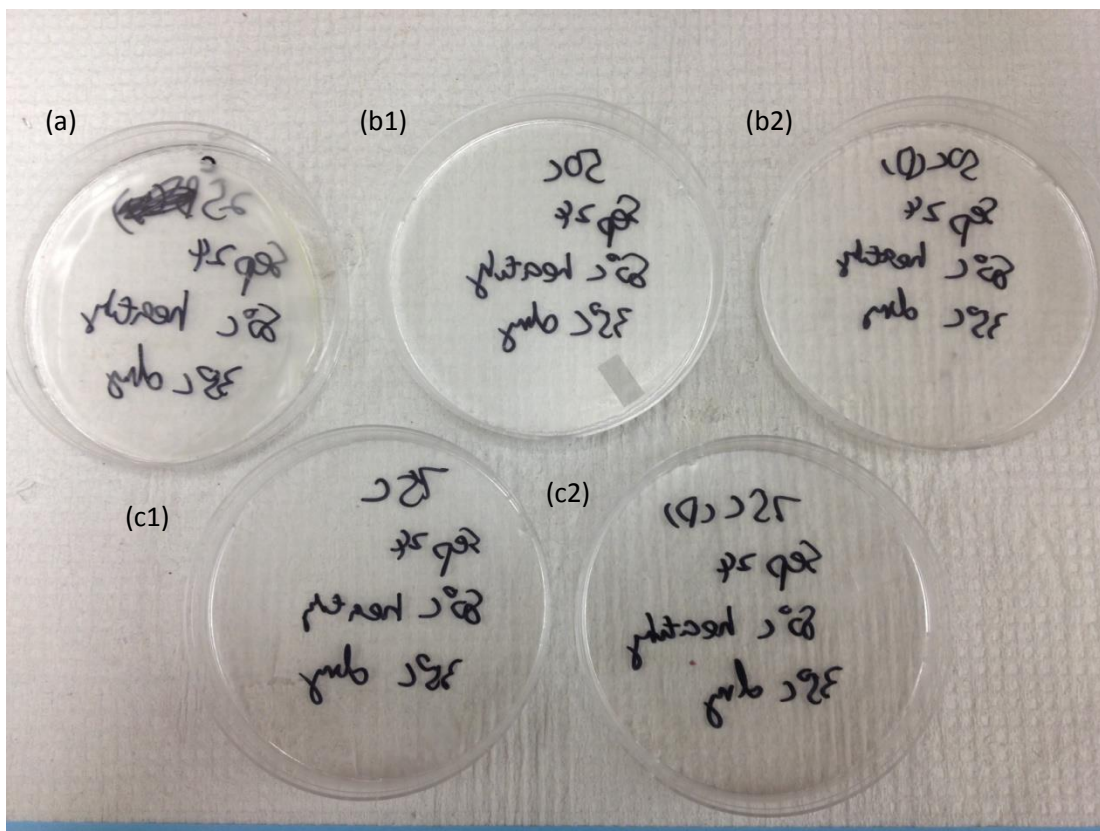
Figure B.3 Digital image of solution-cast regular corn starch film made by added different water amount: (a) starch film using formula A.(b1) starch film using formula B, (c1) starch film using formula C, (b2) and (c2) are their duplicates.
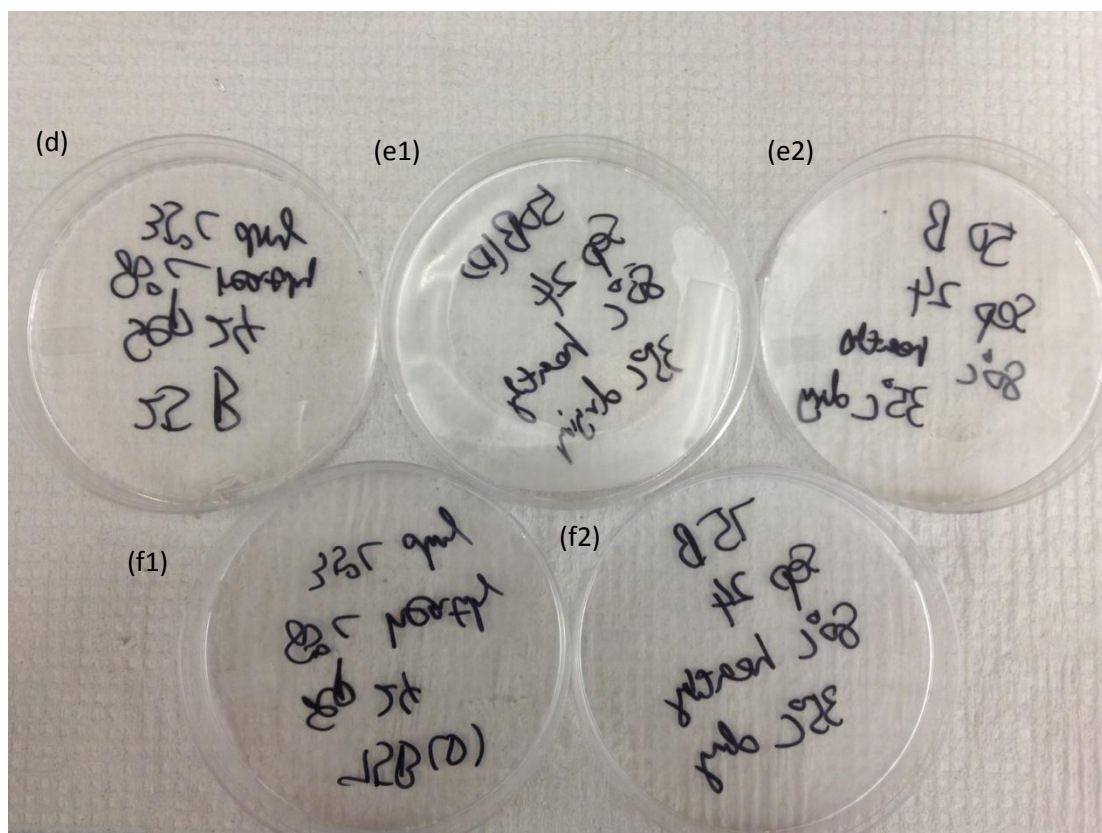
Figure B.4 Digital image of solution-cast high amylose barley starch film made by added different water amount :(d) starch film using using formula A.(e1) starch film using using formula B,(cf1) starch film using using formula C,(e2) and (f2) are their duplicates.

b) Second preliminary experiments

Table B.1 Experimental conditions for preliminary study designed by Design Expert 6.0

Run #	Pressure (bar)	Temperature (°C)	Gallic acid /Starch ratio (mg/g)	Glycerol/starch ratio (g/g)
1	50	75	0	0
2	50	100	10	0.5
3	50	125	20	1
4	120	75	10	1
5	120	100	20	0
6	120	125	0	0.5
7	190	75	20	0.5
8	190	100	0	1
9	190	125	10	0
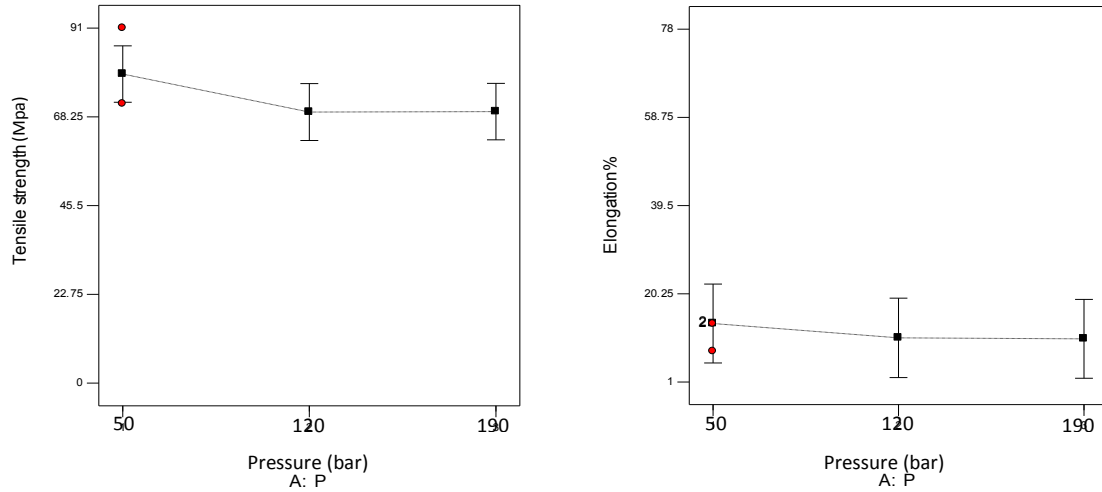
Figure B.5a Predicted results for influence of pressure on the mechanical properties of starch film.
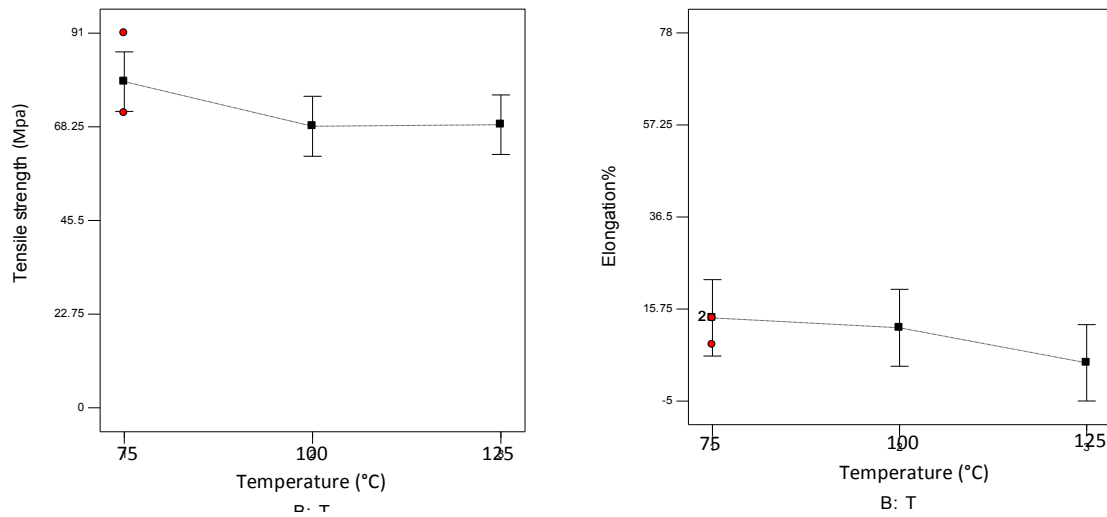
Figure B.5b Predicted results for influence of temperature on the mechanical properties of starch film.

230
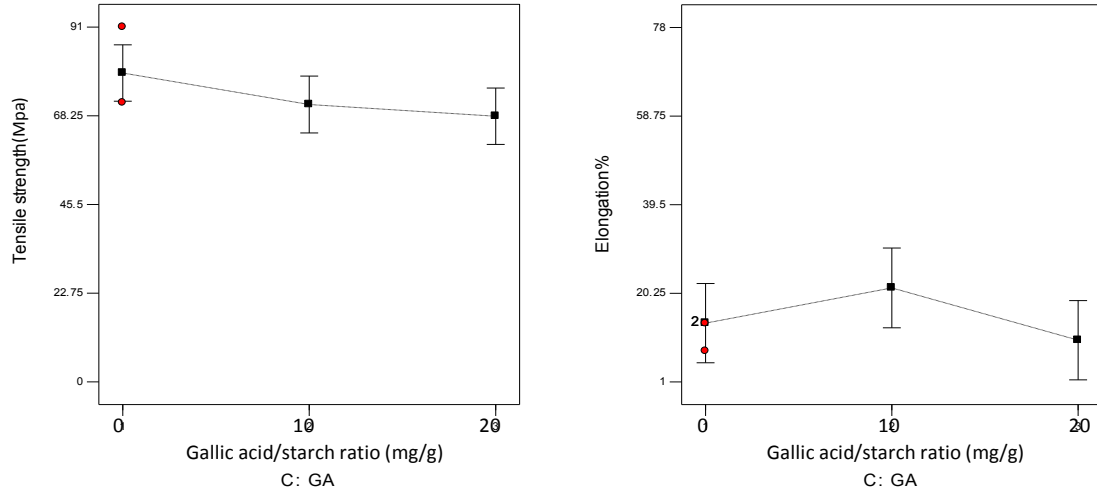
Figure B.5c Predicted results for influence of gallic acid/starch ratio on the mechanical properties of starch film.
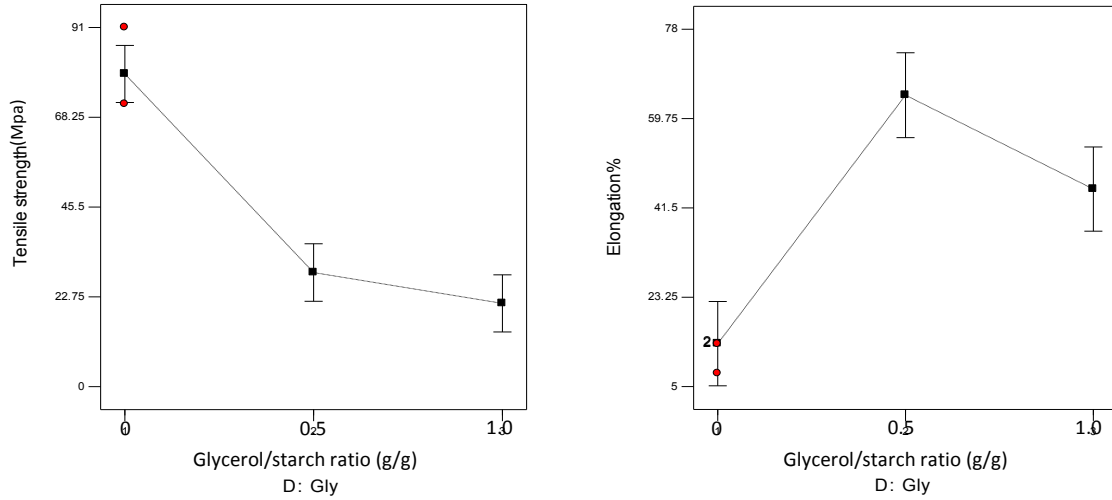
Figure B.5d Predicted results for influence of glycerol/starch ratio on the mechanical properties of starch film.

B.2 Optimization of experiment parameters for starch films

B3a) Experimental condition for starch films

Table B.2 Experimental conditions for final experiment (13 g starch and 260mL water is used in each experiment)

Run#	Pressure (bar)	Temperature (°C)	Phenolic acid /Starch ratio (mg/g)	Glycerol/starch ratio (g/g)
For influence of gallic acid/starch ratio				
10	50	100	0	0.5
2	50	100	10	0.5
11	50	100	20	0.5
12	50	100	40	0.5
13	50	100	60	0.5
14	50	100	80	0.5
15	50	100	100	0.5
16	50	100	250	0.5
17*	50	100	400	0.5
For influence of temperature				
18	50	75	40	0.5
19	50	88	40	0.5
12	50	100	40	0.5
20	50	113	40	0.5
21	50	125	40	0.5
22	50	150	40	0.5
For influence of glycerol/starch ratio				
23	50	100	40	0
12	50	100	40	0.5
24	50	100	40	1
25	50	100	40	1.5
26	50	100	40	2
For influence of pressure				
27	10	100	40	0.5
28	30	100	40	0.5
12	50	100	40	0.5
29	120	100	40	0.5
30	190	100	40	0.5
Optimum condition for other phenolic acids				
31	30	100	40 (Cinnamic acid)	0.5
32	30	100	40 (Ferulic acid)	0.5
33	30	100	40 (Caffeic acid)	0.5
28	30	100	40 (Gallic acid)	0.5
34	30	100	0 (Control)	0.5
Optimum condition for maximum gallic acid				
35	30	100	250	0.5

*Phenolic acid phase separation occurred, recrystallized from the film.

B3b) Characterization of bioactive films

B3b.1) Mechanical properties of bioactive films

Table B.3 Tensile strength and elongation % of bioactive films

Run#	Tensile strength (Mpa)		Average*	Elongation (%)		Average*
	Analysis 1	**Analysis 2**		**Analysis 1**	**Analysis 2**	
Influence of gallic acid/starch ratio						
10	2.08	2.97	2.53 b	103.41	95.47	99.44 a
2	5.45	6.35	5.90 a	75.19	77.04	76.12 abc
11	6.86	6.66	6.76 a	62.13	64.63	63.38 bc
12	7.22	7.29	7.25 a	59.64	53.32	56.48 c
13	7.70	6.13	6.91 a	71.72	76.09	73.91 abc
14	3.99	2.50	3.24 b	77.61	83.55	80.58 abc
15	2.47	2.63	2.55 b	97.56	94.22	95.89 a
16	2.58	1.76	2.17 b	76.07	102.40	89.23 ab
Influence of temperature						
18	2.79	1.78	2.28 c	96.76	91.69	94.23 a
19	2.29	3.59	2.94 bc	75.79	77.90	76.85 b
12	7.22	7.29	7.25a	59.64	53.32	56.48 c
20	4.32	3.50	3.91 bc	68.89	63.60	66.24 bc
21	4.43	5.71	5.07 ab	30.63	33.74	32.19 d
22	2.23	2.95	2.59 bc	11.55	13.41	12.48 e
Influence of glycerol /starch ratio						
23	41.43	64.60	53.02 a	4.33	5.34	4.83 c
12	7.22	7.29	7.25 b	59.64	53.32	56.48 a
24	0.38	0.54	0.46 b	38.13	43.51	40.82 b
25	0.11	0.10	0.11 b	46.18	46.68	46.43 ab
26	0.07	0.08	0.07 b	40.36	35.49	37.92 b
Influence of pressure						
27	4.25	5.25	4.75 a	82.69	82.59	82.64 a
28	6.16	5.80	5.98 a	66.83	78.88	72.86 ab
12	7.22	7.29	7.25 a	59.64	53.32	56.48 b
29	8.00	6.03	7.02 a	63.85	63.08	63.46 ab
30	6.34	6.16	6.25 a	58.41	66.86	62.63 ab
Influence of different phenolic acids						
31	3.22	3.45	3.34 b	51.53	35.90	43.72 a
32	1.53	2.21	1.87 b	65.74	53.31	59.53 a
33	1.63	2.29	1.96 b	62.56	53.98	58.27 a
28	6.16	5.80	5.98 a	66.83	78.88	72.86 a
34	2.83	1.47	2.15 b	74.24	60.69	67.46 a
35	1.95	1.96	1.95 b	69.00	72.30	70.65 a

*Within columns, means followed by the same letter are not significantly different according to Tukey's test (0.05)

B3b.2) Moisture content and water activity of bioactive films

Table B.4 Moisture content and water activity of bioactive films

Run#	Moisture content (%)		Average	Water activity		Average
	Analysis 1	Analysis 2		Analysis 1	Analysis 2	
Influence of gallic acid/starch ratio						
10	26.82	26.88	26.85 a	0.288	0.284	0.286 a
2	24.18	23.50	23.84 abc	0.233	0.241	0.237 a
11	23.23	22.13	22.68 bc	0.232	0.234	0.233 a
12	22.98	21.57	22.28 bc	0.255	0.260	0.257 a
13	21.47	24.38	22.93 abc	0.243	0.253	0.248 a
14	25.22	24.22	24.72 ab	0.284	0.301	0.292 a
15	24.85	22.78	23.82 abc	0.300	0.346	0.323 a
16	19.84	19.72	19.78 c	0.333	0.253	0.293 a
Influence of temperature						
18	24.66	25.86	25.26 ab	0.233	0.258	0.245 b
19	25.66	24.99	25.32 ab	0.333	0.335	0.334 a
12	22.98	21.57	22.28 b	0.2549	0.2595	0.257 b
20	24.79	25.68	25.24 ab	0.243	0.230	0.237 b
21	26.21	24.39	25.30 ab	0.236	0.234	0.235 b
22	27.68	27.61	27.65 a	0.297	0.255	0.276 ab
Influence of glycerol /starch ratio						
23	6.24	6.51	6.37 e	0.281	0.290	0.286 a
12	22.98	21.57	22.28 d	0.2549	0.2595	0.257 a
24	45.46	45.48	45.47 c	0.262	0.268	0.265 a
25	57.12	56.59	56.86 b	0.272	0.273	0.273 a
26	64.14	63.56	63.85 a	0.248	0.271	0.259 a
Influence of pressure						
27	23.95	24.90	24.43 ab	0.273	0.277	0.275 a
28	24.34	25.05	24.70 ab	0.284	0.237	0.260 a
12	22.98	21.57	22.28 b	0.2549	0.2595	0.257 a
29	24.30	24.41	24.35 ab	0.250	0.237	0.243 a
30	24.46	25.11	24.79 a	0.237	0.251	0.244 a
Influence of different phenolic acids						
31	27.54	26.61	27.07 ab	0.316	0.299	0.307 a
32	26.43	26.55	26.49 bc	0.327	0.318	0.322 a
33	25.03	25.31	25.17 cd	0.325	0.294	0.310 a
28	24.34	25.05	24.70 d	0.284	0.237	0.260 a
34	27.98	27.98	27.98 a	0.318	0.360	0.339 a
35	20.90	21.27	21.08 e	0.264	0.270	0.267 a

B3b.3) Water solubility of bioactive films at 4, 25 and 50 °C

Table B.5 Water solubility of bioactive films at 4, 25 and 50 °C

Run#	Solubility (%) at 4°C		Average	Solubility (%) at 25°C		Average	Solubility (%) at 50°C		Average
	Analysis 1	Analysis 2		Analysis 1	Analysis 2		Analysis 1	Analysis 2	
Influence of gallic acid/starch ratio									
10	15.25	15.34	15.29 bc	15.26	17.02	16.14 b	17.88	16.70	17.29 b
2	13.90	11.68	12.79 c	18.97	17.53	18.25 b	20.65	20.77	20.71 b
11	9.74	13.60	11.67 c	21.17	18.71	19.94 b	22.79	21.72	22.25 b
12	20.42	16.47	18.45 bc	24.63	22.35	23.49 b	27.08	24.78	25.93 ab
13	18.78	18.00	18.39 bc	24.78	23.60	24.19 b	29.04	18.00	23.52 b
14	20.26	17.41	18.83 bc	24.13	24.50	24.32 b	12.06	19.88	15.97 b
15	20.74	24.94	22.84 ab	29.22	21.68	25.45 b	19.56	25.98	22.77 b
16	27.92	32.34	30.13 a	39.73	34.92	37.32 a	38.45	44.29	41.37 a
Influence of temperature									
18	15.12	13.74	14.43 bc	15.45	18.52	16.99 b	19.22	20.35	19.78 a
19	10.57	11.30	10.93 c	14.06	17.26	15.66 b	16.59	18.95	17.77 a
12	20.42	16.47	18.45 b	24.63	22.35	23.49 b	27.08	24.78	25.93 a
20	18.96	16.86	17.91 bc	19.37	21.61	20.49 b	23.67	28.74	26.21 a
21	18.97	19.03	19.00 b	21.38	21.89	21.63 b	21.22	32.96	27.09 a
22	31.05	35.50	33.27 a	39.96	50.13	45.04 a	22.74	47.67	35.21 a
Influence of glycerol /starch ratio									
23	2.99	7.94	5.47 b	7.14	8.40	7.77 c	10.39	11.98	11.18 b
12	20.42	16.47	18.45 a	24.63	22.35	23.49 a	27.08	24.78	25.93 a
24	10.41	8.92	9.67 b	20.11	21.42	20.76 a	14.63	20.11	17.37 ab
25	6.81	7.56	7.19 b	17.62	19.55	18.58 ab	18.54	16.89	17.72 ab
26	5.12	5.70	5.41 b	12.48	15.81	14.14 b	15.37	12.87	14.12 b

Table B.5 continued. Water solubility of bioactive films at 4, 25 and 50 °C

Run#	Solubility (%) at 4°C		Average	Solubility (%) at 25°C		Average	Solubility (%) at 50°C		Average
	Analysis 1	Analysis 2		Analysis 1	Analysis 2		Analysis 1	Analysis 2	
Influence of pressure									
27	14.67	12.56	13.62 a	18.28	21.26	19.77 a	24.24	21.63	22.94 a
28	21.26	14.00	17.63 a	21.17	19.57	20.37 a	24.69	22.44	23.57 a
12	20.42	16.47	18.45 a	24.63	22.35	23.49 a	27.08	24.78	25.93 a
29	16.49	13.44	14.96 a	23.15	22.12	22.63 a	25.13	23.33	24.23 a
30	12.09	15.75	13.92 a	21.66	22.50	22.08 a	22.27	24.25	23.26 a
Influence of different phenolic acids									
31	18.67	13.78	16.22 ab	17.64	17.39	17.51 b	12.35	12.61	12.48 bc
32	13.30	20.75	17.02 ab	17.44	22.10	19.77 b	12.76	17.56	15.16 bc
33	19.92	20.67	20.30 ab	21.45	18.61	20.03 b	20.37	16.68	18.53 bc
28	21.26	14.00	17.63 ab	21.17	19.57	20.37 ab	24.69	22.44	23.57 b
34	15.86	12.19	14.03 b	17.35	12.37	14.86 b	10.67	7.13	8.90 c
35	26.99	34.38	30.68 a	35.63	28.60	32.12 a	36.02	45.14	40.58 a

B3b.4) Color of bioactive films

Table B.6 Color of bioactive films

Run#	Total color difference (ΔE)		Average	Yellowness index (YI)		Average	Whiteness index (WI)		Average
	Analysis 1	Analysis 2		Analysis 1	Analysis 2		Analysis 1	Analysis 2	
Influence of gallic acid/starch ratio									
10	1.88	1.26	1.57 a	2.10	1.90	2.00 a	91.00	91.61	91.30 a
2	2.80	2.33	2.57 a	3.04	2.47	2.75 a	90.01	90.47	90.24 ab
11	2.35	2.71	2.53 a	2.60	2.70	2.65 a	90.46	90.09	90.27 ab
12	2.37	2.96	2.66 a	2.80	2.60	2.70 a	90.44	89.86	90.15 b
13	2.02	2.32	2.17 a	2.69	2.72	2.70 a	90.79	90.49	90.64 ab
14	2.10	2.15	2.12 a	3.03	3.42	3.22 a	90.72	90.70	90.71 ab
15	1.78	2.14	1.96 a	3.10	3.25	3.17 a	91.05	90.70	90.88 ab
16	2.30	2.23	2.27 a	2.96	1.95	2.46 a	90.50	90.60	90.55 ab
Influence of temperature									
18	1.94	2.32	2.13 b	2.01	1.92	1.96 d	90.91	90.56	90.74 a
19	2.29	2.32	2.30 b	2.44	2.58	2.51 c	90.52	90.49	90.50 a
12	2.37	2.96	2.66 b	2.80	2.60	2.70 bc	90.44	89.86	90.15 a
20	2.02	3.38	2.70 b	2.70	2.66	2.68 bc	90.85	89.49	90.17 a
21	2.32	2.15	2.23 b	3.19	2.97	3.08 ab	90.60	90.74	90.67 a
22	4.70	5.06	4.88 a	3.41	3.49	3.45 a	88.19	87.82	88.00 b
Influence of glycerol /starch ratio									
23	2.03	2.09	2.06 b	2.47	2.65	2.56 a	90.86	90.81	90.83 a
12	2.37	2.96	2.66 b	2.80	2.60	2.70 a	90.44	89.86	90.15 a
24	3.57	3.28	3.43 ab	2.54	2.91	2.72 a	89.32	89.61	89.47 ab
25	3.64	2.95	3.29 b	2.89	2.24	2.56 a	89.25	89.93	89.59 a
26	5.12	4.47	4.80 a	2.06	2.37	2.22 a	87.81	88.44	88.13 b
Influence of pressure									
27	2.93	2.53	2.73 a	2.76	2.65	2.70 a	89.96	90.36	90.16 a
28	1.98	2.52	2.25 a	2.73	2.87	2.80 a	90.92	90.38	90.65 a
12	2.37	2.96	2.66 a	2.80	2.60	2.70 a	90.44	89.86	90.15 a
29	1.81	3.06	2.44 a	2.72	2.44	2.58 a	91.10	89.83	90.47 a
30	2.84	3.03	2.94 a	2.49	2.98	2.73 a	90.05	89.87	89.96 a
Influence of different phenolic acids									
31	1.96	2.26	2.11 a	2.24	2.16	2.20 b	90.84	90.55	90.69 a
32	2.10	2.25	2.17 a	2.39	2.41	2.40 ab	90.70	90.55	90.62 a
33	2.69	2.19	2.44 a	2.92	3.17	3.05 ab	90.10	90.63	90.37 a
28	1.98	2.52	2.25 a	2.73	2.87	2.80 ab	90.92	90.38	90.65 a
34	2.52	1.95	2.23 a	2.73	1.88	2.31b	90.29	90.88	90.58 a
35	2.42	2.48	2.45 a	3.46	3.32	3.39 a	90.42	90.35	90.38 a

B3b.5) Gloss of both sides and transparency of the bioactive films

Table B.7 Gloss of both sides and transparency of the bioactive films

Run#	Gloss (GU) of bottom surface		Average	Gloss (GU) of top surface		Average	Translucency		Average
	Analysis 1	Analysis 2		Analysis 1	Analysis 2		Analysis 1	Analysis 2	
Influence of gallic acid/starch ratio									
10	88.83	79.97	84.40 a	9.37	11.53	10.45 b	2.30	2.90	2.60 a
2	91.50	81.33	86.42 a	8.73	11.10	9.92 b	5.35	4.65	5.00 a
11	88.97	81.53	85.25 a	8.63	8.63	8.63 b	4.25	5.15	4.70 a
12	90.37	92.50	91.43 a	9.20	15.73	12.47 b	4.91	3.98	4.44 a
13	111.33	90.30	100.82 a	61.60	39.50	50.55 ab	0.68	4.22	2.45 a
14	91.10	66.50	78.80 a	26.60	10.10	18.35 ab	1.26	2.78	2.02 a
15	80.70	101.00	90.85 a	18.50	66.20	42.35 ab	1.65	0.58	1.12 a
16	118.00	115.00	116.50 a	66.30	80.30	73.30 a	0.63	0.87	0.75 a
Influence of temperature									
18	83.57	87.40	85.48 b	12.67	12.03	12.35 c	3.71	4.11	3.91 a
19	67.80	67.10	67.45 c	12.60	11.30	11.95 c	2.72	2.65	2.69 a
12	90.37	92.50	91.43 b	9.20	15.73	12.47 c	4.91	3.98	4.44 a
20	131.00	131.67	131.33 a	118.33	131.00	124.67 a	0.87	0.65	0.76 a
21	91.37	98.53	94.95 b	82.37	71.63	77.00 b	1.34	1.36	1.35 a
22	52.47	47.30	49.88 d	4.27	1.73	3.00 c	13.04	35.76	24.40 a
Influence of glycerol /starch ratio									
23	N/A	N/A	N/A	N/A	N/A	N/A	2.18	5.51	3.85b
12	90.37	92.50	91.43 a	9.20	15.73	12.47 a	4.91	3.98	4.44b
24	86.97	85.53	86.25 a	5.22	6.63	5.93 a	4.27	5.38	4.83b
25	80.00	78.50	79.25 a	5.27	6.02	5.64 a	6.57	7.62	7.10b
26	47.93	38.30	43.12 b	4.23	7.70	5.97 a	66.54	33.14	49.84a
Influence of pressure									
27	83.40	87.77	85.58 a	8.83	8.57	8.70 a	5.88	3.99	4.93 a
28	95.57	91.37	93.47 a	32.83	9.67	21.25 a	1.65	4.25	2.95 a
12	90.37	92.50	91.43 a	9.20	15.73	12.47 a	4.91	3.98	4.44 a
29	89.97	79.97	84.97 a	18.13	9.03	13.58 a	1.72	6.57	4.15 a
30	67.70	86.17	76.93 a	10.07	9.53	9.80 a	1.88	4.33	3.11 a
Influence of different phenolic acids									
31	82.60	86.80	84.70 b	5.80	5.70	5.75 b	6.80	6.40	6.60 a
32	72.70	72.70	72.70 b	7.10	7.50	7.30 b	7.07	7.99	7.53 a
33	80.30	75.00	77.65 b	9.20	10.80	10.00 b	4.76	4.66	4.71 ac
28	95.57	91.37	93.47 ab	32.83	9.67	21.25 b	1.65	4.25	2.95 bc
34	87.10	82.20	84.65 ab	8.20	9.10	8.65 b	4.30	4.37	4.33 ac
35	106.00	122.67	114.33 a	67.80	68.30	68.05 a	0.64	0.51	0.57 c

B3b.6) Contact angle of both sides of the bioactive films

Table B.8 Contact angle of both sides of the bioactive films

Run#	Contact angle° (Bottom surface)		Average	Contact angle° (top surface)		Average
	Analysis (1)	Analysis (2)		Analysis (1)	Analysis (2)	
Influence of gallic acid/starch ratio						
10	87.52	87.39	87.46 a	88.48	86.32	87.40 a
2	91.22	89.58	90.40 a	89.66	86.20	87.93 a
11	79.70	80.80	80.25 b	93.97	92.14	93.06 a
12	80.14	80.37	80.26 b	89.84	84.06	86.95 a
13	80.02	82.42	81.22 b	84.66	89.24	86.95 a
14	88.03	88.48	88.26 a	92.60	92.09	92.35 a
15	92.33	90.20	91.27 a	89.20	89.04	89.12 a
16	88.42	86.10	87.26 a	89.02	88.35	88.69 a
Influence of temperature						
18	84.32	93.92	89.12 ab	82.86	83.62	83.24 b
19	99.17	93.44	96.31 a	88.30	93.19	90.75 ab
12	80.14	80.37	80.26 ab	89.84	84.06	86.95 ab
20	84.63	79.65	82.14 ab	81.25	83.09	82.17 b
21	80.98	79.78	80.38 ab	80.27	81.43	80.85 b
22	76.45	69.69	73.07 b	97.91	92.89	95.40 a
Influence of glycerol /starch ratio						
23	66.75	66.13	66.44 ab	82.04	79.84	80.94 ab
12	80.14	80.37	80.26 a	89.84	84.06	86.95 ab
24	43.89	57.58	50.74 b	96.62	91.12	93.87 a
25	54.39	49.85	52.12 b	66.51	82.19	74.35 ab
26	40.49	53.15	46.82 b	71.86	62.46	67.16 b
Influence of pressure						
27	84.89	82.00	83.45 a	88.19	89.95	89.07 ab
28	72.72	80.16	76.44 a	96.99	92.93	94.96 ab
12	80.14	80.37	80.26 a	89.84	84.06	86.95 b
29	84.10	76.99	80.55 a	96.75	101.78	99.27 a
30	84.97	85.67	85.32 a	90.03	90.30	90.17 ab
Influence of different phenolic acids						
31	92.28	87.91	90.10 b	65.56	70.66	68.11 b
32	87.23	86.81	87.02 bc	96.91	87.84	92.38 a
33	87.66	87.30	87.48 bc	92.92	91.54	92.23 a
28	72.72	80.16	76.44 c	96.99	92.93	94.96 a
34	88.53	93.15	90.84 b	95.98	102.21	99.10 a
35	104.80	101.29	103.05 a	98.88	90.48	94.68 a

B3b.7) Antioxidant activity and total phenolic content of film-dissolving solution

Antioxidant activity results from each assay (FRAP, ABTS and DPPH) were expressed in the unit of mg trolox equivalent/g solution for comparison purpose. This unit conversion was made through trolox standard curves obtained from each antioxidant activity assay in Figure B.6. Besides, total phenolic content of film-dissolving solution were all expressed as mg gallic acid equivalent/g solution through the standard curve in Figure B.6.
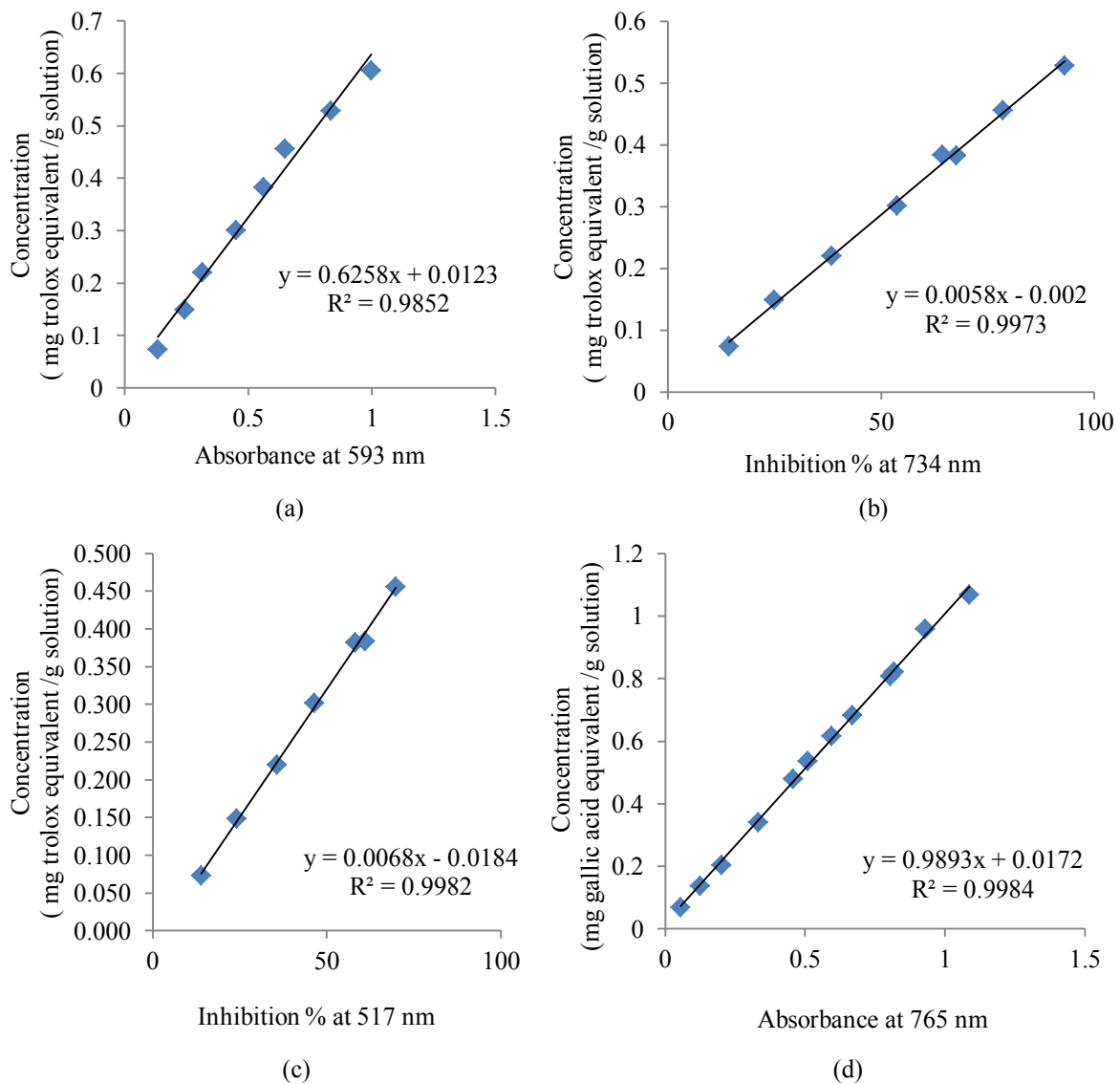
Figure B.6 Antioxidant activity and total phenolic content standard curve
(a)FRAP;(b)ABTS;(c)DPPH;(d) total phenolic content

Table B.9 Antioxidant activity (FRAP,ABTS,DPPH) and total phenolic content of film-dissolving solutions

Run#	FRAP (Trolox equivalent / film mg/g)		Average	ABTS (Trolox equivalent / film mg/g)		Average	DPPH (Trolox equivalent / film mg/g)		Average	Total phenolic content (Gallic acid equivalent / film mg/g)		Average
	Analysis 1	Analysis 2		Analysis 1	Analysis 2		Analysis 1	Analysis 2		Analysis 1	Analysis 2	
Influence of gallic acid/starch ratio												
10	0.00	0.00	0.00 f	0.00	0.00	0.00 d	0.00	0.00	0.00 e	0.74	0.80	0.77 d
2	60.66	105.45	83.05 ef	88.34	123.30	105.82 d	60.86	75.46	68.16 de	7.75	12.12	9.93 d
11	122.30	134.26	128.28 e	175.34	173.70	174.52 cd	102.67	112.00	107.33 cde	16.41	15.07	15.74 d
12	279.35	271.13	275.24 d	411.50	410.78	411.14 bcd	167.92	213.29	190.61 bcd	30.97	32.59	31.78 c
13	438.01	463.66	450.835 c	580.74	567.17	573.95 bc	263.93	348.86	306.40 b	34.61	34.99	34.80 c
14	529.11	441.99	485.55 bc	712.00	584.86	648.43 b	312.15	180.89	246.52 bc	39.40	47.90	43.65 c
15	571.31	625.34	598.32 b	788.71	890.57	839.64 b	269.53	272.33	270.93 bc	57.99	69.27	63.63 b
16	1472.92	1416.85	1444.89 a	1795.29	1390.63	1592.96 a	627.01	687.96	657.48 a	118.26	113.37	115.81 a
Influence of temperature												
18	254.46	260.22	257.34 a	344.42	330.05	337.24 b	233.48	158.42	195.95 a	30.17	28.58	29.37 ab
19	316.19	261.22	288.70 a	350.32	315.65	332.99 b	163.18	138.55	150.87 a	24.19	26.73	25.46 bc
12	279.35	271.13	275.24 a	410.78	411.50	411.14 a	167.92	213.29	190.61 a	30.97	32.59	31.78 a
20	271.58	291.34	281.46 a	362.34	337.56	349.95 b	242.72	184.47	213.60 a	29.09	31.15	30.12 ab
21	245.43	259.77	252.6 a	332.16	347.56	339.86 b	208.84	162.63	185.74 a	29.83	27.95	28.89 abc
22	273.17	258.71	265.94 a	344.95	348.42	346.68 b	252.48	166.96	209.72 a	24.29	22.95	23.62 c

*results obtained from HPLC, as total phenolic assay cannot detect cinnamic acid used in this experiment.

Table B.9 continued. Antioxidant activity (FRAP,ABTS,DPPH) and total phenolic content of film-dissolving solutions

Run#	FRAP (Trolox equivalent / film mg/g)		Average	ABTS (Trolox equivalent / film mg/g)		Average	DPPH (Trolox equivalent / film mg/g)		Average	Total phenolic content (Gallic acid equivalent / film mg/g)		Average
	Analysis 1	Analysis 2		Analysis 1	Analysis 2		Analysis 1	Analysis 2		Analysis 1	Analysis 2	
Influence of glycerol /starch ratio												
23	488.80	417.68	453.24 a	536.22	605.21	570.71 a	368.38	241.06	304.72 a	38.46	34.38	36.42 a
12	271.13	279.35	275.24 b	410.78	411.50	411.14 ab	167.92	213.29	190.61 a	30.97	32.59	31.78 a
24	204.16	196.24	200.2 bc	217.62	299.76	258.69 bc	176.07	125.01	150.54 a	23.79	23.58	23.68 b
25	173.38	153.85	163.61 c	182.50	248.30	215.40 c	136.97	93.92	115.44 a	19.11	18.46	18.78 bc
26	128.48	123.33	125.90 c	202.47	208.80	205.63 c	58.42	138.17	98.29 a	16.88	14.58	15.73 c
Influence of pressure												
27	286.77	282.94	284.86 a	346.51	347.61	347.06 bc	260.44	158.58	209.51 a	32.25	28.27	30.26 a
28	262.14	293.73	277.94 a	353.26	347.68	350.47 bc	237.83	186.08	211.96 a	30.67	32.46	31.57 a
12	271.13	279.35	275.24 a	410.78	411.50	411.14 a	167.92	213.29	190.61 a	32.59	30.97	31.78 a
29	317.55	293.04	305.29 a	349.93	353.61	351.77 b	243.72	179.17	211.45 a	32.13	27.98	30.06 a
30	283.52	240.35	261.93 a	341.57	342.81	342.19 c	276.82	158.27	217.55 a	29.82	28.78	29.30 a
Influence of different phenolic acids												
31	0.89	0.76	0.83 d	0.00	0.00	0.00 e	0.00	0.00	0.00 b	16.18	16.34	16.26 d
32	109.69	94.17	101.93 c	203.10	188.51	195.80 c	8.88	2.29	5.59 b	16.85	18.77	17.81 cd
33	150.82	132.87	141.84 c	93.93	67.45	80.69 d	43.23	32.04	37.63 b	21.78	22.98	22.38 c
28	293.73	262.14	277.94 b	353.26	347.68	350.47 b	186.08	237.83	211.96 b	30.67	32.46	31.57 b
34	0.84	1.05	0.94 d	1.63	1.00	1.31 e	0.00	0.00	0.00 b	0.60	0.63	0.62 e
35	1458.36	1406.13	1432.25 a	1366.42	1380.10	1373.26 a	594.49	792.62	693.56 a	103.76	99.31	101.53 a

*results obtained from HPLC, as total phenolic assay cannot detect cinnamic acid used in this experiment.

242

B3b.8) Water vapor permeability of bioactive films

Table B.10 Water vapor permeability of bioactive films

Run#	Water vapor permeability (g.mm/m^2.h.pa)*10^4			
	Analysis 1	**Analysis 2**	**Analysis 3**	**Average**
34	11.88	10.54	13.07	11.83 a
28	11.15	8.78	11.96	10.63 a
35	10.12	10.25	11.51	10.63 a
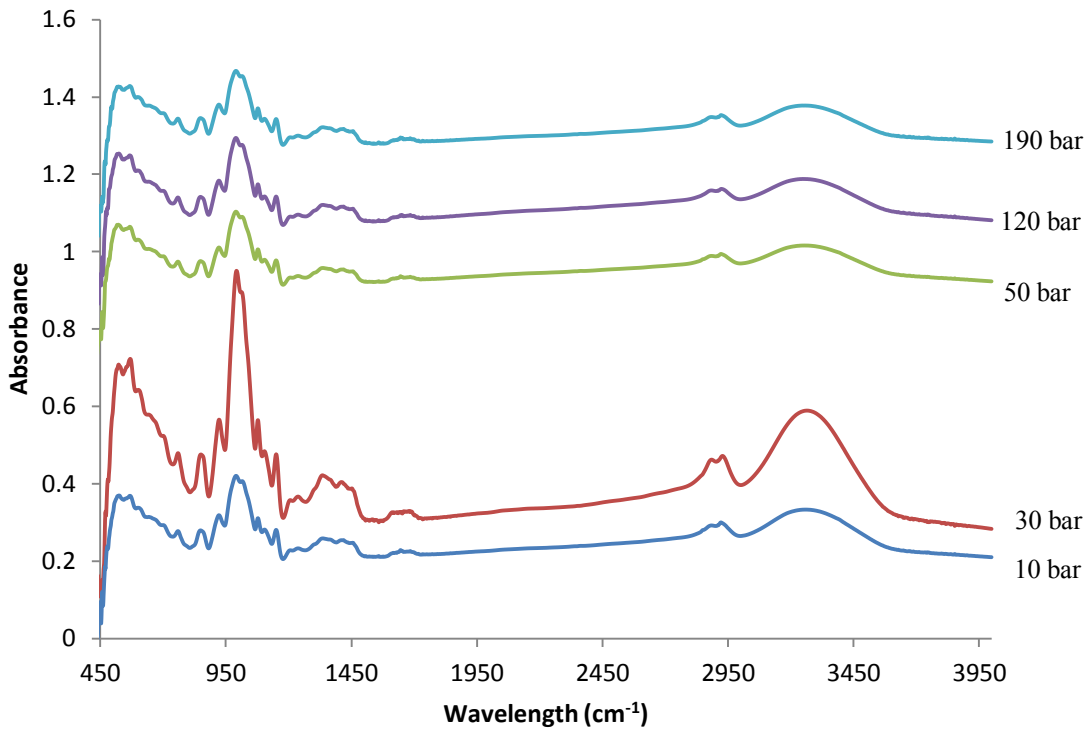
Figure B.7 FTIR of bioactive films produced at different pressures and constant glycerol/gallic acid ratio of 0.5 g/g, gallic acid /starch ratio of 40 mg/g, temperature of 100 °C.

APPENDIX C: Bioactive gels

Table C.1 Physical and functional properties of bioactive gels

Run #	Density (g/cm^3)		Average	Porosity (%)		Average	Swelling degree (%)		Average	Total phenolic content (Gallic acid equvelient / film mg/g)		Average
	Analysis 1	Analysis 2		Analysis 1	Analysis 2		Analysis 1	Analysis 2		Analysis 1	Analysis 2	
Influence of gallic acid/starch ratio												
10	0.088	0.083	0.085 a	56.82	50.93	53.88 a	11.98	13.51	12.75 a	2.09	2.58	2.33 e
2	0.093	0.076	0.085 a	43.56	63.71	53.64 a	6.48	7.22	6.85 d	9.30	15.43	12.37 d
11	0.088	0.086	0.087 a	66.44	55.12	60.78 a	10.97	12.15	11.56 ab	11.14	15.05	13.10 d
12	0.099	0.091	0.095 a	66.02	79.70	72.86 a	10.12	9.64	9.88 bc	22.59	24.69	23.64 c
13	0.098	0.090	0.094 a	69.01	74.99	72.00 a	7.60	6.43	7.02 d	36.90	36.97	36.94 b
14	0.091	0.088	0.089 a	55.87	71.98	63.93 a	7.64	7.26	7.45 cd	48.40	43.50	45.95 b
15	0.102	0.068	0.085 a	35.05	41.62	38.33 a	N/A	N/A	N/A	55.15	56.58	55.87 a
16	N/A	N/A	N/A	N/A	N/A	N/A	N/A	N/A	N/A	N/A	N/A	N/A
Influence of temperature												
18	0.085	0.082	0.084 a	61.29	65.96	63.63 a	14.16	10.03	12.10 a	22.06	22.36	22.21 a
19	0.081	0.096	0.088 a	63.10	53.76	58.43 a	12.56	11.62	12.09 a	21.52	24.75	23.14 a
12	0.099	0.091	0.095 a	66.02	79.70	72.86 a	9.64	10.12	9.88 a	22.59	24.69	23.64 a
20	0.098	0.094	0.096 a	53.55	52.02	52.78 a	8.37	6.36	7.37 a	21.85	23.62	22.74 a
21	0.089	0.080	0.084 a	60.93	72.19	66.56 a	N/A	N/A	N/A	21.87	18.91	20.39 a
22	N/A	N/A	N/A	N/A	N/A	N/A	N/A	N/A	N/A	25.86	18.51	22.19 a
Influence of glycerol /starch ratio												
23	0.05	0.04	0.05 d	53.92	57.80	55.86 ab	N/A	N/A	N/A	7.57	10.17	8.87 c
12	0.10	0.09	0.10 cd	66.02	79.70	72.86 a	9.64	10.12	9.88 a	22.59	24.69	23.64 a
24	0.13	0.12	0.13 bc	37.10	33.70	35.40 bc	7.55	5.60	6.57 b	17.03	17.72	17.37 b
25	0.15	0.17	0.16 ab	37.55	28.54	33.05 c	2.39	2.69	2.54 c	15.02	14.31	14.67 b
26	0.20	0.17	0.19 a	28.51	24.33	26.42 c	4.91	5.69	5.30 b	9.81	10.26	10.04 c

Table C.1 continued. Physical and functional properties of bioactive gels

Run #	Density (g/cm³)		Average	Porosity (%)		Average	Swelling degree (%)		Average	Total phenolic content (Gallic acid equvelient / film mg/g)		Average
	Analysis 1	Analysis 2		Analysis 1	Analysis 2		Analysis 1	Analysis 2		Analysis 1	Analysis 2	
Influence of pressure												
27	0.093	0.095	0.094 a	63.69	64.64	64.17 a	10.73	10.18	10.45 a	25.35	23.93	24.64 a
28	0.096	0.093	0.095 a	66.33	53.46	59.89 a	8.26	8.40	8.33 ab	19.56	22.13	20.85 a
12	0.099	0.091	0.095 a	66.02	79.70	72.86 a	9.64	10.12	9.88 ab	22.59	24.69	23.64 a
29	0.078	0.098	0.088 a	53.47	69.53	61.50 a	8.33	6.06	7.19 b	24.30	23.80	24.05 a
30	0.087	0.072	0.079 a	68.85	48.56	58.71 a	7.20	6.31	6.76 b	22.38	23.91	23.15 a
Influence of different phenolic acids												
31	0.095	0.083	0.089 a	57.62	73.97	65.80 a	9.87	9.75	9.81 a	5.27	9.81	7.54 b
32	0.096	0.097	0.096 a	65.96	69.44	67.70 a	8.79	9.98	9.38 a	21.95	23.40	22.68 a
33	0.099	0.089	0.094 a	60.96	49.77	55.37 a	7.68	7.40	7.54 a	21.90	23.25	22.58 a
28	0.096	0.093	0.095 a	42.11	59.61	50.86 a	8.40	8.26	8.33 a	22.13	19.56	20.85 a
34	0.089	0.080	0.085 a	62.87	72.58	67.73 a	9.29	7.97	8.63 a	2.07	2.42	2.25 b